Universitat de Barcelona

Study of the Electron-Transfer properties of phenolics and their relationship with the biological activity on cancer cells

Anna Carreras Cardona

Study of the Electron-Transfer properties of phenolics and their relationship with the biological activity on cancer cells.

Anna Carreras Cardona, 2012

Programa de doctorat de Biotecnologia. Bienni 2008-2010

Departament de Bioquímica i Biologia Molecular

Facultat de Biologia, Universitat de Barcelona

Study of the Electron-Transfer properties of phenolics and their relationship with the biological activity on cancer cells.

Estudi de la Transferència Electrònica de compostos fenòlics i la seva relació amb l'activitat biològica en cèl·lules canceroses.

Els resultats experimentals d'aquesta tesi han estat obtinguts a l'Institut de Química Avançada de Catalunya (IQAC) en el departament de Química Biològica i Modelització Molecular del Consell Superior d'Investigacions Científiques (CSIC) i a la Facultat de Biologia en el departament de Bioquímica i Biologia Molecular de la Universitat de Barcelona.

Memòria presentada per Anna Carreras Cardona per a optar al títol de doctora per la Universitat de Barcelona

Doctoranda: Anna Carreras Cardona

Co-dirigida per:

Dr. Josep Lluís Torres i Simón

Dr. Lluís Juliá Bargés   Dra. Marta Cascante Serratosa

Agraïments

Voldria agrair al Josep Lluís, al Lluís i a la Marta l'esforç que han dedicat a aquesta tesi. Al Josep Lluís per haver-me concedit la beca, sense la qual no podria haver realitzat aquest doctorat, i per les idees que dia rere dia han donat forma a la tesi, al Lluís per la seva ajuda constant i imprescindible i a la Marta per endinsar-me en el món de la bioquímica cel·lular.

Agrair al Jesús, al Pere, la Irene i la Laura l'ajuda en la síntesi i anàlisi dels glucuronats, a la Venci per la seva ajuda continuada amb l'EPR i a l'Enric, l'Isaac i l'Amado per les seves imprescindibles mesures voltamperomètriques.

Als meus no només companys de laboratori, sinó amics. A la Ari, la Sonia L, al Guillem, al Jose i al Jordi que em van acompanyar en els meus inicis en el món de la investigació, a la Sonia T. qui em va ensenyar i guiar pel complicat món dels polifenols i al Carles que hi ha sigut des de el primer moment. A la Sonia C. i al Marc que em van acompanyar en els dies de foscor i en els moments més radicals de la investigació, i a la Marisa i al Jordi P. amb qui vaig gaudir de treballar amb ells. A la Susana, l'Anna S., la Eunice, la Cris, la Jara, la Mariana, la Esther, el Carel, la Sara, l'Anna Sz, la Livia, l'Alda, l'Antonio, al Dani, a l'Aris, al Bruno i a tots els que heu estat breu però intensament en el laboratori, a tots moltes gràcies per haver-hi sigut dia a dia i per haver compartit tants bons moments.

A tot el laboratori de Bioquímica i Biologia Molecular de la Facultat de Biologia, moltes gràcies a tots per tota l'ajuda, suport i interès que heu mostrat en tot moment.

A les meves amigues Imma, Meri, Mercè, Anna, Rosa, Montse i Tània amb qui he compartit molt bons i imprescindibles moments i a qui sempre he tingut al meu costat.

A la meva amiga Arola que encara que està lluny, sempre m'acompanya i em fa suport.

Agrair a la meva família, especialment als meus pares i al Xavi el recolzament i ajut diari que m'han donat durant tots aquests anys, gràcies per haver-me ajudat a arribar on ara sóc.

Contents

Foreword

During aerobic cell metabolism, molecular oxygen is reduced to water through electron-transfer reactions, and the oxygen not completely reduced is transformed into a set of neutral and free radical molecules with high oxidant ability, generally denominated reactive oxygen species (ROS). Basal concentrations of ROS accomplish physiological functions as secondary messengers, whereas excessive amounts may cause oxidative damage in the susceptible cellular environment. To regulate the cellular ROS content, organisms are endowed with an efficient endogen antioxidant system.

The physiological ROS levels may be excessively increased by different factors including unbalanced diets (e.g. diet rich in fats), ionizing radiations (e.g. solar ultraviolet light), and tobacco smoke among others, leading to the oxidative stress, term referred to the imbalance between ROS production and its neutralization by the endogenous antioxidant system. More importantly, *in vitro* and *in vivo* studies reveal the relationship between suffering oxidative stress and the development of cardiovascular and respiratory diseases, diabetes, and cancer.

To prevent and treat the oxidative stress and its adverse effects, exogenous, readily oxidizable molecules may help the organism to neutralize ROS into less dangerous species. Interestingly, these detoxifying molecules could be already present in our diet. Epidemiologic studies have demonstrated that a diet rich in fruits and vegetables is related to the prevention of diseases caused by oxidative stress, albeit the compounds responsible of this activity are not clearly established. The phenolic compounds or (poly)phenols, a structurally diverse group of hydroxylated molecules very susceptible to oxidation, and abundantly found in our diet (i.e. fruits, vegetables, and beverages such as tea and wine) may be responsible for this antioxidant activity of fruits and vegetables.

Currently, (poly)phenols are regarded as natural antioxidant molecules with outstanding beneficial effects, including anti-aging activity, and the prevention of cancer and diabetes. On the other hand, the scientific studies and clinical surveys on the benefits of (poly)phenols remain incomplete and controversial, and an increasing number of scientists think that they cannot account for the healthy properties of vegetables by themselves.

The antioxidant activity of (poly)phenols is mainly associated with their radical scavenging activity, action conferred by the transfer of a hydrogen atom or an electron to

a free radical, rendering a less reactive molecule. On the other hand, chemical probes and *in vitro* studies have demonstrated that some highly reacting (poly)phenols are able to generate small quantities of ROS. Phenolic compounds have shown antiproliferative activity, induction of apoptosis, and/or arrest of the cell cycle in cancer cell cultures, which may be caused *inter alia* by their ability to scavenge or generate toxic radicals.

To further understand the connection between the redox reactivity of (poly)phenols and their biological actions, studies with more sensitive and selective chemical probes may help to clarify the role of redox reactions in the physiological actions of phenolics and their metabolites.

In this thesis, we have focused on the utilization of two stable radicals as chemical probes to determine the electron-transfer activity of dietary (poly)phenols and some metabolites. The different reducing potential of the two stable radicals facilitates the quantitative evaluation of the radical scavenging capacity of each (poly)phenol, as well as the establishment of the most reactive moieties. The results obtained are compared with two well-established methods for the quantification of electron-transfer capacity. The action of these (poly)phenols on cell cultures of a colon cancer cell line is also presented. This cell line is particularly relevant because dietary (poly)phenols are in contact with epithelial cells of this kind during their transit along the digestive tract and may exert some preventive action on colon cancer. In addition, a chemoenzymatic strategy to prepare glucuronated metabolites of a particularly reactive (poly)phenol was attempted.

This thesis is part of a research project within the *Institut de Química Avançada de Catalunya (IQAC-CSIC)* funded by the Spanish *Ministerio de Ciencia e Innovación* that focuses on valorization of agricultural by-products by examining the mechanisms of action of their putatively bioactive components.

1.Introduction

1.1. Free radicals and reactive oxygen species

1.1.1. Free radicals

In the structure of atoms and molecules, electrons are usually associated in pairs, each pair moving in space according to a distribution of probability (an atomic or molecular orbital). One electron in each pair has a spin quantum number of +1/2, the other -1/2. A free radical is an atom, molecule or ion that contains one or more unpaired electrons, being the electron alone in an orbital, produced by homolytic cleavage of a covalent bond or by gaining or losing one electron. Free radicals are generally highly reactive and unstable species because they readily react to become a more stable molecule by obtaining one electron (1), a hydrogen atom (2) or by scavenging of other free radicals (3) (**Figure 1**).

$$R^{\bullet} \xrightarrow{\;+\,1\,e^{-}\;} R^{-} \qquad \textbf{(1)}$$

$$R^{\bullet} \xrightarrow{\;+\,H^{\bullet}\;} H{-}R \qquad \textbf{(2)}$$

$$R^{\bullet} + R^{\bullet} \longrightarrow R{-}R \quad \textbf{(3)}$$
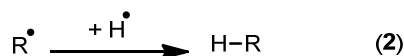
Figure 1. Reactions of a free radical to become more stable molecules.

1.1.2. Reactive Oxygen (ROS) and Reactive Nitrogen Species (RNS) in biological systems

The electronic structure of the molecule of oxygen has a unique configuration with fourteen electrons and two semi-occupied orbitals, being in a triplet state in the ground state (**Figure 2**).

1. Introduction
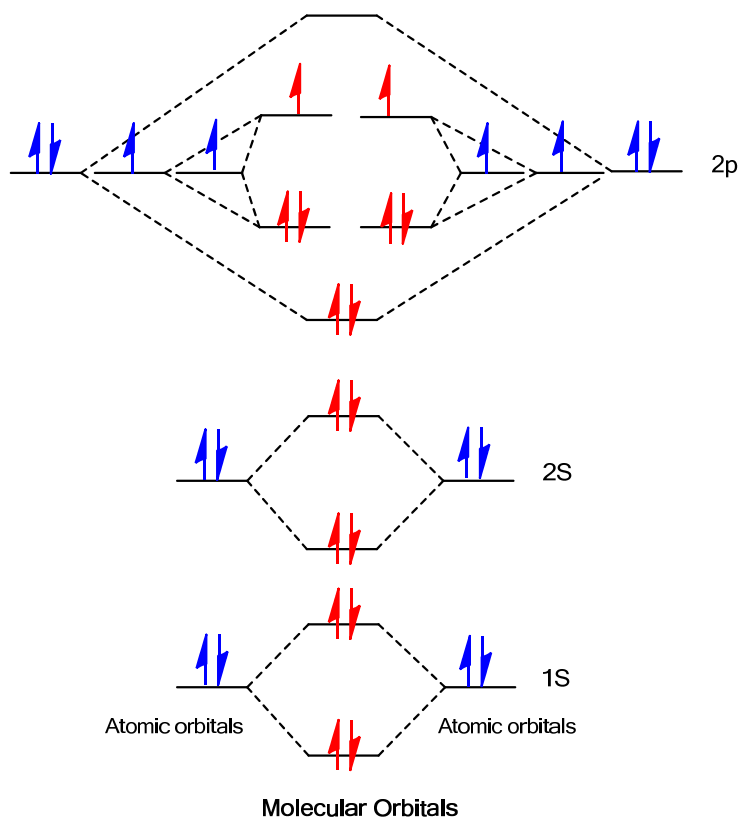
Figure 2. Molecular orbital diagram of oxygen.

Reactive Oxygen Species (ROS) include oxygen radicals (e.g. superoxide anion ($O_2^{\bullet -}$), hydroxyl ($^{\bullet}OH$), alcoxyl ($RO^{\bullet}$) and peroxyl ($ROO^{\bullet}$) radicals), and some derivatives of O_2 that do not contain unpaired electrons, such as hydrogen peroxide (H_2O_2), oxygen singlet (O_2^1), hypochlorus acid (HOCl) and ozone (O_3). Reactive Nitrogen Species (RNS) include derivatives of nitric oxide radical ($NO^{\bullet}$) (e.g. nitrogen dioxide ($NO_2^{\bullet}$)) and non radical species such as peroxynitrite ($ONOO^-$), nitrosyl anion (NO^-), nitrosyl cation (NO^+) and nitrous acid (HNO_2).

ROS/RNS are ubiquitous, highly reactive, short-lived derivatives produced within the cell as byproducts of aerobic respiration and metabolism of biological systems. They are well recognized for playing a dual role as both deleterious and beneficial species, since they can be either harmful or beneficial to living systems.

ROS generation occurs by an incomplete reduction of molecular oxygen (O_2) into two molecules of H_2O. This process requires the successive gain of four electrons. The first electron yields superoxide radical ($O_2^{\bullet-}$) and dismutation of $O_2^{\bullet-}$ produces hydrogen peroxide (H_2O_2) which in turn may be reduced to water and O_2 (**Figure 3**).(*1, 2*) Unlike $O_2^{\bullet-}$, H_2O_2 is stable and can cross the cell membrane.
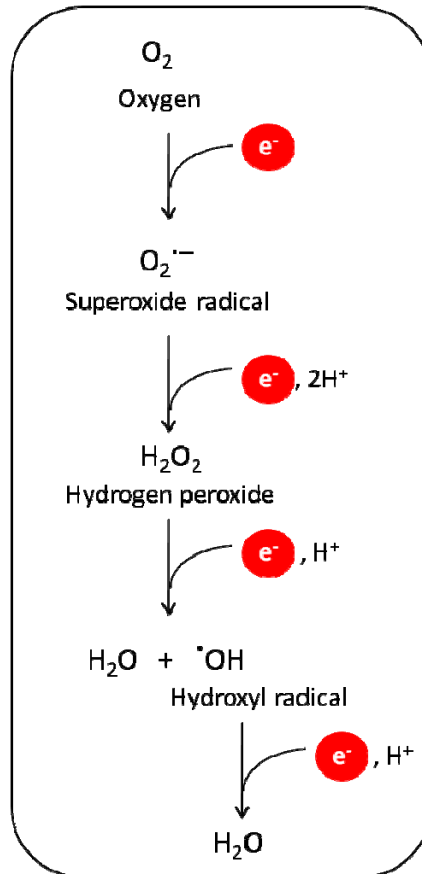
Figure 3. Schematic representation
of oxygen reduction.

ROS and RNS are essential for life of aerobic organisms. They are produced in normal cells and formed as a result of exposure to numerous factors, both chemical and physical. In normal cells, they are neutralized or eliminated by natural defense

1. Introduction

mechanisms that involve enzymatic antioxidants (glutathione peroxidase, superoxide dismutase, and catalase) and non-enzymatic antioxidants (vitamins C and E, glutathione). Under certain conditions, however, ROS/RNS production during cellular metabolism may exceed the natural ability of cells to eliminate them from the organism. These species can also form more potent oxidants leading to cellular damage and oxidative stress. For example, $O_2^{\bullet-}$ and $NO^{\bullet}$ can react to form $OONO^-$, which can then decompose into $^{\bullet}OH$. H_2O_2 is commonly reduced *in vivo* by either Fe^{2+} or Cu^+, resulting in the formation of $^{\bullet}OH$ via Fenton type reactions (Reaction **1**, **Figure 4**). $O_2^{\bullet-}$ forms H_2O_2 upon protonation in aqueous solution. DNA damage is observed directly from $^{\bullet}OH$, and indirectly from $O_2^{\bullet-}$ oxidation of [4Fe–4S] iron–sulfur clusters (contained in some proteins such as metalloproteins, NADH dehydrogenase, coenzyme Q reductase) to form H_2O_2. In addition to H_2O_2 formation, $O_2^{\bullet-}$ also releases Fe^{2+} from enzymes, such as ferritin and the [4Fe–4S]-containing dehydratases by reducing $Fe^{3+,}$ generating an unstable iron–sulfur cluster. $O_2^{\bullet-}$ can also reduce aqueous Fe^{3+} or Cu^{2+}, making these metal ions available to react with H_2O_2, although the rate of iron reduction is slow (10 h is the proposed halftime for this reaction *in vivo*), and it is generally assumed that more abundant cellular reductants such as NADH commonly reduce cellular Fe^{3+}. The Haber–Weiss reaction was once thought to be a source of cellular $^{\bullet}OH$ (Reaction **2**, **Figure 4**), but it has been determined later on that this reaction does not occur *in vivo*.(*3*)

$$Fe^{2+}/Cu^+ \ + \ H_2O_2 \longrightarrow Fe^{3+}/Cu^{2+} \ + \ ^-OH \ + \ ^{\bullet}OH \quad (\mathbf{1})$$

$$O_2^{\bullet \, -} + \ H_2O_2 \longrightarrow O_2 \ + \ ^-OH \ + \ ^{\bullet}OH \quad (\mathbf{2})$$

Figure 4. (**1**) Fenton's reaction and (**2**) Haber-Weiss reaction.

1.1.3. Cellular sources of ROS and RNS

Mitochondria

The production of $O_2^{\bullet-}$ in the cell mainly occurs within the mitochondria. The mitochondrial electron transport chain is the main source of ATP (adenosine-5'-triphosphate) in the mammalian cell and thus it is essential for life. During the energy

transduction, a small amount of O_2 is reduced prematurely, forming the superoxide radical ($O_2^{\bullet-}$) (1-3 % of the electrons in the transport chain generate $O_2^{\bullet-}$ instead of contributing to the reduction of oxygen to H_2O). $O_2^{\bullet-}$ is transformed into H_2O_2 with low rates at physiological conditions and this process can be accelerated by superoxide dismutases (SOD) (See section 1.2.2). (*4*) Mitochondria is also the main cellular source of NO and $ONOO^-$ (*2, 5*).

<u>Endoplasmic reticulum and peroxisome sources</u>

Peroxisomes are single membrane-bounded subcellular organelles with an essentially oxidative type of metabolism (e.g. a major function of the peroxisome is the breakdown of very long chain fatty acids through β-oxidation and detoxification of various toxic substances that enter the blood). They contain at least one H_2O_2-generating oxidase. All of the peroxisomal oxidases, with the exception of urate oxidase, are flavoproteins (proteins that contain a nucleic acid derived from riboflavin: flavin mononucleotide (FMN) or flavin adenine dinucleotide (FAD)). H_2O_2-generating peroxisomal oxidases catalyze reactions in which the protons and electrons produced are transferred from the prosthetic group of the enzyme to molecular oxygen forming H_2O_2. Peroxisomes are probably the major sites of intracellular H_2O_2 production.

The existence of L-arginine-dependent nitric oxide synthase (NOS) activity and the generation of the reactive nitrogen species (RNS), nitric oxide (NO), have been demonstrated in peroxisomes producing $ONOO^-$ through $O_2^{\bullet-}$.(*6*)

Cytochrome P450/P450 reductase and cytochrome b5 reductase are present in the endoplasmic reticulum and nuclear membranes and catalyze desaturation, demethylation and hydroxylation reactions of endogenous or foreign substances (e.g. drugs). They normally require NADPH (Nicotine Adenine Dinucleotide Phosphate) and NADH (Nicotine Adenine Dinucleotide) but under certain conditions, the incomplete oxidation of NADPH to NADH, produce H_2O_2.(*7, 8*)

<u>Respiratory burst</u>

Phagocitic cells (e.g. neutrophils) recognize under stimulus foreign particles (e.g. bacteria) producing a series of reactions called the respiratory burst. NADPH oxidase produces $O_2^{\bullet-}$ for bacterial destruction. $O_2^{\bullet-}$ spontaneously recombines with other

molecules to produce reactive ROS, such as H_2O_2, $^\bullet OH$ and $HOCl$. $O_2^{\bullet-}$ production varies according to the stimulus.(*4, 7, 8*)

Prostaglandin production

The biosynthesis of prostaglandins from arachidonic acid requires hydroperoxides (10^{-7} M), and free radicals are also produced during the process (e.g. $^\bullet OH$).(*7*)

Cytosolic sources

Xanthine oxidase, an enzyme implicated on the hydroxylation of purines, uses NAD^+ as its electron acceptor to convert xanthine or hypoxanthine into uric acid. Both reactions produce $O_2^{\bullet-}$ and H_2O_2.(*7*)

Oxidation of small molecules

Oxidation of small molecules by O_2, such as hydroquinones, leucoflavines, catecholamines and reduced ferredoxins produces $O_2^{\bullet-}$.(*7*)

1.1.4. ROS and RNS: Damage to biomolecules

The injury level produced in biomolecules by ROS/RNS is determined by the duration of oxidant production, the concentration of ROS/RNS, the species of ROS/RNS generated, and the specific intracellular site of ROS/RNS production. At high concentrations, ROS/RNS can mediate damage to cell structures, nucleic acids, lipids and proteins. On the other hand, low levels of ROS/RNS are essential in several biochemical processes, including intracellular messaging, cellular differentiation, growth arrestment, apoptosis, immunity, and defense against microorganisms.

Lipid peroxidation

The oxidation of lipids by ROS/RNS produces a range of reactive products that can concomitantly generate additional radicals. Since compartmentalization is crucial for cell viability, damage to membrane structures usually triggers initiation of cell death. Lipid peroxidation can be initiated by alcoxyl radicals ($RO^\bullet$), peroxyl radicals ($ROO^\bullet$) and $^\bullet OH$.(*7*) ROS/RNS-mediated impairment of membrane function can either occur directly through oxidation of (poly)unsaturated fatty acids present in lipids, or indirectly through inhibition of lipid synthesis, fatty acid desaturation, or activation of lipases.(*4*)

Protein oxidation

ROS/RNS can inhibit the activity of proteins by oxidation of amino acids such as cysteine (thiol-disulphide exange), methionine, histidine, and tryptophan. Oxidation of proteins may induce conformational changes leading to increased hydrophobicity and subsequent denaturation, aggregation, and precipitation. Eventually this process contributes to tissue inflammation and cell death.(4)

DNA damage

The hydroxyl radical ($^\bullet$OH) is known to react with all components of the DNA molecules, damaging both the purine and pyrimidine bases, and also the deoxyribose backbone. Permanent modification of genetic material resulting from this oxidative damage represents the first step involved in mutagenesis, carcinogenesis, and ageing.(7)

Cell signaling

Certain levels of ROS/RNS contribute to signaling cascades that trigger cell death. Conversely, complete depletions of radicals can be detrimental, too. Intracellular signaling is highly sensitive to changes in redox homeostasis, so a cellular response to high levels of ROS/RNS may lead to cell cycle arrest and apoptosis.(4)

1. Introduction

1.2. Antioxidant defense system

1.2.1. Antioxidant

An antioxidant is a substance capable of preventing or significantly delaying the oxidation of an oxidizable substrate (e.g. DNA) when is present in lower concentrations than the substrate. To be an antioxidant or not depends on the oxidizable target structure and the ROS or RNS under study.

1.2.2. Antioxidant endogenous system

Intracellular ROS/RNS production and propagation are controlled by a highly complex and integrated antioxidant system. Mammalian cells have evolved a variety of interrelated enzymatic and non-enzymatic antioxidant mechanisms which enable them to cope with oxidative environments.

The antioxidant control system of ROS/RNS production is formed by ROS/RNS-scavenging enzymes (superoxide dismutases (SODs), catalase (CAT), and glutathione peroxidases (GPX)), enzymes detoxifying lipid peroxidation products (glutathione-S-transferase (GST), phospholipid hydroperoxide glutathione peroxidase (PHGPX)) (**Table 1**) (*9*) and low molecular mass antioxidants (ubiquinone (Coenzyme Q), uric acid, albumin-bound bilirubin, glutathione (GSH), thioredoxin, transferrin, ceruloplasmin and lipoic acid) (**Table 2**).(*10, 11*) In addition, a whole array of enzymes (e.g. glutathione reductase (GSR) and methionine sulfoxide reductase (MsrA)) (*12*) is needed for the regeneration of the antioxidants (**Table 1**).

Table 1. Enzymes of the enzymatic antioxidant system.

Enzyme	Function	Location
Superoxide dismutases (SODs)	Scavenger of superoxide radical	Cytosol, mitochondria and in extracellular fluids
Catalase (CAT)	Scavenger of hydroperoxides	Peroxisomes
Glutathione peroxidase (GPX)	Scavenger of hydroperoxides	Cytosol, microsomes, mitochondria
Glutathione-*S*-transferases (GST)	Scavenger of lipidic peroxides	Cytosol, microsomes, mitochondria
Phospholipid hydroperoxide glutathione peroxidase (PHGPX)	Scavenger of hydroperoxides	Cytosol, microsomes, mitochondria
Glutathione reductase (GSR)	Reduces the oxidized glutathione	Cytosol, microsomes, mitochondria
Methionine sulfoxide reductase (MsrA)	Repairs the oxidized residues of methionine	Cytosol, nucleus, mitochondria (*13*)

Table 2. Non-enzymatic antioxidants.

Non-enzymatic antioxidants	Function	Location
Uric acid	Scavenger of free radicals (singlet oxygen, peroxynitrite, peroxides) (*14*)	Blood
Albumin-Bound Bilirubin	Scavenger of peroxyl radicals (*15*)	Blood
Glutathione (GSH)	Substrate of the enzymes GPX and GST	Cytosol, microsomes, mitochondria
Ubiquinol-10 (Coenzyme Q10)	Prevent peroxidative damage to lipids (*16*)	Mitochondria, Golgi apparatus, endoplasmic reticulum
Ceruloplasmin	Scavenger of free radicals (*17*)	Blood
Transferrin	Scavenger of free radicals (*17*)	Blood
Lipoic acid	Scavenger of free radicals (*5*)	Mitochondria

1. Introduction

Due to its high concentration and its central role in maintaining the cell's redox state, glutathione is one of the most important cellular antioxidants. Glutathione (GSH) is a tripeptide synthesized in the body from the amino acids L-cysteine, L-glutamic acid, and glycine. GSH reduces disulfide (R-S-S-R) bonds formed within cytoplasmic proteins to cysteines by serving as an electron donor. The reducing agent of GSH is the thiol group from the cysteine. In the process, GSH is converted to its oxidized form, the glutathione disulfide (GSSG). Glutathione peroxidase (GPX) catalyzes the reaction. Glutathione reductase (GSR) catalyzes the reduction of GSSG to GSH with NADPH as the reducing agent (**Figure 5**). Glutathione-S-transferase (GST) plays an important role in detoxifying reactive metabolites by catalyzing their conjugation with GSH.
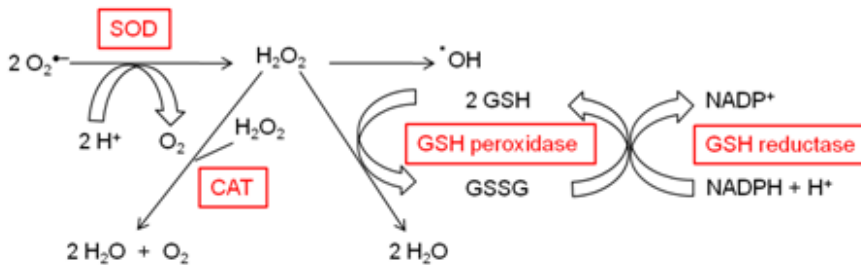
Figure 5. Suppression of ROS by SOD, CAT and GSH.

1.3. Oxidative stress

Generation of ROS/RNS and the activity of antioxidant defenses appear more or less balanced *in vivo*. In fact, the balance may be slightly tipped in favor of the ROS/RNOS so that there is continuous low-level oxidative damage in the human body. This creates a need for repairing systems that can deal with oxidatively damaged molecules.(*18*) However, if the net amount of ROS/RNS exceeds the antioxidant capacity as a consequence of a general increase in ROS/RNS generation, a depression of the endogenous antioxidant systems, or both, the so called oxidative stress is produced.

1.3.1. Causes of oxidative stress

Oxidative stress can be imposed in several ways. Tissue damage by disease, trauma, poisons, and other causes usually lead to the formation of increased amounts of injury mediators, such as prostaglandins, leukotriens (lipid oxidation) and interferons (in response to pathogens) among others.

Causes of tissue damage:

A. Alcohol consumption: alcohol increases lipid peroxidation as well as the modification of proteins.(*19*)

B. Tobacco smoking: smoke contains enormous amounts of oxidant material (aldehydes, epoxides, peroxides, NO and semiquinones) that may cause damage to the lung alveoli and it can origin micro-hemorrhages that produces iron deposition in the lung tissue, thus originating hydroxyl radical from H_2O_2 (Fenton's reaction). Elevated amounts of neutrophils are found in the lower respiratory tract increasing the formation of free radicals. Moreover, smoke oxidants deplete intracellular antioxidants.(*20*)

C. Ionizing radiation (ultraviolet light, α and β particles, gamma rays, X-rays and radioisotopes): radiation generates primary radicals by transferring their energy to cellular components and its high energy level can split water into hydroxyl and hydrogen radicals. Furthermore, radiation may generate organic radicals through direct collision with organic cellular components.(*21*)

D. Drugs: antibiotics with quinoid groups or bound metals and antineoplastics such as bleomycin, anthracyclines and methotrexate can increase free radical

production.(*22*) Long time exposure to estrogens induces DNA damage through metabolic formation of reactive species.(*4*)

E. Inorganic substances: mineral dust (asbestos, quartz and silica) can produce lung injury mediated in part by free radical production and phagocytosis by pulmonary macrophages releasing proteolytic enzymes which increase free radical levels.(*23*)

F. Other factors: physiologic stress,(*24*) exercise to excess (*25, 26*) and unbalanced diets (e.g. rich in fat) (*27*) can increase the amount of ROS.

1.3.2. Consequences of oxidative stress

Oxidative stress has been implicated in various pathological conditions involving different diseases and ageing. These diseases fall into two groups:

A. Diseases characterized by pro-oxidant shifting the thiol/disulphide redox state (protein oxidation) and impairing glucose tolerance (i.e. pre-diabetes) (*28*), the so called mitochondrial oxidative stress: cancer and diabetes mellitus.(*29, 30*)

B. Diseases characterized by inflammatory oxidative conditions and enhanced activity of either NAD(P)H oxidase (atherosclerosis and chronic inflammation) (*31*) or xanthine oxidase-induced formation of ROS (ischemia and reperfusion injury).(*32*)

The process of aging is to a large extent due to the damaging consequences of free radical action (lipid peroxidation, DNA damage and protein oxidation).(*8*)

1.4. (Poly)phenols. Importance in the diet

To avoid or treat the oxidative stress and to prevent cardiovascular, neurodegenerative, and cancer diseases, exogenous antioxidants may help to remove the excess of ROS/RNS.

- (Poly)phenols in the diet

(Poly)phenols possess one common structural feature, a phenol (an aromatic ring bearing at least one hydroxyl substituent). (Poly)phenols comprise simple phenols (one phenolic moiety bearing one or more hydroxyl groups), and di-, tri- and tetraphenols, as well as more complex polyphenolic structures. In the last five decades, (poly)phenols have attracted growing global interest as exogenous antioxidants because of their great abundance in our diet, (fruit, vegetables, cereals, olive and chocolate and in beverages, such as tea, coffee, beer and wine) and their possible role in the prevention of various diseases associated with oxidative stress. Their total dietary intake could be as high as 1 g/day, which is much higher than that of all other classes of phytochemicals and known dietary antioxidants. The high diversity of (poly)phenols in food and the complexity of their chemical structures complicate the systematic structure/activity relationships.

- (Poly)phenols as antioxidants

The protective effects of (poly)phenols in biological systems are ascribed to their scavenging activity by transfer electrons and/or hydrogen to free radicals, to their chelating activity, to activate antioxidant enzymes and to inhibit oxidases. The propensity of (poly)phenols to scavenge free-radicals is governed by their chemical structure (See section 1.4.2).

- (Poly)phenols as pro-oxidants

Oxidation of (poly)phenols produces $O_2^{\bullet-}$, H_2O_2 and a complex mixture of semiquinones and quinones, all of which are potentially cytotoxic. This pro-oxidant effect can also be beneficial by the hormetic principle (a low-dose stimulation of the defense systems with a subsequent beneficial effect).([33]) Imposing a mild degree of oxidative stress, the levels of antioxidant defenses and xenobiotic-metabolising enzymes might be raised, leading to overall cytoprotection.([34, 35])

1. Introduction

- Health benefits associated with (poly)phenols

The health benefits associated with the consumption of some (poly)phenols have been corroborated in animal studies of cancer chemoprevention, hypercholesterolemia, atherosclerosis, Parkinson's disease, Alzheimer's disease, and other aging-related disorders. Cancer chemoprevention refers to the use of agents to inhibit, reverse or retard tumorogenesis.(*36*) Epidemiological and preclinical evidences suggest that (poly)phenols, such as (–)-epigallocatechin-3-*O*-gallate (EGCG) from green tea, the flavonoids quercetin and genistein from onions and soya, respectively, curcumin of curry spice, and resveratrol from red grapes constitute a class of diet constituents with notable efficacy in human preclinical models of carcinogenesis, including those of the colorectum, breast and prostate.(*37*)

Nevertheless more evidence is needed in humans. Plant-derived foods and beverages containing (poly)phenols appear to be good for us but the contribution of the antioxidant/pro-oxidant effect of the phenolics remain still unclear.(*30*)

- Bioavailability of (poly)phenols

Most *in vitro* studies have focused on the activity of the native (poly)phenols found in food. However, after food intake, dietary (poly)phenols are absorbed and metabolized as conjugates (phase II) and as smaller phenolic acids (phase I). Very little is currently known regarding the biological activities of metabolites and further insights are required to evaluate the biological antioxidant activity of (poly)phenol conjugates and other derivatives.(*38*)

1.4.1. Types and distribution of (poly)phenols in the diet

(Poly)phenols are the most widely distributed plant secondary metabolites (8.000 (poly)phenolic structures). (Poly)phenols play many different roles in plant biology, including UV protective agents, defensive compounds against herbivores and pathogens, contributors to plant colors and to the taste of food and drink (astringency and bitterness). (Poly)phenols include phenolic acids, flavonoids, tannins, and the less abundant stilbens and lignans.

A. Phenolic acids can be divided into two classes: derivatives of benzoic acid such as gallic acid, and derivatives of cinnamic acid such as coumaric, caffeic and ferulic acid (**Figure 6**).
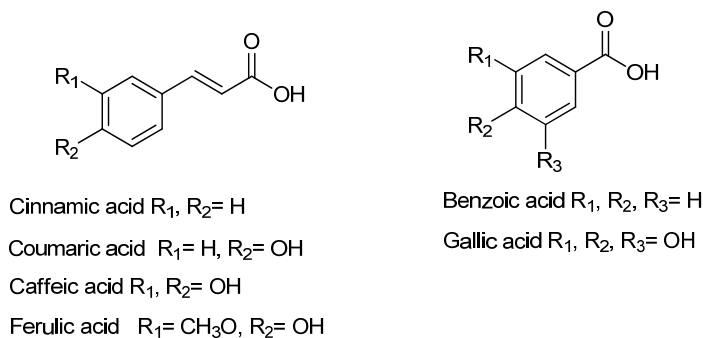
Figure 6. Phenolic acid structures.

The content of benzoic acid derivatives in edible plants is generally very low and can be found in certain red fruits, black radish, onions and tea (important source of gallic acid). In mango, raspberry and blackberry they are found as components of complex structures such as hydrolyzable tannins (On this section look at C. Hydrolyzable tannins).(*39*)

Cinnamic acids are normally found as glycosylated derivatives or esters of different acids. Caffeic acid and quinic acid (cyclitol) combine to form chlorogenic acid, which is found in many types of fruit (blueberries, kiwis, plums, cherries, apples) and in high concentrations in coffee (a single cup may contain 70-350 mg of chlorogenic acid). Ferulic acid is the most abundant phenolic acid found in wheat grain, rice and oat and maize flours.

B. Flavonoids are the most abundant (poly)phenols in our diet. Flavonoids present a common basic structure of C_6-C_3-C_6 as it is shown in the **Figure 7**.
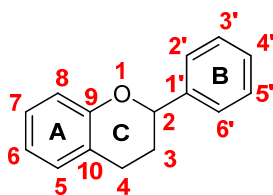
Figure 7. Basic structure of flavonoids.

1. Introduction

Flavonoids are divided into six subgroups: flavones, flavonols, flavanols/flavan-3-ols, flavanones, isoflavones and anthocyanidins, according to the oxidation state of the central C ring. Flavonoids are present in glycosylated forms except flavanols which are in their free form (aglycone). Aglycones of flavonols are shown in **Figure 8**. The associated sugar moiety is very often glucose or rhamnose, but other sugars may also be involved (e.g. galactose, arabinose, xylose, glucuronic acid).

Flavone
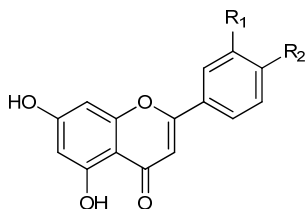
Flavonol

Luteolin R_1, R_2= OH

Apigenin R= H, R_2= OH
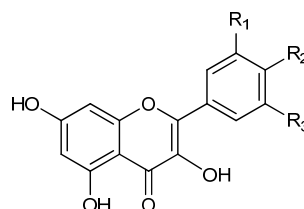
Myricetin R_1, R_2, R_3= OH

Quempferol R_2= OH, R_1, R_3= H

Flavanol/Flavan-3-ol
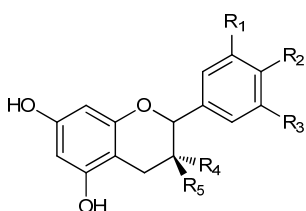
Flavanone

(-)-Epicatechin R_2, R_3, R_4= OH R_1, R_5= H

(-)-Epigallocatechin-3-O-gallate R_1, R_2, R_3= OH, R_5= H
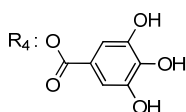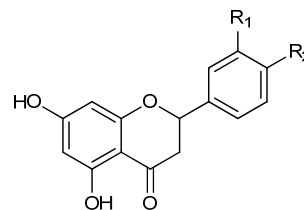
Naringenin R_1= H, R_2= OH

Hesperetin R_1= OH, R_2= OCH$_3$

R_4 :

Isoflavone
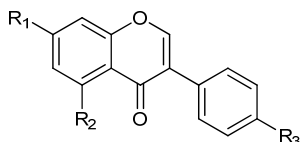
Anthocyanidin

Genistein R_1, R_2, R_3= OH

Daidzein R_1, R_3= OH, R_2= H
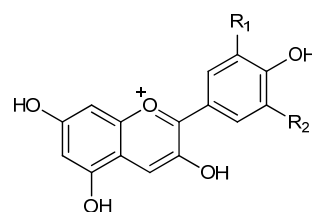
Cyanidin R_1= OH, R_2= H

Delphinidin R_1, R_2= OH

Figure 8. Aglycones of flavonols.

1. Introduction

The only important edible source of flavones is parsley and celery. Flavonols are the most ubiquitous flavonoids in food. The richest sources are onions, leeks, broccoli and blueberries. These flavonols are accumulated in the outer and aerial tissues (skin and leaves) because their biosynthesis is stimulated by light. Flavanols exist in both monomeric (catechins, gallocatechins) and polymeric forms (procyanidins, prodelfinidines). (On this section look at section C. Condensed tannins). (+)-Catechin and (−)-epicatechin are the main flavanols in fruits such as the apricot, and grape (red wine), and chocolate, whereas (+)-gallocatechin, (−)-epigallocatechin, and (−)-epigallocatechin-3-*O*-gallate are found in certain seeds of leguminous plants, and more importantly in tea. Flavanones are found in tomatoes, in certain aromatic plants and in citrus fruit. Isoflavones are found exclusively in leguminous plants, soya and its processed products are the main source. Anthocyaninds are found in red wine, certain varieties of cereals, and some leafy and root vegetables (aubergines, cabbage, beans, onions, radishes), but they are most abundant in fruit (blackcurrant and blackberries). They are found mainly in the skin, where they impart a pink, red, blue, or purple color.

C. <u>Tannins.</u> Tannins have traditionally been divided into two groups: the hydrolyzable and the condensed tannins. Hydrolyzable tannins (HTs) are made up of a carbohydrate core whose hydroxyl groups are esterified with phenolic acids (mainly gallic and hexahydroxydiphenic acid). The condensed tannins (CT), or proanthocyanidins, are polymers of flavanol units (flavan-3-ol, flavan-3,4-diol) (**Figure 9**).

Hydrolyzable tannin **Condensed tannin**
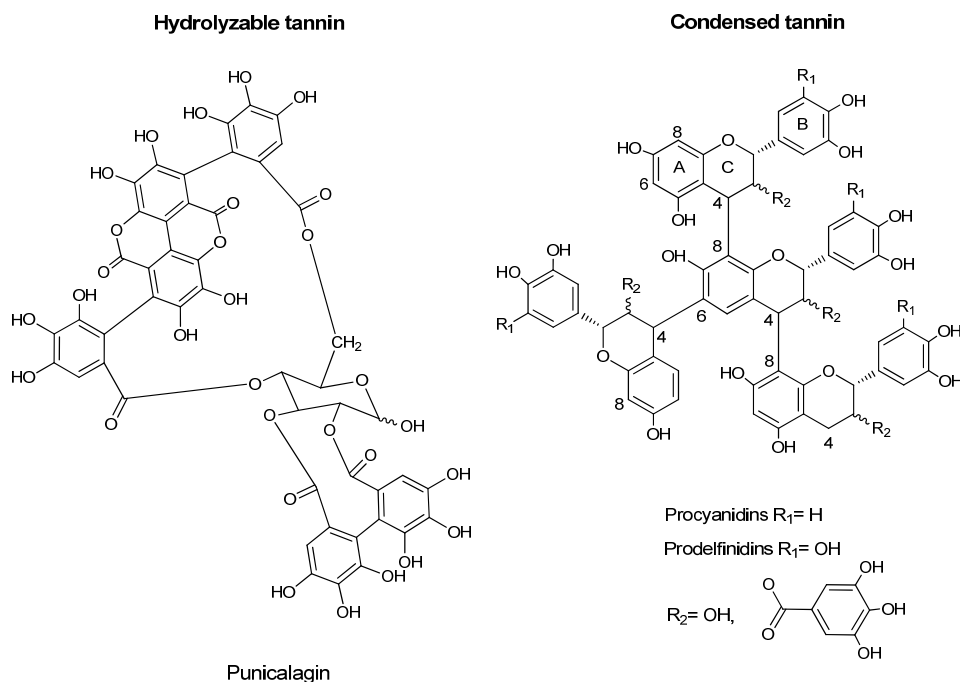
Figure 9. Structures of hydrolyzable and condensed tannins.

Hydrolyzable tannins are found in fruits such as pomegranate, in nuts such as chest nuts and in oak-aged red wine.(*40*) Condensed tannins are found in fruit such as, grapes, peaches, kakis, apples, pears, and berries and in beverages such as wine, cider, beer and in chocolate. Through the formation of complexes with salivary proteins, condensed tannins are responsible for the astringent character of food and beverages.(*39*)

D. <u>Stilbens and Lignans.</u> Stilbens are widely distributed in liverworts and higher plants, in monomeric form and as dimeric, trimeric and polymeric stilbenes, the so-called viniferins. Stilbens are 1,2-diarylethenes. Ring A (**Figure 10**) usually carries two hydroxyl groups in the *m*-position, while ring B (**Figure 10**) is substituted by hydroxyl and methoxy groups in the *o*-,*m*- and/or *p*-position. Lignans are defined as compounds possessing a 1,4-diarylbutane structure (**Figure 10**).(*41*)

1. Introduction
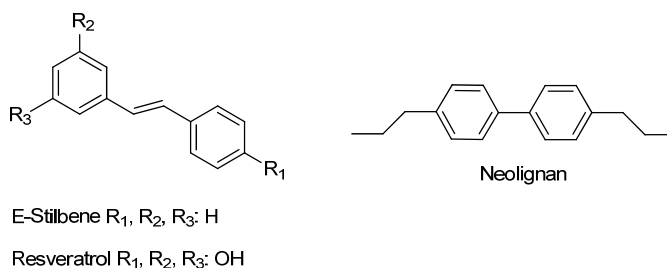
Figure 10. Structures of stilbenes and lignan.

The richest dietary source of lignans is linseed. As minor sources, lignans are found in other cereals such as triticale and wheat, in lentils, in garlic, asparagus, carrots, pears and prunes.(*39*) The stilbene resverastrol is found in low quantities in red wine.

1.4.2. Properties of (poly)phenols: chemical structures and behavior

1.4.2.1. Antioxidant properties of (poly)phenols

The antioxidant properties of a (poly)phenol (PhOH) ((PhOH) instead of $((Ph)_n(OH)_m)$ to simplify the reaction schemes) are defined by its activity to scavenge free radicals, to prevent the formation of free radicals, and to inhibit enzymes involved in free radical production.

1. Free radical scavenging activity: (Poly)phenols (PhOH) eliminate free radicals (R•) with the formation of a more stable and less damaging intermediate radical (PhO•) (reaction **1**). These more stable radicals may terminate the propagation route of other free radicals (reaction **2**).

$$R^\bullet + PhOH \longrightarrow RH + PhO^\bullet \quad (\mathbf{1})$$

$$PhO^\bullet + R^\bullet \longrightarrow PhOR \quad (\mathbf{2})$$
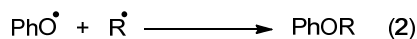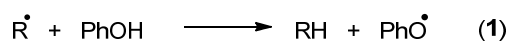
Figure 11. Scavenging reaction between a (poly)phenol (PhOH) and a free radical (R•).

The radical scavenging activity of (poly)phenols is conferred by their capacity to donate a hydrogen atom or an electron to a free radical and the velocity in doing this. The aromatic (poly)phenolic system stabilizes the odd electron from the newly formed (poly)phenolic radical (**Figure 12**). The number and position of the hydroxyl functions found in each (poly)phenol is key to establish the reactivity of the molecule and the stability of its radical form.
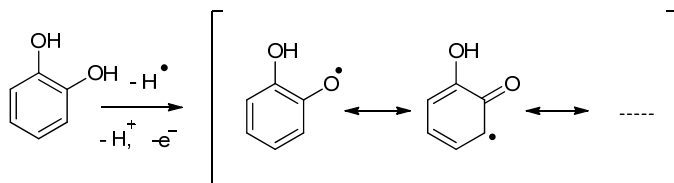
Figure 12. Oxidation of the catechol and the resonance effect of the oxidized radical.

The radical scavenging activity of phenolic acids (i.e. benzoic acid and cinnamic acid derivatives) and their esters depends on the number of free hydroxyl groups. The radical scavenging activity of flavonols is determined by their high number of hydroxyl groups and their capacity to stabilize the odd electron by delocalization. The B-ring hydroxyl configuration and the 3-OH are the most significant determinant of scavenging of ROS/RNS (**Figure 13** in red), and the 2,3-double bond and the 4-oxo function of the C ring (**Figure 13** in green), enhance the stability of the oxidized (poly)phenol radical.(*42, 43*) Finally, the radical scavenging activity of hydrolyzable tannins is conferred by the number of gallate groups contained, their molecular weight, and the presence of *ortho*-hydroxyl structures.(*44*)

1. Introduction
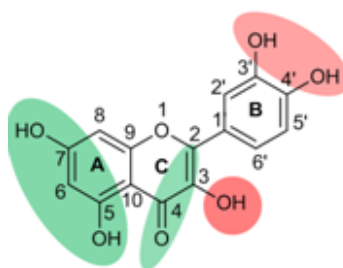
Figure 13. Quercetin and the structural features which confers its scavenging properties.

2. Ability to prevent the formation of free radicals: Most biological iron (i.e. Fe^{3+} and Fe^{2+}) is bound to proteins (e.g., transferrin, ferritin) to regulate its concentration, although a very small amount of iron is found free within the cytoplasm. This labile iron pool represents < 5 % of the total cellular iron,(*45*) and contains free Fe^{2+}, which catalyzes ROS formation (Fenton's reaction (Section 1.1.2, **Figure 4**, reaction **1**)). (Poly)phenolic prevention of ROS formation is conferred by the Fe^{2+} chelating ability of anions of catechol (e.g. Quercetin, B-ring), pyrogallol (e.g. EGCG, B-ring) and gallate (e.g. ECG, D-ring) groups (**Figure 14**). Flavonols possess a second iron-binding site between the carbonyl oxygen at the 4-position and either the 3-OH or 5-OH groups (Quercetin, A and C-ring, **Figure 14**).
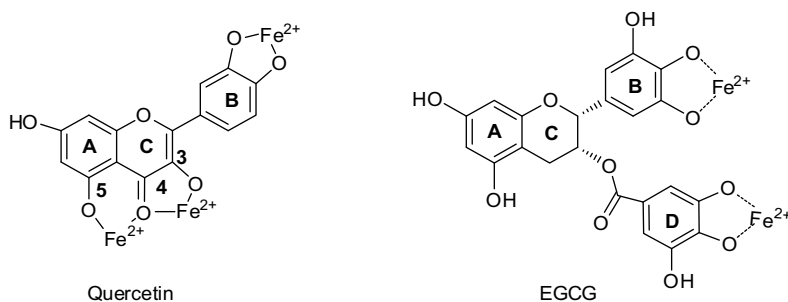
Figure 14. Iron-binding sites of Quercetin and EGCG.

The ability of (poly)phenols to prevent ROS formation by quelation is explained by two mechanisms:

A (Poly)phenols bind Fe^{2+}, and prevent its reaction with H_2O_2 in the Fenton's reaction (**Figure 15**).
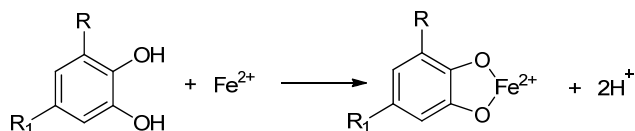
Figure 15. Chelate formation of Fe^{2+} by catechol (R, R_1 = H), pyrogallol (R = OH, R_1 =H) or gallate (R = OH, R_1 = COO) anions.

B The Fe^{2+}-phenol complex reacts with O_2 to generate a Fe^{3+}-phenol complex (**Figure 16**). The product of this reaction has not been elucidated, although participation of O_2 is thought to generate the pro-oxidant species $O_2^{\bullet-}$. In this reaction, Fe^{2+} is oxidized to Fe^{3+} complex which cannot participate in the Fenton reaction (Section 1.1.2, **Figure 4**, reaction **1**).
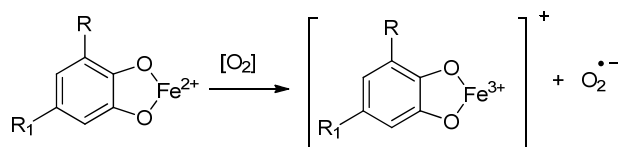
Figure 16. Proposed reaction of Fe^{2+}-(poly)phenol complex with O_2 (catechol (R, R_1 = H), pyrogallol (R = OH, R_1 =H) or gallate (R = OH, R_1 = COO) anions).(*46*)

3. Ability to inhibit the formation of free radicals: (Poly)phenols can inhibit some enzymes involved in free radical production (e.g. xantine-oxidase, peroxidases, lipooxigenases and cyclooxygenases).(*47*) Lin *et al.* demonstrate the capacity of EGCG as a competitive inhibitor in front of xanthine as substrate of xantine-oxidase enzyme.(*48*)

1.4.2.2. Dangerous molecules formed by (poly)phenols

At low concentrations, some (poly)phenols act as antioxidants, but at higher concentrations they may damage biomolecules. The explanation of this action can be, *inter alia*, the generation of free radicals by (poly)phenols, and (poly)phenol oxidation into more reactive or toxic molecules (e.g. oligomers, semiquinones and quinones). (Poly)phenols containing the pyrogallol group behave as pro-oxidants at whatever concentration by reaction with molecular oxygen (O_2) to produce superoxide radical ($O_2^{\bullet-}$) and other related ROS (H_2O_2 and $^{\bullet}OH$). Some (poly)phenols reduce Fe^{3+} and Cu^{2+} to Fe^{2+} and Cu^{+} respectively, which act as pro-oxidant molecules by formation of hydroxyl radical ($^{\bullet}OH$) by Fenton's reaction.

At high concentrations, dietary flavonoids (e.g. silymarin) inhibit cell growth, deplete glutathione concentration, decrease cell viability and induce DNA breakage in normal human lymphocytes and transformed cells.([49]) Fan *et. al.* showed that low concentrations of procyanidin B4, catechin, and gallic acid prevent oxidative damage to cellular DNA, but at higher concentrations, these compounds may induce cellular DNA damage.([50])

(Poly)phenols containing the pyrogallol group are the most potent to reduce O_2 to $O_2^{\bullet-}$ by formation of the corresponding quinone (**Figure 17**, reaction **1**). Within the cell, superoxide dismutase (SOD) catalyzes the dismutation of $O_2^{\bullet-}$ to H_2O_2 (**Figure 17**, reaction **2**) and, by Fenton's reaction, $^{\bullet}OH$ radical is obtained as the most dangerous ROS (**Figure 17**, reaction **3**).([51])
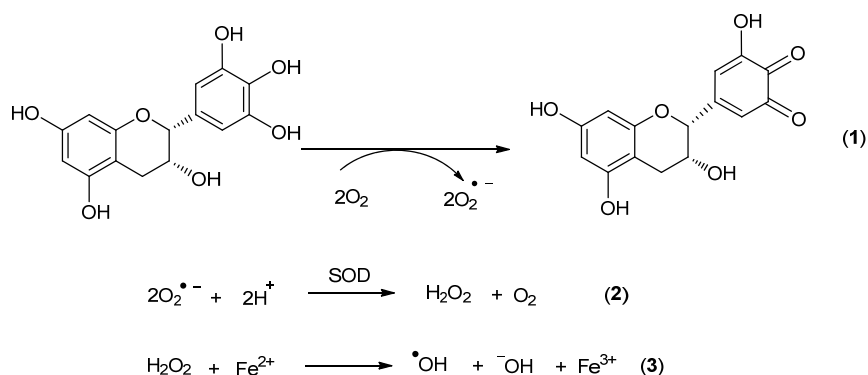
Figure 17. Reduction of O_2 to $O_2^{\bullet-}$ by pyrogallol group of (–)-epigallocatechin (EGC).

Nakagawa *et al.* studied the antitumor mechanism of (–)-epigallocatechin (EGC) and (–)-epigallocatechin-3-*O*-gallate (EGCG) in human T-cell acute lymphoblastic leukemia Jurkat cells.(*52*) The cytotoxicity of the two catechins in certain tumor cells was given by their ability to produce H_2O_2, which triggers the Fe(II)-dependent formation of the highly toxic $^{\bullet}OH$, an apoptotic cell death inductor. Li *et al.* demonstrated the pro-oxidative activity of EGCG *in vivo* and *in vitro* in human lung cancer H1299 cultures and in xenograft tumors.(*51*) The antiproliferative action of EGCG in culture cell was mostly abolished by the presence of superoxide dismutase (SOD) and catalase, which decompose the ROS formed in the culture medium. It is important to notice that the production of H_2O_2 by EGCG and EGC depends on the medium used in the culture cell. Treatment with EGCG also caused the generation of intracellular and mitochondrial ROS producing apoptosis and DNA damage. *In vivo*, tumor growth was dose dependently inhibited by EGCG introduced in diet.(*53, 54*)

<u>Reduction of Fe^{3+} and Cu^{2+} by (poly)phenols</u>

Anions of catechol, pyrogallol and gallate groups form complexes with Fe^{3+}. The formation of these complexes leads to the reduction of Fe^{3+} to Fe^{2+} and the oxidation of the (poly)phenol to a semiquinone. The semiquinone is able to reduce another equivalent of Fe^{3+}, rendering Fe^{2+} and the corresponding quinone (**Figure 18**, reaction **1**).(*55*) The Fe^{2+} thus obtained can participate in the Fenton's reaction to form $^{\bullet}OH$ (**Figure 18**, reaction **2**).

1. Introduction

$$H_2O_2 + Fe^{2+} \longrightarrow {}^{\bullet}OH + {}^{-}OH + Fe^{3+} \quad (2)$$
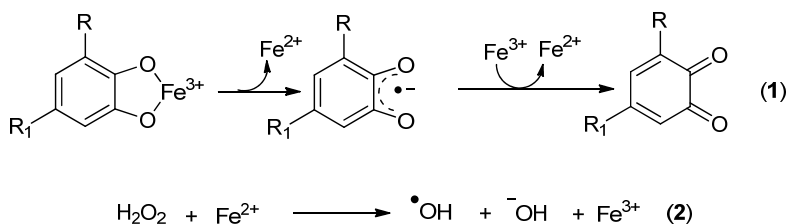
Figure 18. (**1**) Reduction of two equivalents of Fe^{3+} to Fe^{2+} and concomitant quinone formation (catechol (R, R_1 = H), pyrogallol (R = OH, R_1 =H) or gallate (R = OH, R_1 = COO) anions) (**2**) Fenton's reaction.

Similarly to Fe^{2+}, Cu^+ mediates ROS generation. Cu^{2+} is reduced by (poly)phenols to form Cu^+ (**Figure 19**, reaction **1**), which generates $^{\bullet}OH$ in the Fenton's reaction (**Figure 19**, reaction **2**).

$$H_2O_2 + Cu^+ \longrightarrow {}^{\bullet}OH + {}^{-}OH + Cu^{2+} \quad (2)$$
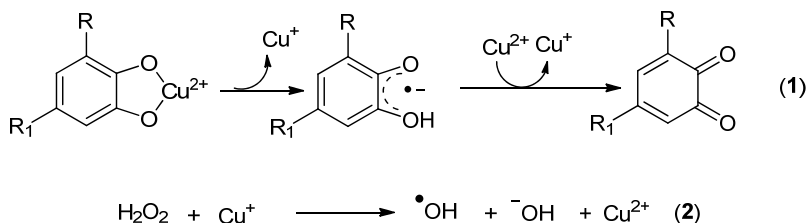
Figure 19. (**1**) Reduction of two equivalents of Cu^{2+} to Cu^+ and concomitant quinone formation (catechol (R, R_1 = H), pyrogallol (R = OH, R_1 =H) or gallate (R = OH, R_1 = COO) anions). (**2**) Fenton's reaction.

Perron *et. al.* tested the effects of catechins on the Cu^+/H_2O_2-mediated DNA damage and observed both antioxidant and pro-oxidant behaviors. EGCG showed antioxidant effect by inhibition of Cu^+. In contrast, EC and EGC exhibited pro-oxidant activity under the same conditions, whereas ECG showed both pro-oxidant and antioxidant activity. The greatly diminished antioxidant potency for (poly)phenols in the copper system is attributed to the weak interactions between (poly)phenols and Cu^+.(*56*) Nevertheless, it should be noticed that the biological concentrations of Cu^{2+}/Cu^+ are much lower than that of Fe^{3+}/Fe^{2+} in healthy individuals.

1.4.3. (Poly)phenols as chemopreventive agents against cancer

Strong and consistent epidemiologic evidence indicates that a diet with high consumption of fruits and vegetables rich in (poly)phenols significantly reduces the risk of many cancers, suggesting that certain dietary (poly)phenols could be effective agents for the prevention of cancer incidence and mortality.(*43*) Different *in vitro* and *in vivo* systems have been employed to determine the anticarcinogenic and anticancer potential of natural (poly)phenols as pure compounds or extracts.

<u>*In vitro* effect of (poly)phenols</u>

(Poly)phenolic extracts and isolated (poly)phenols from different vegetal sources have been studied with a number of cancer cell lines representing different evolutionary stages of cancer.

Berry extracts prepared form blackberry, raspberry, blueberry, cranberry, strawberry (the major classes of berry (poly)phenols were anthocyaninds, flavonols, flavanols, ellagitannins, gallotannins, proanthocyanidins, and phenolic acids), and the isolated (poly)phenols from strawberry including anthocyaninds, kaempferol, quercetin, esters of coumaric acid and ellagic acid, were found to inhibit the growth of human oral (KB, CAL-27), breast (MCF-7), colon (HT-29, HCT-116), and prostate (LNCaP, DU-145) tumor cell lines in a dose-dependent manner with different sensitivity between cell line.(*57, 58*) Ethanol extracts of 10 edible berries and bilberry extract were very effective at inhibiting the growth of HL60 human leukemia cells and HCT116 human colon carcinoma cells *in vitro*.(*59*) Ross and co-workers showed that the antiproliferative activity of raspberry extract in human cervical cancer (Hela) cells was predominantly associated with ellagitannins.(*60*)

Red wine is a rich source of (poly)phenols, and their antioxidant and tumor arresting effects have been demonstrated in different *in vitro* systems. Damianaki *et al.* measured the antiproliferative effect of red wine and purified catechin, epicatechin, quercetin, and resveratrol, which account for more than 70 % of the total (poly)phenols in red wine, on the proliferation of hormone sensitive (MCF7, T47D) and resistant (MDA-MB-231) breast cancer cell lines, indicating a decrease in cell proliferation in a dose- and a time-dependent manner.(*61*) Kampa *et al.* studied the effect of (−)-catechin, (−)-epicatechin, quercetin, and resveratrol on the growth of three prostate cancer cell lines (LNCaP, PC3, and DU145) and a dose- and time-dependent inhibition of cell growth

1. Introduction

by (poly)phenols was found. The proliferation of LNCaP and PC3 cells was preferentially inhibited by flavonoids ((−)-catechin, (−)-epicatechin, and quercetin), whereas resveratrol was the most potent inhibitor of DU145 cell growth.(*62*) Zhang and co-workers showed that green, Oolong and black tea extracts dose-dependently inhibited proliferation and invasion of a rat ascites hepatoma cell line of AH109A but did not affect the proliferation of the normal mesentery-derived mesothelial cells (M-cells) from rats. Furthermore, (−)-epigallocatechin-3-*O*-gallate (EGCG), (−)-epicatechin gallate (ECG) and (−)-epigallocatechin (EGC) from green tea, as well as the mixture of theaflavin and theaflavin gallates from black tea, were shown to be the most effective components against the invasion and proliferation of AH109A.(*63*) The antiproliferative effects of tea (poly)phenolic extracts and EGCG were more pronounced towards immortalized, tumourigenic (CAL27, HSC-2, and HSG1) and non-tumourigenic (S-G) human oral cavity cells than in normal (GN56 and HGF-1) fibroblasts, and green tea was more toxic than black tea.(*64*) McCan *et al.* demonstrated that a crude apple extract from waste, rich in phenolic compounds, beneficially influences key stages of carcinogenesis in colon cells: genotoxicity (HT-29), invasion and metastatic potential (HT-115), and colonic barrier function (CaCo-2).(*65*) Grape procyanidins showed a significant capacity to induce apoptosis in colon cancer cells (HT-29 cell line) while being inactive in non-cancer control cells (IEC-6).(*66*) Lizárraga *et al.* showed that Witch Hazel fractions block the cell cycle of HT-29 cells in the S phase by scavenging ROS, with subsequent inhibition of DNA synthesis.(*67*)

In vivo effect of (poly)phenols with animal models

Many experimental animal studies tested Green Tea Extract (GTE) and EGCG, and analyzed biomarkers of cancer risk or cancer development. Many of these studies reported that GTE and EGCG protect against chemical carcinogens in various organs such as intestine, lung, liver, prostate, and breast. Dietary ingestion of green tea (0.1–2.0 % of diet) or EGCG was tested in hamsters demonstrating a decrease in the number of duodenal or colon tumors induced by various promoters. Assays using rats as model showed that the ingestion of EGCG decreased the incidence of gastric carcinogenesis and colorectal cancer. In mice, ingestion of green tea (2 % of diet) decreased the number of induced lung tumors and the growth and the progression of prostate cancer. Furthermore, EGCG inhibits metastasis of this cancer to distinct organ sites (lymph, lungs, liver, and bone).(*68*)

Curcumin, a yellow (poly)phenolic pigment commonly used as a spice and food-coloring agent, was tested with different induced tumors in mice. Feeding 0.5-2.0 % of curcumin in the diet decreased the number of induced forestomach tumors per mouse by 51-53 % when administrated during the initiation period, and 47-67 % when administered during the post-initiation period. Feeding 0.5-2.0 % of curcumin in the diet decreased the number of induced duodenal tumors per mouse by 47-77 % when administered during the post-initiation period. Administration of 0.5-4.0 % of curcumin in the diet, both during the initiation and post-initiation periods, decreased the number of induced colon tumors per mouse by 51-62 %. Administration of 2 % of curcumin in the diet inhibited the number of induced colon tumors per mouse by 66 % when fed during the initiation period, and 25 % when fed during the post-initiation period. Administration of curcumin in the diet to treated mice resulted in development of colon tumors which were generally smaller in number and size as compared to the control group of treated mice. These results indicate that curcumin control the number of tumors per mouse and the percentage of mice with tumors, and reduced tumor size.(*69*) Genistein and daidzein (isoflavones derived from soybeans) inhibit the development of different cancers in mouse model, i.e. breast, prostate, and skin cancer.(*70*) A high isoflavone diet was also found to inhibit induced prostate tumors in rats with induced tumor.(*71*)

In vivo effect of (poly)phenols in human studies

Studies with (poly)phenols in healthy individuals. Oral consumption of tea (poly)phenols has been associated with an increase of the antioxidant activity in plasma and urine. Sung and co-workers measured the Plasma Antioxidant Activity (PAA) with the Trolox Equivalent Capacity Assay (TEAC, See Section 1.5.2.3) after ingestion of tea extract. PAA raised by 12.7 % in the plasma of individuals 2 hours after ingestion of 7.5 g green tea extract.(*72*) Consumption of 6 cups of black tea was associated with a 76 % increase in PAA determined by the Ferric Reducing Antioxidant Power Assay (FRAP, See section 1.6) at 7 hours.(*73*) Some reports suggest that consumption of green tea also protected against smoking and radiation induced DNA damage in healthy individuals.(*74, 75*)

Studies with (poly)phenols in patients with premalignancy. Relatively few cancer types are associated with a definite premalignant stage, which facilitates an early detection and treatment. A good example is a recent double-blind trial, in which individuals with high-grade of neoplasia (abnormal proliferation of cells) of prostate

received either 600 mg (3 capsules of 200 mg/day (=6-8 cups of tea) of green tea catechins daily or placebo. After 1 year of treatment, only one tumor was diagnosed among the 30 green tea catechins treated men (incidence ˜3 %), whereas nine cancers were found among the 30 placebo treated men (incidence, 30 %).(*76*) In another study, a mixed tea product was administrated to two groups of 59 patients with oral mucosa leukoplakia (oral lesion described as precancerous). After the six month trial period, the oral lesion size was decreased in 37.9 % of the 29 treated patients and increased in 3.4 %; whereas the oral lesion was decreased in 10.0 % of the 30 control patients and increased in 6.7 %.(*77*) These studies indicate that dietary (poly)phenols may have a significant beneficial effect on cancer premalignancy.

Studies with (poly)phenols in patients with cancer. In a chemotherapeutic study, in which 17 patients with advanced lung cancer received green tea extract (0.5 g per day), none of the 17 participants experienced a 50 % or greater decrease in tumor diameter for 4 weeks.(*78*) Results are not surprising because it seems unlikely that a relatively short course of a diet-derived chemopreventive agent can cause obvious chemotherapeutic responses in advanced cancer. Hence, chemotherapeutic effects should be determined by the study of cancer related biomarkers. Studies with patients with advanced colorectal cancer who consumed up to 3.6 g curcumin daily for up to 4 months showed a consistent reduction in inducible PGE2 levels, as an indicator of COX-2 (enzyme responsible of inflammation and pain) activity, in peripheral blood samples. Significant reductions in the level of deoxyguanosine adduct (M1G), a marker of oxidative DNA damage, occurred in malignant colorectal tissue following ingestion of 3.6 g curcumin for 7 days.(*79*)

1.4.4. Bioavailability and metabolism of (poly)phenols

The biological activity of polyphenols is conditioned by their bioavailability. The bioavailability of (poly)phenols is the quantity or fraction of (poly)phenols that is absorbed to bloodstream of the organism after its ingestion or skin contact. There are many factors that influence the extent and rate of absorption of ingested compounds. These include physicochemical factors such as molecular size, lipophylicity, solubility, pKa and biological factors including gastric and intestinal transit time, lumen pH, membrane permeability, active transport, and metabolism.

Recent studies show that the absorption extent of dietary (poly)phenols in the small intestine is relatively small (10-20 %).(*80*) Most (poly)phenols are present in the diet in the form of esters, glycosides, or polymers but mainly unconjugated monomers can be absorbed in the small intestine (some procyanidins and anthocyanidins are absorbed as glycosides.(*81-83*)) Esters, glycosides and polymers undergo hydrolysis by intestinal enzymes or by the colonic microbiota before they can be absorbed. When the microbiota of the colon (the colon contains ≈10^{12} microorganisms/cm^3) is involved, (poly)phenols are hydrolyzed, dehydroxylated, deconjugated, decarboxylated, and ring cleavage is produced. Various simple aromatic acids are formed: 3,4-dihydrophenylacetic acid, 3-hydroxyphenylacetic acid, homovainillic acid, and their conjugates derived from the B-ring, phenolic acid form the C-ring and phenylvalerolactones metabolites (**Figure 20**). These are called phase I metabolites.
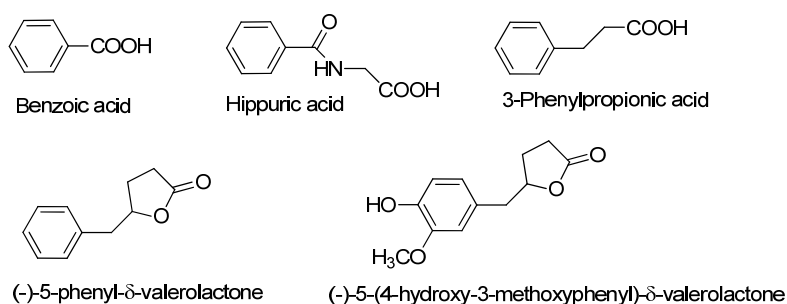
Figure 20. Metabolites observed in human urine after consumption of a variety of (poly)phenols.

Some monomeric and small (poly)phenols are already conjugated in the small intestine and later in the liver. The conjugates are called phase II metabolites. Simple phenolic acid metabolites are absorbed in the colon and highly conjugated in the liver by methylation, sulfatation and glucuronidation:

• Methylation is produced by the catechol-*O*-methyl transferase, which catalyzes the transfer of a methyl group form S-adenosyl-L-methionine to (poly)phenols having an *O*-diphenolic moiety (catechol). Catechol-*O*-methyl transferase is present in a wide range

of tissues and it is mostly active in the liver and kidneys. Studies with model animals show significant methylation of catechins in the small intestine of rats.(*84*)

• Sulfotransferases catalyze the transfer of a sulfate moiety from 3'-phophosdenosine-5'-phophosulfate to a hydroxyl group of phenolics. Sulfation occurs mainly in the liver.

• UDP-glucuronosyltranferases are membrane-bound enzymes that are located in the endoplasmic reticulum in many tissues, and catalyze the transfer of a glucuronic acid from UDP-glucuronic acid to phenolic compounds. Glucuronidation first occurs in the enterocytes (intestinal epithelial cells) before further conjugation in the liver. Some conjugated (poly)phenols are secreted by the bilis into the duodenum, where they are subjected to the action of bacterial enzymes (e.g. β-glucuronidase) to be reabsorbed (entherohepatic recycling). (Poly)phenols and simple phenolic acids are conjugated as glucuronides to achieve a higher hydrophylicity for a better biliary and urinary excretion (**Figure 21**). Although the liver has been considered the most important organ involved in glucuronidation, studies from Cheng *et al.* indicate the important role of the gastrointestinal tract in the glucuronidation of xenobiotics.(*85*)
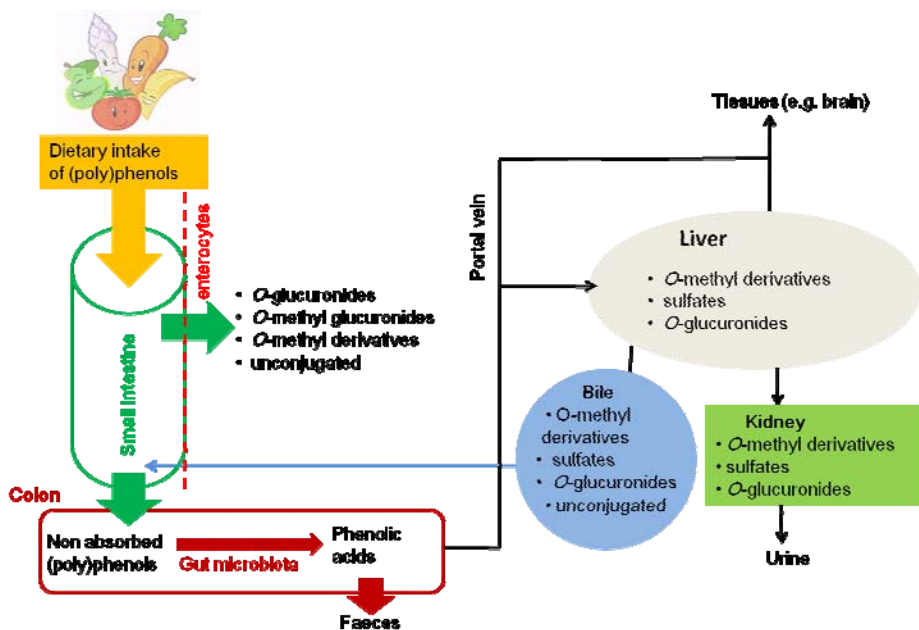
Figure 21. Metabolism of dietary intake (poly)phenols.(*39, 86-90*)

The study of the bioavailability and metabolism of (poly)phenols by its detection in physiological fluids (blood, faces and urine) is required to determine the different phenolic derivatives that may take part in the antioxidant activity of (poly)phenol intake.

1.4.4.1. Importance of (−)-epigallocatechin-3-*O*-gallate (EGCG) bioavailability

Tea infusion is a beverage with a very high (poly)phenol content. It is consumed worldwide at greatly varying levels and it is the most widely consumed beverage aside from water with a per capita worldwide consumption of approximately 0.12 liter per year. (*91*)Tea leaves are manufactured in three basic forms. Green tea is prepared with freshly harvested leaves, which precludes the oxidation of green leaf (poly)phenols. Black tea is produced by an oxidation process, and Oolong tea is a partially oxidized product. Of the total of dried tea manufactured worldwide, 20 % is green tea and less than 2 % is Oolong tea.

Fresh tea leaves contain a diversity of (poly)phenols, and are unusually rich in catechins, which constitute up to 30 % of the dry leaf weight. EGCG is the most abundant and the major biologically active component of green tea owing to it is associated with the reduction of cancer risk through its pro-oxidant property (i.e. inhibition of cell growth, deregulation of cell cycle, and apoptosis induction).(*52*)

1.4.4.2. Bioavailability and metabolism of EGCG

During the ingestion process, a fraction of the EGCG is degalloylated by saliva estereases to form EGC. After absorption, EGCG undergoes methylation, glucuronidation, and sulfation in the small intestine, liver, kidney, and other organs.

The study of EGCG metabolism in model animals is highly relevant to study different aspects of their biological effect that result difficult with human, such as toxic dose, accumulation in different tissues, and experimentation with modified animals that bear illnesses. Hence, we should first compare the metabolism in human and in animals in order to determine the accuracy of the model. A few works *in vivo* in human have studied the conjugated metabolites of EGCG. Lambert and coworkers used mouse as animal model to evaluate de bioavailability of EGCG. Results showed that after administration of EGCG intravenously or intragastrically, the free EGCG is the most

1. Introduction

abundant form found in lung, prostate, small intestine and colon, and in plasma the EGCG-glucuronides (50-60 %).(*92*) Comparison of these results with previous studies in humans, mice and rats indicates that humans and mice have similar (and higher) EGCG bioavailability than rats. However, the high degree of conjugation of EGCG in mice plasma differs from previous results in humans in which plasma EGCG was largely in the free form.(*93, 94*) Considering the published differences on the biotransformation of EGCG in studies with human and animals,(*93, 94, 96, 97*) the biotransformation of EGCG is just beginning to be understood (**Figure 22**).

The major products of EGCG degradation in the colon characterized by Lee *et al.*(*93*) and Meng *et. al.*(*95*) were M1, M2, and M3, in which M2 and M3 appear to be the dehydroxylated products of M1 (**Figure 22**). Some of these ring-fission products were reabsorbed into systemic circulation, and significant amounts appeared in the plasma and urine. These ring-fission products could also be further metabolized in the colon into simple phenolic acids, such as 4-hydroxybenzoic acid, 3,4-dihydroxybenzoic acid, 3-methoxy-4-hydroxy-hippuric acid, and 3-methoxy-4-hydroxybenzoic acid, which were detected in human urine after tea ingestion (**Figure 22**).
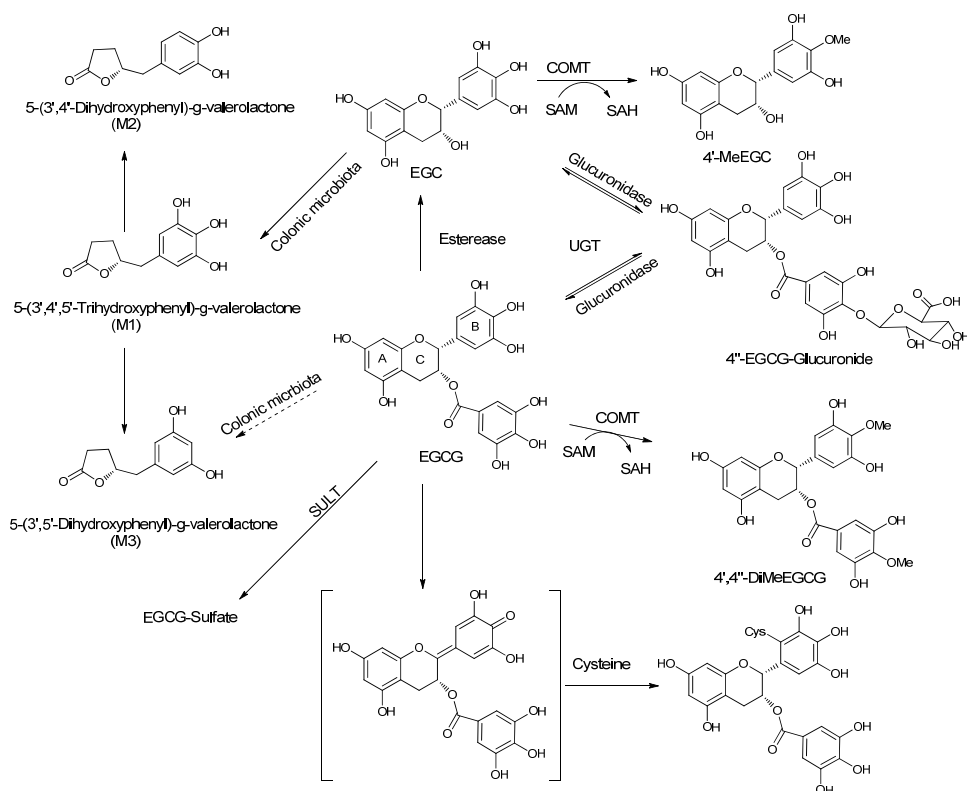
Figure 22. Biotransformation of the EGCG. Abbreviations. 4'-*O*-MeEGC: 4'-*O*-methyl-(–)-epigallocatechin; 4',4''-DiMeEGCG: 4',4''-di-*O*-methyl-(–)-epigallocatechin-3-*O*-gallate; COMT: catechol-*O*-methyltransferase; EGC: (–)-epigallocatechin; EGCG: (–)-epigallocatechin-3-*O*-gallate; SAM: (S)-adenosyl-L-methionine; SAH: (S)-adenosyl-L-homocysteine; SULT: sulfotransferase; UGT: UDP-glucuronosyltranferases.(*95*)

1.4.4.3. Synthesis of EGCG-glucuronides

Investigations over the past three decades have shown that dietary (poly)phenols are only moderately bioavailable, and that the fraction of (poly)phenols crossing the intestinal barrier is extensively metabolized in the intestinal and hepatic cells (See section 1.4.4). Thus, the potential cell effects of dietary (poly)phenols must be mainly mediated by their metabolites, of which glucuronides make the largest contribution. Hence, there is a growing interest for (poly)phenol glucuronides as standards for identification of *in vivo* metabolites and as biologically relevant compounds for cell studies with the aim of elucidating the potential health effects of (poly)phenols.

The chemical and enzymatic syntheses of some metabolites have been reported, but in the case of catechins, the high number of hydroxyl groups present in their structures makes this task a challenge.

The metabolite EGCG-4''-*O*-glucuronide was first synthesized in 2003 by Lu *et al.* in human, mouse, and rat liver microsomes as the major EGCG glucuronide followed by EGCG-3'-*O*-glucuronide, EGCG-7-*O*-glucuronide and EGCG-3''-*O*-glucuronide. Moreover, they demonstrated that the position of glucuronidation of EGCG affected its scavenging capacity with DPPH, since EGCG-7-*O*-glucuronide and EGCG-4''-*O*-glucuronide were less active than EGCG, whereas the 3'-and 3''-*O*-glucuronides showed the same activity as the EGCG.(*98*) Direct enzymatic glucuronidation of (poly)phenols is a useful technique to ascertain the preferential glucuronidation positions, albeit the isolation of the glycosides is tedious and small amounts of products are typically prepared. In this context, an efficient synthesis to obtain sufficient amounts of EGCG glucuronides for chemical and biological assays was the main goal of this part of this thesis.

1.4.4.3.1. Glucuronidation

1.4.4.3.1.1. Enzymatic glucuronidation (microsomes)

The enzymes involved in the glucuronidation of xenobiotics are known as UDP-glucuronosyltranferases (UDPGTs). These enzymes are located in the endoplasmic reticulum of cells from a number of tissues but usually have a greater abundance in the liver. The microsomes are fragments of pieces of the endoplasmic reticulum obtained by centrifugal fractionation. Microsomes are prepared by homogenization of the tissue, mostly liver and gut in a more or less defined and reproducible manner.(*98*) The

utilization of microsomes has been concerned with establishing the glucuronidation pathway of various drugs and their metabolites which were only required in small quantities for detection in HPLC and mass spectrometry assays.(*99*)

1.4.4.3.1.2. Chemical glucuronidation

No convenient synthetic methodology is currently reported to replace biosynthetic methods using liver microsomes, or the purification of metabolite-glucuronides from urinary and/or biliary samples. The chemical glucuronidation can be advantageous for the preparation of sufficient amounts of (poly)phenol glucuronides for biological testing, albeit the regiospecificity of the chemical reaction may differ from that given in human metabolism.

The chemical synthesis of glucuronide conjugates begins with the formation of a glycosidic bond. This reaction requires two reactants: a glucuronic acid derivative as a donor substrate with protecting groups (acetyls or benzoyls groups) in all its hydroxylic positions except for the anomeric carbon, which bears an activating group that enhances its electrophilicity and a nonconjugated molecule as acceptor substrate, which contains one or more hydroxyl functions acting as nucleophile. In the case of (poly)phenols, the different hydroxyl groups present diverse nucleophilicity and steric hindrance, which introduces some regioselectivity to the glycosidation reaction. A fully regioselective control requires the protection of alternative reacting hydroxyl groups.

The nucleophilic attack of the reactive hydroxyl functions of the acceptor onto the anomeric carbon of the donor is catalyzed by a number of promoters (e.g. silver carbonate, mercuric oxide, cadmium carbonate). During the glycosidation reaction, an acetyl or benzoyl group at the C2 position creates the so-called neighboring group effect, which means that the carbonyl group forms a five member ring intermediate with the anomeric carbon (**Figure 23**). Therefore, the nucleophilic attack is forced to take place from the β face, leading to the desired β anomer. The stereochemistry of the starting sugar derivative does not affect the formation of the β anomer (**Figure 23**).

1. Introduction
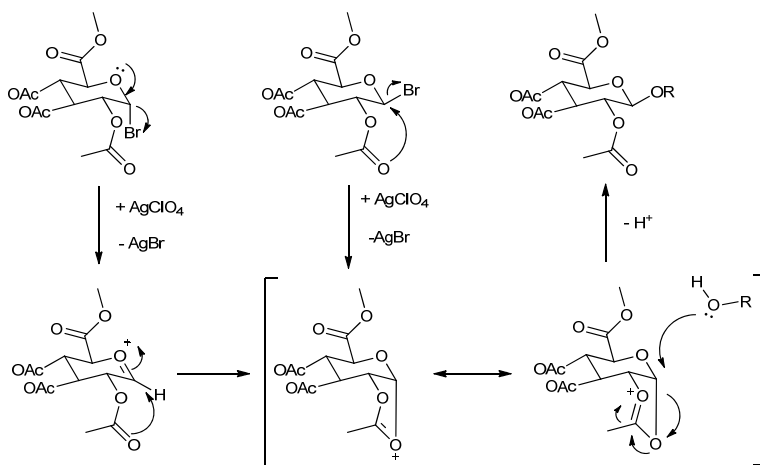
Figure 23. Glycosidation reaction mediated by a neighboring group.

The Koenigs-Knorr method, which utilizes halide glycosides as donors, remains the most popular for the synthesis of a wide range of (poly)phenol glucuronides.(*100*) This method produces stereochemically pure compounds (**Figure 23**). The most commonly used monosaccharide derivative in this reaction is the commercial methyl-2,3,4-tri-*O*-acetyl-1-*O*-bromo-α-D-glucuronate under various conditions. Alternatively, the use of glycosyl imidates as donors has recently increased but its use implies more complex synthetic and purification procedures (**Figure 24**).(*101*)

Methyl-2,3,4-tri-*O*-acetyl-1-*O*-bromo-α-D-glucuronate

R:

Methyl-2,3,4-tri-*O*-acetyl-1-*O*-(trichloroacetimidoyl)-D-glucuronate

Methyl-2,3,4-tri-*O*-acetyl-1-*O*-(trifluoroacetimidoyl)-D-glucuronate
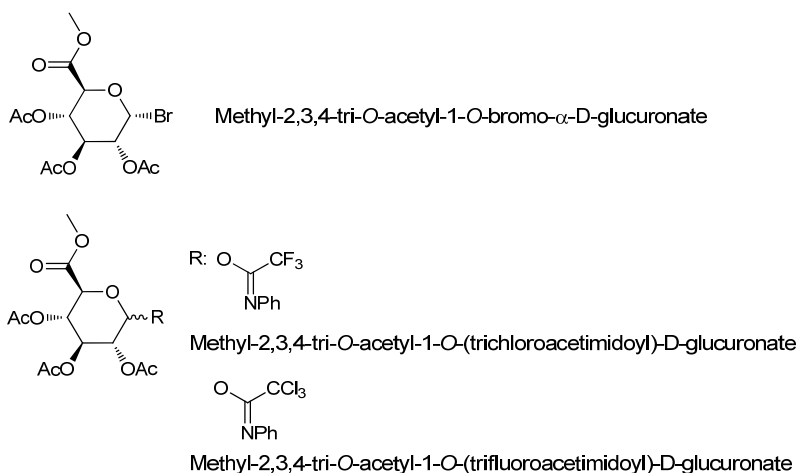
Figure 24. The most common monosaccharide derivatives used in glucuronide conjugate synthesis.

In the Koenigs-Knorr reaction, the electrophilic character of the anomeric carbon of the methyl-2,3,4-tri-*O*-acetyl-1-*O*-bromo-α-D-glucuronate, is enhanced by a promoter (e.g. silver carbonate, mercuric oxide, cadmium carbonate) that facilitates the nucleophilic attack of the (poly)phenolic anion (PhO⁻) leading to glucuronide conjugate (**Figure 25**).

methyl-2,3,4-tri-*O*-acetyl-1-*O*-bromo-α-D-glucuronate
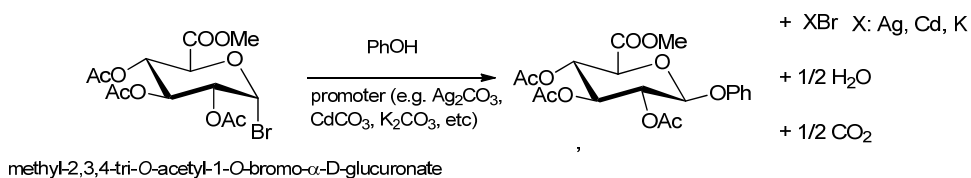
Figure 25. Koenigs-Knorr reaction between the methyl-2,3,4-tri-*O*-acetyl-1-*O*-bromo-α-D-glucuronate and a phenol (PhOH).

An interesting example of the Koenigs-Knorr reaction is the synthesis of the catechin acetylglucuronides by Gonzalez-Manzano *et al.* using K_2CO_3 as promoter and methyl-2,3,4-tri-*O*-acetyl-1-*O*-bromo-α-D-glucuronate as glycosyl halide. A mixture of catechin glucuronides was obtained according to the reactivity of each hydroxyl group of

catechin: catechin-4'-*O*-acetylglucuronide, catechin-3'-*O*-acetylglucuronide, catechin-5-*O*-acetylglucuronide, catechin-7-*O*-acetylglucuronide, and catechin-3-*O*-acetylglucuronide.(*102*)

1.4.4.3.2. Deacetylation reaction

1.4.4.3.2.1. Chemical deacetylation

The deacetylation process is the most sensitive step for obtaining the glucuronide conjugates due to the instability of (poly)phenols in the basic conditions typically used. The Zemplén reaction is the most common treatment for deacetylation of the *O*-acetylated substrates. Using this procedure, Gonzalez-Manzano *et al.* obtained catechin glucuronides using methanol and a catalytic amount of sodium methoxide (NaOMe).(*102*)

Milder base conditions may be preferable to avoid (poly)phenol damage by ring opening. For example, Needs *et al.* obtained quercetin-3-glucuronide by addition of sodium carbonate (Na_2CO_3) in aqueous methanol and Boumendjel *et al.* deacetylated the persicogenin-3'-*O*-β-D-acetylglucuronide with zinc acetate ($Zn(OAc)_2$) in dry methanol.(*103, 104*) However, (poly)phenols containing ester groups (e.g. EGCG) may suffer hydrolysis under most basic conditions, and alternative procedures are required.

1.4.4.3.2.2. Enzymatic deacetylation

Enzymatic techniques are very attractive for deacylation because they are mild and efficient, although little attention has been paid to hydrolase-catalysed deacetylation of glucuronide conjugates. Lipases (esterases) are enzymes which hydrolyze fat in the digestive tract and are extremely versatile for the regioselective acylation or deacylation (depending on the solvent system used) of a wide range of unnatural substances. Unlike most other enzymes, they can accommodate a wide range of substrates and are quite stable in aqueous and non-aqueous organic solvents (e.g. THF, toluene, DMSO). Since many substrates are only sparingly soluble in water, the addition of co-solvents (5-20 %), such as alcohols (methanol, ethanol, *tert*-butanol), water-soluble ethers (THF, dioxane), acetone, DMSO, and DMF, will be advantageous. An important consideration on acetyl hydrolysis in water is the concomitant formation of acetic acid, which requires the utilization of a buffer (e.g. phosphate, citrate buffers) to preserve the activity and stability of the enzyme and substrates.

Interestingly, some lipases have been used to selectively remove sugar acetyl groups without affecting 1-β-*O*-acyl functions. For example, Baba *et al.* chemoselectively removed protecting acetyl groups of 1-β-*O*-acylglucuronide methyl ester of three non-steroidal anti-inflammatory drugs, diclofenac (DF), mefenamic acid (MF) and (S)-naproxen (NP) using lipase AS Amano (LAS) (**Figure 26 a**).(*105*) Therefore, the hydrolysis catalyzed by lipases is a promising strategy for a selective deprotection of acetyl groups found in chemically sensitive glucuronide conjugates (e.g. (poly)phenolic conjugates containing ester groups) obtained with the Koenigs-Knorr reaction (**Figure 26 b**).
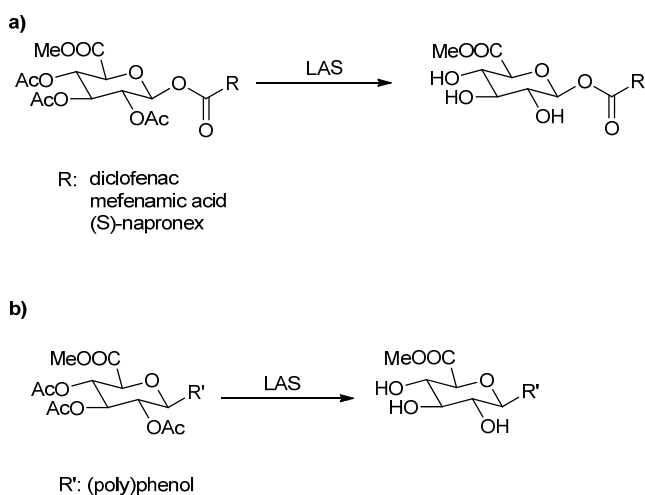
Figure 26. a) Lipase-catalyzed deprotection of acetyl groups in glucuronide conjugates.(*105*) **b)** Potential application of lipase deprotection towards the preparation of (poly)phenol-glucuronide conjugates.

1.4.4.3.3. Enzymatic hydrolysis of the methyl ester

1.4.4.3.3.1. Enzymatic hydrolysis of the methyl ester:

Porcine Liver Esterase (PLE) is an effective enzyme for the hydrolysis of the methyl moiety from the methyl ester of 1-β-O-acylglucuronides and 1-β-O-glucuronides. Baba *et al.* used PLE to obtain the corresponding free 1-β-O-acylglucuronides of diclofenac (DF), mefenamic acid (MF) and (S)-naproxen (NP) in high yields (90-94 %)

1. Introduction

(**Figure 27 a**).(*105*) PLE is a promising strategy to hydrolyze the methyl ester of the (poly)phenol-glcucuronide conjugates (**Figure 27**, **b**). Moreover, the lipase CAL-B from Candida Antarctica was used to remove the carboxylic methyl ester of diverse carboxylic acids.(*106, 107*)}

a)

MeOOC
HO
HO
OH
O
R
O
→ PLE →
HOOC
HO
HO
OH
O
R
O

R: diclofenac
   mefenamic acid
   (S)-napronex

b)

MeOOC
HO
HO
OH
O
R
→ PLE →
HOOC
HO
HO
OH
O
R
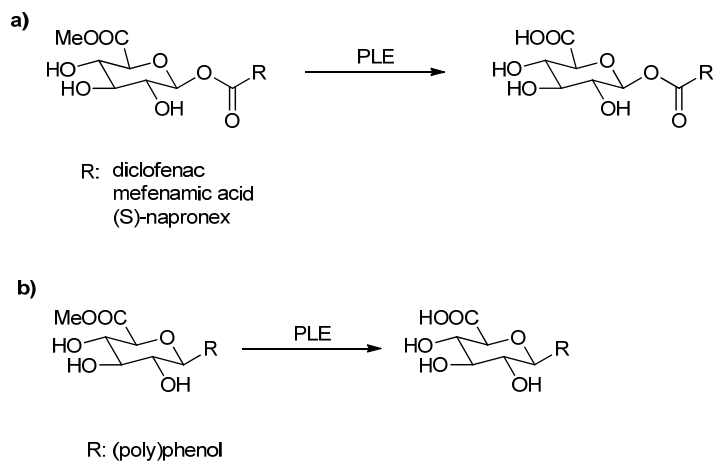
R: (poly)phenol

Figure 27. a) Esterase-catalyzed the hydrolysis of the methyl ester in glucuronide conjugates.(*105*) **b)** Potential application of esterase hydrolysis towards the preparation of (poly)phenol-glucuronide conjugates.

1.5. Methods for measuring the radical scavenging activity of (poly)phenols

1.5.1. Reaction mechanisms

There are two types of scavenge mechanisms involving (poly)phenols and free radicals:

A. Reaction in which a hydrogen atom is transferred in a single step, Hydrogen Atom Transfer (HAT). The bond dissociation enthalpy (BDE) of the phenolic O-H bond is an important parameter in evaluating the radical scavenging activity; the lower the BDE value, the easier the hydrogen abstraction and the reaction with free radicals.(*108*)

B. Reactions in which an electron and a proton are transferred in two steps, electron-transfer and a proton-transfer or viceversa. These include Sequential Proton Loss Electron Transfer (SPLET), Electron Transfer-Proton Transfer (ET-PT) and Proton Coupled Electron Transfer (PCET). The ionization potential (IP) of the (poly)phenol is the most significant parameter in this kind of mechanism; the lower the IP value, the easier the electron abstraction and the reaction with free radicals.(*108*)

Hydrogen Atom Transfer (HAT): the (poly)phenol (PhOH) reacts with the free radical (R$^{\bullet}$) by transfer of a hydrogen atom through homolytic rupture of the O-H bond (**Figure 28**). This mechanism is mainly found in non-ionizing solvents.(*109*)

$$PhOH + R^{\bullet} \xrightarrow{\text{HAT}} PhO^{\bullet} + HR$$

Figure 28. HAT mechanism.

Sequential Proton-Loss Electron Transfer (SPLET): initially, a proton of (poly)phenol is transferred to the solvent (X) in an acid-base reaction. This mechanism takes place by the fast electron-transfer from the corresponding phenolate formed (PhO$^-$) to the free radical, followed by a proton transfer from the solvent to the corresponding anion of the radical (R$^-$) (**Figure 29**).

1. Introduction
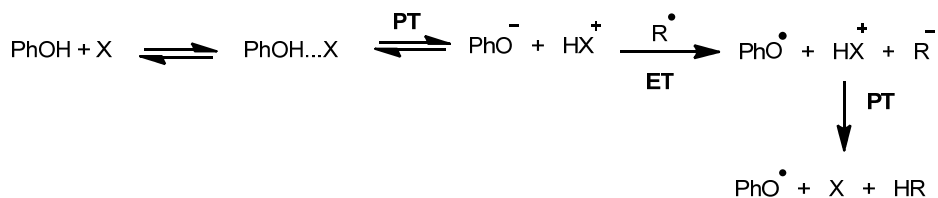
Figure 29. SPLET mechanism.

This reaction mechanism is enhanced in solvents that support PhOH ionization (notably methanol among organic solvents) and with PhOH having low pKa's. In many solvents, the addition of base (e.g. sodium methoxide) increases the degree of (poly)phenol ionization and consequently, increases the reaction rate of the process while the addition of acid (e.g. acetic acid) exerts the opposite effect.(*110, 111*)

Electron Transfer-Proton Transfer (ET-PT): the electron-transfer is the first and the determining reaction step of this mechanism followed by the deprotonation of the phenoxy cation radical formed (PhOH•+) (**Figure 30**).(*112*) This mechanism takes place in non-ionizable solvents and with strong oxidant radicals.
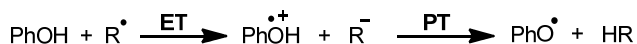
Figure 30. ET-PT mechanism.

Proton-Coupled Electron Transfer (PCET): the reaction involves an intermediate hydrogen-bonding complex between the (poly)phenol (PhOH) and the radical (R•).(*109*) Within the complex, the electron and the proton are transferred in a sequential way (**Figure 31**).
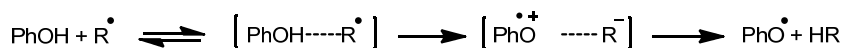
Figure 31. PCET mechanism.

46

In all these four mechanisms, the product obtained, PhO$^\bullet$, is a phenoxy radical in which the odd electron has the possibility to be spread over the entire molecule resulting into a more stable and less reactive radical than R$^\bullet$.

It is very important to notice that the relative contributions of HAT and SPLET are sensitive to both reactants and solvent. Interestingly, the Electron-Transfer (ET) more specifically the SPLET mechanism is the more biologically significant mode of (poly)phenols action. SPLET is a much more probable mechanism in biofluids such as blood plasma and cellular cytosol.(*113, 114*)

1.5.2. Evaluation of the radical scavenging activity of (poly)phenols against free radicals

The words ability, activity, or efficiency, when are referred to the free radical scavenging of a (poly)phenol, have the same meaning, and includes both the capacity (number of radicals scavenged) and velocity.

In general, the evaluation of the radical scavenging activity of a (poly)phenol is determined by the measure of its Radical Scavenging Capacity (RSC), and kinetic parameters are underestimated. Interestingly, Sánchez-Moreno and co-workers defined the Antiradical Efficiency of a (poly)phenol as the value which combines the capacity and the reaction rate of a (poly)phenol against a free radical.(*115*) The knowledge of the kinetics of HAT and ET is important because free radicals, in the organism, are short-lived species, what entails that the impact of an antioxidant depends on its fast reactivity towards them.

Several chemical assays allow us to determine the RSC of pure (poly)phenols and (poly)phenolic fractions. In these methods, the RSC of (poly)phenols is measured by indirect techniques, measuring the reduction of a stable free radical or a free radical generated in the medium by radiolysis, photolysis or Fenton reaction. Reactions can be monitored by Electron Paramagnetic Resonance (EPR), by the Ultraviolet-Visible (UV-Vis) (See section 1.7) and fluorescence spectroscopies, and/or by gas chromatography. These methods that measure the RSC of (poly)phenols can be classified according to different criteria. The following classification is done according to their reaction mechanism.

1. Introduction

1.5.2.1. Evaluation method by both Hydrogen Atom Transfer (HAT) and Electron-Transfer (ET)-based reactions. The activity of (poly)phenols tested with this method is presumed to be close to the scavenging of peroxyl radicals (ROO•).(*109*)

   2,2-Diphenyl-1-picrilhidrazyl radical (DPPH) assay: the method is fast (20-60 min), simple, inexpensive and widely used to measure the radical scavenging activity of pure (poly)phenols and (poly)phenolic fractions in MeOH. The kinetics and the RSC of (poly)phenols is measured easily by measuring the decay of the radical spectrum band by EPR or by the decay of the absorbance of the radical by UV-Vis. DPPH gives a characteristic five band spectrum by EPR and a strong absorption maximum by UV-Vis at 517 nm, conferring it a purple color. The color turns from purple to yellow when DPPH is reduced by (poly)phenols (**Figure 32**). A hydrogen atom or/and an electron is transferred from the (poly)phenol to DPPH to form the reduced *H*-DPPH yellow form. The resulting change in color and the decay of the spectrum band by EPR are related to the number of hydrogen atoms or electrons captured but it is not necessarily related to the number of hydroxyl groups contained in pure (poly)phenols. This can be explained by the hydroxyl regeneration.(*116, 117*)

Figure 32. Reaction and expected products formed in the reaction of DPPH with a (poly)phenol (PhOH).

   Litwinienko and co-workers demonstrated experimentally that in polar and ionizable solvents (e.g. MeOH, EtOH) and in polar and non-hydroxylic solvents (e.g. ACN, DMSO (solvents which can support the ionization) kinetic analysis of reactions of DPPH with different (poly)phenols indicates that the most probable mechanism is the SPLET. On the other hand, in apolar solvents, the mechanism is the HAT (See section 1.5.1). The contribution of one or the other pathway depends on the nature of the solvent, the redox potentials of the species involved and the bond dissociation energy (BDE) of the phenolic O-H bond.(*111, 118*)

1.5.2.2. Evaluation methods by Hydrogen Atom Transfer (HAT). These assays measure the activity of (poly)phenols to quench generally peroxyl radicals (ROO$^\bullet$) by hydrogen atom donation.

Oxygen Radical Absorbance Capacity (ORAC) assay: the ORAC assay is a method used primarily for water soluble (poly)phenols. It can also be used to measure the radical scavenging activity of biological samples such as human plasma, blood serum or organ tissue. This method is based on the HAT of (poly)phenols to peroxyl radicals generated in aqueous solution from a free radical generator such as the hydrochloride of 2,2'-azobis-2-methyl-propanimidamide (AAPH). The activity of peroxyl radicals to quench the fluorescence of fluorescein (λ (emission)= 521 nm in water) (or β-phycoerythrin) and the activity of (poly)phenols to protect the fluorescein from the radical damage is measured by fluorescence decay. ORAC measures are evaluated by the area under the curve (AUC) of the fluorescence decay versus time in the absence and in presence of (poly)phenols, and the difference between AUC of sample and blank is correlated to (poly)phenol concentration in the sample. Results are compared to those of Trolox (water soluble vitamin E analogue (**Figure 33**)) as standard scavenger.
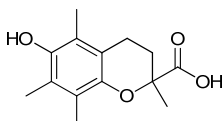
Figure 33. Trolox structure.

The ORAC method is standardized and integrates both degree and time of (poly)phenol reaction. In the ORAC assay, different free radical generators can be used (AAPH as a ROO$^\bullet$ generator, H_2O_2-Cu^{2+} as a $^\bullet OH$ generator). This is important because the measure of the RSC of a compound depends on the free radical used in the assay. A general drawback of this method is the sensitivity of fluorescein towards pH which has to be maintained above pH=7.

Total Oxidant Scavenging Capacity (TOSC) assay: this method measures the radical scavenging activity of biological tissues with lipid and water soluble (poly)phenols. Peroxyl radicals generated by the thermal homolysis of 2,2'-Azobis(2-methyl-propionamidine) dihydrochloride (ABAP) oxidize alpha-keto-gamma-methyolbutyric

acid (KMBA) to produce ethylene which is quantified by gas chromatography. Ethylene production is reduced in the presence of (poly)phenols owing to the scavenging of the peroxyl radicals. The decrease in ethylene production with the time, compared to a control reaction without (poly)phenol provides a relative measure of the radical scavenging activity. The advantage of the TOSC assay against ORAC assay is the capability of the former to discriminate between faster acting and slower acting (poly)phenols, as it is a kinetically based assay.

Stable potassium nitrosodisulphonate (Férmy's salt assay): a Férmy's salt (**Figure 34**) is a stable free radical which responds to highly reactive hydrogen donors. This method is similar to that of DPPH albeit with longer reactions times (2h). This is used as a model for peroxyl radicals, and it is measured by Electron Paramagnetic Resonance (EPR).
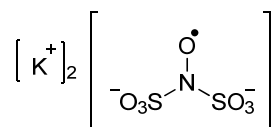
Figure 34. Férmy's salt.

2,6-Di-tert-butyl-α-(3,5-di-tert-butyl-4-oxo-2-,5-cyclohexadien-1-ylidene)-*p*-tolyloxy free radical (Galvinoxyl radical): similarly to the DPPH, the stable free radical galvinoxyl (**Figure 35**) is used to measure and compare the radical scavenging activity of (poly)phenols in a range time of 20-60 min. Galvinoxyl shows an spectrum band by EPR and a strong absorption band by UV-Vis at 428 nm of wavelength (in ethanol). The absorption vanishes by the radical scavenging activity of (poly)phenols, and the resulting decolorization from yellow is stoichiometric with respect to the amount of hydrogen transferred.
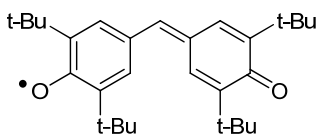
Figure 35. Galvinoxyl radical.

1.5.2.3. Evaluation methods by Electron-Transfer (ET)

Trolox Equivalent Antioxidant Capacity (TEAC) assay: this method is broadly applied in assaying food and biological samples. The method is very fast (6 min) and can be used over a wide range of pH values in both aqueous and organic solvent systems (it enables the simultaneous determination of hydrophilic and lipophilic antioxidants). The TEAC assay measures the relative activity of (poly)phenols to scavenge the ABTS$^{\bullet+}$ cation radical generated in aqueous phase *in situ* by persulfate oxidation of ABTS^{2-} (2,2'-azinobis(3-ethylbenzothiazoline-6-sulfonic acid). Results are compared with those from Trolox, as standard. The radical scavenging activity of (poly)phenols is measured easily by detection of the decay of the radical spectrum band by EPR or by the decay of the absorbance of the radical (λ= 734 nm) by UV-Vis (**Figure 36**). It is a simple method to perform and it is widely used.
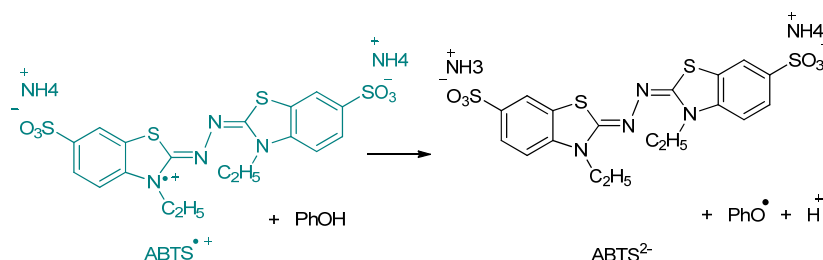
Figure 36. Reaction and products formed in the reaction of the ABTS cation with a (poly)phenol (PhOH).

The TEAC values for pure (poly)phenols do not show clear correlation with the number of electrons that a (poly)phenol can give away. The assay is not highly reproducible because it is too dependent on the chromogenic radical-generation method. Moreover, it may not be suitable for slow reacting (poly)phenols because an end-point is achieved within a protocol time of 6 min for ABTS$^{\bullet+}$. Finally, it has not been correlated with biological effects; hence, its actual relevance to *in vivo* antioxidant efficacy is unknown.(*119*)

1. Introduction

Free stable organic radicals of the TTM and PTM series. Tris(2,4,6-trichloro-3,5-dinitrophenyl)methyl radical (HNTTM) assay: Organic radicals are very little known species because of their instability. They are easily degraded in contact with oxygen, moisture, and light. During the last decades the design and synthesis of stable organic radicals have been developed owing to their application as constituents of stable molecular magnets. In 1964, Ballester and co-workers (*120*) discovered a new class of stable free radicals, the paradigm being the perchlorotriphenylmethyl radical (PTM), and later on Veciana *et al.*(*121*) synthesized the 1,3,5-trichlorophenylmethyl radical (TTM) (**Figure 37**).
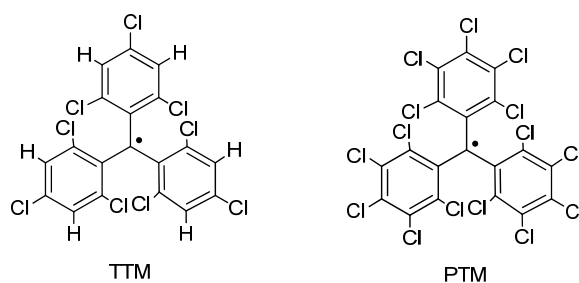
Figure 37. Structures of TTM and PTM.

Free radicals of the TTM and PTM series have a high stability both in solid state and in solution in the dark due to the steric hindrance of the six *ortho*-chlorine atoms to the trivalent carbon atom which greatly impedes the direct interaction with any external molecule.

As these radical species can be reduced to charged molecules by oxidation-reduction processes, we are interested in exploring the potential of these radicals as chemosensors of the radical scavenging activity of natural and synthetic (poly)phenols. The introduction of functional groups in the molecular structure of these radicals modulates their redox properties. Thus, each radical species can have a different standard redox potential, as determined by cyclic voltammetry (CV). A number of stable free radicals of the TTM and PTM series can be synthesized and tested as chemosensors to evaluate the electron donating properties of (poly)phenols.

In 2003, a stable free radical of the TTM series with nitro groups ($-NO_2$) on the *meta-aromatic* positions, the tris(2,4,6-trichloro-3,5-dinitrophenyl)methyl radical (HNTTM) was synthesized in the laboratory of halogenated organic materials of the *Institut d'Investigacions Quimiques i Ambiental de Barcelona del Centro Superior de Investigaciones Científicas* (IIQAB-CSIC) (**Figure 38**).

HNTTM

E^o (CH_2Cl_2)= 0.58 V
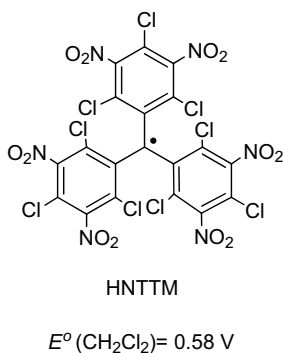
Figure 38. Structure of HNTTM.

HNTTM is stable in solid form and in solution (stability > 99% after two days) in organic solvents such as $CHCl_3$, $CHCl_3$/MeOH mixtures, CH_2Cl_2, benzene, toluene and CH_3CN in the dark. HNTTM reacts exclusively by Electron-Transfer (ET) reactions (*122*) in different organic solvents, having an adequate reduction potential value (E^o_{HNTTM}=0.58 V in CH_2Cl_2) to react with the catechol, pyrogallol and gallate esters.(*123*) HNTTM has been used as a chemosensor to measure the radical scavenging activity of natural and synthetic (poly)phenols and (poly)phenolic extracts.(*122-126*)

HNTTM (**Figure 38**) is soluble in organic solvents with different polarity. The standard assay with (poly)phenols is performed in $CHCl_3$/MeOH (2:1), and followed by UV-Vis or EPR. The UV-Vis spectrum of HNTTM (orange in color) is characterized by three radical bands (**Figure 40**) at $\lambda(\varepsilon)$ ($CHCl_3$) 385(21170), 513(740) and 560(800) nm(dm^3 mol^{-1} cm^{-1}). The EPR spectrum of HNTTM gives a characteristic single band. The color turns to an intense red when HNTTM is reduced by (poly)phenols to its stable anion HNTTM$^-$. This process is monitored and observed by UV-Vis with a characteristic band at λ (ε) ($CHCl_3$)= 497 nm (26700) nm (dm^3 mol^{-1} cm^{-1}) (**Figure 39**), and the decay of the single band of HNTTM is observed by EPR. Slowly, the colored solution turns into a non-

colored solution by the formation of the protonated form α*H*-HNTTM (**Figure 39**). The standard reaction time is 7h, which allows to study the Radical Scavenging Capacity (RSC) and kinetics of both fast and slowly reacting (poly)phenols.
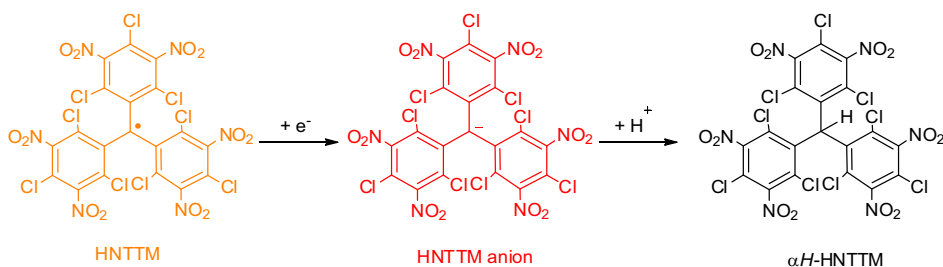
Figure 39. Structures of HNTTM, its stable anion and its protonated form α*H*-HNTTM.
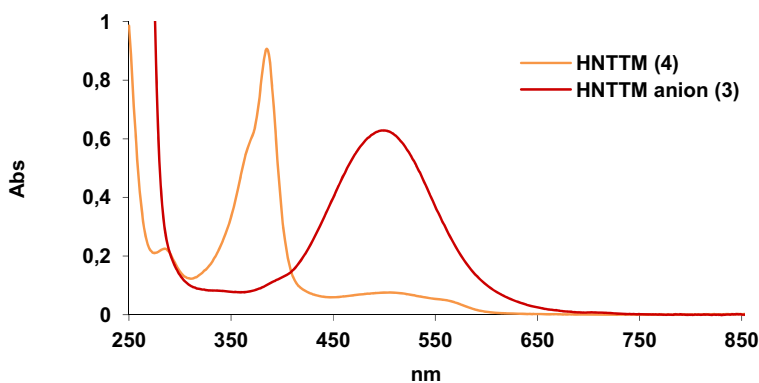
Figure 40. UV-Visible spectrum of HNTTM and its anion HNTTM¯ in CHCl₃/MeOH (2:1). The HNTTM anion (HNTTM⁻) spectrum was obtained from a solution of the Bu₄N⁺ ⁻ HNTTM salt in CHCl₃/MeOH (2:1).

The resulting change in color detected by UV-Vis and the decay of the main spectrum band by EPR of HNTTM is roughly stoichiometric with respect to the number of electrons transferred and with the number of reactive hydroxyl groups contained in catechol, pyrogallol and gallates.

1.6. Evaluation of the metal-reducing activity of (poly)phenols

Several methods evaluate the reducing activity of (poly)phenols towards certain metallic cations.

Ferric Reducing Antioxidant Power (FRAP) assay: this method is based on the reduction of Fe^{3+} to Fe^{2+} at low pH (pH= 3.6) by the action of (poly)phenols. Subsequently, the interaction of Fe^{2+} with 2,4,6-tris(2pyridyl)-s-triazine (TPTZ) provides a strong absorbance at λ= 593 nm (**Figure 41**). The method has its limitations, especially because of its measurements under non-physiological conditions (pH= 3.6) values, and is not useful for the determination of lipophylic antioxidants, especially in human plasma, because the Fe(III)-TPTZ complex has more affinity toward the aqueous phase. In addition, this method is not able to detect slowly reactive (poly)phenolic compounds and thiols (e.g., GSH).(*127*)
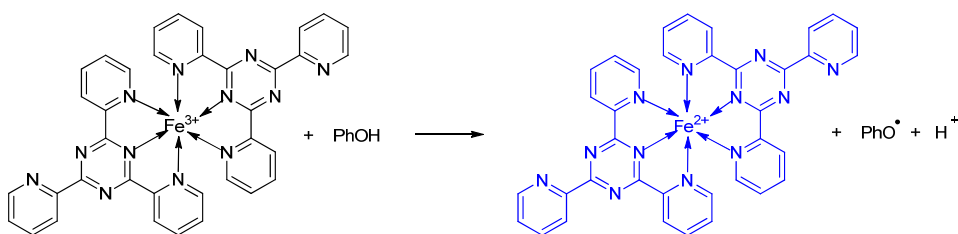
Figure 41. Reaction and products formed in the reaction of the TPTZ complex with a (poly)phenol (PhOH).

There are different ferric ion-based reducing activity assays: 1,10-phenanthroline method, batho-phenanthroline method, modified FRAP method, original ferricyanide method, and modified ferricyanide method. The main difference between them is the different redox potential of the Fe^{2+} chromogenic complexes formed in each method. A suitable selection of the Fe(II)-stabilizing chromogenic ligands may provide a selective reactivity towards a range of physiologically important (poly)phenols. In all methods, each mole of *n* electron-reductants would produce *n* moles of Fe(II)–ligand complex.

1. Introduction

The disadvantage of these methods is the activity of some (poly)phenols to act as ligands of Fe^{2+}, avoiding the formation of the $Fe(TPTZ)_2^{2+}$ complex, and giving a wrong measure of absorbance. The production of $^{\bullet}OH$ in biological samples by the reaction of Fe^{2+} with H_2O_2 produces erroneous results by the redox cycling of this unbound iron (Fenton's reaction. **Figure 42**).(*128*)

$$Fe^{2+} \ + \ H_2O_2 \longrightarrow Fe^{3+} \ + \ ^{\bullet}OH \ + \ ^{-}OH$$

Figure 42. Oxidation of Fe^{2+} by Fenton's reaction.

Cupric Ion Reducing Antioxidant Capacity (CUPRAC) assay: The chromogenic redox reagent used for the CUPRAC assay is bis(neocuproine) copper(II) chelate $(Cu(Nc)_2^{2+}$ (light blue). This reagent is useful at pH=7, and the absorbance of the Cu(I)-chelate $(Cu(Nc)_2^{+}$ (yellow orange) formed as a result of the redox reaction with reducing (poly)phenols is measured at $\lambda= 450$ nm. The CUPRAC capacity is in accordance with the number and position of the hydroxyl groups of the (poly)phenol as well as the conjugation level of the molecule. Results are compared with Trolox values. Compared to the FRAP assay, CUPRAC is superior because the pH is close to the physiological pH, the redox potential ($E^{\circ}= 0.6$ V) is more favorable, and applicability to lipophilic (poly)phenols as well as hydrophilic ones. CUPRAC assay is complete in minutes for ascorbic acid, uric acid, gallic acid, and quercetin but requires 30–60 min for more complex molecules. Flavonoid glycosides need to be hydrolyzed to their corresponding non-conjugated flavonoids to fully exhibit their reducing activity, and slow-reacting (poly)phenols require higher incubation temperature to complete their oxidation with the CUPRAC reagent.(*129*)
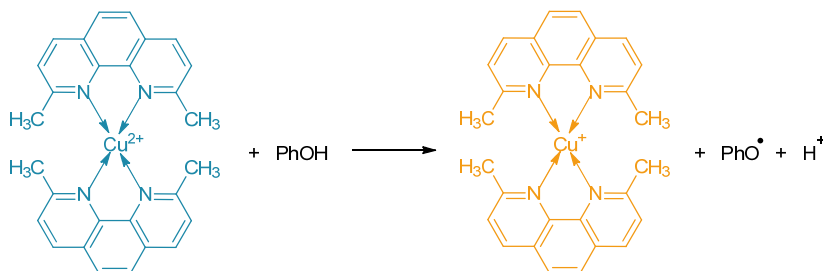
Figure 43. Reaction and products formed in the reaction of the Cu(II)-Nc with a (poly)phenol (PhOH).

1.7. Analytical methods for the study of the radical scavenging and reducing activity of (poly)phenols

1.7.1. Electronic Paramagnetic Resonance (EPR) technique

The EPR is essential for the study of free radicals and their reactions with different molecules. Its basis lays on the existence of two magnetic Zeeman states that, under the influence of an external magnetic field, have different energy, producing absorption of electromagnetic radiation. Each electron possesses an intrinsic magnetic dipolar moment (μ) given by its spin. For this reason, compounds with odd electrons, such as free radicals, have the total spin number (S) different from zero and they interact with the electromagnetic radiation giving a signal on the EPR. That is, when an electron is under the influence of an external and uniform magnetic (H) field, the magnetic dipole of the electron (S= 1/2) turns around of the externally magnetic applied field. The projection of the spin angular momentum vector on the axis of the extern applied field H gives two values $M_s = \pm 1/2$. In the absence of an external magnetic field, both levels ($\pm 1/2$) are degenerated (they have the same energy), but when a magnetic field is applied, each level has different energy. This is called Zeeman effect (**Figure 44**). Between these two levels, there will be transition if:

1. the selection rule is fulfilled $\Delta M_s = 1$

2. exists condition of resonance:

$$h\upsilon = \Delta U = g_e \beta_e H$$

$h\upsilon$ (radiation energy), ΔU (Zeeman levels separation), g_e (Lande's factor), β_e (Bohr magneton).

1. Introduction
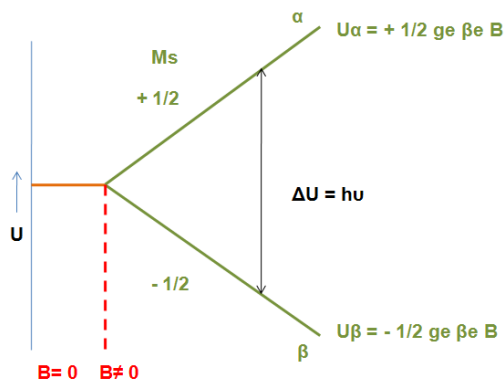
Figure 44. Zeeman effect. Energy levels (α, β) of a free electron are produced when a magnetic field is applied (B) and the corresponding absorption of the EPR transition is obtained. U_α and U_β represent energies of the states M_s=+ 1/2 and M_s=- 1/2, respectively.

To obtain resonance conditions on the EPR, a variable magnetic field is applied and a radio frequency is fixed (approximately 9.5 GHz). The sample absorbs this energy and the electron is promoted to an excited level. Subsequently, the absorbed energy is emitted, but results are given by a net absorption. This absorption is shown in the spectrum in the form of its derivative. So, the spectrum records the derivative of the absorption band versus the magnetic field in Gauss.

Given an EPR spectrum, a free radical can be characterized with different parameters:

1. Lande's Factor (g): It is a measure of the spin-orbital interaction of the electron. The g value for a free electron is 2.0023 and for free organic radicals, only the last two digits of g can vary.

2. Hyperfine coupling (a): The odd electron can interact with the atoms of the molecule with a nuclear spin I≠0 (e.g. ^{1}H, ^{14}N, ^{13}C). Each nuclear moment divides a line of the spectra in 2·M·I + 1 line (M, equivalent nuclei, I, nuclear spin) and the intensity of lines is defined by the Pascal's triangle (**Figure 45**).
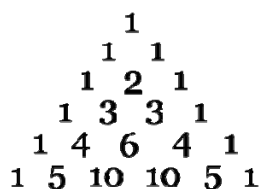
Figure 45. Pascal's triangle.

When the coupling is only with a number of magnetically equivalent nuclei, the distance between two consecutive lines measures the hyperfine coupling, and its magnitude depends on the electron spin density on each nucleus and on its magnetic moment. These couplings give very important structural information i.e. the location of the odd electron.

Example: **HNTTM**
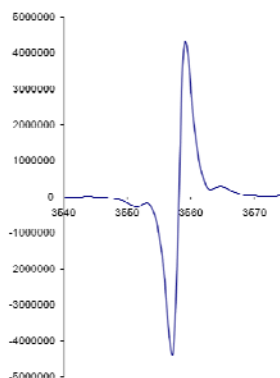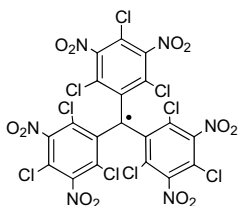
1.7.2. Ultraviolet-Visible (UV-Vis) spectroscopy

The UV-Vis spectrum is comprised between wavelength values from 200 to 800 nm. The only molecular moieties likely to absorb light in the 200 to 800 nm region are π-electron functions and heteroatoms having non-bonding electrons. Such light absorbing groups are referred to as chromophores. When sample molecules are exposed to light having an energy that matches a possible electronic transition, some of the light energy will be absorbed and an electron will be promoted to a higher energy orbital. An optical spectrophotometer records the wavelengths at which the absorption occurs. The resulting spectrum is presented as a graph of absorbance (A) versus wavelength (λ).

1. Introduction

The absorbance of a sample is proportional to the number of absorbing molecules in the spectrometer light beam, so it is necessary to correct the absorbance value for this and other operational factors if the spectra of different compounds are to be compared in a meaningful way. The corrected absorption value is called "molar absorptivity (ε)", and is particularly useful when comparing the spectra of different compounds and determining the relative strength of light absorbing functions (chromophore):

$$\varepsilon = \frac{A}{c.l}$$

Where A = absorbance, c = sample concentration in mol/L, and l = length of light path through the sample in cm (normally 1 cm).

UV-Vis and EPR are two complementary techniques for the study of the behavior of (poly)phenols against different free radicals. The advantage of EPR is that it exclusively detects species with odd electrons, avoiding interferences with other molecules. On the other hand, this technique cannot detect the corresponding anions of the reduced radical species (e.g. the HNTTM anion), which are relevant to elucidate the reaction mechanism. UV-Vis technique shows the spectrum of the molecules with chromophore groups, producing in some cases interferences (substrates or/products absorb at the same wavelength) and incorrect results. On the other hand, this technique can give the opportunity to study and understand in a more extensive way the mechanism of reaction of (poly)phenols with different free radicals. Overall, the combination of both techniques is a good way for the characterization of stable free radicals, for the study of their reactivity and their reaction mechanisms in front of (poly)phenols.

1.8. Cell models to measure the cancer preventive activity of (poly)phenols

Because the study of the biological activity of (poly)phenols in human and animal models is costly, cellular models are used to study *in vitro,* the biological effect of (poly)phenols.

Catechins from green tea, hydrolyzable tannins and anthocyaninds from berries have been assayed in different normal and cancer cell lines producing a preventive effect against different types of cancer.(*58, 59, 62, 63, 130*)

(Poly)phenols act on cancer cells by producing necrosis, inducing apoptosis (cancer cells lack this mechanism), and/or arresting the cell cycle avoiding cell proliferation. They also inhibit angiogenesis.(*131*) The mechanisms of action of (poly)phenols are not well known. Thus, some of these mechanisms can be related with the scavenging and metal chelating activities of (poly)phenols as antioxidants, and their pro-oxidant and metal reducing activity as damaging ones. Interestingly, Nakagaua and co-workers demonstrated that the mechanism that make catechins cytotoxic in certain tumor cells is their ability to produce H_2O_2 and the resulting increase in H_2O_2 levels triggering the Fe(II)-dependent formation of highly toxic hydroxyl radical (Fenton's reaction (See section 1.4.2.2)), which in turn induces apoptotic cell death.(*132*) This is the case of EGCG which causes apoptotic cell death in osteoclastic cells (a type of bone cell that destroys bone tissue by removing its mineralized matrix and breaking up the organic bone)(*133*), and EGCG and EGC which decrease the viability of Jurkat cells (cells from an immortalized line of T lymphocytes) causing concomitant increase in cellular caspase-3 activity (protein that plays a central role in the execution-phase of cell apoptosis) by the formation of the hydroxyl radical ($^{\bullet}$OH).(*132*)

1.8.1. Assays to study the antiproliferative effect of (poly)phenols in cell cultures

The inhibition of cell proliferation by (poly)phenols will be produced by cytotoxicity, induction of apoptosis, and/or arrest of the cell cycle.

Cell proliferation is the increase in cell number as a result of cell growth and division. It is a controlled process in healthy organisms but, in certain conditions, this can be out of control with an excess of proliferation (cancer). (Poly)phenols can exert effects on the cellular proliferation machinery producing antiproliferative activity trough toxicity, induction of apoptosis and inhibition of some stage of the cell cycle. The

1. Introduction

antiproliferative activity exerted by some (poly)phenols in cancer cells and the absence of effect on normal cells is a good way to prevent and/or treat cancer.(*134, 135*) The most commonly used method to quantify the antiproliferative effect exerted by (poly)phenols of (poly)phenolic extracts is the MTT assay. The MTT assay consists on the reduction of the yellow MTT (3-(4,5-Dimethylthiazol-2-yl)-2,5-diphenyltetrazolium bromide) to purple formazan by mitochondrial reductase enzymes (living cells). The absorbance of this purple solution is quantified by spectrophotometry at 570 nm of wavelength. The amount of formazan produced by cells treated with a (poly)phenol or a (poly)phenolic extract is compared with the amount of formazan produced by untreated control cells, and the effectiveness of the (poly)phenol or (poly)phenolic extract in causing cell death is deduced through a dose-response curve. In this thesis the inhibition of the cell proliferation has been quantified using this method.

Cell toxicity can be produced by extreme variations of the physiological cell conditions such as hypoxia, hypothermia, or by agents that can damage the plasmatic membrane (e.g. virus). This effect produces swell and lyses or rupture by the loose of the cell (necrosis). Necrosis can also be detected by the MTT method.

Necrosis and apoptosis are distinct mechanisms of cell death with very different characteristics. Apoptosis is the capacity of a cell to undergo programmed cell death in response to a stimulus. The pathway triggered leads to the destruction of the cell by a characteristic set of reactions that require energy. The cascade of events that causes apoptosis is controlled genetically by the cell, does not cause swelling, and completely removes the cell from the tissue or the body. On the other hand, necrosis is caused by catastrophic toxic or traumatic events with cell swelling, injury to cytoplasmic organelles including mitochondria, and rapid collapse of internal homeostasis. Necrosis leads to membrane lysis, release of cellular contents, and resulting inflammation.

During apoptosis the loss of phospholipid asymmetry of the cell membrane is produced and phosphatidylserine (PS) residues found in the inner membrane are externalized and recognized by macrophages.

Flow cytometry is one of the most used methods to detect and quantify the induction of apoptosis. FACS (Fluorescence-Activated Cell Sorting), is a technique based on the high affinity of the protein Annexin by PS. Annexin detects the early apoptosis

and can interact with PS of necrotic cells. To differentiate apoptotic and necrotic cells, the Propidium Iodide (PI) is used to stain the DNA of leaky necrotic cells.
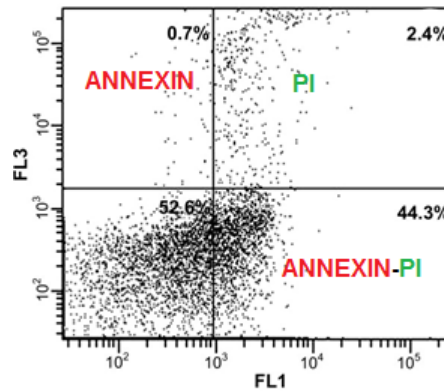
Figure 46. Diagram adapted from Tognon *et al.*(*136*) Dot-plot diagram of FITC/annexin-V/PI flow cytometry of control mononuclear cells treated with 25 μM. Quadrant 1 represents the apoptotic cells, FITC-Annexin V positive and PI negative, demonstrating cytoplasmic membrane integrity. Quadrant 2 contains the non-viable, necrotic cells, IP positive, and negative for FITC-Annexin V binding. Quadrant 3 shows the viable cell, which exclude PI and are negative for FITC-Annexin V binding. Quadrant 4 contains the non-viable, necrotic cells, positive for FITC-Annexin V binding and for PI uptake.

2. Objectives

This thesis focuses on the radical scavenging activity of selected (poly)phenols measured by their ability to donate electrons to stable free radicals of the series of PTM and TTM as electron-acceptor chemosensors, and the possible relationship with their activity on cancer cell cultures, assessed by *in vitro* assays with the human colorectal adenocarcinoma cell line HT-29. This cancer type was chosen because of its high incidence and because dietary phenolic compounds may be largely accessible to such cells in the digestive tract.

A stable free radical exclusively sensitive to the electron-transfer was available in our research group, the tris(2,4,6-trichloro-3,5-dinitrophenil)methyl radical (HNTTM). The chemistry of the stable free radicals of the PTM and TTM series opened up the possibility to devise assays to evaluate the activity of (poly)phenols and (poly)phenolic metabolites to transfer electrons, using selective chemosensors with different oxidation power.

To define the electron-transfer activity of different naturally occurring (poly)phenols and metabolites and to contribute to the understanding of its relation to their biological activity, the following objectives were pursued:

1. The study of the kinetics, the Radical Scavenging Capacity (RSC), and the reaction mechanisms of natural and synthetic (poly)phenols with HNTTM (**4**) as electron-acceptor chemosensor.

2. The synthesis of another stable free radical with a lower redox potential (less oxidant) than that of HNTTM, the tris(2,3,5,6-tetrachloro-4-nitrophenyl)methyl radical (TNPTM) sensitive only to the most reactive phenolic positions.

3. The evaluation of TNPTM as electron-acceptor chemosensor of natural and synthetic (poly)phenols (kinetics, RSC, and mechanism).

4. The evaluation of the antiproliferative activity of (poly)phenols in HT-29 cells to suggest relationships between electron-transfer and biological activities of (poly)phenols.

5. The synthesis of the main metabolites (glucuronides) of the biologically active (−)-epigallocatechin-3-*O*-gallate (EGCG) to be used in future structure/relationship studies.

2. Objectives

This thesis is part of a larger project aimed at obtaining a collection of stable radicals selectively sensitive to different phenolic hydroxyls within complex (poly)phenolic structures with the final goal of conveniently assessing the possible biological activity of complex natural mixtures or new synthetic compounds.

3. Materials and Methods

3.1. Materials

3.1.1. Reagents

3.1.1.1. Chemistry

Substrates

1,3,5-trichlorobenzene, 1,2,4,5-tetrachlorobenzene, (–)-catechol (**10**) (≥ 99%), pyrogallol (**11**) (≥99 %), methylgallate (**12**) (≥98 %), (–)-epicatechin (EC, **13**) (≥98 % (HPLC) from green tea), (–)-epigallocatechin (EGC, **14**) (≥95 % (HPLC), from green tea), (–)-epicatechin-3-*O*-gallate (ECG, **15**) (≥98 % (HPLC) from green tea), (–)-epigallocatechin-3-*O*-gallate (EGCG, **16**) (≥95 % from green tea), hamamelitannin (HT, **17**) (≥98.0 % (HPLC)), ellagic acid (**21**) (≥95 % (HPLC)), and acetobrom-α-D-glucuronic acid methyl ester (**22**) were from Sigma-Aldrich, Cysteine (–)-epigallocatechin (**14A**), Cysteine (–)-epigallocatechin-3-*O*-gallate (**16A**), Cysteamine (–)-epigallocatechin (**14B**), Cysteamine (–)-epigallocatechin-3-*O*-gallate (**16B**) and Cysteamine (–)-epicatechingallate (**15B**) were obtained from the thiolisis of proanthocyanidies from *Hamamelis Virginiana*, pentagalloylglucose (PGG, **18**) (≥ 90 % (HPLC)) was extracted and purified in our laboratory from *Hamamelis Virginiana*, and punicalagin (**19**) (≤ 95 % HPLC) was from Chengdu Biopurify Phytochemicals (Sichuan, China).

Enzymes

Lipase Novozyme-345 (N-345), Pancreatic Porcine Lipase (PPL), Lypozyme (LIM), Lipase A (LA) and Lipase AS (LAS) were from Amano, and Porcine Liver Esterase (PLE) was from Sigma-Aldrich.

Solvents

Chloroform (CHCl₃, spectrophotometric grade), dichloromethane (CH₂Cl₂, analytical standard), distilled benzene, toluene, acetone, dimethylformamide (DMF), anhydrous methanol (MeOH), dimethylsulfoxide (DMSO) (analytical grade), tetrahydrofurane (THF), acetonitrile (CH₃CN) (HPLC grade), diisopropyl eter and hexane.

Other reagents

Anhydride aluminium chloride (AlCl₃), chlorhidric acid (HCl), sodium hydrogen carbonate (NaHCO₃), anhydride magnesium sulphate (MgSO₄), fuming nitric acid (HNO₃ x NO₂), fuming sulfuric acid (H₂SO₄ x SO₃), chromium (VI) oxide, sodium sulfate

3. Materials and Methods

(Na$_2$SO$_4$), tetrabutylammonium hydroxide (TBAH), tetrachloro-p-quinone, potassium carbonate (K$_2$CO$_3$), potassium hydroxide (KOH), cesium carbonate (Cs$_2$CO$_3$), formic acid, sodium methoxide (NaMeO), zinc acetate (Zn(Ac)$_2$), o-phenanthroline and iron (III) chloride (FeCl$_3$) were from Sigma-Aldrich.

3.1.1.2. Biochemistry

Dulbecco's Modified Eagle's Medium (DMEM), Tripan Blue solution (0,2 %), MTT (3-(4,5-dimethylthiazol-2yl)-2,5 diphenyltetrazolium bromide), Binding Buffer 4x, Propidium Iodide (PI) and hydrogen peroxide (H$_2$O$_2$) 30 % were from Sigma Chemical Co. Fetal Bovine Serum (FBS) and Streptomycin/Penicilin (S/P) were both from Invitrogen. Dulbecco's Phosphate Buffer Saline (PBS) was from Gibco-BRL, and tripsine EDTA (0,05 % trypsin-0,02 % EDTA) was from Biological Industries (Kibbutz Beit Haemet, Israel). The Anexin V/FITC (Bender System Kit) and the PeroXOquant Quantitative Peroxide Assay Kit (lipid-compatible formulation) were from Pierce, Rockford, Illinois.

3.1.2. Instruments

3.1.2.1. Chemistry (characterization, detection and measuring)

Ultraviolet-Visible (UV-Vis) spectrometer
The UV-Vis spectra of stable radicals and of (poly)phenols, the kinetics, the Radical Scavenging Capacity (RSC), the Reducing Rates (RR) and the Reducing Capacity (RC) of (poly)phenols were recorded with a Varian Cary 300 Bio and with a Varian Cary 50 Bio models. For monitoring the absorbance of reactions, cuvettes of quartz suprasil of 3.5 mL of capacity and 1 cm of optic way from Hellma, and cuvettes of poliestirene of 1 mL of capacity and 1 cm of optic way from Ficher Scientific, were used.

Electron Paramagnetic Resonance (EPR) spectrometer
EPR spectra of radicals, the kinetics and the RSC of (poly)phenols were recorded with an EPR Varian spectrometer E-109E (E-Line Century Series) and with an EPR Bruker BioSpin spectrometer EMX-Plus 10/12. A tube of quartz was used for all experiments and the spectra simulations were performed with the Winsim program.

Infrared (IR) spectrometer
IR spectra of compounds were recorded in potassium bromide (KBr) tablets with a Nicolette AVATAR 360 FT-IR.

Nuclear Magnetic Resonance (NMR) spectrometer

^{1}H-NMR spectra of compounds were recorded with a Varian Mercury-500, with a Varian Mercury-400 and with a Varian Gemini 300. ^{13}C-NMR, HMBC and HSQC were recorded with a Varian Mercury-400.

Voltamperometer

Cyclic voltamperometries were carried out in a standard thermostated three-electrode cell. A platinum (Pt) disk of 0.093 cm[2] of area was used as the working electrode and a Pt wire as the counter electrode. The reference electrode was a Saturated Calomel Electrode (SCE), submerged in a salt bridge of the same electrolyte, which was separated from the test solution by a Vycor membrane. Electrochemical measurements were performed under argon atmosphere (25 °C) using an Eco Chemie Autolab PGSTAT100 potentiostat-galvanostat controlled by a computer with Nova 1.5 software. Measures were obtained at the *Departament de Química Física* from the *Universitat de Barcelona*.

Analytic HPLC-DAD

An HPLC with Diode Array Detector (DAD) Elite LaChrome from VWR was used to follow synthesis of EGCG glucuronides and the stability of (poly)phenols.

Semipreparative HPLC

A Waters Prep LC 4000 system with a UV-detector Hitachi L-4000 from Merck was used to purify products.

HPLC-HR-DAD-ESI-TOF-MS

High-resolution electrospray mass spectrometry (HR-ESI-MS) analyses were performed on a LC/MSD-TOF from Agilent Technologies to characterize oxidation products of DHHDP (**20**) by HNTTM (**4**) and TNPTM (**8**), and to follow the synthesis of EGCG glucuronides at the *Unitat d'Espectrometria de Masses, Centres Científics i Tecnològics de la Universitat de Barcelona, Facultat de Química*.

Elemental analyzer

Elemental analyses were performed with an EA1108-Elemental analyzer by the *Servei de Microanàlisi Elemental de l'Institut de Química Avançada de Catalunya (IQAC-CSIC).*

3. Materials and Methods

X-ray diffraction

The diffraction pattern was measured on a SIEMENS D5000 powder diffractometer (Bragg-Brentano geometry) equipped with a secondary graphite-monochromator (CuKa1,2 radiation, 45 kV; 35 mA; 2_ range measured 2-100°; step scan 0.02°; 2_ range used 2-65°, counting time, 5 s; FWHM(full width at half-maximum), 0.135 of 2_ at 20°). Programs used to resolution and refinement were: for the cell refinement and data collection, the CAD4 Express Software, for the data reduction, the WINGX32; for the resolution, the XLENS94; for the refinement, the SHELXL93; and for the plots, the PLUTON and the ORTEP32. X-ray diffraction was carried out by the *Institut de Ciència de Materials (CSIC) de la Universitat Autònoma de Barcelona.*

Thermogravimetric analyzer (TG)

Thermogravimetry was performed with a thermogravimetric analyzer Mettler, model TG50 by the *Servei d'Anàlisi Tèrmica i Calorimetria de l'Institut de Química Avançada de Catalunya (IQAC-CSIC).*

Differential scanning calorimeter (DSC)

Thermal stability was measured with a DSC 821E Mettler Toledo calorimeter by the *Servei d'Anàlisi Tèrmica i Calorimetria de l'Institut de Química Avançada de Catalunya (IQAC-CSIC).* Measures were processed with a Mettler Toledo software Star 6.1 version.

3.1.2.2. Biochemistry

ELISA

A UV-Vis ELISA System MIOS (3.2 version) from Merck was used to measure the results of the antiproliferative activity of (poly)phenols on HT-29 cells.

Flux cytometer

A flow cytometer Epics XL (Coulter Corporation, Hialeah, FL,USA) was used for fluorescence-activated cell sorting (FACS) analysis. Results were obtained with the Epics ELITE program.

3.2. Methods

3.2.1. Chemical probes to study the Electron-Transfer (ET) activity of (poly)phenols

3.2.1.1. Synthesis of organic stable free radicals

<u>3.2.1.1.1. Synthesis of the tris(2,4,6-trichloro-3,5-dinitropehnyl)methyl radical (HNTTM)</u>

*Synthesis of tris(2,3,5,6-tetrachlorophenyl)methane (**1**)*

1,3,5-Trichlorobenzene (50.8 g; 279.7 mmol), chloroform (2.6 mL; 32.4 mmol), and anhydride aluminium chloride (13.0 g; 97.3 mmol) were poured into a hermetic and dry reactor of glass. The reactor was heated at 110 °C into a silicon bath (5.5 h). The reaction mixture was extracted with a diluted solution of aqueous HCl in ice-water and CHCl$_3$. The organic phase was washed with an aqueous solution of sodium hydrogen carbonate (NaHCO$_3$) (2 %, 200 mL) and water (3 x 100 mL). The organic phase was dried with anhydride magnesium sulfate (MgSO$_4$) and the solvent was removed under reduced pressure obtaining a brown precipitate, which was digested in hexane (100 mL) at reflux during 1 h. The insoluble fraction, separated by filtration and dried, was identified as tris(2,3,5,6-tetrachlorophenyl)methane (**1**) (29.5 g; 57 %). ^{1}H-NMR (CDCl$_3$) δ, 7.29 (d, 3Harom), 7.17 (d, 3Harom), 7.19 (s, 1H) ppm.

*Synthesis of tris(2,4,6-trichloro-3,5-dinitrophenyl)methane (**2**)*

Fuming sulfuric acid (30 % SO$_3$) (25 mL) was added slowly to a solution of tris(2,4,6-trichloro-3,5-dinitrophenyl)methane (2.0 g; 3.6 mmol) in fuming nitric acid (100 mL), and the resulting mixture was stirred at 80 °C (3 days), and poured into an excess of ice-water. The precipitate, separated by filtration and dried under reduced pressure, was identified as tris(2,4,6-trichloro-3,5-dinitrophenyl)methane (**2**) (2.52 g; 85 %). IR (KBr) υ 2894 (w), 1564 (h), 1244 (w), 1213 (w), 1020 (m), 949 (m), 832 (m), 783 (m), 631 (m) cm^{-1}. ^{1}H-NMR (CDCl$_3$) δ 8.3 (s) ppm.

*Synthesis of the tris(2,4,6-trichloro-3,5-dinitrophenyl)methyl radical (HNTTM, **4**)*

Tetrabutylammonium hydroxide (TBAH) (1.5 M; 0.9 mL) was added to a solution of tris(2,4,6-trichloro-3,5-dinitrophenyl)methane (1.0 g; 1.21 mmol) in acetone (50 mL) and the mixture was stirred (20 min) at room temperature (rt). Chromium (VI) oxide (0.6 g; 3.0 mmol) was added to the reaction mixture and stirred in the dark at rt under inert atmosphere of Ar (20 h). The reaction mixture was poured into an excess of aqueous solution of hydrochloric acid and an excess of CHCl$_3$ was added. The organic solution was

3. Materials and Methods

washed with water, dried with anhydride sodium sulfate (Na$_2$SO$_4$) and filtered, and the solvent was dried under reduced pressure. The solid obtained was purified by chromatography in column (silica gel) eluting with CHCl$_3$, and it was identified as HNTTM (**4**) (0.63 g; 63 %). UV-Vis (CHCl$_3$) λ (ε), 285 (6345), 384 (23240), 504 (1260), 553 (1080) nm (dm^3 mol^{-1} cm^{-1}). IR (KBr) 1549 (h), 1340 (h), 1279 (w), 949 (m), 842 (m), 787 (m), 691 (w) cm^{-1}.

3.2.1.1.2. Synthesis of the tris(2,3,5,6-tetrachloro-4-nitrophenyl)methyl radical (TNPTM)

*Synthesis of tris(2,3,5,6-tetrachlorophenyl)methane (**5**)*

1,2,4,5-Tetrachlorobenzene (28.8 g; 133.4 mmol), chloroform (1.5 mL; 18.4 mmol), and anhydride aluminium chloride (2.6 g; 19.5 mmol) were poured into a hermetic and dry reactor of glass. The reactor was heated at 160 °C into a silicon bath (2 h 15 min). The reaction mixture was extracted with a diluted solution of aqueous HCl in ice-water and CHCl$_3$. The organic phase was washed with an aqueous solution of sodium hydrogen carbonate (NaHCO$_3$) (2 %, 200 mL) and water (3 x 100 mL). The organic phase was dried with anhydride sodium sulfate (Na$_2$SO$_4$) and the solvent was removed under reduced pressure obtaining a light-brown precipitate, which was purified by sublimation at 150 °C (30 min), and by chromatography in silica flash-gel eluting with hexane. The solid obtained was identified as tris(2,3,5,6-tetrachlorophenyl)methane (**5**) (16.4 g; 56 %) IR (KBr) υ 3111 (w), 3068 (w), 1539 (m), 1410 (h), 1388 (h), 1348 (m), 1322 (m), 1235 (m), 1199 (m), 1163 (h), 1098 (m), 974 (m), 865 (h), 844 (m), 781 (m), 646 (m), 626 (m), cm^{-1}. ^{1}H-NMR (CDCl$_3$) δ, 7.65 (s, 3Harom), 6.98 (s, 1H, CH) ppm.

*Synthesis of tris(2,3,5,6-tetrachloro-4-nitrophenyl)methane (**6**)*

Fuming nitric acid (50 mL) was added to a solution of tris(2,3,5,6-tetrachlorophenyl)methane (5.1 g; 7.8 mmol) and the resulting mixture was stirred at reflux (21 h) and poured into an excess of ice-water. The precipitate, separated by filtration, dried under reduced pressure, and purified by chromatography in silica gel eluting with CHCl$_3$, was identified as tris(2,3,5,6-tetrachloro-4-nitrophenyl)methane (**6**) (4.97 g; 81 %). IR (KBr) u, 1555 (s), 1345 (s), 1303 (m), 1131 (m), 882 (w), 784 (m), 757 (m), 730 (m), 664 (w), 567 (m) cm^{-1}. ^{1}H-NMR (CDCl$_3$) δ, 7.01 (s, 1H) ppm. Anal. Calcd for C19HCl12N3O6: C, 28.8; H, 0.1; Cl, 53.7; N, 5.3. Found: C, 28.9; H, 0.2; Cl, 53.7; N, 5.1.

*Synthesis of the tris(2,3,5,6-tetrachloro-4-nitrophenyl)methyl radical (TNPTM, **8**)*

Tetrabutylammonium hydroxide (TBAH) (1.5 M; 3.7 mL,) was added to a solution of tris(2,3,5,6-tetrachloro-4-nitrophenyl)methane (3.4 g; 4.3 mmol) in THF (50 mL) and the mixture was stirred (2 h) at 0 °C (2 h). Tetrachloro-*p*-quinone (1.5 g; 6.0 mmol) was added to the reaction mixture and stirred in the dark at 0 °C under inert atmosphere (Ar) (30 min). The mixture was dried and purified by chromatography in silica gel eluting with hexane/CHCl₃ (3:1) to give TNPTM (**8**) (3.0 g; 88 %) UV-Vis (CHCl₃) λ (ε), 287 (6320), 378 (17153), 493 (871) nm (dm³ mol⁻¹ cm⁻¹). IR (KBr) υ 1556 (h), 1343 (h), 1268 (w), 1148 (w), 1048 (w), 888 (w), 788 (w), 765 (m), 724 (w), 572 (w) cm⁻¹. Anal. Calcd for $C_{19}Cl_{12}N_3O_6$: C, 28.8; Cl, 53.7; N, 5.3. Found: C, 28.8; Cl, 54.0; N, 5.1.

3.2.1.2. Crystallization of the tetrabutylammonium (Bu₄N⁺) salt of HNTTM anion and TNPTM

3.2.1.2.1. Tetrabutylammonium tris(2,4,6-trichloro-3,5-dinitrophenyl) methyde salt (Bu₄N⁺·⁻HNTTM)

An aqueous solution of tetrabutylammonium hydroxide (TBAH) (1.5 M) (26 μL; 0.4 mmol) was added to a stirred solution of tris(2,4,6-trichloro-3,5-dinitrophenyl)methane (269.0 mg; 0.3 mmol) in THF (15 mL), and the mixture was left in Ar at rt for a period of time (6 h). The precipitate (253.0 mg) was filtrated off, washed with water, and dried under reduced pressure to give the tetrabutylammonium tris(2,4,6-trichloro-3,5-dinitrophenyl)methide salt (253.0 mg; 73 %). The salt yield small dark violet needles by slow evaporation of a saturated solution in MeOH. IR (KBr) 2973 (w), 2929 (w), 2871 (w), 1553 (s), 1465 (w), 1358 (m), 1222 (w), 945 (w), 833 (w), 784 (w), 735 (w), 677 (w), 638 (w) cm. Anal. calcd. for $C_{35}H_{36}Cl_9N_7O_{12}$: C, 39.4; H, 3.4; N, 9.2; Cl, 29.9. Found: C, 39.7; H, 3.6; N, 8.8; Cl, 29.2.

3.2.1.2.2. Tris(2,3,5,6-tetrachloro-4-nitrophenyl)methyl radical (TNPTM)

TNTPM (**8**) (102.5 mg; 0.13 mmol) was dissolved in CHCl₃ (15 mL) and the solution was stirred (70 °C). As the solution was being concentrated, hexane was slowly added up to a CHCl₃/hexane proportion of 10:90 (v/v) approximately. The final solution was kept at the dark at rt and TNPTM (**8**) was crystallized in nice dark red crystals.

3. Materials and Methods

3.2.1.3. Synthesis of dimethyl-4,4',5,5',6,6'-hexahydroxy-2,2'-diphenyl-dicarboxylate (DHHDP)

DHHDP (**20**) was synthesized following the procedure described by Quideau, *et al.*(*137*) **20** was identified by NMR, ^{1}H NMR (400 MHz, CD$_3$COCD$_3$) δ 3.47 (s, 6 H), 7.12 (s, 2H) ppm; ^{13}C NMR (101 MHz, CD$_3$COCD$_3$) δ 167.60, 144.52, 137.52, 122.66, 118.75, 110.68, 51.45 ppm.

3.2.1.4. Reaction of stable free radicals with toluene

3.2.1.4.1. Reaction of DPPH with toluene

DPPH (**9**) (10.0 mg; 0.03 mmol) was dissolved in deoxygenated toluene (10 mL) and stirred at reflux (24 h) in inert atmosphere (Ar). The solution color changed from violet to yellow. Toluene was removed from the solution under vacuum to give **9** and *H*-DPPH identified by IR spectroscopy. The recovered **9** and *H*-DPPH was quantitative.

3.2.1.4.2. Reaction of HNTTM with toluene

HNTTM (**4**) (9.9 mg; 0.01 mmol) was dissolved in deoxygenated toluene (10 mL) and stirred at reflux (24 h) in inert atmosphere (Ar). The red solution did not change in color. Toluene was removed from the solution under vacuum to give **4** identified by IR spectroscopy. The recovered **4** was quantitative.

3.2.1.4.3. Reaction of TNPTM with toluene

TNPTM (**8**) (31.0 mg; 0.04 mmol) was dissolved in deoxygenated toluene (31 mL) and stirred at reflux (24 h) in inert atmosphere (Ar). The red solution did not change in color. Toluene was removed from the solution under vacuum to give **8** identified by IR spectroscopy. The recovered **8** was quantitative.

3.2.1.5. Reaction of TNPTM with ascorbic acid

TNTPM (**8**) (0.9 mg; 0.001 mmol) was dissolved in deoxygenated CHCl$_3$/MeOH (2:1) (v/v) (10 mL). An excess of ascorbic acid (2 mg; 0.011 mmol) was added to the solution. The solution became first violet and then colorless. The reaction was followed by UV-Vis at λ= 378 nm for a time (1 h).

3. Materials and Methods

3.2.1.6. Cyclic voltamperometries

Determination of the standard redox potential (E°) and the anodic and cathodic peak potentials ($E_p{}^a$, $E_p{}^c$) of radicals, and the anodic and anodic onset peak potentials ($E_p{}^a$, $E_o{}^a$) of (poly)phenols

Cyclic voltammograms were obtained with an electrolytic cell and the use of three electrodes; the working electrode (platinum (Pt)), the reference electrode (saturated calomel electrode (SCE)), and the counter electrode (Pt). The solvents used were $CHCl_3$, $CHCl_3/MeOH$ (2:1) (v/v), DMF and benzene. Tetrabutylammonium perchlorate (TBAP) 0.1 M was used as electrolyte with the three first solvents, and tetrahexylammonium hexafluorophosphate ($THAPF_6$) 0.3 and 0.2 M was used as electrolyte with benzene as solvent.

Measuring of the standard redox potential (E°) and the anodic and cathodic peak potentials ($E_p{}^a$, $E_p{}^c$) of HNTTM and TNTPM

Radicals HNTTM (**4**) and TNPTM (**8**) (1mM) were dissolved in deoxygenated $CHCl_3/MeOH$ (2:1). A variable potential was applied for **4** from 1.0 to 0.3 V. Different scan rates were applied (200, 100, 50 and 20 mV s^{-1}). The potential applied for the reduction and oxidation of **8** was from 0.6 to 0.0 V, and the processes were also run at different scan rates (200, 100, 50 and 20 mV s^{-1}).

Measuring of the anodic peak potentials ($E_p{}^a$) of catechol and pyrogallol

Catechol (**10**) and pyrogallol (**11**) (1mM) were dissolved in deoxygenated $CHCl_3$, benzene and $CHCl_3/MeOH$ (2:1). The variable potential applied for the reduction and oxidation of **10** in $CHCl_3$ were from 1.6 to 0.6 V, in benzene was from 2.0 to 0.3 V, and in $CHCl_3/MeOH$ (2:1) from 1.25 to 0.25 V. Different scan rates were applied (200, 100, 50 and 20 mV s^{-1}). The potential applied for the reduction and oxidation of **11** in $CHCl_3$ was from 1.4 to 0.3 V, in benzene was from 3.0 to 0.0 V, and in $CHCl_3/MeOH$ (2:1) from 1.0 to 0.0 V.

Measuring of the anodic peak potentials ($E_p{}^a$) of the anions of catechol and pyrogallol

Catechol (**10**) (1mM) was dissolved in deoxygenated $CHCl_3/MeOH$ (2:1). A variable potential was applied from 1.1 to 0.0 V at different scan rates (200, 100, 50 and 20 mV s^{-1}). Tetrabutylammonium hydroxide (TBAH) (4 mM) in water was added to the solution and a potential from 0.5 to -0.7 V was applied at different scan rates (200, 100, 50

and 20 mV s^{-1}). A range of potential from 1.1 to 0.0 V was applied to a solution of pyrogallol (**11**) (1mM) in deoxygenated CHCl$_3$/MeOH (2:1) at different scan rates (200, 100, 50 and 20 mV s^{-1}). TBAH (3 mM) in water was added to the solution of **11** and a variable potential from 0.3 to -0.7 V was applied at different scan rates (200, 100, 50 and 20 mV s^{-1}).

Measuring of the anodic onset potential ($E_o{}^a$) of catechol, pyrogallol, methylgallate and DHHDP

Catechol (**10**) (1mM) was dissolved in deoxygenated DMF. The potential range from 1.3 to 0.0 V was applied to obtain the oxidation potential of **10**. Different scan rates were applied (200, 100, 50 and 20 mV s^{-1}). The potential range applied for the oxidation of pyrogallol (**11**), methylgallate (**12**) and DHHDP (**20**) was from 1.6 to 0.0 V at different scan rates (200, 100, 50 and 20 mV s^{-1}).

3.2.1.7. Determination of the stability of HNTTM, TNPTM, and (poly)phenols

The stability of HNTTM (**4**) and TNPTM (**8**) was monitored by UV-Vis spectroscopy measuring the characteristic band of each radical in the different deoxygenated solvents (CHCl$_3$, CHCl$_3$/MeOH (2:1), MeOH, CH$_3$CN, DMF, DMSO) during 7 h and 48 h, respectively.

The stability of (poly)phenols in different solvents was measured by HPLC-DAD at different times during 48 h. HPLC-DAD analysis were carried out using a column C-18 *Mediterranea Sea18* (5μm, 4.6 x 250 mm) from Teknokroma. The solvents employed were (A) water with 0.1 % acetic acid, and (B) 100 % methanol. The eluting gradient established was from 10 to 90 % of B over 45 min using a flow rate of 0.8 mL min^{-1} detecting at 214 and 280 nm of wavelength.

3.2.1.8. Analysis of the products of the reaction between catechol or pyrogallol with HNTTM and TNPTM

Reaction of catechol or pyrogallol with HNTTM. Equimolar solutions (1:1) of (poly)phenols catechol (**10**) or pyrogallol (**11**) (6.7 and 7.7 mg, respectively) and HNTTM (**4**) (49.7 mg) were dissolved in deoxygenated CHCl$_3$, or benzene or CHCl$_3$/MeOH (2:1) (v/v) (50 mL). The solutions were left at rt in the dark and under inert atmosphere (N$_2$) during a time (47 h). The organic phase was extracted with a diluted aqueous solution of hydrochloric acid and water, dried with anhydride sodium sulphate (Na$_2$SO$_4$), and finally

filtered. The organic solvent was removed under vacuum, and the solids were identified by UV-Vis and IR spectroscopies. Experiments were carried out in duplicate (n=2).

Reaction of catechol or pyrogallol with TNPTM. Equimolar solutions (1:1) of (poly)phenols catechol (**10**) or pyrogallol (**11**) (7.5 mg and 8.5 mg, respectively) and TNTPM (**8**) (52.9 mg) were dissolved in deoxygenated CHCl$_3$ or CHCl$_3$/MeOH (2:1) (v/v) (50 mL). The solutions were left at rt in the dark and under inert atmosphere (N$_2$) during a time (48 h). The organic phase was extracted with a diluted aqueous solution of hydrochloric acid and water, dried with anhydride sodium sulphate (Na$_2$SO$_4$), and finally filtered. The organic solvent was removed under vacuum, and the solids were identified by UV-Vis and IR spectroscopies. Experiments were carried out by duplicate (n=2).

3.2.1.9. Determination of the kinetics and Radical Scavenging Capacity (RSC) of the reactions of HNTTM or TNPTM with (poly)phenols

Second-order kinetics. The kinetics of the reactions between HNTTM (**4**) or TNPTM (**8**) with (poly)phenols were determined at rt by Electronic Paramagnetic Resonance (EPR) or by UV-Vis spectroscopies. Fresh solutions of HNTTM (**4**) or TNPTM (**8**), and (poly)phenols **10**-**21** were prepared in deoxygenated CHCl$_3$/MeOH (2:1) with a radical/(poly)phenol molar ratio of 5:1. The reaction started when the solution of **4** or **8** (2 mL) was mixed with the solution of a (poly)phenol **10**-**21** (2 mL) (1:1, v/v). Assays were carried out between two and five repetitions (n=2-5). The intensity of the EPR signal or the absorbance of the band of the radical **4** or **8** in the UV-Vis spectrum was recorded each second, in the case of fast reactions, and each 15 or 30 min in the case of slow reactions, until the signal or band remained constant (7 h and 48 h, respectively). The rate constant (k) and the number of electrons transferred (n$_e$) were estimated with a simple and general kinetic model reported by Dangles *et al.*(*116*)

The reaction rate is defined as **Equation 3**, and values of k$_1$ or k are obtained from the representation of the integrated equation (**Equation 4** and **Figure 48**):

$$-d\frac{[\text{radical}]}{dt}=k'.2[(\text{poly})\text{phenol}].[\text{radical}]=k[(\text{poly})\text{phenol}].[\text{radical}] \quad (\textbf{Equation 3})$$

$$\ln\frac{1-\frac{I_f}{I_x}}{1-\frac{I_f}{I_o}}=-\frac{k.c}{\frac{I_o}{I_f}-1}.t \quad (\textbf{Equation 4})$$

3. Materials and Methods

Where I_f is the final intensity, I_x represents the intensity at different times, I_o is the initial intensity, c is the initial (poly)phenol concentration and t is the reaction time.
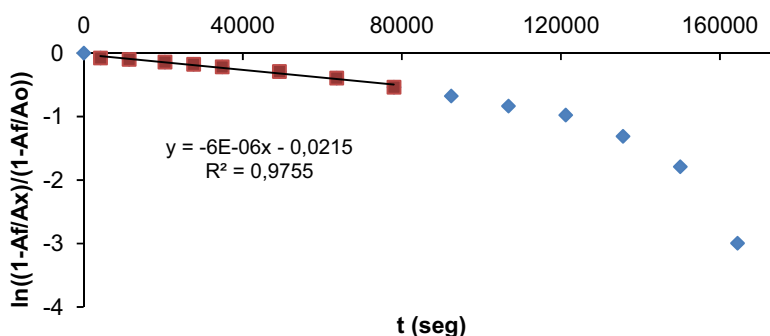
Figure 48. Representation of the kinetics of the reaction of **11** with **8** *vs* time (s), using the EPR technique in deoxygenated CHCl$_3$/MeOH (2:1), with a **8**/**11** molar ratio of (5:1). Final reaction time: 48 h.

The n_e values were calculated using the **Equation 5**:

$$n_e = \frac{I_o - I_f}{\varepsilon \cdot c} \quad \text{(\textbf{Equation 5})}$$

Where I_o is the initial intensity; I_f the final intensity; ε the molar absorption coefficient; and c the initial (poly)phenol concentration (A_o and A_f are used in the case of UV-Vis spectroscopy).

3.2.1.10. Determination of the Radical Scavenging Capacity (RSC) of (poly)phenols

Evaluation of the Efficient Concentration at 50 % (EC$_{50}$). RSC of (poly)phenols was determined per duplicate from mixtures (1:1, v/v) of fresh solutions of HNTTM (**4**), TNPTM (**8**) and DPPH (**9**), (120 µM), and fresh solutions of (poly)phenols **10**-**21** in deoxygenated CHCl$_3$/MeOH (2:1) at five different concentrations (1-120 µM) at rt in the dark. Final reaction time, 30 min for the radical **9**, 7 h for the radical **4**, and 48 h for the radical **8**. The EC (**13**) was used as the control (poly)phenol and a calibration curve for each radical was obtained for a better precision of the radical concentration. RSC of hydrolyzable tannins with radicals **4**, **8** or **9** cannot be measured by UV-Vis spectroscopy because of the overlapping bands of both reagents. For a better comparison of the RSC of

all (poly)phenols **10**-**21**, all the experiments were performed by EPR. Operating conditions were magnetic center field, 3615 G; scan range, 250 G; microwave power, 5.2 mW; microwave frequency, 9.86 GHz; modulation frequency, 100 KHz; receiver gain, 6 × 10^3 and time constant, 4.1 s. The percentage of reacted radical (**Equation 6**) as a function of the concentration of (poly)phenol per concentration of radical ([**13**]/[**4**]) gives the straight line, as depicted in **Figure 49** for the reaction of **13** with the radical **4**.

$$\left(1 - \frac{I_x}{I_o}\right).100 \quad (\textbf{Equation 6})$$

Where I_o and I_x are the EPR band signal intensities of the radical at initial and at final reaction time.
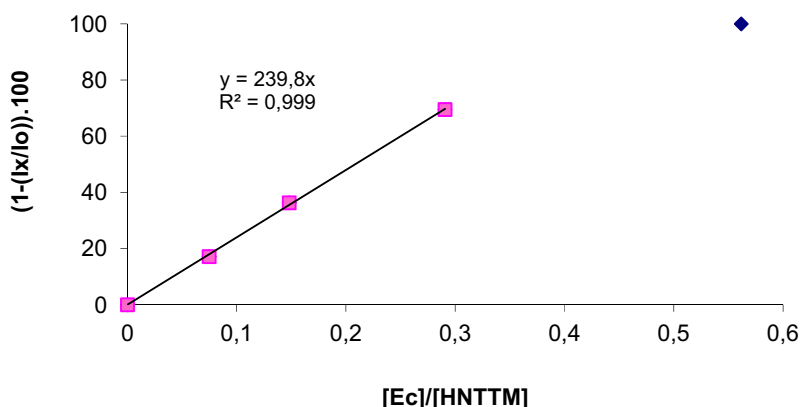
Figure 49. Representation of the calibration line as explained in the text, obtained from the reaction of EC (**13**) with the radical **4** in deoxygenated CHCl$_3$/MeOH (2:1) and expressed in μmol of EC per μmol of HNTTM. Concentrations of **13** (5-40 μM range) and concentration of **4**, 60 μM.

The RSC values of (poly)phenols in the reactions with the radicals **4**, **8** or **9** are calculated from the straight line depicted in **Figure 49**. The calculated value (EC$_{50}$, μmol of (poly)phenol per μmol of radical or μg of (poly)phenol per μmol of radical) is the Efficient Concentration of the (poly)phenol to decrease half of the concentration of the radical divided by the moles of initial radical. The Stoichiometric Value (SV, EC$_{50}$ x 2), the Antiradical Power (ARP, 1/EC$_{50}$) and the number of electrons or hydrogen atoms

transferred ($n_{e/H}$, 1/SV) per molecule of (poly)phenol are the parameters obtained from the EC_{50} for each (poly)phenol.

3.2.1.11. Detection of some of the oxidized products of DHHDP by reaction with TNPTM

The reaction of DHHDP (**20**) (43.0 µM) with TNPTM (**8**) (119.7 µM) was performed at rt in the dark and under inert atmosphere (N_2) (48 h) in deoxygenated $CHCl_3$/MeOH (2:1). The reaction products were analyzed and characterized by mass spectrometry (HPLC-HR-ESI-TOF-MS). Conditions of the mass spectrometer in the negative ion mode were capillary voltage, 3.5 kV; fragmentor voltage, 175 V; gas temperature, 325 °C; nebulizing pressure, 15 psi; and flow of dried gas, 7.0 L min^{-1}. The carrier solution was H_2O/CH_3CN (1:1).

3.2.1.12. Determination of the Reducing Rates (RR) of (poly)phenols with the Ferric-Reducing Antioxidant Power (FRAP) method

Fresh solutions of (poly)phenols at four different concentrations (8-50 µM) in deoxygenated water (pH=3.6, sodium acetate buffer) were added (1:1, v/v) to a solution of the same buffer with o-phenanthroline (1.2 mg mL^{-1}) and $FeCl_3$ (1 mM). The mixture was incubated at rt (20 s) then, the UV absorbance of the Fe(II)-o-phenanthroline complex (λ = 510 nm) was measured. The RR values were assessed by the formation of the Fe(II)-o-phenanthroline complex and expressed relative to the activity of the flavanol EGCG (**16**).

3.2.1.13. Measuring of the Reducing Capacity (RC) of (poly)phenols with the Ferric-Reducing Antioxidant Power (FRAP) method

Fresh solutions of (poly)phenols at four different concentrations (8-50 µM) in deoxygenated water (pH= 3.6, sodium acetate buffer) were added (1:1, v/v) to a solution of the same buffer with o-phenanthroline (1.2 mg mL^{-1}) and $FeCl_3$ (1 mM). The mixture was incubated at rt in the dark (1 h), then, the UV absorbance of the Fe(II)-o-phenanthroline complex (λ = 510 nm) was measured. The activity was assessed by the formation of the Fe(II)-o-phenanthroline complex and expressed relative to the capacity of the flavanol EGCG (**16**).

3.2.2. Biochemical assays to study the effect of (poly)phenols. *In vitro* studies

3.2.2.1. Cell Culture

Human colorectal adenocarcinoma cell line HT-29 was obtained from the American Type Culture Collection. HT-29 were cultured in DMEM, supplemented with 10 % Foetal Bovine Serum (FBS), and antibiotics penicillin (100 U mL^{-1}) and streptomycin (100 mg L^{-1}) at 37 °C in a humidified atmosphere of CO_2 (5 %). Experiments were carried out in a monolayer of 80 % of confluence.

3.2.2.2. Cell tripsinization

HT-29 cells grew adhered in the plate and they duplicated in 24 h. When the plate was in 80-90 % of confluence, DMEM was aspired and cells were cleaned with PBS (3 mL, 2 min). PBS was aspired and 3 mL of tripsine were added into the plate to resuspend the cells. Cells were incubated during 5 min at 37 °C and resuspended in 9 mL of DMEM to inhibit the tripsine effect (3 x 3mL of tripsine volume). Finally, the resuspended cells were centrifuged (1500 rpm, 5 min), supernatant liquid was removed and the precipitate (*pellet*) was resuspended in PBS (1mL). The resultant solution was used to maintain the cellular line and to count the number of cells for its use in different assays.

3.2.2.3. Cell counting

Following the tripsinization (Section before), 10 μL of resuspended pellet was diluted with PBS in a 1/8 proportion (dilution volume depends on the initial cell concentration). Tripan blue (TB, 10 μL) was added to an aliquot of cells (10 μL) and finally, 10 μL of them were added into the Neubauer chamber to observe and counter the cells with the microscope (**Figure 50**). Cells of each quadrant were counted and the **Equation 7** was applied.

3. Materials and Methods
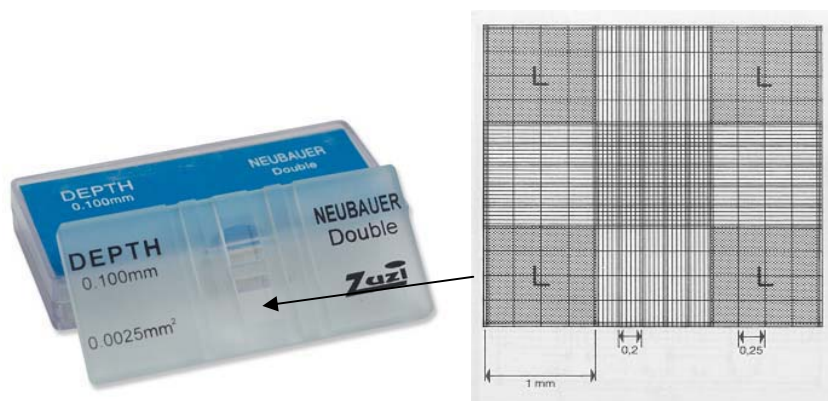
Figure 50. Neubauer chamber

$$\text{(Cell average)}.\big(\text{dilution factor (PBS)}\big).\big(\text{dilution factor (TB)}\big).10^4 = \text{cells } ml^{-1} \quad \textbf{(Equation 7)}$$

3.2.2.4. Cell viability

The effect of the treatment with different (poly)phenols upon proliferation of HT-29 cells was measured by the 3-(4,5-dimethylthiazol-2-yl)-2,5-diphenyl tetrazolium bromide (MTT) assay, which is based on the ability of live cells to cleave the tetrazolium ring, thus producing formazan, which absorbs at $\lambda = 570$ nm in the UV-Vis spectrum. HT-29 cells were tripzinized and counted (See Materials and Methods, Sections 3.2.2.2 and 3.2.2.3). HT-29 cells (3000 cells/well) were grown on a 96-well plate for 24 h and then incubated with the different (poly)phenols at concentrations ranging from 10 to 900 µM. The most hydrophobic (poly)phenols were dissolved in dimethylsulphoxide (DMSO), except ellagic acid (EA, **21**) which was dissolved in N-methyl-pyrrolidone because of their poor solubility in DMSO. After 72 h, the supernatant was aspirated and then, 100 µL of filtered solution of MTT in cell culture medium (0.5 mg mL^{-1}) was added to each well. The cell plates were incubated during 1 h and metabolically active cells reduced the dye to purple formazan. The supernatant was removed, and the precipitated dark blue MTT formazan was dissolved in 100 µL of DMSO. Some of the experiments were also run in the presence of catalase (100 U mL^{-1}) in DMEM and optical density (OD) was measured at $\lambda = 550$ nm on a multiwall ELISA plate reader. The IC$_{50}$ or compound concentration causing a 50 % of reduction of the dye in the mean OD value relative to the control was estimated using the Graph Pad program or the Excel.
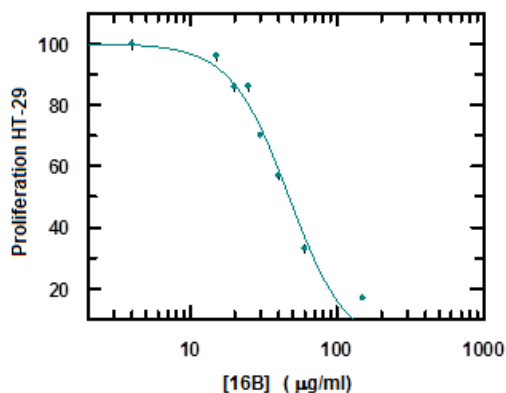
Figure 51. Proliferation curve obtained for HT-29 cells treated with thio-flavanol **16B**.

3.2.2.5. Apoptosis

Apoptosis quantification was conducted by flow cytometry. HT-29 cells were seeded into six well plates at 8×10^4 cells per well and incubated for 24 h at 37 °C prior to addition of the (poly)phenols. The supernatant was aspired and the (poly)phenols were added with 1500 μl of DMEM. Well plates were incubated during 72 h at 37 °C. DMEM of each well was collected separately and added in its corresponding eppendorf. The cells were cleaned with PBS (1 mL) and added to the subsequent eppendorf. The eppendorfs were centrifuged (5 min, 1800 rpm). Each well was tripsinized with Tripsin (400 μl) at 37 °C during 3 min. To neutralize the Tripsin, DMEM (1.2 mL) was added and each well was collected and centrifuged again (5 min, 1500 rpm). The supernatant was removed and Binding Buffer 1X was added. The cells were incubated with Anexin V-FITC (30 min). Binding Buffer 1x (800 μl) and PI (20 μl) were added. The cells, double stained with PI and FITC–annexin V, were processed by flow cytometry and laser-scanning cytometry, which collected green (λ= 525 nm) fluorescence for FITC-conjugated antibody and red (λ= 675 nm) fluorescence for PI, under λ= 488 nm of excitation.

3. Materials and Methods

3.2.3. Synthesis of EGCG-glucuronides

3.2.3.1. Glucuronidation reaction of flavanol EGCG. Modified Koenigs-Knorr reaction.

3.2.3.1.1. Glucuronidation reaction of EGCG with K_2CO_3 and acetobrom-α-D-glucuronic acid methyl ester using different solvents

Synthesis of EGCG (**16**) glucuronides was carried out following the reaction conditions employed by Gonzalez-Manzano and co-workers to prepare catechin glucuronides.(*102*) EGCG (**16**) (5.10 mg; 0.01 mmol) and acetobrom-α-D-glucuronic acid methyl ester (**22**) (25.2 mg; 0.06 mmol) were dissolved in different deoxygenated solvents, such as acetone, CH_2Cl_2, DMSO, and DMF (0.25 mL). After the addition of K_2CO_3 (5.20 mg; 0.04 mmol), the mixtures were stirred for 6 h at rt under inert atmosphere (N_2) and in the dark. In addition, the reaction in CH_2Cl_2 was performed at 40 °C. All the reactions were followed by analytic HPLC-DAD and HPLC-HR-DAD-ESI-TOF-MS (See Materials and Methods, Section 3.2.3.3.1.1 and 3.2.3.3.2.1).

3.2.3.1.2. Glucuronidation reaction of EGCG with KOH and acetobrom-α-D-glucuronic acid methyl ester in deoxygenated DMF as solvent

Regev-Shoshani G *et al.,* synthesized glucosides of resverastrol using KOH as promoter.(*138*) Following their procedure, EGCG (**16**) (9.77 mg; 0.01 mmol) and acetobrom-α-D-glucuronic acid methyl ester (**22**) (18.5 mg; 0.05 mmol) were dissolved in anhydrous (molecular sieves (3Å)) and deoxygenated DMF (N_2) (0.36 mL). After addition of KOH (1.77 M) (24 μL; 0.43 mmol), the mixture was stirred at rt (6 h) under inert atmosphere (N_2) and in the dark. Reaction was followed by analytic HPLC-DAD (See Materials and Methods, Section 3.2.3.3.1.2).

3.2.3.1.3. Glucuronidation reaction of EGCG with Cs_2CO_3 and acetobrom-α-D-glucuronic acid methyl ester in deoxygenated CH_3CN as solvent

Glucuronidation reaction of EGCG (**16**) was assayed using Cs_2CO_3 as promoter in deoxygenated CH_3CN as solvent, following the reaction conditions used by Yamazoe and co-workers.(*139*) **16** (10.4 mg; 0.02 mmol) and acetobrom-α-D-glucuronic acid methyl ester (**22**) (26.6 mg; 0.06 mmol) were dissolved in deoxygenated CH_3CN (1 mL). After addition of Cs_2CO_3 (7.11 mg; 0.02 mmol), the mixture was stirred at rt (6 h), under inert

atmosphere (N_2) and in the dark. Reaction was followed by analytic HPLC-DAD (See Materials and Methods, Section 3.2.3.3.1.2).

<u>3.2.3.1.4. Preparative glucuronidation reaction of EGCG with acetobrom-α-D-glucuronic acid methyl ester to obtain EGCG-4"-*O*-triacetylglucuronide methyl ester using deoxygenated DMF as solvent</u>

EGCG (**16**) (150 mg; 0.33 mmol) and acetobrom-α-D-glucuronic acid methyl ester (**22**) (750 mg; 1.88 mmol) were dissolved in anhydrous (molecular sieves (3Å)) and deoxygenated DMF (7.5 mL). After addition of K_2CO_3 (150 mg; 1.09 mmol), the mixture was stirred at rt (6 h) under inert atmosphere (N_2) and in the dark. Reaction was followed by analytic HPLC-HR-ESI-TOF-MS. The resulting mixture was added into an ice/H_2O (1:1) mixture (45 mL) and then adjusted to acidic conditions by adding a few drops of formic acid. The DMF/H_2O was removed by liophylization. The residue obtained was dissolved in MeOH/H_2O (1:1) and purified with a semipreparative HPLC (See Materials and Methods, Section 3.2.3.3.3.1) to remove the remaining reagents and side products of the reaction. Three fractions were collected. The methanol was evaporated under reduced pressure and the water was removed by liophylization. Studies of NMR were carried out in D_2O (^{1}H-NMR, ^{13}C-NMR, HSQC, and HMBC) to determine the side of union of the triacetylglucuronide methyl ester to the EGCG (**16**).

3.2.3.2. Synthesis of EGCG-*O*-4"-glucuronide from EGCG-*O*-4"-triacetylglucuronide methyl ester

<u>3.2.3.2.1. Chemical synthesis of EGCG-4"-*O*-glucuronide from EGCG-4"-*O*-triacetylglucuronide methyl ester with sodium methoxide (NaMeO)</u>

The conditions of the deacetylation of catechin acetylglucuronides used by Gonzalez-Manzano and co-workers(*102*) were tested to deacetylate and hydrolyze the methyl ester of EGCG-4"-*O*-triacetylglucuronide methyl ester (**A16**) to obtain EGCG-4"-*O*-glucuronide (**C16**).

A solution of NaMeO (72 μL) (28:72, v/v NaMeO/MeOH) was added to a solution of **A16** (2.03 mg; 0.003 mmol) in MeOH (5 mL) at 4 °C during a time (30 min) to remove the acetyl moieties bound to the glucuronide residue. After addition of ultrapure deoxygenated water (1.5 mL), the reaction was performed at rt (45 min) in order to hydrolyze the methyl ester. The solution was neutralized with HCl and then adjusted to

3. Materials and Methods

acidic conditions by adding a few drops of formic acid. The reaction was followed by HPLC-DAD (See Materials and Methods, Section 3.2.3.3.1.2).

<u>3.2.3.2.2. Chemical synthesis of EGCG-4''-*O*-glucuronide methyl ester from EGCG-4''-*O*-triacetylglucuronide methyl ester with zinc acetate (Zn(Ac)₂)</u>

EGCG-4''-*O*-triacetylglucuronide methyl ester (**A16**) (9.10 mg) was dissolved in deoxygenated anhydrous MeOH (3 mL). Zn(Ac)₂ (11.1 mg; 0.06 mmol) was added and stirred at 35 °C (1.5 h) to obtain EGCG-4''-*O*-glucuronide methyl ester (**B16**). The reaction was followed by HPLC-DAD (See Materials and Methods, Section 3.2.3.3.1.2).(*104*)

<u>3.2.3.2.3. Chemical synthesis of EGCG-4''-*O*-glucuronide methyl ester from EGCG-4''-*O*-triacetylglucuronide methyl ester with *para*-toluenesulfonic acid (*p*-TsOH)</u>

EGCG-4''-*O*-triacetylglucuronide methyl ester (**A16**) (3.96 mg; 0.005 mmol) was dissolved in deoxygenated CH₂Cl₂/MeOH (9:1) (2 mL). *p*-TsOH (5.20 mg; 0.016 mmol) was added and stirred at 30 °C (48 h) in the dark to obtain EGCG-4''-*O*-glucuronide methyl ester (**B16**). The reaction was followed by HPLC-HR-ESI-TOF-MS. The reaction was assayed at rt using 4 equivalents of *p*-TsOH (6.78; 0.02 mmol) in CH₂Cl₂/MeOH (9:1) (2 mL) or in MeOH/CH₂Cl₂ (4.5:1) (2 mL).

<u>3.2.3.2.4. Enzymatic synthesis of EGCG-4''-*O*-glucuronide from EGCG-4''-*O*-triacetylglucuronide methyl ester</u>

3.2.3.2.4.1. **Route A.** *Analytical deacetylation of EGCG-4''-O-triacetylglucuronide methyl ester to obtain EGCG-4''-O-glucuronide methyl ester testing different lipases*

EGCG-4''-*O*-triacetylglucuronide methyl ester (**A16**) (3.65-0.50 mg) was dissolved in different deoxygenated solvents (from 1 to 0.4 mL) and conditions. As solvents, deoxygenated THF, diisopropyl eter or water were used. THF and diisopropyl eter were used with an ion exchange resin (IRA) (50 mg) and water was used at different pH (5.0, 6.1, 6.7 and 8.0) and with a co-solvent (10 % or 20 % of MeOH, DMSO or THF). Lipase (from 7.36 to 80.8 mg) Novozyme-435 (N-435), Lipase A (LA), Lypozime IM (LIM), Pancreatic Porcine Lipase (PPL) or Lipase AS (LAS)) was added to the solution with different **A16**:lipase ratios, (1:15) and (1:30) approximately to obtain EGCG-4''-*O*-glucuronide methyl ester (**B16**). The reaction was stirred softly at different temperatures

(30 or 40 °C) during different reaction times (from 4.5 to 24 h) and followed by HPLC-HR-DAD-ESI-TOF-MS (See Materials and Methods, Section 3.2.3.3.2.2).

3.2.3.2.4.2. Preparative deacetylation of EGCG-4''-O-triacetylglucuronide methyl ester to obtain EGCG-4''-O-glucuronide methyl ester

EGCG-4''-*O*-triacetylglucuronide methyl ester (**A16**) (50.7 mg) was dissolved in deoxygenated water at pH 6.1 (Na₂HPO₄, 25 mM, 20 mL) and deoxygenated DMSO as co-solvent (5 mL). Lipasse AS (LAS) (1.5 g) was added to the solution, and the reaction was conducted with soft stirring at 40 °C (6h) in the dark to obtain EGCG-4''-*O*-glucuronide methyl ester (**B16**). The reaction was followed by HPLC-DAD (See Materials and Methods, Section 3.2.3.3.1.2). To purify the sample, it was filtered several times with a filter paper to remove the precipitated lipase, albeit the complete elimination of lipase was difficult, making impossible the purification of the sample by semipreparative-HPLC (See Materials and Methods, Section 3.2.3.3.3.3).

3.2.3.2.4.3. **Route B.** Analytical methyl ester hydrolysis and deacetylation of EGCG-4''-O-triacetylglucuronide methyl ester with Lipase AS (LAS) and Lipase A (LA) to obtain EGCG-4''-O-glucuronide (one pot reaction)

EGCG-4''-*O*-triacetylglucuronide methyl ester (**A16**) (4.12 mg) was dissolved in deoxygenated water (1.8 mL) at different pH (5.0, 6.2 and 7.3) with deoxygenated DMSO as co-solvent (0.4 mL). Porcine Liver Esterase (PLE) (8.24 mg) was added to the solutions with soft stirring at 40 °C (30 min). Then, LAS (from 24.75 to 121.42 mg) was added to the reaction at different **A16**/LAS ratios (1:30, 1:13 and 1:6) or LA (25.5 mg) with a **A16**/LA ratio of 1:6, maintaining the same reaction conditions to obtain EGCG-4''-*O*-glucuronide (**C16**). The reaction time varied from 1.5 to 22.5 h. The reactions were followed by HPLC-DAD and the final products were detected and characterized by HPLC-HR-DAD-ESI-TOF-MS (See Materials and Methods, Section 3.2.3.3.2.2).

3.2.3.2.4.4. Preparative methyl ester hydrolysis of EGCG-4''-*O*-triacetylglucuronide methyl ester to obtain EGCG-4''-*O*-triacetylglucuronide with Porcine Liver Esterase (PLE) and its deacetylation to obtain EGCG-4''-*O*-glucuronide with Lipase A (LA)

EGCG-4''-*O*-triacetylglucuronide methyl ester (**A16**) (34.6 mg) was dissolved in deoxygenated sodium bisphosphate buffer (pH 7.3, 50 mM, 15.6 mL) and deoxygenated DMSO (1.56 mL) as co-solvent. PLE (69.4 mg) was added to the solution with soft stirring

3. Materials and Methods

at 40 °C (30 min) to obtain EGCG-4"-O-triacetylglucuronide (**A16-Me**). After this time, LA (217.3 mg) was added to the reaction maintaining the same reaction conditions to obtain EGCG-4"-O-glucuronide (**C16**). The reaction was followed by HPLC-DAD (14 h) (See Materials and Methods, Section 3.2.3.3.1.2). The sample obtained was lyophilized, dissolved in MeOH (1mL) and purified by semipreparative HPLC (See Materials and Methods, Section 3.2.3.3.3.2) to obtain **C16** (3.7 mg) characterized by ^{1}H-NMR (D$_2$O, 400 MHz).

3.2.3.2.4.5. *Modified Route A. Deacetylation of EGCG-4"-O-triacetylglucuronide methyl ester to obtain EGCG-4"-O-glucuronide methyl ester with immobilized Lipase AS (LAS)*

Immobilization of LAS. Sodium phosphate buffer (pH 6.0; 25 mM; 1.0 mL) was added on a macroporous acrylic resin (1 g) followed by the addition of LAS (100 mg (A), 300 mg (B) and 600 mg (C)). The compounds were mixed softly and the solvent was lyophilized.

EGCG-4"-O-triacetylglucuronide methyl ester (**A16**) (2.07 mg) was dissolved in water at pH 6.0 (25 mM; 0.8 mL) and DMSO as co-solvent (0.2 mL). Immobilized LAS was added to the solution (from 20.1 to 60.4 mg) and softly stirred at 40 °C from 6 to 22.5 h to obtain EGCG-4"-O-glucuronide methyl ester (**B16**). Immobilized LAS was readily removed by filtration with a filter paper. The reactions were followed by HPLC-DAD and HPLC-HR-DAD-ESI-TOF-MS (See Materials and Methods, Section 3.2.3.3.1.3 and 3.2.3.3.2.3).

3.2.3.2.4.6 Methyl ester hydrolysis of *EGCG-4"-O-glucuronide methyl ester to obtain EGCG-4"-O-glucuronide with Porcine Liver Esterase (PLE)*

PLE (4.3 mg) was added to the solution containing EGCG-4"-O-glucuronide methyl ester (**B16**) obtained on the section before (3.2.3.2.4.5). The solution was kept with soft stirring at 40 °C (5.5 h) to obtain EGCG-4"-O-glucuronide (**C16**). The reaction was followed by HPLC-DAD (See Materials and Methods, Section 3.2.3.3.1.3).

3.2.3.3. Analytical methods

3.2.3.3.1. HPLC-DAD methods

3.2.3.3.1.1. HPLC-DAD method used to analyze the Koenigs-Knorr reaction products

HPLC-DAD analyses were performed using a C-18 *Mediterranea Sea18* (5μm, 25x0.46) column from Teknokroma. Solvents employed for all procedures were (A) water and 0.1 % acetic acid and (B) methanol 100 %. The eluting gradient established was from 20 to 80 % of B over 34 min using a flow rate of 0.8 mL min^{-1}, detecting at 214 and 280 nm of wavelength.

*3.2.3.3.1.2. HPLC-DAD method used to analyze the chemical deacetylation, the enzymatic deacetylation obtained with lipases N-435, LA, LIM, PPL, and LAS (**Route A**), and the methyl ester hydrolysis with PLE and later deacetylation obtained with LAS and LA (**Route B**) reaction products*

HPLC-DAD analyses were carried out using a C-18 *Mediterranea Sea18* (5 μm, 25x0.46) column from Teknokroma. Solvents employed for all procedures were (A) water and 0.1 % acetic acid and (B) 80 % CH_3CN, 20 % H_2O and 0.095 % acetic acid. The eluting gradient established was from 5 to 80 % of B over 40 min using a flow rate of 1 mL min^{-1}, detecting at 214 and 280 nm of wavelength.

3.2.3.3.1.3. HPLC-DAD method used to analyze the enzymatic deacetylation products obtained with immobilized LAS

HPLC-DAD analysis was conducted using a C-18 *Mediterranea Sea18* (5 μm, 25x0.46) column from Teknokroma. Solvents employed for all procedures were (A) water and 0.1 % trifluoroacetic acid (TFA) and (B) CH_3CN 80 %, H_2O 20 % and 0.095 % TFA. The eluting gradient established was from 10 to 80 % of B over 30 min using a flow rate of 1 mL min^{-1}, detecting at 214 and 280 nm of wavelength.

3. Materials and Methods

3.2.3.3.2. HPLC-HR-DAD-ESI-TOF-MS methods

3.2.3.3.2.1. HPLC-HR-DAD-ESI-TOF-MS method used to analyze the Koenigs-Knorr reaction products

HPLC-HR-DAD-ESI-TOF-MS analyses were carried out using a column C-18 *Mediterranea Sea18* (5µm, 25x0.46) from Teknokroma. Solvents employed were (A) water and 0.1 % acetic acid and (B) methanol 100 %. The eluting gradient established was from 20 to 80 % of B over 34 min using a flow rate of 0.8 mL min^{-1} detecting at 214 nm and 280 nm of wavelength. The mass detector operated in negative ion mode. The mass conditions were acquisition, *m/z* 100-2000; fragmentor, 175 V; drying gas flow, 10 L min^{-1}; nebulizer pressure, 35 psig; drying gas temperature, 350 °C; and capillary voltage, 3500 V.

*3.2.3.3.2.2. HPLC-HR-DAD-ESI-TOF-MS method used to analyze the chemical deacetylation, the enzymatic deacetylation obtained with lipases N-435, LA, LIM, PPL, and LAS (**Route A**), and the methyl ester hydrolysis reaction with PLE and later deacetylation with LAS and LA (**Route B**) reaction products*

HPLC-HR-DAD-ESI-TOF-MS analyses were performed using a C-18 *Mediterranea Sea18* (5 µm; 4.6 x 250 mm) column from Teknokroma. Solvents employed were (A) water and 0.1 % acetic acid and (B) 80 % CH$_3$CN, 20 % H$_2$O and 0.095 % acetic acid. The eluting gradient established was from 5 to 80 % of B over 40 min using a flow rate of 0.8 mL min^{-1} detecting at 214 nm and 280 nm of wavelength. The mass detector operated in negative ion mode. The mass conditions were acquisition, *m/z* 100-2000; fragmentor, 175 V; drying gas flow, 10 L min^{-1}; nebulizer pressure, 35 psig; drying gas temperature, 350 °C; capillary voltage 3500 V.

3.2.3.3.2.3. HPLC-HR-DAD-ESI-TOF-MS method used to analyze the enzymatic deacetylation reaction products with immobilized LAS

HPLC-HR-DAD-ESI-TOF-MS analyses were conducted using a C-18 LiChospher 100 RP-18 (5 µm, 4 x 250 mm) column from Merck. Solvents employed were (A) water and 0.1 % acetic acid and (B) 80 % CH$_3$CN, 20 % H$_2$O and 0.095 % acetic acid. The eluting gradient established was from 10 to 80 % of B over 30 min using a flow rate of 1 mL min^{-1} detecting at 214 nm and 280 nm of wavelength. The mass detector operated in

negative ion mode. The mass conditions were acquisition, *m/z* 100-2000; fragmentor, 175 V; drying gas flow, 10 L min^{-1}; nebulizer pressure, 35 psig; drying gas temperature, 350 °C; and capillary voltage, 3500 V.

<u>3.2.3.3.3. Semipreparative methods</u>

3.2.3.3.3.1 Semipreparative-HPLC method used to purify the Koenigs-Knorr reaction products

HPLC purification was carried out using a column C-18 X-Terra (10 μM; 19 x 250 mm) from Waters. Solvents employed were those used on the analytic HPLC-DAD (See Materials and Methods, Section 3.2.3.3.1.1) with a eluting gradient from 5 to 20 % of B over 5 min followed by a gradient form 20 to 80 % of B over 40 min using a flow rate of 8 mL min^{-1} detecting at 214 nm of wavelength.

*3.2.3.3.3.2. Semipreparative-HPLC method used to purify the preparative methyl ester hydrolysis of EGCG-4"-O-triacetylglucuronide methyl ester to obtain EGCG-4"-O-triacetylglucuronide with PLE and its deacetylation to obtain EGCG-4"-O-glucuronide with LA (**Route B**) reaction products*

This purification was performed using a column C-18 X-Terra (10 μM; 19 x 250 mm) from Waters. Solvents employed were those used on the analytic HPLC-DAD (See Materials and Methods, Section 3.2.3.3.1.2) with an eluting gradient from 5 to 15 % of B over 5 min, from 15 to 20 % in 40 min, from 20 to 40 % of B in15 min, and from 40 to 95 % of B in 15 min, using a flow rate of 10 mL min^{-1}, detecting at 214 nm of wavelength.

4. Results and Discussion

4.1. Study of the kinetics and the evaluation of the Radical Scavenging Capacity (RSC) of (poly)phenols using HNTTM and TNPTM as chemosensors by Electron-Transfer (ET) reactions

4.1.1. Chemical probes to measure kinetic parameters and the RSC of (poly)phenols by Electron-Transfer (ET)

The Trolox Equivalent Antioxidant Capacity (TEAC) method is the only available assay to measure the radical scavenging activity of (poly)phenols by ET, using the ABTS cation radical (ABTS$^{\bullet+}$). This assay presents some relevant drawbacks (See Introduction, Section 1.5.2.3), and the finding of more generally applicable methods remains as a rewarding challenge.

HNTTM (**4**) was used as a highly oxidant chemosensor to determine the radical scavenging activity of different (poly)phenols (i.e. catechol (**10**), pyrogallol (**11**), EC (**13**), a series of synthetic flavanol thio-derivates, and different fractions of pine bark and grape extracts).(*122, 123, 125, 140*) The radical **4** reacts exclusively by ET and it is a useful tool to quantify the number of electrons transferred by each (poly)phenolic molecule or (poly)phenolic fraction. The use of the radical **4** does not discriminate the (poly)phenols according to their different reactivity due to its high oxidation power.

The tris(2,3,5,6-tetrachloro-4-nitrophenyl)methyl radical (TNPTM, **8**) (**Figure 52**), a stable free radical with a lower oxidant power than that of the radical **4**, was also available in our Laboratory as a potentially selective chemosensor for the most reactive (poly)phenols by ET.

In this thesis, the radicals **4** and **8** were synthesized, characterized, and used to measure kinetic parameters and the RSC of different (poly)phenols and (poly)phenolic fractions by ET. The RSC values obtained were compared with those values obtained with the 1,1-diphenyl-2-picrylhydrazyl radical (DPPH, **9**). Additionally, the reducing-metal power of (poly)phenols was measured with the Ferric Reducing Antioxidant Power (FRAP) method (See Introduction, Section 1.6).

4. Results and Discussion
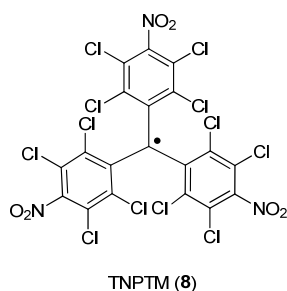
TNPTM (**8**)

Figure 52. Structure of the radical **8**.

4.1.2. Synthesis of tris(2,4,6-trichloro-3,5-dinitrophenyl)methyl radical (HNTTM) and tris(2,3,5,6-tetrachloro-4-dinitrophenyl)methyl radical (TNPTM)

<u>4.1.2.1. Synthesis of HNTTM</u>

The synthesis of HNTTM (**4**) was achieved following the procedure in the Materials and Methods, Section 3.2.1.1.1.

Synthesis of tris(2,4,6-trichlorophenyl)methane

The alkylation reaction of the 1,3,5-trichlorobenzene with chloroform and anhydride aluminum trichloride as catalyst (Friedel-Crafts reaction conditions), gave tris(2,4,6-trichlorophenyl)methane (**1**) in 57 % yield, as a white solid (**Figure 53**).
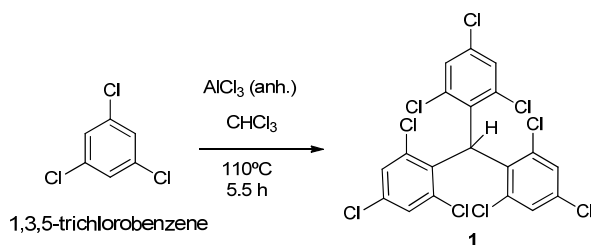
Figure 53. Friedel-Crafts reaction to obtain **1** from 1,3,5-trichlorobenzene.

<u>Synthesis of the tris(2,4,6-trichloro-3,5-dinitrophenyl)methane (α*H*-HNTTM)</u>

Nitration of **1** was achieved by electrophylic aromatic substitution (S$_E$2) of the aromatic protons by nitronium ions (NO$^+$). Nitronium ions were produced by the

activation of fuming nitric acid with fuming sulfuric acid. α*H*-HNTTM (**2**) was obtained in 85 % yield, as a white solid (**Figure 54**).
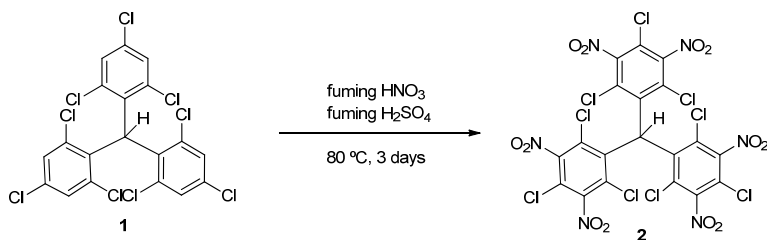
Figure 54. Nitration of **1**.

Synthesis of the tris (2,4,6-trichloro-3,5-dinitrophenyl)methyl radical (HNTTM)

The carbanion **3** was obtained from **2** by deprotonation with tetrabutylammonium hydroxide (TBAH) in acetone. The radical **4** was obtained by oxidation with chromium (VI) oxide in 63 % yield, as an orange solid (**Figure 55**).
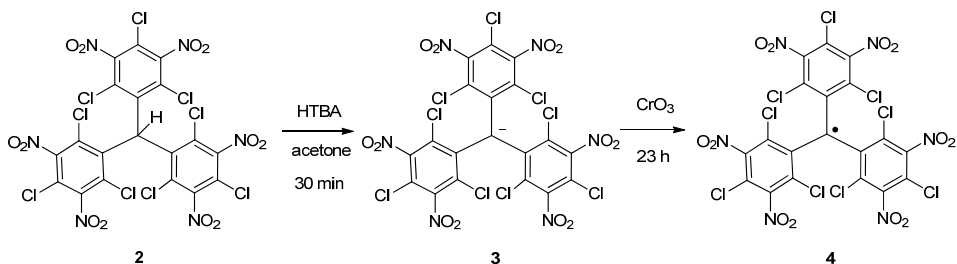
Figure 55. Reduction of **2** to obtain **3** and its oxidation to yield **4**.

4.1.2.2. Synthesis of TNPTM

The synthesis of TNPTM (**8**) was achieveded following the procedure of the Materials and Methods, Section 3.2.1.1.2.

Synthesis of tris(2,3,5,6-tetrachlorophenyl)methane (**5**)

The alkylation of 1,2,4,5-tetrachlorobenzene with chloroform and aluminum trichloride as catalyst (Friedel-Crafts reaction conditions), gave tris(2,3,5,6-tetrachlorophenyl)methane (**5**) in 56 % yield, as a white solid (**Figure 56**).

4. Results and Discussion
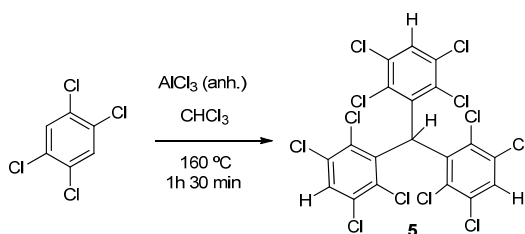
Figure 56. Friedel-Crafts reaction to obtain **5** from 1,2,4,5-tetrachlorobenzene.

Synthesis of tris(2,3,5,6-tetrachloro-4-nitrophenyl)methane (α*H*-TNPTM)

Nitration of **5** was achieved by electrophylic aromatic substitution (S$_E$2) of aromatic protons by nitronium ions (NO$_2$$^+$) to obtain α*H*-TNPTM (**6**) in 81 % yield, as a white solid (**Figure 57**).

Figure 57. Nitration of **5**.

Synthesis of the tris(2,3,5,6-tetrachloro-4-nitrophenyl)methyl radical (TNPTM)

The carbanion **7** was obtained from **6** by deprotonation with tetrabutylammonium hydroxide (TBAH) in THF. The final product TNPTM (**8**) was obtained by oxidation with *p*-chloranil in 88 % yield, as a red solid (**Figure 58**).

Figure 58. Reduction of **6** to obtain **7** and its oxidation to yield **8**.

The syntheses of the radicals **4** and **8** were simple, inexpensive and the radicals were obtained in good yields, and in a very reproducible manner. Yang and co-workers obtained the radical **4** in similar yield using the procedure described by us.(*141*)

4.1.3. HNTTM as chemosensor of (poly)phenols by Electron-Transfer (ET)

In previous works in our group, HNTTM (**4**) was thoroughly characterized by Electron Paramagnetic Resonance (EPR), Ultraviolet-Visible (UV-Vis), and Infrared (IR) spectroscopies and elemental analysis. Its redox potential was determined by Cyclic Voltammetry (CV).(*122, 123*) The most important characteristic of the radical **4** is its exclusive reactivity by ET. This feature was demonstrated, in this thesis, 1) by its inalterability in the presence of toluene, a good hydrogen donor molecule, contrary to DPPH (**9**) which gives *H*-DPPH by hydrogen abstraction (*142*) (NH absorption band at 3286 cm^{-1} in the infrared (IR) spectrum of the resulting product)(*143*) (See Materials and Methods, Sections 3.2.1.4.1 and 3.2.1.4.2 and Annex 1. A and C and Annex 2. A and C), and 2) by the detection (UV-Vis) of the stable anion **3** in the presence of catechol (**10**), (–)-epicatechin (EC, **13**), and two EC thio-derivates in CHCl₃/MeOH (2:1).(*122, 123*) Interestingly, the X-ray crystallography of the salt of **3** with tetrabuthylammonium (Bu₄N$^+$) as counter ion was obtained and analyzed in this thesis, confirming the stability of the reduced species **3**. The Hydrogen Atom Transfer (HAT) reaction from toluene is not feasible by the radical **4** because of the steric hindrance shown by the voluminous *ortho*-chlorine atoms around the trivalent carbon.(*144*)

4.1.3.1. Physicochemical properties of HNTTM

The study of the physicochemical properties of HNTTM (**4**) was essential to provide a supporting base to use the radical **4** as chemosensor of the radical scavenging activity of (poly)phenols.

4.1.3.1.1. Electron-accepting ability of HNTTM

The electron-accepting ability of HNTTM (**4**) was determined by CV. HNTTM was reduced and oxidized in a quasi-reversible process (E_p^a-E_p^c > 60 mV, E_p^a, anodic peak potential, E_p^c, cathodic peak potential), and showed strong oxidant properties in CH₂Cl₂ solution.(*123*) The strong oxidant power and the reversibility of the electrochemical process is indicative of the great stability of both the radical **4** and its reduced anionic species **3**. The high standard potential (E°) value in CV is a consequence of the strong

4. Results and Discussion

electron-acceptor properties of the six *m*-nitro groups in the phenyl rings, as it is shown in **Table 3** that compares the potential value of the radical **4** with that of its non-nitrated precursor, the tris(2,4,6-trichlorotriphenyl)methyl radical (TTM).(*122*) The nitro group has traditionally been considered as a strong electron-withdrawing group, with two modes of action, inductive and resonance effects, being the first effect the strongest in the particular case of the radical **4** (the twisted phenyl rings around the sp^2 central carbon atom partially inhibits the resonant effect (See below)).

Table 3. Electrochemical parameters for the reduction of the radicals TTM and **4** in CH_2Cl_2 (10^{-3} M) with 0.1 M Bu_4NClO_4 on Pt at scan rate of 100 mV s^{-1} vs SCE (NaCl-saturated calomel electrode).

Radicals	$E°/V$ ($E_p{}^a$-$E_p{}^c$/mV)[a]
TTM	-0.66 (100)
4	0.58 (90)

[a]Values of the difference between $E_p{}^a$ and $E_p{}^c$ of the radical showing quasi-reversible reduction processes.

4.1.3.1.2. Characterization of the salt of tris(2,4,6-trichloro-3,5-dinitrophenyl)carbanion (**3**) with tetrabutylammonium as counter ion, by X-ray crystallography

Tetrabutylammonium hydroxide (TBAH) was used as electron-donor to reduce HNTTM (**4**) to the triphenylcarbanion **3** as Bu_4N^+ ⁻HNTTM salt form. The one-electron reducing power of the hydroxide ion (⁻OH), assisted by the presence of powerful electron-acceptor substrates in polar solvents other than water, such as DMSO, HMPT, and THF has been reported in the literature.(*120, 145, 146*)

The reaction of **4** with an aqueous solution of TBAH in THF yielded a strong blue solution of the salt Bu_4N^+⁻HNTTM (salt of **3**). The Bu_4N^+ salt of **3** is very stable in solid and in solution at room temperature (rt). The UV-Vis spectrum of the Bu_4N^+ salt of **3** was obtained in $CHCl_3$ solution showing a typical broad band at λ (ε)= 499 (26700) nm (dm^3 mol^{-1} cm^{-1}) (UV-Vis is included as Annex 3). The thermal stability was measured by thermogravimetric (TG) and differential scanning calorimetry (DSC) analysis,

demonstrating its stability at temperatures up to 273 °C (TG and DSC spectra are included as Annex 4).

The Bu_4N^+ salt of **3** yields small, dark, violet needles by slow evaporation of a saturated solution in MeOH (See Materials and Methods, Section 3.2.1.2.1). The molecular and crystal structure of this salt was solved from an X-ray powder diffraction pattern measured with conventional laboratory equipment (See Materials and Methods, Section 3.1.2.1) from the *Institut de Ciència de Materials (CSIC)* form the *Universitat Autònoma de Barcelona (UAB)*. The perspective view with atom numbering is shown in **Figure 59**.(*144*)

Figure 59. Perspective view of the salt of **3** with atom numbering.

The most reliable and useful information supplied by the refinement of the structure obtained by X-ray were the torsion angles and the dihedral angles between mean planes describing the overall geometry of the molecule (**Table 4**) (Annex 5 includes extra information about the X-ray of Bu_4N^+ ⁻HNTTM). All distances and bond angles of the trivalent carbon (C7) with the three aromatic carbons (C4, C4', C4") are in accordance with a sp^2 hybridation of the central carbon (C7) forming the plane **D** (**Figure 60**).

Hibridation sp^2

Figure 60. Plane **D**.

4. Results and Discussion

The molecule is formed geometrically by 10 planes: plane D, three planes corresponding to the phenyl rings (A, A', A''), these phenyl planes are twisted around the plane D with angles of 51°, and six planes corresponding to the nitro groups (NO2) (B, C, B', C', B'',C'') (**Figure 59**). The NO2 planes are forced out of the phenyl planes ($^-80°$) by the presence of *ortho*-chlorine atoms (**Table 4**).

Table 4. Dihedral angles (degrees (°)) between planes[a] of the molecular structure of HNTTM anion (**3**).

A-D (=A'-D = A''-D)	A-B (=A'-B' = A''-B'')	A-C (=A'-C' = A''-C'')
51	79	80

[a]Planes are defined as follows: A (C1, C2, C3, C4, C5, C6, C7, N1 N2), B (C2, N1, O2, O3), C (C6, N2, O3, O4), D (C4, C4', C4'', C7).

4.1.3.2. Reactivity of catechol and pyrogallol with HNTTM

The reactivity of catechol (**10**) and pyrogallol (**11**) (**Figure 61**) with the radical **4** was determined by the evaluation of the rate constant (k) and the Radical Scavenging Capacity (RSC) The studies to determine the RSC of (poly)phenols using DPPH (**9**) as a persistent free radical sensor, do not provide clear information of the mechanism involved because both mechanisms, Hydrogen Atom Transfer (HAT) and Electron-Transfer (ET) have been proposed (See Introduction, Section 1.5.1 and Section 1.5.2.1). As the radical **4** cannot directly abstract hydrogen atoms from H-donating compounds as it was demonstrated in this thesis, it can be used as a privileged tool to evaluate the reactivity of (poly)phenols by ET exclusively.

Figure 61. Structures of **10** and **11**.

4.1.3.2.1. Reactivity of catechol and pyrogallol with HNTTM in solvents with different polarity

The reactivity of simple phenols such as catechol (**10**) and pyrogallol (**11**) with HNTTM (**4**) was measured from equimolecular solutions (0.12 M) of both reactants in solvents of different polarity such as the apolar benzene, the polar and aprotic $CHCl_3$ and the ionizable mixture $CHCl_3$/MeOH (2:1) (methanol is a ionizable solvent, able to accept/release protons). The experiments were conducted for short (4 h) and long (47 h) reaction times to identify any possible HNTTM derived products of the reaction. The experiments were carried out as it is shown in the Materials and Methods, Section 3.2.1.8, and the reactivity results obtained are summarized in **Table 5**.

Table 5. Reactivity of catechol and pyrogallol with HNTTM in benzene, $CHCl_3$ and $CHCl_3$/MeOH (2:1) (equimolar solutions)[a].

Solvent	Time (h)	Simple phenol			
		10		**11**	
		4 (%)[b]	**2 (%)**[c]	**4 (%)**[b]	**2 (%)**[c]
Benzene	4	92	8	76	24
	47	71	29	51	49
$CHCl_3$	4	96	4	75	25
	47	73	27	50	50
$CHCl_3$/MeOH (2:1)	4	34	66	< 5	> 95
	47	11	89	0	100

[a]Initial concentration of (poly)phenol and the radical **4**, 0.12 M; [b]Recovered radical; [c]α*H*-HNTTM (**2**) reduced species of **4**.

The reactions were analyzed by UV-Vis spectroscopy and the products were characterized by IR spectroscopy. All reactions were very clean and simple processes yielding the diamagnetic species α*H*-HNTTM (**2**) as the result of the reduction of **4** by the (poly)phenols. In some of the tested experiments, the compounds reacted very slowly or did not react at all, and part of the initial radical **4** was recovered.

From the results in **Table 5**, it was concluded that pyrogallol (**11**) reacts with the radical **4** faster than catechol (**10**) in the tested solvents, and the reaction was significantly faster in the $CHCl_3$/MeOH (2:1) mixture than in plain benzene or $CHCl_3$.

4. Results and Discussion

<u>4.1.3.2.2. Kinetics and Radical Scavenging Capacity (RSC) of catechol and pyrogallol measured with HNTTM in solvents with different polarity</u>

The rate constant values (k) and the number of electrons transferred (n_e) per molecule of (poly)phenol (RSC) were determined in reactions of catechol (**10**) or pyrogallol (**11**) with HNTTM (**4**) in benzene, $CHCl_3$ and $CHCl_3$/MeOH (2:1) as solvents (Graphics of the kinetics are shown in Annex 6). The reactions were monitored by UV-Vis spectroscopy, recording the decay of the maximum absorbance of the radical **4** (λ_{max} of 387 nm in benzene, and at 384 nm in $CHCl_3$ and $CHCl_3$/MeOH (2:1)) as a consequence of the electron addition to give the anion **3**. The experiments were carried out with a **4**/(poly)phenol molar ratio of ⁻5:1 and an initial concentration of **4** of 54 μM. The reactions were completed when the absorptivity on the UV-Vis spectrum remained constant. The experiments were carried out following the procedure of the Materials and Methods, Section 3.2.1.10 and the rate constants (k) and the n_e values for the reactions of the simple phenols **10** and **11** with **4** were estimated by using a simple kinetic model reported by Dangles *et al.*(*116*). Results are shown in **Table 6**.

In the course of the reducing processes in $CHCl_3$/MeOH (2:1) two steps of the decay of the absorbance of HNTTM (**4**) were observed with both simple phenols **10** and **11**, the first step being faster than the second. On the other hand, a single slow step can be distinguished for both simple phenols (**10** and **11**) in benzene and in $CHCl_3$ solvents (See Annex 6). Rate constant values in $CHCl_3$/MeOH (2:1) were calculated for the fast step (k_1).

Table 6. Observed rate constants (k_1 or k) and number of electrons transferred (n_e) per molecule of simple phenol in the reactions[a] of catechol or pyrogallol with HNTTM in solvents with different polarity.

Simple phenol	Solvent	4/(poly)phenol molar ratio	k_1[b] k[c] ($M^{-1} s^{-1}$)	n_e[d]
10	CHCl$_3$/MeOH (2:1)	5.1	1123 ± 95[b]	1.9
11	CHCl$_3$/MeOH (2:1)	4.6	5115 ± 82[b]	3.1
10	Benzene	5.1	0.41 ± 0.2[c]	0.5[e]
11	Benzene	5.1	14.5 ± 0.4[c]	3.0
10	CHCl$_3$	5.0	0.47 ± 0.1[c]	0.3[e]
11	CHCl$_3$	5.1	0.95 ± 0.4[c]	0.7[e]

[a]Number of assays performed by each (poly)phenol, n= 2-4. k and n_e calculated at a reaction time of 5.5 h. Initial concentrations between 52.1–55.9 μM and 10.3–10.9 μM (molar ratio, 5:1) for the radical **4** and (poly)phenols, respectively; [b]Reactions with two kinetic steps; (k_1) rate constant of the first step; [c]Reactions with one distinguishable kinetic step; (k) total rate constant; [d]Number of electrons transferred per molecule of phenol; [e]Unfinished reactions. (± SD =Standard Deviation).

From the corresponding RSC values, a molecule of catechol (**10**) reduces two molecules of the radical **4** in CHCl$_3$/MeOH (2:1), whereas a pyrogallol (**11**) molecule reduces three molecules of the radical **4** in CHCl$_3$/MeOH (2:1) and in benzene. Hence, the number of electrons transferred (n_e) is in accordance with the number of hydroxyl groups of the simple phenols **10** and **11**. It is confirmed that the rate of reaction of the radical **4** with pyrogallol (**11**) is higher than the reactivity with catechol (**10**); approximately 5-fold higher in CHCl$_3$/MeOH (2:1), 35-fold higher in benzene, and 2-fold higher in CHCl$_3$. Generally the reactivity of the radical **4** with either **11** or **10** follows the order CHCl$_3$/MeOH (2:1) >> benzene ≈ CHCl$_3$. Kinetics of **10** in benzene and CHCl$_3$, and **11** in CHCl$_3$ were very slow (k ≤ 0.95 $M^{-1} s^{-1}$) and the reactions were not completed at the time tested (5.5 h).

4. Results and Discussion

4.1.3.2.3. Electrochemical parameters of the reactions of catechol and pyrogallol with HNTTM in solvents with different polarity

The redox potential of reactants, the thermodynamic behavior, and the Gibbs' free energy of the reactions between catechol (**10**) or pyrogallol (**11**) with HNTTM (**4**) were determined in different solvents.

A. *Determination of the redox potentials of catechol, pyrogallol, their corresponding anions and HNTTM in solvents with different polarity*

Each (poly)phenol presents a different oxidation potential, which may vary depending on the solvent used. The lower the oxidation potential, the easier the oxidation of the molecule. (Poly)phenols dissolved in ionizable solvents are partially ionized, due to the acidity of the   groups, losing a proton to give the corresponding anions, species more reactive than the neutral entities. The increased reducing activity of these species in $CHCl_3$/MeOH (2:1) can be confirmed by obtaining the oxidation potentials of the same in alkaline conditions.

Standard (E^o) and cathodic peak potentials ($E_p{}^c$) of the radical **4** (oxidant species) and anodic peak potential ($E_p{}^a$) of the neutral and anionic forms of the simple phenols **10** and **11** (reducing species) were determined in different solvents by Cyclic Voltammetry (CV) at the *Departament de Química Física* of the *Universitat de Barcelona* (See Materials and Methods, Section 3.2.1.6 and Votammograms are included as Annex 7).

Table 7. Electrochemical parameters for the oxidation of the simple phenols **10** and **11** and their corresponding anions, and for the reduction of the radical **4** in organic solvents.

Solvent	10 E_P^a/V[a] (E_P^a/V,anion)[b]	11 E_P^a/V[a] (E_P^a/V,anion)[b]	4 E^o/V[a] (E_P^c/V)[a]
Benzene	1.64	–[c]	0.65 (0.48)
CHCl$_3$	1.27	1.15	0.58 (0.50)
CHCl$_3$/MeOH (2:1)	1.00 (0.20)	0.78 (0.03)	0.55 (0.46)

[a] E_p^a, E_p^c and $E°$ for the substrate (10^{-3} M) with 0.3 and 0.2 M of THAPF$_6$ in benzene for **10** and **11**, respectively, and 0.1 M TBAP in CHCl$_3$ or CHCl$_3$/MeOH (2:1), on Pt at scan rates of 100 mV s^{-1} and 25.0 °C; [b]E_p^a of catechol (**10**) and pyrogallol (**11**) (10^{-3} M) with an excess of 4 and 3 mM, respectively, of tetrabutylammonium hydroxide (TBAH) at scan rates of 100 mV s^{-1}; [c]Not determined due to partial adsorption of **11** on Pt.

Potential values represented in **Table 7** show that the anionic forms of simple phenols **10** or **11** (E_P^a values obtained under alkaline conditions) are much more oxidizable than the neutral forms.

B. *Exergonic or endergonic character of the reactions of catechol or pyrogallol with HNTTM*

An electrochemical reaction is thermodynamically allowed when the difference between the E_p^c of the oxidant (e.g. HNTTM) and the E_p^a of the reducing agent (e.g. (poly)phenols) is a positive value (E_p^c-E_p^a > 0). **Table 8** summarizes the E_p^c-E_p^a values for the reactions of the simple phenols **10** and **11** with the radical **4** in different solvents.

4. Results and Discussion

Table 8. $E_p{}^c$-$E_p{}^a$ values for the substrates used in the reactions of **10** or **11** with the radical **4** in different solvents. $E_p{}^c$ and $E_p{}^a$ values are found in **Table 7**.

Simple phenol	10	11
Solvent	$E_p{}^c$-$E_p{}^a/mV$ [a] ($E_p{}^c$-$E_p{}^a/mV$ [b])	$E_p{}^c$-$E_p{}^a/mV$ [a] ($E_p{}^c$-$E_p{}^a/mV$ [b])
Benzene	-1.16	–
CHCl₃	-0.77	-0.65
CHCl₃/MeOH (2:1)	-0.54 (0.26)	-0.32 (0.43)

[a] $E_p{}^c$-$E_p{}^a$ values obtained from the $E_p{}^c$ of **4** and from the $E_p{}^a$ of the molecular form of simple phenols **10** and **11** in different solvents; [b] $E_p{}^c$-$E_p{}^a$ values obtained from the $E_p{}^c$ of **4** and from the $E_p{}^a$ of the anions of **10** or **11** in CHCl₃/MeOH (2:1).

From results shown above, only the reactions of the simple phenols **10** and **11** with the radical **4** in CHCl₃/MeOH (2:1) are thermodynamically allowed (exergonics) reactions owing to their $E_p{}^c$-$E_p{}^a$ positive values. The partial ionization of the simple phenols **10** and **11** by MeOH may explain this result. The charge species (PhO⁻) (**Figure 62**) are much more oxidazable than the corresponding molecular species (PhOH).

C. Gibbs energy of the reactions of catechol or pyrogallol with HNTTM in CHCl₃/MeOH (2:1) as solvent.

The Gibbs energy is a function of thermodynamic potential that indicates the spontaneity of a chemical reaction. If $\Delta G_{et} < 0$, the reaction is exergonic or spontaneous.

$$\Delta G_{et} = -\left(E_p^c - E_p^a \right) \times F$$

F (Faraday constant, 96487 C mol⁻¹)

Table 9. Gibbs energy calculated for reactions of the anions of **10** or **11** with HNTTM (**4**) in CHCl₃/MeOH (2:1).

(Poly)phenol	ΔG_{et} (J mol⁻¹)
anion **10**	-20262
anion **11**	-38595

112
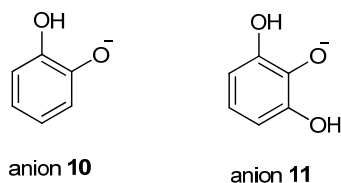
anion **10**

anion **11**

Figure 62. Structure of the anion **10** and the
most probable structure of the anion **11**.

In conclusion, the values in **Tables 8** and **9** show that the constant rates (k or k_1) of
the reaction of the radical **4** with the simple phenols **10** or **11** in benzene, CHCl$_3$ and in
CHCl$_3$/MeOH (2:1) are in accordance with their different $E_p{}^a$ values obtained by CV, $E_p{}^a$ (**11**
and its anion) < $E_p{}^a$ (**10** and its anion), respectively. The $E_p{}^c$-$E_p{}^a$ values of the difference
between peak potentials of the radical **4** and the simple phenols **10** or **11** demonstrate that
only reactions of **10** or **11** with the radical **4** in CHCl$_3$/MeOH (2:1) are thermodynamically
allowed, and that the reaction of **11** with the radical **4** is the most exergonic. On the other
hand, radical **4** slowly reacts with pyrogallol in benzene, but the Gibbs energy's value for
this reaction is not calculated due to the difficulty to determine the $E_p{}^a$ value in this
conditions (**Table 7**).

<u>4.1.3.2.4. Reaction mechanisms of catechol or pyrogallol with HNTTM in solvents with
different polarity</u>

- *Reaction of catechol or pyrogallol with HNTTM in CHCl$_3$/MeOH (2:1)*

The rather fast reaction of catechol (**10**) or pyrogallol (**11**) with HNTTM (**4**) in
CHCl$_3$/MeOH (2:1) is due to the presence in the medium of much more reactive species,
the phenolic anions (PhO$^-$). These species are generated by partial ionization of the
neutral phenol. As mentioned above, (PhO$^-$) is more easily oxidized than (PhOH) (**Table
7**). The electron-deficient radical **4** reacts very fast by Electron-Transfer (ET) with the
generally low concentration of (PhO$^-$) present in equilibrium with (PhOH). Thus, the
Sequential Proton Loss Electron Transfer (SPLET) mechanism (See Introduction, Section
1.5.1), first reported by Litwinienko and co-workers, and Foti and co-workers, takes place
in these processes.(*118, 147*)

4. Results and Discussion

The presence of the HNTTM anion (**3**) in the reactions between the simple phenols **10** or **11** with the radical **4**, has been confirmed by UV-Vis spectroscopy. **Figure 63** shows the UV-Vis spectrum of the products present in the course of the reaction between the radical **4** and the simple phenol **11** in CHCl₃/MeOH (2:1). The band corresponding to the reaction mixture resulting after a few minutes of mixing both reactants **4** and **11** together with a combination of the spectra of single species HNTTM (**4**) and HNTTM anion (**3**) are shown in **Figure 63**. The simulated spectra was a linear combination of the spectrum of **4** (19 %) and **3** (81 %), showing that both species are present in solution.
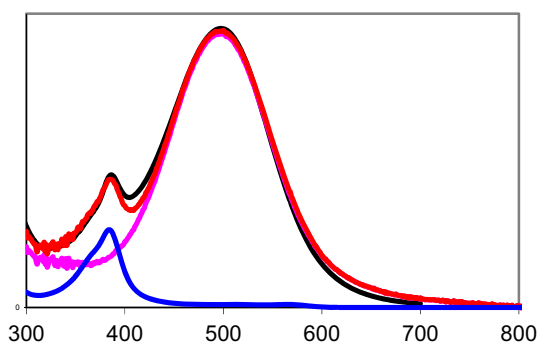
Figure 63. The absorption spectra of radical **4** (blue) (λ= 384 nm), **3** (purple) (λ = 494 nm), **4** + **11** in CHCl₃/MeOH (2:1) after a few minutes of reaction (black), and a simulation of the black spectrum by a combination of **4** and **3** (red). **4**/phenol molar ratio of ⁻5:1, and an initial concentration of **4** of 54 µM.

Proposed reaction mechanism of catechol with HNTTM: **Figure 64** shows the proposed Sequential Proton Loss Electron Transfer (SPLET) mechanism for the reaction of the simple phenol **10** with the radical **4**. In this reaction, each molecule of **10** reduces two molecules of **4** (**Table 6**) in accordance with the number of hydroxyl groups of the simple phenol **10** to give α*H*-HNTTM (**2**) and the *ortho*-quinone (**10A**).
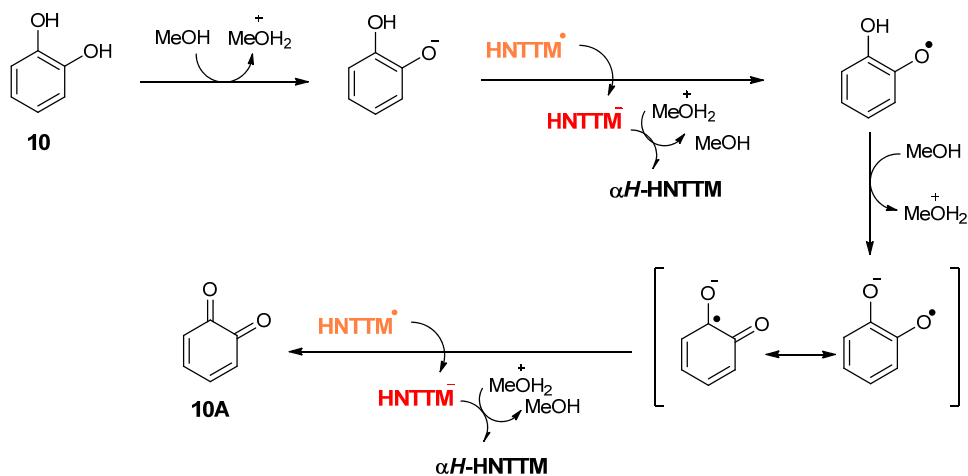
Figure 64. Proposed SPLET mechanism (*148*) of the simple phenol **10** with the radical **4** in CHCl₃/MeOH (2:1).

Proposed reaction mechanism of pyrogallol with HNTTM: **Figure 65** shows the SPLET mechanism for the reaction of the simple phenol **11** with the radical **4**. In this reaction, each molecule of **11** reduces 3 molecules of **4** (**Table 6**) in accordance with the number of hydroxyl groups of **11** albeit not all electrons have to be provided from each hydroxyl. From this result, three different mechanisms may be proposed:
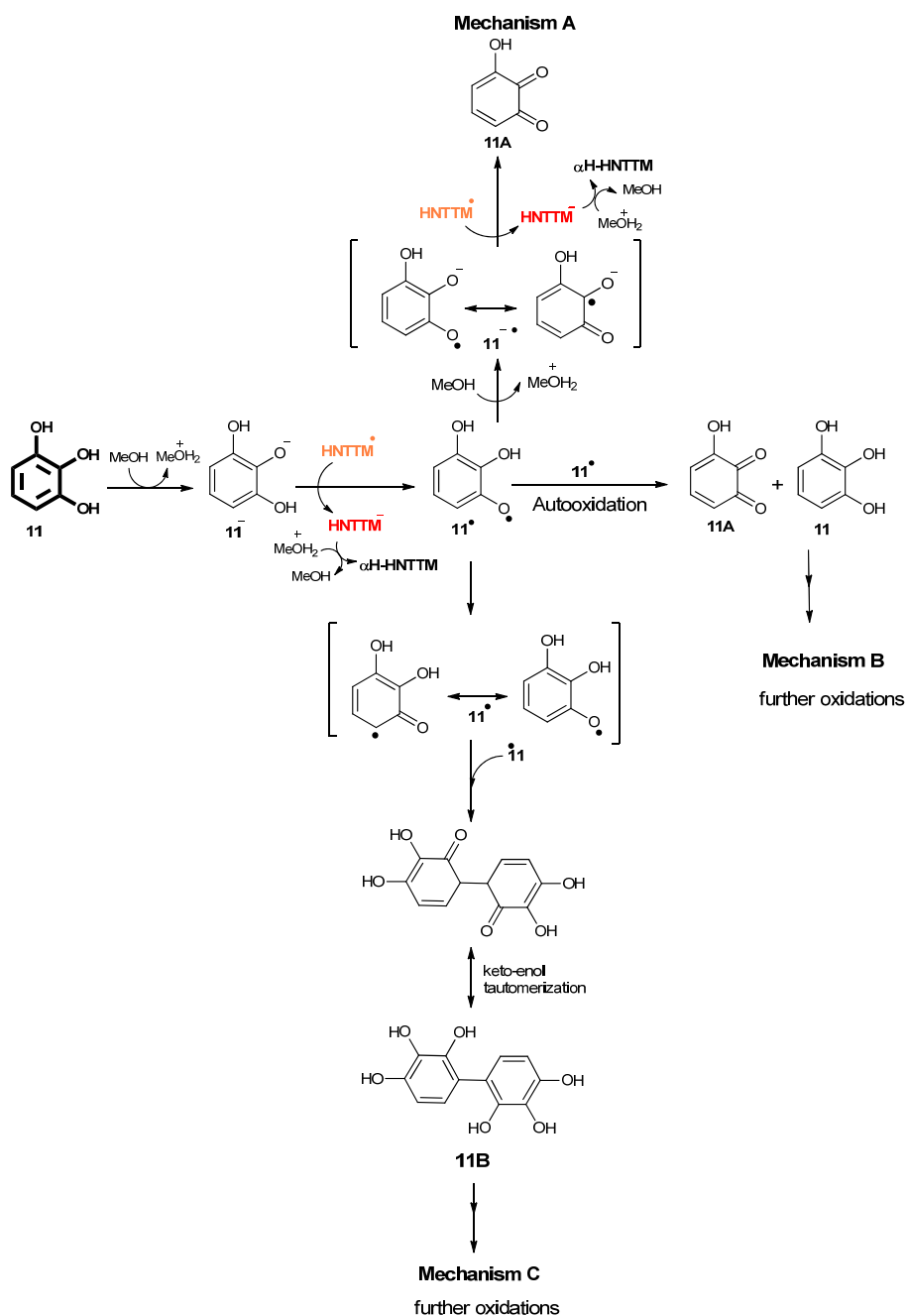
Figure 65. SPLET mechanisms proposed for reaction of the simple phenol **11** with the radical **4** in CHCl₃/MeOH (2:1).

In mechanism A, two molecules of the radical **4** are scavenged by a molecule of **11** obtaining **11A** (3-hydroxi-*o*-quinone) and two molecules of α*H*-HNTTM (**2**) as products. In mechanism B, two molecules of radical **4** are reduced by two molecules of pyrogallol (**11**) giving **11A** and **11**, the later suffering further oxidations. In the last mechanism proposed, the mechanism C, two molecules of radical **4** are reduced by two molecules of pyrogallol (**11**), and differently to mechanism B, the product **11B** is formed by a termination step between two pyrogallol radicals (**11•**). The product **11B** can suffer further oxidations. Zhu *et al.* purified and identified the dimeric theasinensin (**11B**) (⁻5 % of yield) as a product of the reaction between pyrogallol (**11**) and DPPH (**9**). (*149*) To sum up, one, two, and/or the three proposed SPLET mechanisms are suitable for the scavenging reaction of **11** with **4**, and further oxidation reactions should be considered to attain the experimental n_e value.

In summary, the SPLET mechanism of the reactions of the simple phenols **10** and **11** as scavengers of the radical **4** in CHCl$_3$/MeOH (2:1) is supported by electrochemical analysis (exergonic reaction only for anionic forms of the phenols) and by UV-Vis spectroscopy showing the HNTTM anion (**3**) as the stable and characteristic intermediate.

- *Reaction of catechol and pyrogallol with HNTTM in benzene*

Proposed reaction mechanism of catechol with HNTTM:

Benzene is a non-ionizable solvent with a very low dielectric constant and it shows weak interactions with charged and polar species. The very slow reaction of catechol (**10**) with HNTTM (**4**) in benzene was followed by UV-Vis spectroscopy, and the formation of the reduced species of **4**, the HNTTM anion (**3**), was not observed. Since the radical **4** does not react by Hydrogen Atom Transfer (HAT), a concerted mechanism of electron- and proton-transfer is proposed. The Proton-Coupled Electron Transfer (PCET) mechanism (See Introduction, Section 1.5.1) was suggested as possible reaction mechanism between the simple phenol **10** and the radical **4** in benzene.

Proposed reaction mechanism of pyrogallol with HNTTM:

The slow reaction of pyrogallol (**11**) with HNTTM (**4**) in benzene deserves special mention. The reaction shows a low rate constant (k) value (**Table 6**), albeit the generation of the corresponding HNTTM anion (**3**) is observed by UV-Vis spectroscopy, as it is shown in **Figure 66**.
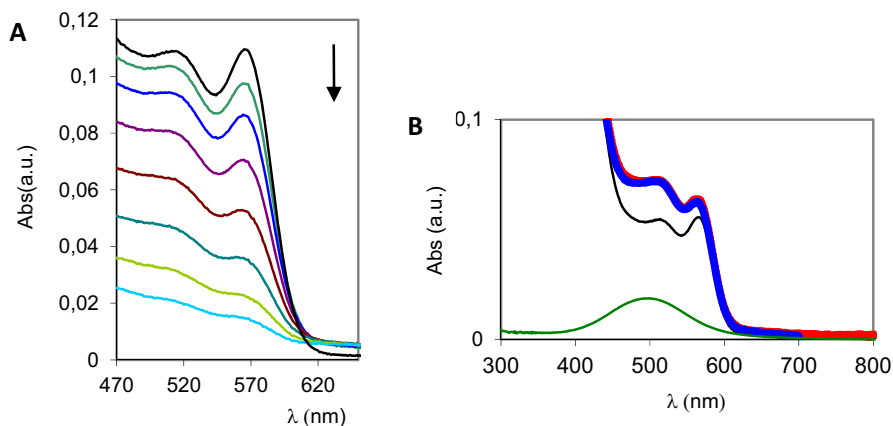
Figure 66. A. Evolution of the lowest-energy band intensity of a solution of radical **4** (120.2 μM) and pyrogallol (**11**) (1.63 mM) in benzene at different times (intervals of 10 min) (first band in black). **B.** The lowest-energy band in the absorption spectra of **4** (black), **3** (green) (λ, 499 nm), theoretical combination: **4** + **3** (red), and **4** (54.0 μM) + **11** (10.6 μM) in benzene after three minutes of reaction (blue).

In **Figure 66 B**, the lowest-energy band (blue band) for the products resulting after a few minutes of mixing of both reactants, HNTTM (**4**) and pyrogallol (**11**), are displayed together with a simulation (red). The simulated spectrum was obtained by a linear combination of the spectra of the radical **4** and its anion **3** showing that both species are present in solution in ˜99 % and ˜1 %, respectively. **Figure 66 A**, displays the evolution of the absorption band of a more concentrated solution of the radical **4** and the simple phenol **11**, clearly observing the presence of the small absorption band of the anion **3** (increase of the band at λ= 520 nm with time) within the very large band of the radical **4**.

By CV we could not obtain the $E_p{}^a$ of pyrogallol (**11**) in benzene because of the partial absorption of the simple phenol **11** on the Pt electrode. For this reason, the anodic onset potential ($E_o{}^a$) was obtained instead (See Materials and Methods, Section 3.2.1.6 and Annex 7). The $E_o{}^a$ of the simple phenol **11** and the cathodic onset potential ($E_o{}^c$) of the radical **4** in benzene are $E_o{}^a$ ˜ 1.1V and $E_o{}^c$ ˜0.75V, respectively. The result obtained from the $E_o{}^c - E_o{}^a$ = −0.35, is a negative value that indicates that the Electron-Transfer (ET) reaction between **11** and **4** in benzene would be endergonic. This seems to contradict the experimental results. To overcome this contradiction, it is reasonable to envisage the

formation of a complex intermediate between both species. The strength of the interactions between the phenol **11** and the radical **4** may affect the electrochemistry of both reactants providing an efficient intermolecular ET from the simple phenol **11** to the radical **4**.(*150*) This intermediate may be generated by hydrogen-bonding between the nitro oxygen atoms of radical **4** and the hydroxyl hydrogen atoms of **11**, increasing the electron density on the phenolic oxygen and making it easier to be oxidized (**Figure 67**).
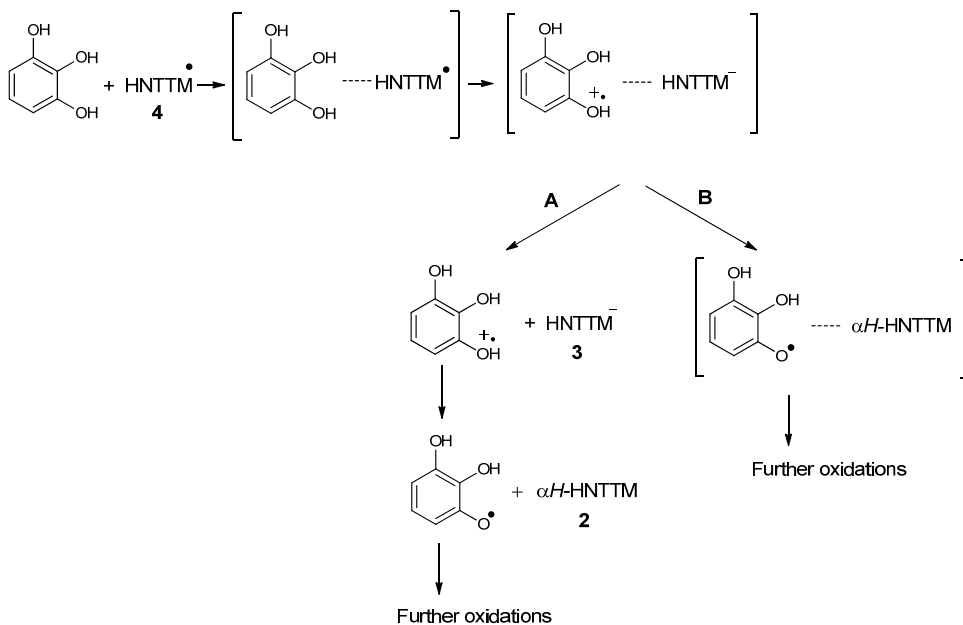
Figure 67. Proposed mechanism for the reaction between **11** and **4** in benzene.

This sequence of steps explains favorably the detection of the HNTTM anion (**3**) by UV-Vis spectroscopy (**Figure 66**). Thus, once the electron is transferred within the complex, it rapidly dissociates leading to the free ions. The HNTTM anion (**3**) has been clearly detected by UV-Vis spectroscopy before the protonation of **3** takes place (**Figure 67,** pathway **A**). However, it is not discarded that the protonation of **3** might take place in part within the complex as the acidity of the phenol significantly increases after one-electron oxidation to the radical cation (Ph(OH)$_2$(OH$^{\bullet+}$)) (PCET mechanism, See Introduction, Section 1.5.1) (**Figure 67,** pathway **B**).(*144*)

4. Results and Discussion

- *Reaction of catechol and pyrogallol with HNTTM in CHCl₃*

   The HNTTM anion (**3**) formed by Electron-Transfer (ET) of the (poly)phenol to HNTTM (**4**) was not detected by UV-Vis spectroscopy in the reactions of catechol (**10**) or pyrogallol (**11**) with the radical **4** in CHCl₃. As mentioned above, as the radical **4** does not react by Hydrogen Atom Transfer (HAT), consequently, a concerted mechanism, such as the PCET, (See Introduction, Section 1.5.1) would explain the reactivity between the phenols **10** or **11** with the radical **4** in CHCl₃.

   To sum up, the reactions between the simple phenols **10** or **11** with the radical **4** in different solvents occur by ET to the SOMO (Semi Occupied Molecular Orbital) of **4** to give the charged HNTTM anion (**3**), which is protonated to α*H*-HNTTM (**2**). In ionizable solvents (i.e. CHCl₃/MeOH (2:1)), the ET is a very rapid process and the real electron-donating species are the charged phenolates of **10** and **11**, whereas in non-ionizable solvents (CHCl₃ and benzene), the ET is slower and facilitated by an assumed intermediate complex between the phenols **10** or **11** with the radical **4**. The formation of this intermediate would account for the low concentration observed for the anion **3**, which is rapidly protonated after the ET.

4.1.4. Radical Scavenging Capacity (RSC) of simple phenols, flavanols, synthetic thio-flavanols, and hydrolizable tannins with HNTTM

   In our group, HNTTM (**4**) was used as chemosensor to measure the RSC of natural and synthetic (poly)phenols and fractions of different natural products.(*122-125*) To complete the picture of phenolic reactivity with this radical the RSC of a more comprehensive set of (poly)phenols was determined in CHCl₃/MeOH (2:1). The collection of compounds included simple phenols (catechol (**10**), pyrogallol (**11**) and methylgallate (**12**)) (**Figure 68**, in blue), flavanols from green tea, commonly known as catechins ((−)-epicatechin (EC, **13**), (−)-epigallocatechin-3-*O*-gallate (EGC, **14**), (−)-epicatechingallate (ECG, **15**) and (−)-epigallocatechin-3-*O*-gallate (EGCG, **16**) (**Figure 68**, in green), five synthetic thio-flavanols derived from EGC (**14**), ECG(**15**) and EGCG (**16**) (**Figure 70**), hydrolyzable tannins classified as gallotannins (hamamelitannin (HT, **17**) and pentagalloylglucose (PGG, **18**)) from *Hamamelis virginiana,* and ellagitannins (punicalagin (**19**) and its substructures dimethyl-hexahydroxydiphenyl-dicarboxylate (DHHDP, **20**) (NMR characterization included as Annex 8) and ellagic acid (EA, **21**))

from pomegranate (**Figure 68**, in black and in red, respectively). The results are summarized in **Table 10**.
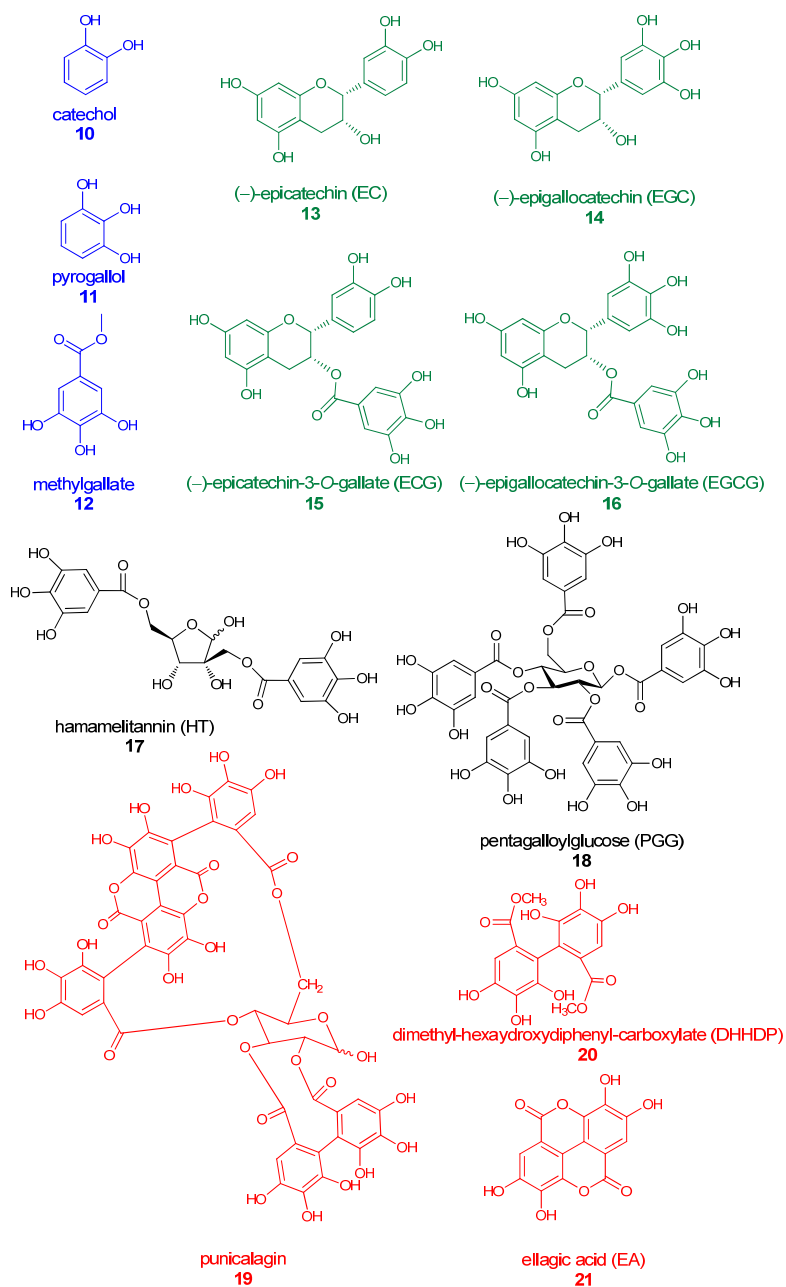
Figure 68. Structures of (poly)phenols **10**-**21**.

4. Results and Discussion

Thio-flavanols **14A**, **16A**, **14B**, **16B** and **15B** were obtained in a previous work in our laboratory from depolymerization of proanthocyanidins extracted from grape, pine and *Hamamelis Virginiana* by thioacidolysis with L-Cysteine (Cys) or L-Cysteamine (Cya) (**Figure 69**).(*125, 126, 151*)

Figure 69. Thioacydolysis of proanthocyanidins

4β–(*S*-cysteinyl)epigallocatechin
14A

4β–(*S*-cysteinyl)epigallocatechin-3-*O*-gallate
16A

4β–(2-aminoethylthio)epigallocatechin
14B

4β–(2-aminoethylthio)epigallocatechin-3-*O*-gallate
16B

4β–(2-aminoethylthio)epicatechin-3-*O*-gallate
15B
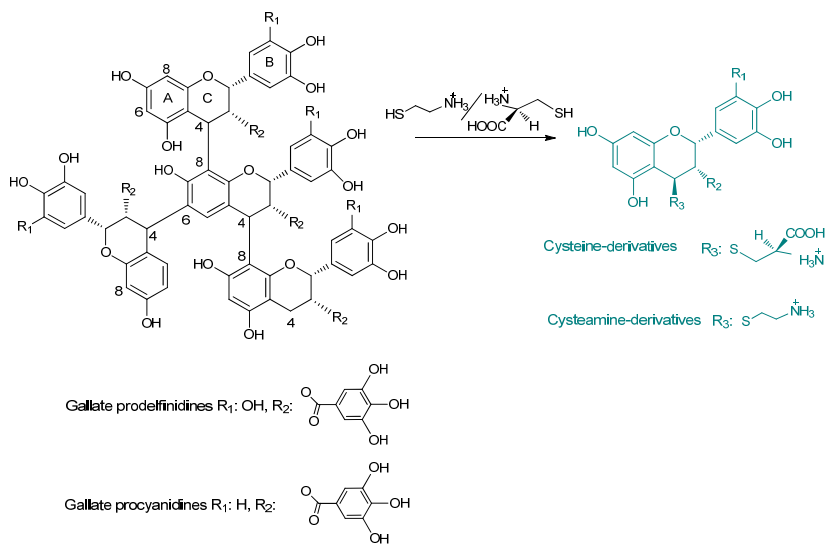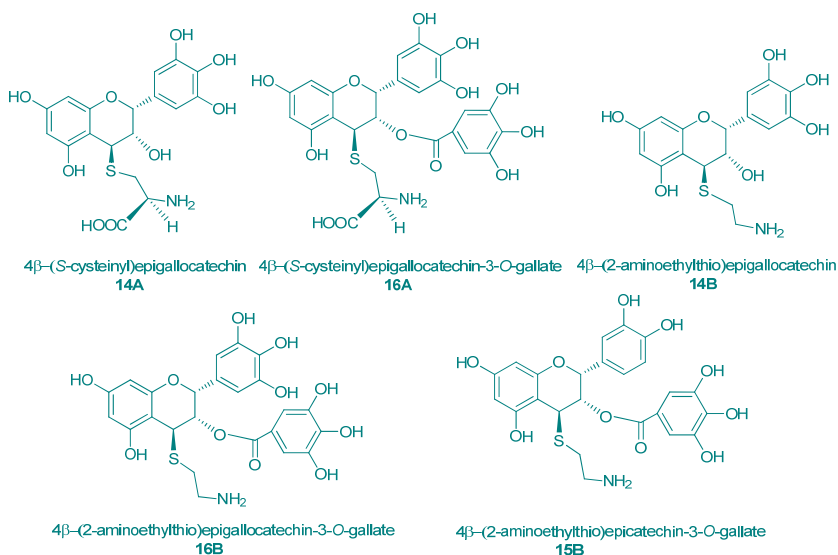
Figure 70. Structures of thio-flavanols.

The Electronic Paramagnetic Resonance (EPR) spectroscopy was used to monitor the decrease of the EPR radical signal in the reactions of these (poly)phenols with radical **4**, because of the overlapping bands of HNTTM (**4**) and hydrolyzable tannins in UV-Vis spectroscopy. Kinetics of (poly)phenols **10-21** with **4** could not be measured by EPR spectroscopy because the reactions were too fast. Therefore, the RSC of (poly)phenols **10-21** with the radical **4** was measured in $CHCl_3/MeOH$ (2:1) following the procedure described on Materials and Methods, Section 3.2.1.10 (See Annex 9, sections A in µg µmol^{-1} and B in µmol µmol^{-1}). The results were expressed as EC$_{50}$ (Efficient Concentration of the (poly)phenol to decrease half of the concentration of the radical divided by the moles of initial radical), as Antiradical Power (ARP = 1/EC$_{50}$) which helps to compare efficiencies among (poly)phenols. The Stochiometric Value (SV= EC$_{50}$*2) is the molar ratio of reactivity between **4** and the (poly)phenol, and its inverse (n$_e$) which is the number of HNTTM (**4**) moles reduced per mole of (poly)phenol or the number of electrons transferred per molecule of (poly)phenol.

In agreement with previous work in our group, the RSC of (poly)phenols will be expressed in ARP. Moreover, to relate the structural features of each (poly)phenol and their RSC, the number of electrons (n$_e$) transferred per molecule of (poly)phenol will be discussed.

The n$_e$ obtained for the three groups of (poly)phenols, the simple phenols, flavanols and thio-flavanols (**Table 10**, last column), are roughly in accordance with the number of hydroxyl groups present in their structures. It should be noticed that the simple phenols **10**, **11**, **12** are substructures of the flavanols EC (**13**), EGC (**14**), ECG (**15**) and EGCG (**16**). Comparing the n$_e$ values obtained for the simple phenols and flavanols, the phenol **10** is the responsible for the RSC value of EC (**13**), the phenol **11** for that of EGC (**14**), and **11** and **12** for that of EGCG (**16**) (**Table 10**). ECG (**15**) is an exception and the most active scavenger of radical **4** among catechins. The high electron-transfer capacity of **15** may be accounted for its oxidation to dimmers or trimers, with a particularly efficient hydroxyl regeneration.(*117*)

The n$_e$ values of the synthetic thio-flavanols derived from catechins (**Figure 70**), were compared with those of their (poly)phenol precursors, the flavanols EGC (**14**), ECG (**15**) and EGCG (**16**). The introduction of the cysteine group at the 4 position of the flavanols EGC (**14**) and EGCG (**16**), increased by one the n$_e$ values (**Table 10**). On the

other hand, the introduction of the cysteamine group at the same position maintained the n_e values of **14B** and **16B**, and lowered that of **15B** respect to their precursors.

The gallotannins HT (**17**) and PGG (**18**) are structurally formed by a different number of gallate groups linked to a carbohydrate (**Figure 68**). The simple phenol **12** transferred ~3 electrons per molecule to the radical **4**, in agreement with its number of hydroxyl groups, whereas HT (**17**) and PGG (**18**) transferred ~1.7 electrons for each gallate group found in their structures (2 and 5 methylgallate groups, respectively). The higher n_e value of **12** may be explained by its ability to form intermediate products (e.g. dimmers, hydroxyl regeneration) that facilitate its further oxidation.

The n_e values of the ellagitannin punicalagin (**19**) and its substructures DHHDP (**20**) and EA (**21**) (**Figure 68**) was shown to be not fully related with their number of hydroxyl groups, albeit the number of electrons transferred (n_e) by punicalagin (**19**) is in accordance with those transferred by its substructures DHHDP (**20**) and EA (**21**).That is, from the 14 electrons transferred by punicalagin (**19**) to the radical **4**, ~ 5 electrons could be given by the hexahydroxydiphenyl (HHDP) moiety, ~5 more by the ellagic acid central group, and ~2 electrons from each of the two gallate groups linked to the ellagic acid moiety by a C-C bond, finally reducing 14 molecules of the radical **4** (**Figure 71**).
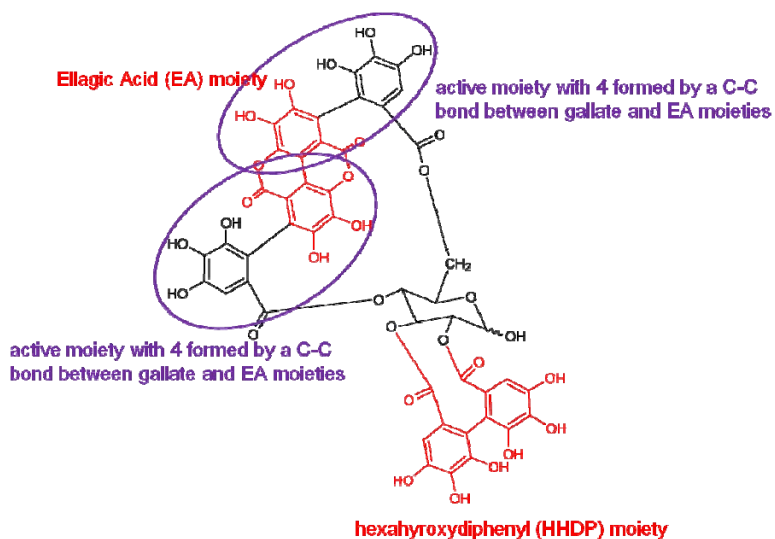
Figure 71. Reactive positions of **19** with the radical **4**.

ARP values are represented in micromols (μmol) of radical **4** per μmol of (poly)phenol and in milimol (mmol) of **4** per microgram (μg) of (poly)phenol (**Table 11**, second and fourth column) to facilitate the comparison of the RSC of (poly)phenols per milligram (mg) of ingested dose within a pharmacological context.

4. Results and Discussion

Table 10. RSC values of (poli)fenols **10-21** determined with HNTTM in CHCl$_3$/MeOH (2:1).

(Poly)phenols	EC$_{50}$[b]	ARP[c]	EC$_{50}$[d]	ARP[e]	SV[f]	n$_e$
Simple phenols[a]						
10	23.1	43.3	0.21	4.76	0.42	2.3
11	19.7	50.8	0.16	6.25	0.31	3.2
12	28.4	35.2	0.15	6.67	0.31	3.2
Flavanols						
13	51.2	19.5	0.25	4.00	0.51	2.0
14	50.2	19.9	0.16	6.25	0.32	3.1
15	22.2	45.0	0.05	20.0	0.1	10
16	40.6	24.6	0.09	11.1	0.18	5.7
Thio-flavanols						
14A	64.9	15.4	0.12	8.33	0.24	4.1
16A	48.5	20.6	0.07	14.3	0.14	7.4
14B	79.3	12.6	0.16	6.25	0.32	3.1
16B	58.4	17.1	0.09	11.1	0.18	5.6
15B	44.2	22.6	0.07	14.3	0.14	7.2
Hydrolizable tannins						
Gallotannins						
17	71.2	14.0	0.15	6.67	0.30	3.4
18	54.8	18.2	0.06	16.7	0.12	8.6
Ellagitannins						
19	38.1	26.2	0.04	25.0	0.07	14
20	42.2	23.7	0.12	8.33	0.23	4.3
21	30.4	32.9	0.10	10.0	0.20	5.0

[a]Number of assays performed for each (poly)phenol, n=2; [b]µg of (poly)phenol per µmol of **4**; [c]mmol of **4** per µg of (poly)phenol; [d]µmol of (poly)phenol per µmol of **4**; [e]µmol of **4** per µmol of (poly)phenol; [f]µmol of (poly)phenol per µmol of **4**.

The RSC values of (poly)phenols **10-21** and thio-flavanols measured with the radical **4**, expressed as ARP are represented in **Figures 72** and **73** in mmol of **4** per µg of (poly)phenol, (**Table 10**, second column) and in µmol of **4** per µmol of (poly)phenol, (**Table 10**, fourth column), respectively. The simple phenol with highest RSC value per µg was pyrogallol (**11**), from flavanols, ECG (**15**), from thio-flavanols, Cya-ECG (**15B**), from

gallotannins, PGG (**18**), and from ellagitannins, EA (**21**) (**Figure 72** in blue). On the other hand, simple phenols with highest RSC value per µmol were pyrogallol (**11**) and methylgallate (**12**), from flavanols, ECG (**15**), from thio-flavanols, Cys-EGC (**14A**) and Cya-ECG (**15B**), from gallotannins, PGG (**18**), and from ellagitannins, punicalagin (**19**) (**Figure 73** in yellow).
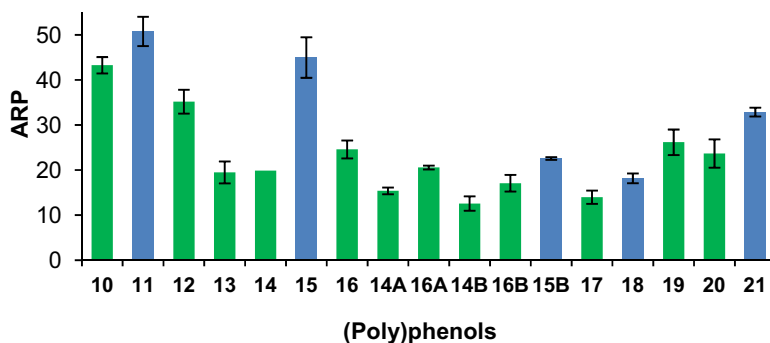
Figure 72. ARP values of (poly)phenols **10**-**21** measured with the radical **4**. Values represented in mmol of **4** per µg of (poly)phenol.
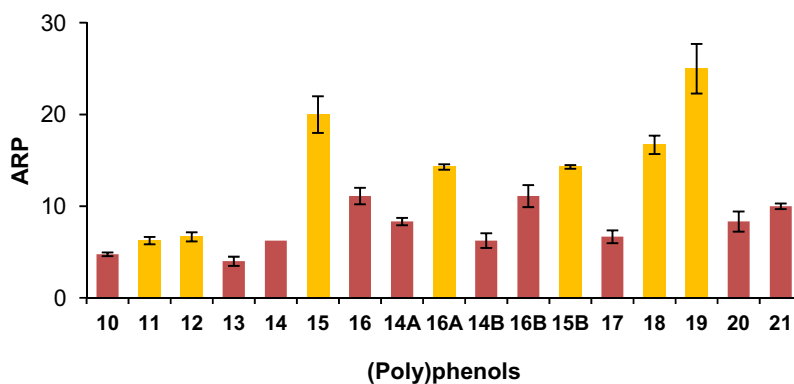
Figure 73. ARP values of (poly)phenols **10**-**21** measured with the radical **4**. Values represented in µmol of **4** per µmol of (poly)phenol.

4. Results and Discussion

In conclusion, the RSC values of (poly)phenols with the radical **4** was roughly related with the number of hydroxyls, which indicates that the oxidation potential of HNTTM (**4**) is high enough to react with all the intermediate species obtained from the successive oxidations of the hydroxyl groups.

4.1.5. TNPTM as chemosensor of (poly)phenols by Electron-Transfer (ET) reactions

A radical from the perchlorotriphenylmethyl radical (PTM) series, the tris(2,3,5,6-tetrachloro-4-nitrophenyl)methyl radical (TNPTM, **8**) was designed and prepared with the objective to obtain a chemosensor of (poly)phenols with a lower redox potential than that of HNTTM (**4**), to be able to react only with the most reactive hydroxylic positions within the (poly)phenols.

4.1.5.1. Physicochemical properties of TNPTM

4.1.5.1.1. Electron-accepting ability of TNPTM

The cyclic voltammogram of **8** was obtained in $CHCl_3$/MeOH (2:1) and CH_2Cl_2 solutions ($\sim 10^{-3}$ M) giving, like the radical **4**, a quasi-reversible process (E_p^a-E_p^c > 60 mV) of reduction by the addition of an electron to the trivalent carbon in both solvents, demonstrating that both species, radical **8** and its reduced anionic species **7** have very similar stability (**Table 11**) (Voltammograms of **8** and **4** in $CHCl_3$/MeOH (2:1) are included as Annex 7).

The $E°$ value of **8** is displayed in **Table 11** along with the $E°$ values of the non-nitrate precursor of radical **4** (TTM), the radical **4** and the non-nitrated precursor of **8** (PTM), determined under the same conditions. The $E°$ values for the reduction of these stable radicals in CH_2Cl_2 increase in following the sequence: TTM < PTM < TNPTM (**8**) < HNTTM (**4**). The radical **8** has a lower positive $E°$ value than that of the radical **4** as a consequence of the different number of nitro groups (3 instead of 6). It is also remarkable the significant influence of a *para*-NO_2 group instead of a *para*-chlorine on the $E°$ values of **8** and PTM. In spite of the restricted conjugation of the NO_2 group with the phenyl rings, substitution of chlorine by NO_2 resulted in a positive shift (0.43 V) of $E°$. Results of **Table 11** show that the $E°$ values of **4** and **8** in $CHCl_3$/MeOH (2:1) are slightly shifted to lower positive values.

Table 11. Electrochemical parameters for the oxidation of catechol and pyrogallol and for the reduction of radicals TTM, **4**, PTM and **8** in organic solution (10^{-3} M) with 0.1 M Bu$_4$NClO$_4$ on Pt at scan rate of 100 mV s^{-1}.

Radicals	E°/V[a] (E_p^a-E_p^c/mV)[b]	E°/V[c] (E_p^a-E_p^c/mV)[d]
TTM	—[e]	-0.66(100)
4	0.55 (90)	0.58(90)
PTM	—[e]	-0.15(150)
8	0.20(120)	0.28(123)

[a]E° in CHCl$_3$/MeOH (2:1); [b]Values of the difference between E_p^a (anodic peal potential) and E_p^c (cathodic peak potential) of radicals showing quasi-reversible reduction processes; [c]E° in CH$_2$Cl$_2$ solution; [d]Values of the difference between E_p^a and E_p^c of radicals showing a quasi-reversible reduction processes in CH$_2$Cl$_2$. [e]Values of potential not measured.

4.1.5.1.2. Characterization of the TNPTM by X-ray crystallography

Dark red crystals of the radical **8** were obtained from a solution of **8** in CHCl$_3$/hexane following the procedure of the Section 3.2.1.2.2 of Materials and Methods. The structure of **8** was elucidated by X-ray crystallography from a single red crystal (See Materials and Methods, Section 3.1.2.1) at the *Institut de Ciència de Materials (CSIC)* form the *Universitat Autònoma de Barcelona (UAB)*. A perspective view of the molecular structure with the atom numbering is shown in **Figure 74**.
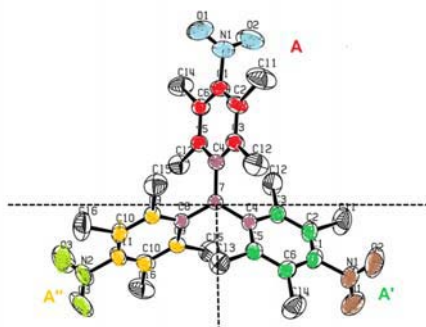
Figure 74. Perspective view of the structure of the radical **8** with the atom numbering.

4. Results and Discussion

All of the distances and angles between the central carbon atom (C7) and the aromatic carbons (C4, C4' and C8) are in good agreement with a sp² hybridation of the C7, lying all of them in the same plane (**D**), like the HNTTM anion (**3**). Phenyl rings are twisted around this plane with angles of ˜50° (**Table 12**) by the presence of the six chlorine atoms in *ortho* to C7.

Table 12. Angles (deg) between planes[a] of the molecular structure of TNPTM.

A-D	A'-D	A''-D	A-B (=A'-B')	A''-B''
50.41	50.41	54.07	82.06	83.30

[a]Planes are defined as follows: **A** (C1, C2, C3, C4, C5, C6, C7, N1); **A'** (C1', C2', C3', C4', C5', C6', C7', N1'); **A''** (C8, C9, C10, C8, C10, C9, C7, N2); **D** (C7, C4, C4, C8); **B** (C1, N1, O1, O2); **B'** (C1', N1', O1', O2'); **B''** (C8, N2, O3, O3).

In collaboration with the group of *Química Teòrica i Computacional* of *IQAC-CSIC*, the spin density of radical **8** was calculated with the UB3LYP method, with the EPR-II basis set for carbon, nitrogen, and oxygen atoms, and the D95/(d) basis set for chlorine atoms using the geometry determined by X-ray crystallography. **Figure 75** shows that the spin density occurs mainly on the trivalent carbon atom (C7) by the large twisting of the phenyl rings around this atom, meaning that the odd electron is localized mainly on the trivalent carbon atom, C7. Values of the spin density on nitrogen atoms are negligibly small owing to the large twisting (practically 90°) of the NO₂ plane around the phenyl ring.
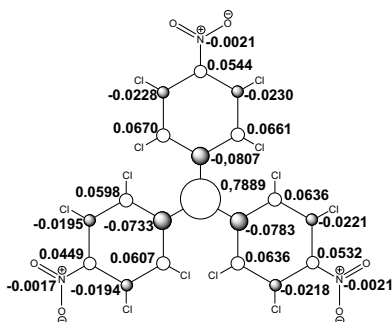
Figure 75. Total atomic spin densities of **8**.

4.1.5.2. Electron-accepting ability of TNPTM

The general assay used previously to establish the stability of TTM, PTM and HNTTM (**4**) and applied to radical TNPTM (**8**) resulted in the absence of hydrogen atom abstraction from a boiling solution of **8** in toluene (24 h) (**Figure 76**, pathway **A**) (See Materials and Methods, Section 3.2.1.4.3 and IR spectra are included as Annexes 1B and 2B). The reduction of the radical **8** with ascorbic acid in CHCl3/MeOH (2:1) gave the stable TNPTM anion (**7**) (λ= 577 nm) detected by UV-Vis spectroscopy, showing the exclusive reactivity of **8** by Electron-Transfer (ET) (**Figure 76**, patway **B**) (See Materials and Methods, Section 3.2.1.5 and UV-Vis spectra of **7** and **8** are included as Annex 10). A suggested mechanism of the reduction is detailed in **Figure 77**. As previously established for the radical **4**, direct Hydrogen Atom Transfer (HAT) to the C7 of the radical **8** from any reducing species is not allowed by steric hindrance of the *ortho*-chlorine groups, as shown by the X-ray crystallographic structure.
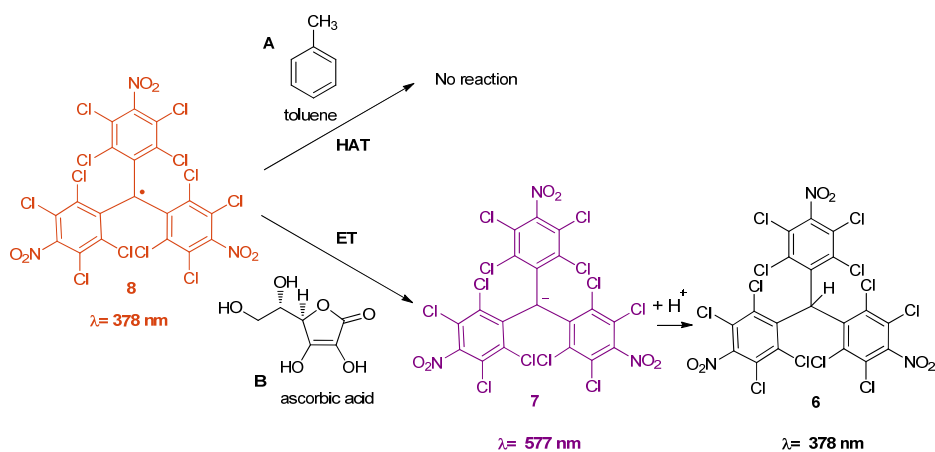
Figure 76. A) Reaction of the radical **8** with toluene. **B**) Reaction of ascorbic acid with the radical **8** in deoxygenated CHCl3/MeOH (2:1).

4. Results and Discussion
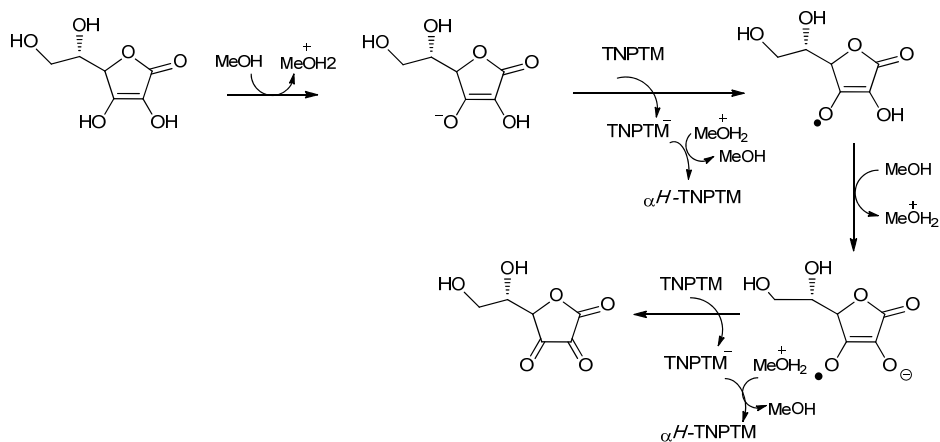
Figure 77. Proposed SPLET mechanism of the oxidation of ascorbic acid with the radical **8**.

4.1.5.3. Reactivity of catechol, pyrogallol, methylgallate, and DHHDP with TNTPM by Electron-Transfer (ET)

4.1.5.3.1. Reactivity of catechol and pyrogallol with TNPTM in solvents with different polarity

The reactivity of the simple phenols catechol (**10**) and pyrogallol (**11**) with the radical **8** was measured from equimolecular solutions (1.26 mM) of **10** or **11** and **8** in CHCl₃, and in CHCl₃/MeOH (2:1). The reaction time was long (48 h) to detect any TNPTM-derived reaction products (**Table 13**).

Table 13. Equimolecular reactions of simple phenols **10** or **11** with the radical **8** in CHCl₃ and CHCl₃/MeOH (2:1).

Simple phenol	10		11	
Solvent	8 (%)[a]	6 (%)[b]	8 (%)[a]	6 (%)[b]
CHCl₃	96	n.d[c]	100	–
CHCl₃/MeOH (2:1)	92	n.d[c]	48	52

[a]Recovered radical **8**; [b]Recovered αH-TNPTM (**6**); [c]Non-detected

132

The diamagnetic species α*H*-TNPTM (**6**) and the recovered radical **8** were identified by IR and UV-Vis spectroscopy. No other species were found in the reaction mixtures between **10** or **11** with **8**. These assays provided relevant information from **Table 13**: the radical **8** is stable in the presence of both simple phenols **10** or **11** in CHCl₃ solution, and with the phenol **10** in CHCl₃/MeOH (2:1). Interestingly, the radical **8** slowly reacted with the phenol **11** in CHCl₃/MeOH (2:1) and α*H*-TNPTM (**6**) was obtained as the only TNPTM-derived product. To sum up, the radical **8** exclusively reacts with the simple phenol **11** in CHCl₃/MeOH (2:1) where the phenol (Ph(OH)₃) (**11**) and its phenolate anion (Ph(OH)₂O⁻) are in equilibrium (**Figure 78**).
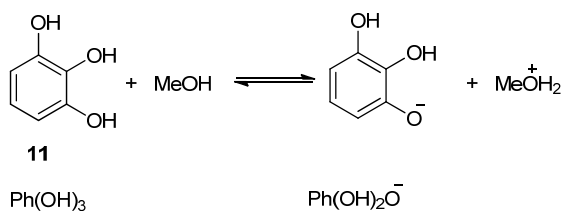
Figure 78. Equilibrium between the phenol **11** and its phenolate anion.

4.1.5.3.2. Kinetics and Radical Scavenging Capacity (RSC) of different (poly)phenols determined with TNPTM in CHCl₃/MeOH (2:1)

The kinetics and the RSC of catechol (**10**), pyrogallol (**11**), methylgallate (**12**), DHHDP (**20**), and EA (**21**) as (poly)phenolic moieties of the flavanols **13**-**16** and hydrolizable tannins **17**-**19**, were determined with TNTPM (**8**) in CHCl₃/MeOH (2:1).

Kinetics measurements of the Electron-Transfer (ET) reaction of catechol (**10**), pyrogallol (**11**), methylgallate (**12**), DHHDP (**20**) or EA (**21**) with the radical **8** were performed to determine the rate constant (k) and the number of electrons transferred (nₑ) per molecule of (poly)phenol. The rate constant and the nₑ values were calculated using the kinetic model reported by Dangles and co-workers.(*116*) (Materials and Methods, Section 3.2.1.9). The course of the reaction was monitored by EPR by recording the decay of the radical **8** band as a consequence of the addition of (poly)phenol to a solution of **8**. The experiments were carried out with a **8**/(poly)phenol molar ratio of 5:1 with an initial concentration of radical **8** of 121.2 μM, and a long reaction time (48 h) to ensure the

4. Results and Discussion

complete consumption of the (poly)phenol (See Materials and Methods, Section 3.2.1.9 and the graphics of kinetics are included as Annex 11). In the course of the reducing process of radical **8** with **10**, **11**, **12**, **20** or **21**, the decay of the EPR band of the radical **8** was observed exclusively with the phenol **11** and the ellagitannin **20**. There was no reaction between the simple phenols **10**, **12** or the ellagitannin **21** with **8** (**Figure 79**).
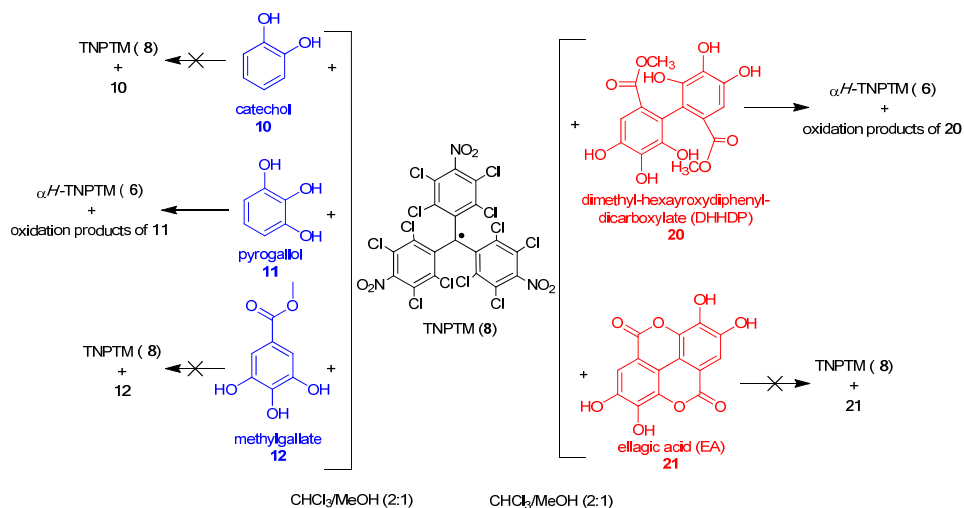
Figure 79. Selectivity of the radical **8** with the (poly)phenols **10**, **11**, **12** and **20**.

Table 14. Observed rate constants (k) and number of electrons transferred (n_e) per molecule of (poly)phenol of the reactions[a] of pyrogallol (**11**) or DHHDP (**20**) with TNPTM (**8**) in CHCl₃/MeOH (2:1).

(Poly)phenol	8/(Poly)phenol molar ratio[a]	k (M⁻¹ s⁻¹)	n_e
11	4.6	0.388 ± 0.070	3.6
20	4.9	0.115 ± 0.010	1.9

[a]Reaction time of 48 h. Initial concentrations between 119.3-122.7 µM and 24.3-25.7 µM (molar ratio, 5:1) for **8** and **10** or **11**, respectively. Number of assays performed by each (poly)phenol, n= 2-5.

The rate constant values (k) show that the reaction of the phenol **11** is 1.5-fold faster than that of the ellagitannin **20** (**Table 14**). As shown in **Table 14** (last column), one molecule of the phenol **11** reduces three molecules of the radical **8** whereas one molecule

4. Results and Discussion

of the ellagitannin **20** reduces two molecules of the radical **8** in CHCl₃/MeOH (2:1). The number of electrons transferred (n_e) per molecule of (poly)phenol is in accordance with the number of hydroxyl groups of **11**. In contrast **20** containing 6 hydroxyl groups transferred only 2 electrons to the radical **8**.

4.1.5.3.3 Electrochemical parameters for the reactions of catechol, pyrogallol, methylgallate, DHHDP and EA with TNPTM in solvents with different polarity

A. Determination of the redox potentials of catechol, pyrogallol, methylgallate, DHHDP, EA and TNPTM in CHCl₃/MeOH (2:1)

Cyclic voltammograms of the phenols **10** and **11** in CHCl₃/MeOH (2:1) were obtained as it is described on the Materials and Methods, Section 3.2.1.6, and their values are shown in **Table 7**. Cyclic voltammograms of methylgallate (**12**), DHHDP (**20**), and EA (**21**) were carried out in CHCl₃/MeOH (2:1) to determine the $E_p{}^a$ of (poly)phenols and with a little excess of tetrabutylammonium hydroxide (TBAH) to determine the $E_p{}^a$ of their corresponding (poly)phenolic anions, albeit the $E_p{}^a$ of the (poly)phenols and of their corresponding anions could not be obtained because of the partial adsorption of the substrate on the Pt electrode. Redox potential (E^o) and cathodic peak potential ($E_p{}^c$) of TNPTM (**8**) was determined in CHCl₃/MeOH (2:1) with values of 0.20 and 0.14 V, respectively (Voltammograms are included as Annex 7).

B. Exergonic or endergonic character of the reactions of catechol or pyrogallol with TNPTM

The $E_p{}^a$ of the simple phenols **10** ($E_p{}^a$ = 1.00 V) and **11** ($E_p{}^a$ = 0.78 V) (**Table 15**) are not high enough to reduce the radical **8** in CHCl₃/MeOH (2:1); however, the $E_p{}^a$ of their phenolates (PhO⁻) formed in CHCl₃/MeOH (2:1) by equilibrium with their molecular forms (PhOH), will be involved in the reduction of **8** by an Electron-Transfer (ET) reaction. In our particular case, the anion of **11** ($E_p{}^a$ = 0.03 V) and not that from **10** ($E_p{}^a$ = 0.20), was able to react with the radical **8** as it is shown in **Table 15** (reaction thermodynamically allowed $E_p{}^c$-$E_p{}^a$ > 0):

4. Results and Discussion

Table 15. Calculation of the $E_p{}^c$-$E_p{}^a$ values for the substrates used in the reactions of catechol or pyrogallol with TNPTM in CHCl$_3$/MeOH (2:1). $E_p{}^c$ and $E_p{}^a$ values are found in **Table 7**.

Simple phenol	10	11
Solvent	$E_p{}^c$-$E_p{}^a$/V [a] ($E_p{}^c$-$E_p{}^a$/V [b])	$E_p{}^c$-$E_p{}^a$/V [a] ($E_p{}^c$-$E_p{}^a$/V [b])
CHCl$_3$/MeOH (2:1)	-0.86 (-0.11)	-0.68 (0.08)

[a]Values of the difference between $E_p{}^c$ of **8**, and $E_p{}^a$ of **10** and **11**; [b]Values of the difference between $E_p{}^c$ of **8**, and $E_p{}^a$ of the anions of **10** and **11**.

C. *Gibbs energy value for the reaction of pyrogallol with TNPTM in CHCl$_3$/MeOH (2:1) as solvent*

The results obtained above for pyrogallol (**11**) are consistent with the negative free energy change value of the Electron-Transfer (ET) from **11** to the radical **8** (ΔG_{et}= -($E_p{}^c$-$E_p{}^a$) x F = -7719 J mol^{-1}). The reaction of **11** with **8** in CHCl$_3$/MeOH (2:1) is an exergonic or spontaneous reaction.

D. *Anodic onset peak potential ($E_o{}^a$) of catechol, pyrogallol, methylgallate, DHHDP and EA in dimethylformamide (DMF)*

The $E_o{}^a$ of the simple phenols **10**, **11**, **12**, and the ellagitannins **20**, and **21** was measured in DMF by CV to compare their reducing powers without problems of the partial adsorption of the substrate o the Pt electrode (**Table 16**) (See Materials and Methods, Section 3.2.1.6 and Voltammograms are included as Annex 7).

Table 16. $E_o{}^a$ for the oxidation of the selected (poly)phenols.

(Poly)phenols	$E_o{}^a$/V [a]	$E_o{}^a$/V [b]
10	0.54	0.60
11	0.45	0.45
12	0.65	— [c]
20	0.50	— [c]
21	0.64	— [c]

[a]DMF and [b]CHCl$_3$/MeOH (2:1) solutions (10^{-3} M) with Bu$_4$NClO$_4$ (0.1 M) on Pt *vs.* SCE at scan rate of 50 mV s^{-1}; [c]Values could not be measured.

The lower the E_o^a value, the easier is the (poly)phenol oxidation. These E_o^a values indicate that pyrogallol (**11**) and DHHDP (**20**) are more easily oxidized than catechol (**10**), methylgallate (**12**) and EA (**21**) in DMF as solvent. The E_o^c of the radical **8** in DMF could not be measured because of the instability of **8** in DMF. In addition to this, the E_o^a values of the phenols **10** and **11** were obtained in CHCl₃/MeOH (2:1) (10⁻³ M) with Bu₄NClO₄ (0.1 M) on Pt *vs*. SCE at scan rate of 50 mV s⁻¹ with values of 0.60 V and 0.45 V, respectively (**Table 16**). From the similarity of the E_o^a values of **10** and **11** obtained in both solvents, we can advance that the E_o^a values of the phenol **12** and the ellagitannins **20** and **21** in CHCl₃/MeOH (2:1) would be very similar to those found in DMF.

4.1.5.3.4. Reaction mechanisms of pyrogallol and DHHDP with TNPTM in CHCl₃/MeOH (2:1)

The reactions of pyrogallol (**11**) and DHHDP (**20**) with the radical **8** take place through the formation of the phenolate anions of **11** and **20**. According to this, the reaction mechanism is the SPLET (See Introduction, Section 1.5.1), and the first reaction step is the formation of the phenolate anions of **11** and **20** induced by the solvent, followed by an Electron-Transfer (ET) to the radical **8** to form the stable TNPTM anion (**7**), and the final protonation of **7** by MeOH₂⁺.

To obtain more information about the oxidation of ellagitannin **20**, their reaction products with the radical **8**, with a molar ratio **8**/ **20** of 3:1, were analyzed in deoxygenated CHCl₃/MeOH (2:1) by high-resolution mass spectrometry (MS chromatogram is included as Annex 11). **Figure 80** depicts structures compatible with the experimental results. Among others, a low signal was detected at *m/z* 363.0355, corresponding to the mass of the loss of two electrons and two protons (two hydrogen atoms) from **20**. A possible structure of this peak could be the *o*-quinone **20A**.(*152*)

4. Results and Discussion
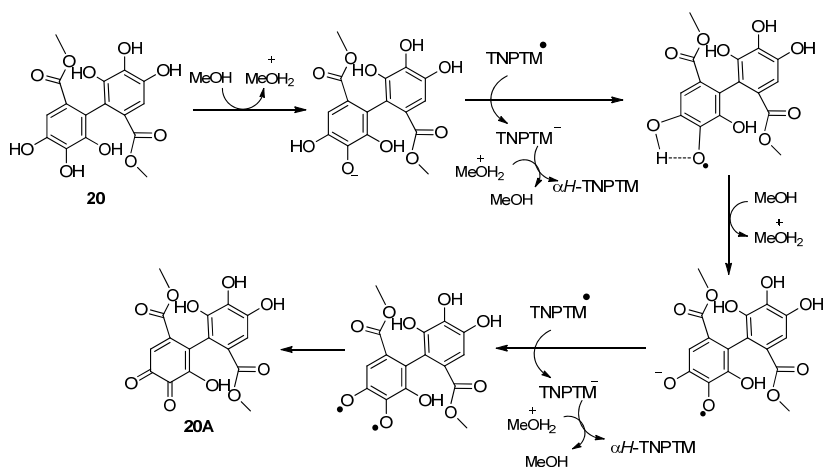
Figure 80. Proposed oxidation mechanism of the (poly)phenol **20** with the radical **8**.

In summary, TNPTM (**8**), like HNTTM (**4**), is only active in Electron-Transfer (ET) reactions and therefore, it is a good candidate to measure the reaction rates (kinetics) by ET and the electron-donating capacity of (poly)phenols. As the $E°$ for the reduction of the radical **8** to its anion **7** is comprised between those of PTM and **4**, and the E_p^c of the radical **8** ranges between the E_p^a for the oxidation of the phenolate anions of catechol (**10**) and pyrogallol (**11**), the radical **8** can selectively distinguish between the reducing properties of the simple phenols **10** and **11**. In an ionizable medium the radical **8** only reacts with the phenolate anion of the simple phenol **11**. The E_o^a of methylgallate (**12**), and the ellagitannins **20** and **21** in DMF can give us a rough estimation of their reactivity with the radical **8**. While **20** reduces radical **8**, phenol **12** and ellagitanin **21** do not react.

4.1.5.4. Kinetics and Radical Scavenging Capacity (RSC) of simple phenols, flavanols and hydrolyzable tannins with TNPTM.

The rate constant values (k) and the number of electrons transferred (n_e) per molecule of (poly)phenols **10**-**21** (**Figure 68**) with TNPTM (**8**) in CHCl₃/MeOH (2:1) were determined. The reactions were monitored by EPR spectroscopy recording the decay of the EPR spectrum band of the radical **8** as a consequence of the addition of (poly)phenol. The experiments were performed with a **8**/(poly)phenol molar ratio of ˜5:1, with an initial concentration of radical **8** of 120.1 μM and, a long reaction time (48 h) to ensure the

complete consumption of the (poly)phenol (See Materials and Methods, Section 3.2.1.9). The decay of the band was exclusively produced by pyrogallol (**11**), the flavanols EGC (**14**) and EGCG (**16**), the gallotannin HT (**17**), and the ellagitannins punicalagin (**19**) and DHHDP (**20**)(Graphics of kinetics are included as Annex 12). The k and n_e values were calculated using the kinetic model and equations reported by Dangles and co-workers(*116*) and showed that all reactions performed with the assayed and active (poly)phenols were slow with some differences among them (**Table 17**). From all (poly)phenols assayed, the flavanol **16** is the only one that shows two reaction steps, one fast (k_1) with the transfer of 1.9 electrons and one slow (Annex 12. 3). The reaction of the radical **8** with pyrogallol is 1.5-fold faster than with EGC (**14**), flavanol containing **11**. Among the ellagitannins, punicalagin (**19**) and its substructure DHHDP (**20**) have very similar values as those presented by the gallotannin HT (**17**), however they differ greatly in the number of electrons transferred. If the active scavenging substructures of flavanols and ellagitannins are compared, the phenol **11** is ⁻3.5-fold faster than the ellagitannin **20** (**Table 17**). The observed rate constant values in **Table 17** are the average of the rate constants of each one of the electrons transferred by each (poly)phenol.

Table 17. Rate constant values (k) and electrons transferred per molecule of (poly)phenol (n_e) of the reactions[a] of the (poly)phenols active with TNPTM in CHCl₃/MeOH (2:1).

(Poly)phenol	TNPTM:polyphenol molar ratio[b]	k ($M^{-1} s^{-1}$) k_1($M^{-1} s^{-1}$)[c]	n_e
11	4.6	0.388 ± 0.070	3.6
14	4.9	0.266 ± 0.035	3.0
16	4.9	71.8 ± 1.02[c]	2.6
17	5.0	0.130 ± 0.024	1.2
19	5.0	0.125 ± 0.041	3.5
20	4.9	0.115 ± 0.010	1.9

[a]Reaction time of 48 h; number of assays performed by each (poly)phenol, n= 2; [b]Initial concentrations between 119.2-121.6 μM and 24.1-25.4 μM (molar ratio, 5:1) for **8** and (poly)phenols **11**, **14**, **16**, **17**, **19**, and **20**, respectively; [c]rate constant of the fast step.

4. Results and Discussion

<u>4.1.5.5 Radical Scavenging Capacity (RSC) of simple phenols, flavanols and hydrolyzable tannins with TNPTM</u>

The RSC of the simple phenols **10-12**, flavanols **13-16** and hydrolyzable tannins **17-21** was measured with TNPTM (**8**) with the experimental method previously used with HNTTM (**4**) (See Materials and Methods, Section 3.2.1.10) to obtain consistent and comparable results.

The RSC of (poly)phenols **10-21** was determined with the radical **8** in CHCl$_3$/MeOH (2:1) by monitoring the decrease of the EPR radical band at 48 h of reaction time (**Table 18**) (Graphics are included as Annex 9, sections C in µg µmol^{-1} and D in µmol µmol^{-1}).

Table 18. RSC values of (poly)phenols **10-21** determined with TNPTM in CHCl$_3$/MeOH (2:1).

Families of (poly)phenols[a]	EC$_{50}$[b]	ARP[c]	EC$_{50}$[d]	ARP[e]	SV[f]	n$_e$
Simple phenols						
10	243	4.12	2.2	0.45	4.41	0.23
11	21.7	46.1	0.17	5.88	0.35	2.90
12	164	6.1	0.89	1.12	1.78	0.56
Flavonols						
13	307	3.25	1.06	0.94	2.12	0.47
14	83.3	12.0	0.18	5.56	0.36	2.75
15	355	2.82	0.80	1.25	1.60	0.63
16	55.2	18.1	0.18	5.56	0.36	2.78
Hydrolyzable tannins						
Gallotannins						
17	232	4.30	0.45	2.22	0.96	1.04
18	2404	0.42	2.55	0.39	5.11	0.20
Ellagitannins						
19	50.3	19.9	0.15	6.67	0.31	3.30
20	51.2	19.6	0.26	3.89	0.51	2.00
21	382	2.62	1.66	0.60	3.32	0.30

[a]Number of assays performed for each (poly)phenol, n= 2; [b]μg of (poly)phenol per μmol of **8**; [c]mmol of **8** per μg of (poly)phenol; [d]μmol of (poly)phenol per μmol of **8**; [e]μmol of **8** per μmol of (poly)phenol; [f]μmol of (poly)phenol per μmol of **8**.

The RSC values of the simple phenols **10-12** were compared with those values obtained with the flavanols **13-16**, the lasts containing the simple phenols **10-12** as substructures. On the section before (Section 4.1.4.4) results shown that the radical **8** is effectively reduced by pyrogallol (**11**), with those flavanols containing this substructure, i.e. EGC (**14**) and EGCG (**16**), by the ellagitannin punicalagin (**19**) and its substructure DHHDP (**20**), and by the gallotannin HT (**17**), the last acting as a weak scavenger of the radical **8**. On **Table 18**, are shown the RSC values of all (poly)phenols tested albeit the (poly)phenols with values of n$_e$ lower than one have been discarded as active scavengers with **8** (i.e. catechol (**10**), methylgallate (**12**), EC (**13**), ECG (**15**), PGG (**18**), and EA (**21**)).

4. Results and Discussion

Values of n_e presented in **Table 18** are in accordance with those obtained in **Table 17** from the kinetic calculations. The n_e values of the flavanols **14** and **16** are in agreement with that of **11**, each one reducing three molecules of the radical **8** per molecule of (poly)fenol. The DHHDP (**20**) molecule is structurally formed by a C-C bond between two gallates, and this linkage appears to activate one of the hydroxyls of each phenolic ring making possible the transfer of two electrons to the radical **8** per molecule of **20**. The reduction of the radical **8** produced by the addition of different amounts of the phenols **11** or **12** or by the ellagitannin **20** is graphically shown in **Figure 81** by the decrease of the EPR band of the radical **8**.
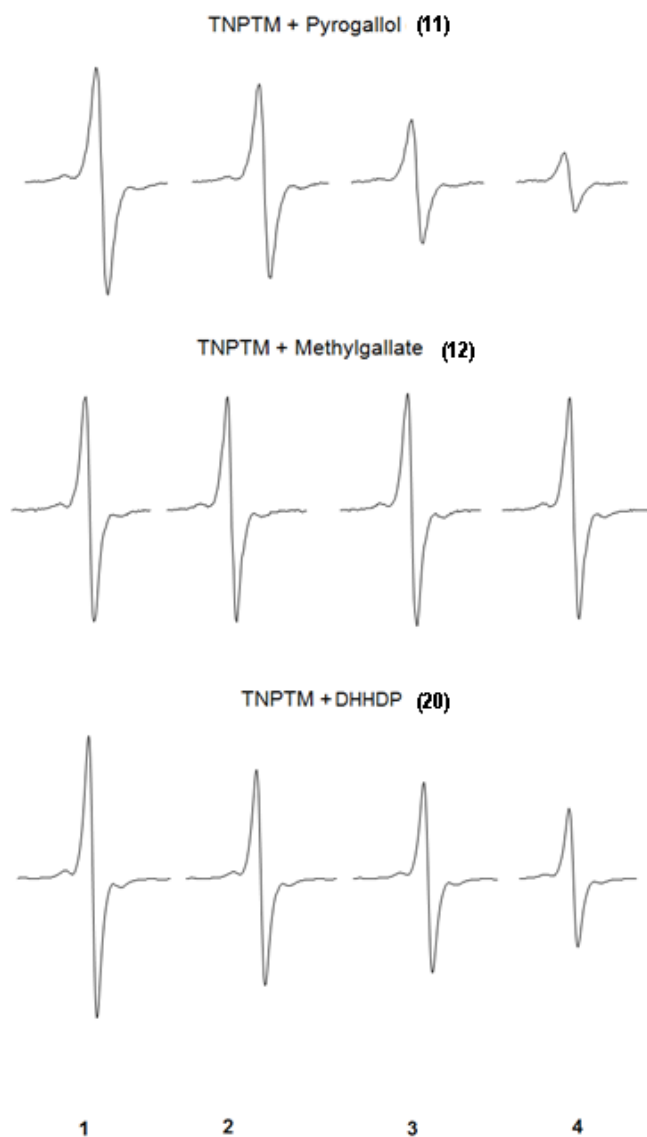
Figure 81. EPR band intensity after the reaction of the radical **8** (120.26 µM) with different concentrations of **11**, **12** and **20** (**1**, negative control; **2**, 5.71 µM; **3**, 18.1 µM and **4**, 55.13 µM) in CHCl₃/MeOH (2:1) at the same reaction time (48 h).

4. Results and Discussion

The examination of the structure of punicalagin (**19**) and the number of electrons transferred (n_e= 3.3) to the radical **8** (**Table 18**, last column), suggests that the C-C bond between the gallate and the ellagic acid moieties (**Figure 82**, position **B**) produces a similar hydroxyl activation that we found for the DHHDP structure (**Figure 82**, position **A**) (**Figure 82**). Notably, despite of the higher number of hydroxyl functions found in punicalagin (**19**), it contains a similar number of highly reactive hydroxyl groups as pyrogallol (**11**) with the radical **8** (n_e= 2.9).
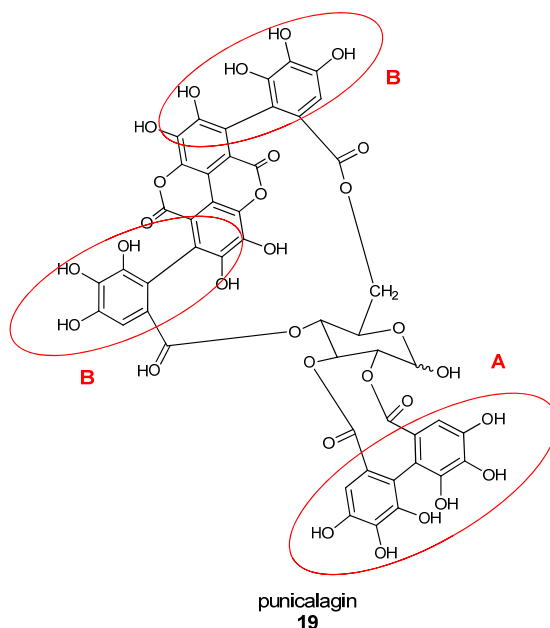
Figure 82. Activated positions of punicalagin (**19**) to reduce the radical **8**.

A structural explanation for the different RSC values in the reaction of the gallotannins HT (**17**) and PGG (**18**) with the radical **8** is more speculative. Ellagitannins **17** and **18** are very similar structurally: they both contain gallates. However, in the case of **17** there is a hydroxyl moiety geminal to one of the gallate esters and this might explain the differences detected in the reactivity with the radical **8**. The extra hydroxyl group might participate in a hydrogen bond with the carbonyl group of the gallate moiety to form a seven member ring. This could introduce a conformational restriction with loss of planarity between the carbonyl froup and the vicinal phenyl, and subsequent loosening

of the conjugation within the gallate moiety. This would make **17** more reactive than **18**. The extended conjugation of the carbonyl and the phenyl groups may be also the reason why gallates are less reactive than pyrogallols.(*153*)

The RSC of the (poly)phenols **10**-**21** measured with TNPTM (**8**) and expressed as ARP (**Table 18**, second and fourth columns), is shown in **Figure 83** in mmol of **8** per µg of (poly)phenol and in **Figure 84** in µmol of **8** per µmol of (poly)phenol, to compare the RSC of (poly)phenols per amount of ingested dose within a pharmacological context. The (poly)phenols with highest RSC values expressed in mmol of **8** per µg of (poly)phenol were the simple phenol pyrogallol (**11**) as the most active (poly)phenol from those assayed, EGC (**14**) and EGCG (**16**) from flavanols, HT (**17**) from gallotannins, and punicalagin (**19**) and DHHDP (**20**) from ellagitannins (**Figure 83**). On the other hand, the (poly)phenols with high RSC values expressed in µmol of **8** per µmol of (poly)phenol were the ellagitannin **19** as the most active (poly)phenol from those assayed, the simple phenol **11**, the flavanols **14** and **16** with a very similar ARP values, and the gallotannin **17** as the less active (**Figure 84**).
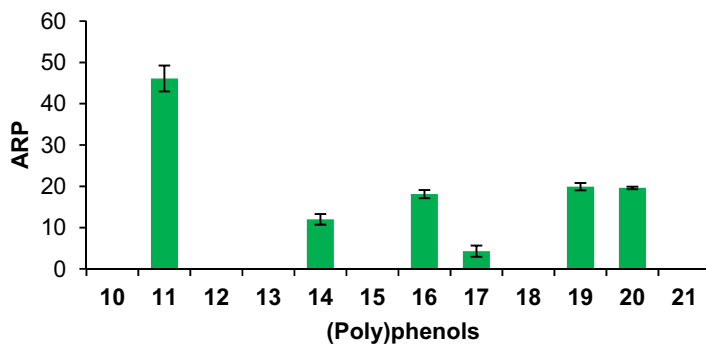
Figure 83. ARP values of (poly)phenols **10**-**21** measured with the radical **8**. Values represented in mmol of **8** per µg of (poly)phenol.
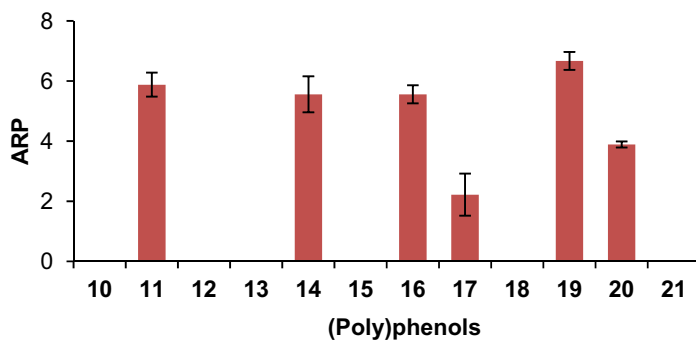
Figure 84. ARP values of (poly)phenols **10**-**21** measured with radical **8**. Values represented in μmol of **8** per μmol of (poly)phenol.

In conclusion, the more active (poly)phenols require the presence of certain moieties in the molecular structure responsible for the electron-transfer to the selective radical **8**.

4.2. DPPH as chemosensor of (poly)phenols by Hydrogen Atom Transfer (HAT)/Electron Transfer (ET)

One of the most extensively used methods to evaluate the RSC of (poly)phenols is the reduction of the commercially available stable radical 1,1-diphenyl-2-picrilhidrazyl (DPPH, **9**).

4.2.1 Physicochemical properties of DPPH

4.2.1.1 Electron-accepting ability of DPPH

The cyclic voltammogram of **9** was obtained in CHCl₃/MeOH (2:1) solution (˜10⁻³ M) and like HNTTM (**4**) and TNTPM (**8**), **9** participates in a quasi-reversible reduction process ($E_p{}^a$-$E_p{}^c$ > 60 mV). This proves that both species, the radical **9** and its anion have very similar stability (**Figure 85** and **Table 19**)(Voltammogram of **9** is included as Annex 7).
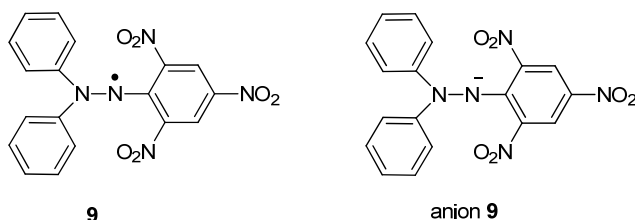
Figure 85. Molecular structures of the radical **9** and its anion.

Table 19. Electrochemical parameters for the reduction of HNTTM, TNPTM and DPPH in CHCl₃/MeOH (2:1) solution (10⁻³ M) with 0.1 M Bu₄NClO₄ on Pt at scan rate of 100 mV s⁻¹.

Radicals	$E°$/V($E_p{}^a$-$E_p{}^c$/mV)[a]
4	0.55 (90)
8	0.20 (120)
9	0.21 (90)

[a]Values of the difference between $E_p{}^a$ and $E_p{}^c$ of **4**, **8** and **9** showing quasi-reversible reduction processes.

4. Results and Discussion

4.2.2. Radical Scavenging Capacity (RSC) of simple phenols, flavanols and hydrolyzable tannins with DPPH in CHCl₃/MeOH (2:1)

The reaction mechanism of DPPH (**9**) with a (poly)phenol depends on the nature of the (poly)phenol and the solvent used. As it was mentioned before, these reactions have been largely admitted to occur by Hydrogen Atom Transfer (HAT), although recently some authors have shown that in ionizable solvents they can proceed by an electron transfer from the phenolate anion, in equilibrium with its molecular counterpart, to the radical **9** (SPLET) (See Introduction, Section 1.5.1).(*111, 118, 154*)

Table 20. RSC values of (poly)phenols **10-21** determined with DPPH in CHCl₃/MeOH (2:1).

Families of (poly)phenols[a]	EC$_{50}$[b]	ARP[c]	EC$_{50}$[d]	ARP[e]	SV[f]	$n_{H/e}$
Simple phenols						
10	18.7	53.4	0.17	5.88	0.34	2.9
11	12.6	79.4	0.10	10.0	0.20	5.0
12	34.0	29.4	0.18	5.56	0.36	3.2
Flavanols						
13	38.0	26.3	0.13	7.72	0.26	3.8
14	32.7	30.6	0.11	9.10	0.21	4.7
15	26.7	37.5	0.06	16.7	0.12	8.3
16	26.4	37.9	0.06	16.7	0.12	8.7
Hydrolyzable tannins						
Gallotannins						
17	27.8	36.0	0.06	16.7	0.11	8.9
18	23.8	42.0	0.03	33.3	0.05	20
Ellagitannins						
19	18.9	52.9	0.02	50.0	0.04	29
20	30.1	33.2	0.08	12.5	0.16	6.1
21	22.5	44.2	0.07	14.3	0.15	6.7

[a]Number of assays performed for each (poly)phenol, n=2; [b]µg of (poly)phenol per µmol of **9**; [c]mmol of **9** per µg of (poly)phenol; [d]µmol of (poly)phenol per µmol of **9**; [e]µmol of **9** per µmol of (poly)phenol; [f]µmol of (poly)phenol per µmol of **9**.

The reactivity of the radical **9** as chemosensor and the RSC of (poly)phenols **10**-**21** is discussed in a similar way as the reactivity of HNTTM (**4**) and TNPTM (**8**) (**Table 20**) (Graphics are included as Annex 9, sections E in µg µmol^{-1} and F in µmol µmol^{-1}). The RSC is represented in **Figure 86** and **Figure 87** as ARP values in mmol of **9** per µg of (poly)phenol and per µmol of **9** per µmol of (poly)phenol, respectively, showing the (poly)phenol **11** as the most active simple phenol, the flavanols **15** and **16** with very similar values, the gallotannin **18**, and the ellagitannin **19**, in both units (**Figure 86** in blue and **Figure 87** in yellow).
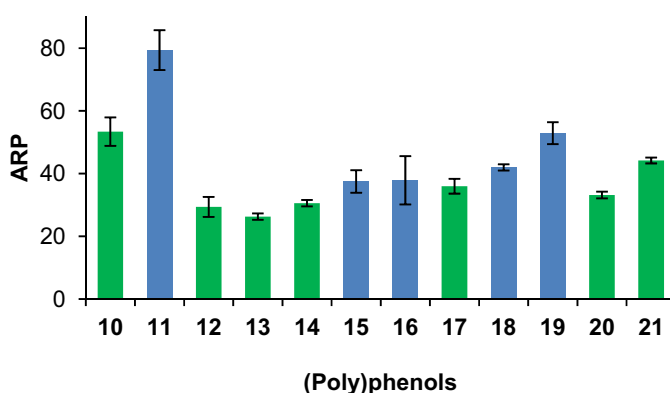
Figure 86. ARP values of (poly)phenols **10**-**21** measured with the radical **9**. Values represented in mmol of **9** per µg of (poly)phenol.
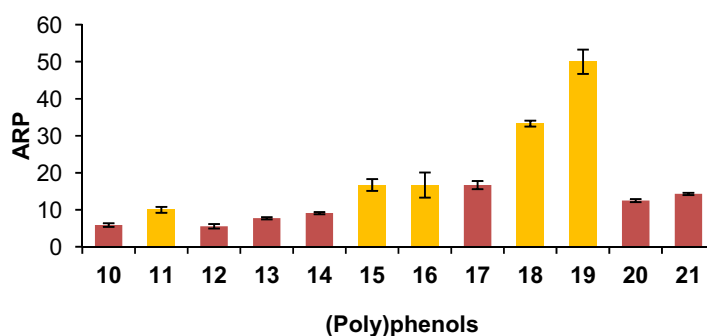
Figure 87. ARP values of (poly)phenols **10**-**21** measured with the radical **9**. Values represented in µmol of **9** per µmol of(poly)phenol.

4. Results and Discussion

The RSC values obtained with the radical **9**, in contrast to those obtained with HNTTM (**4**) and TNPTM (**8**), are not directly related with the number of hydroxyls nor with the presence of certain phenolic moieties. It can be explained because of the hydroxyl regeneration from MeOH.(*155, 156*)

4.2.3. Reaction mechanism of the assayed (poly)phenols with DPPH in CHCl₃/MeOH (2:1)

The redox potential (E°) value for the reduction of DPPH (**9**) has been compared with that of TNPTM (**8**) (**Table 19**). As it was demonstrated before, the radical **8** is selective and reacts only with the most active phenolic positions (See Results and Discussion, Section 4.1.4.4). Interestingly, the E° value of the radical **9** ($E^\circ = 0.21$ V) is practically the same as that of the radical **8** ($E^\circ = 0.20$ V) albeit it reacts with all assayed (poly)phenols without distinction (**Table 20**). These results suggest that both radicals **8** and **9** react with the assayed (poly)phenols through different mechanisms. If the radical **8** reacts by Electron-Transfer (ET) with (poly)phenols, most probably the radical **9** reacts mainly by Hydrogen Atom Transfer (HAT) in this solvent.(*111, 118*)

4.3. The Ferric Reducing Antioxidant Power (FRAP) method to measure the Reducing Power of (poly)phenols

The FRAP method was used to determine the kinetics and the capacity of (poly)phenols as metal-reducing molecules. The Reducing Rates (RR) values were obtained at short reaction time (20 s) and the Reducing Capacity (RC) values were obtained at long reaction time(1 h) to ensure the complete reaction of (poly)phenols (See Materials and Methods, Sections 3.2.1.12 and 3.2.1.13). All these reactions take place via an electron transfer mechanism in which the Fe^{3+} accepts an electron from the (poly)phenol.

4.3.1. Reducing Rates (RR) of (poly)phenols

The FRAP assay was tested with (poly)phenols in aqueous solution (pH=3.6, sodium acetate buffer) at short incubation time (20 s). Results of the RR of (poly)phenols with the Fe(III)-*o*-phenantroline complex were expressed in µg of (poly)phenol per mL and µmol of (poly)phenol per L (Graphics are included as Annex 13, sections A in µg mL^{-1} and B in µmol L^{-1}). The results in **Figure 88** expressed in µg per mL of (poly)phenol reveal that the simple phenol pyrogallol (**11**), the flavanol EGCG (**16**), the gallotannin HT (**17**), and the ellagitannin DHHDP (**20**) (in red) are the fastest reducing (poly)phenols with the ferric ion (Fe (III)). The results expressed in µmol per L of (poly)phenol (**Figure 89**) reveal that the simple phenol **11**, the flavanol **16**, the gallotannin **17**, and the ellagitannin, **19** (in yellow) are the most active (poly)phenols.
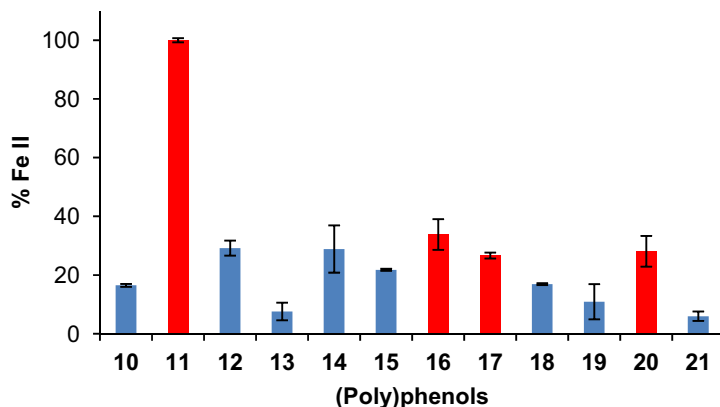
Figure 88. Relative RR of (poly)phenols **10-21** determined with the FRAP method using equal µg mL^{-1} amounts of each (poly)phenol.
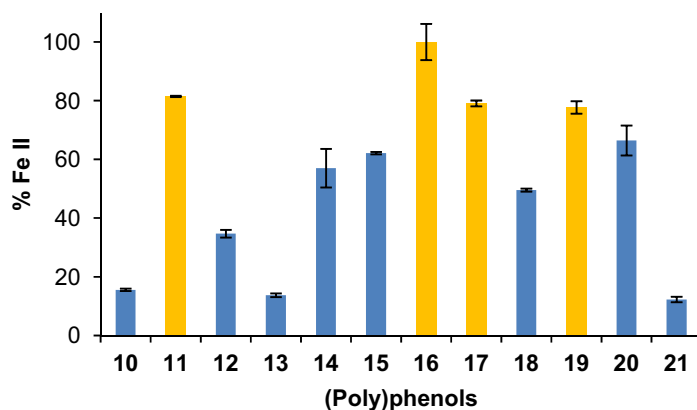
Figure 89. Relative RR of (poly)phenols **10-21** determined with the FRAP method using equal µmol L^{-1} amounts of each (poly)phenol.

4.3.2 Reducing capacity (RC) of (poly)phenols

The FRAP assay was tested with (poly)phenols in aqueous solution (pH=3.6, sodium acetate buffer) with a long incubation time (1 h). Results of the RC of (poly)phenols with the Fe(III)-o-phenantroline complex were expressed in µg of (poly)phenol per mL and in µmol of (poly)phenol per L (Graphics are included as Annex 13, sections C in µg mL^{-1} and D in µmol L^{-1}). The simple phenols pyrogallol (**11**) and

methylgallate (**12**), the flavanol ECG (**15**), the gallotannin PGG (**18**) and the ellagitannin punicalagin (**19**) are the most sensitive (poly)phenols with the FRAP method (green) (**Figure 90**, results expressed in µg per mL of (poly)phenol). RC values of the flavanols **13**, **14**, **15** and **16** and of the gallotannins **17** and **18** are very similar. When the results are expressed in µmol per L of (poly)phenol (**Figure 91**), the simple phenol **12**, the flavanol **15**, the gallotannin **18**, and the ellagitannin **19** (in pink) are the (poly)phenols with higher RC values. RC values of the simple phenols **11** and **12**, of the flavanols **13-16** and of the gallotannins **17** and **18** are very similar.
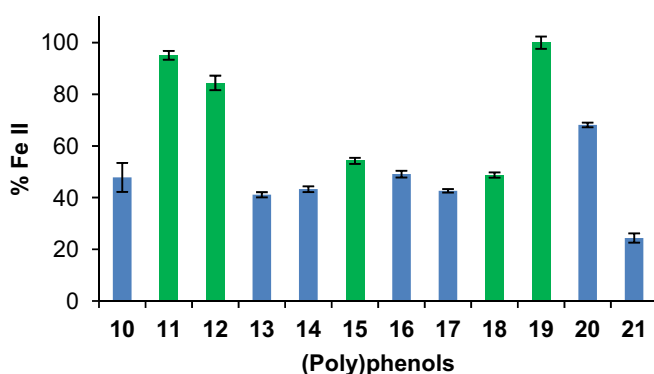
Figure 90. Relative RC values of (poly)phenols **10-21** determined with the FRAP method using equal µg mL-1 amounts of each (poly)phenol.
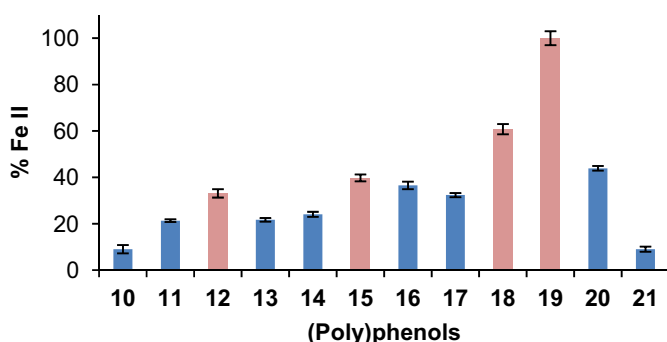
Figure 91. Relative RC values of (poly)phenols **10-21** determined with the FRAP method using equal µmol L-1 amounts of each (poly)phenol.

4.4. Comparison of the Radical Scavenging Capacity (RSC) of (poly)phenols obtained with HNTTM, TNPTM, DPPH and the Reducing Capacity (RC) obtained with the Ferric Reducing Antioxidant Power (FRAP) method

The RSC of (poly)phenols **10**-**21** was determined with HNTTM (**4**), TNPTM (**8**), and DPPH (**9**) under the same experimental conditions (See Materials and Methods, Section 3.2.1.10), and the RC was evaluated with the FRAP method.

The outcome of assays with the (poly)phenols and the radicals **4** and **9**, as well as from the FRAP method provide similar relative results, even though the reactions proceed through different reducing mechanisms, and are conducted in different solvents (**Table 21**). Essentially all the hydroxyls within the substructures containing catechol and pyrogallol functions are detected by these three methods. In contrast, radical **8** is a selective chemosensor, reacting only with the most reactive moieties of the assayed (poly)phenols (i.e. pyrogallol group, structures formed by a C-C bond between two phenols, such as the DHHDP group and C-C bond between the gallate and the ellagic acid moieties present in punicalagin (**19**)). In conclusion, the radicals **4** and **8** are two valuable and complementary electron-transfer chemosensors: the radical **4** is useful to evaluate the total RSC of (poly)phenols, whereas the radical **8** detects selectively their most scavenging moieties among them. This is important because the biological activity and toxicology associated to catechols and pyrogallols seem to be different (see below).

4. Results and Discussion

Table 21. The RSC and RC values[a,b] of (poly)phenols **10-21** determined with HNTTM, TNPTM and DPPH, and the RC values with FRAP method.

	HNTTM		TNPTM		DPPH		FRAP	
	% mmol µg^{-1}	µmol µmol^{-1}	% mmol µg^{-1}	µmol µmol^{-1}	% mmol µg^{-1}	mmol µmol^{-1}	µg mL-1	µmol L^{-1}
10	85	76	-	-	67	59	50	42
11	100	100	100	100	100	100	100	100
12	69	107	-	-	37	56	89	155
13	38	64	-	-	33	77	43	102
14	39	100	26	95	39	91	46	113
15	89	320	-	-	47	167	57	186
16	48	178	39	95	48	167	52	171
17	28	107	9	38	45	167	45	152
18	36	267	-	-	53	333	51	285
19	52	400	43	113	67	500	105	469
20	47	133	42	106	42	125	72	206
21	65	160	-	-	56	143	26	42

[a]Values expressed in % respect to the RSC as ARP (mmol of radical per µg of (poly)phenol and µmol of radical per µmol of (poly)phenol) or RC (µg per mL of (poly)phenol and µmol per L of (poly)phenol) of pyrogallol (**11**). [b](-) Values ≤ 13 (mmol/µg) and 21 (µmol/µmol).

Table 21 shows that the Electron-Transfer capacity values of the assayed (poly)phenols determined with radicals **4**, **9** and with the FRAP method, generally show that the (poly)phenols pyrogallol (**11**) (in red), ECG (**15**) (in green), PGG (**18**) (in blue), and punicalagin (**19**) (in yellow) are the most effective scavenging and reducing (poly)phenols from each group in CHCl$_3$/MeOH (2:1) or in water.

4. Results and discussion

4.5. Biological effect of synthetic and natural (poly)phenols in colon adenocarcinoma HT-29 cells

4.5.1. Biological effect of thio-flavanols in colon adenocarcinoma HT-29 cell line

<u>4.5.1.1. Antiproliferation produced by flavanols derived with cysteine (Cys) and cysteamine (Cya)</u>

The influence of thio-flavanols of cysteine (Cys) and cysteamine (Cya) derived from EGC (**14**), ECG (**15**) and EGCG (**16**) on the viability of HT-29 cells was determined with the MTT (3-(4,5-dimethylthiazol-2-yl)-2,5-diphenyltetrazolium bromide) assay (See Materials and Methods, Section 3.2.2.4 and the graphics of the % of viability are included as Annex 14, A.

Table 22. Viability of HT-29 cells in the presence of (poly)phenols[a].

Thio-flavanols	IC$_{50}$ (μg mL^{-1})
14	24.1± 2.75
15	53.7 ± 11.9
16	17.5 ± 3.21
14A	32.7 ± 2.21
16A	37.2 ± 3.36
14B	35.5 ± 5.21
16B	47.3 ± 2.53
15B	103 ± 6.45

[a]Values are means (± (SD) standard deviation) of three (n=3) experimental measurements

All thio-flavanols **14A**-**15B** and their precursors (**14**, **15** and **16**) tested produce significant antiproliferation in HT-29 cells (**Table 22**). The antiproliferative effect produced by thio-flavanols on HT-29 cells was lower than that the effect produced by their precursors EGC (**14**), ECG (**15**) and EGCG (**16**). The antiproliferation produced by **14A** and **14B** is lower albeit similar than its precursor **14**, the effect produced by **16A** and

16B is 2-fold and 3-fold lower than that of its precursor **16**, respectively, and **15B** is 2-fold lower than its precursor **15**.

<u>4.5.1.2. Induction of apoptosis produced by flavanols derived with cysteine (Cys) and cysteamine (Cya)</u>

To examine the apoptotic effect of thio-flavanols on HT-29 cells at concentrations equal to their IC$_{50}$, cells were treated with the different thio-flavanols during 72 h and analyzed by flow cytometry (See Materials and Methods, Section 3.2.2.5). The results obtained show that all thio-flavanols assayed produce significant early apoptosis and lower late apoptosis and necrosis. Thio-flavanols containing cysteamine produce higher early and late apoptosis values than those containing cysteine. The early apoptosis produced by **14A** and **16A** is 2-fold, by **14B** and **16B** is 3-fold, and **15B** is 6-fold than the control (**Figure 92**). There is not a direct relation between the number of electrons transferred (n$_e$) by these thio-flavanol and the induction of apoptosis values (See **Table 10**).
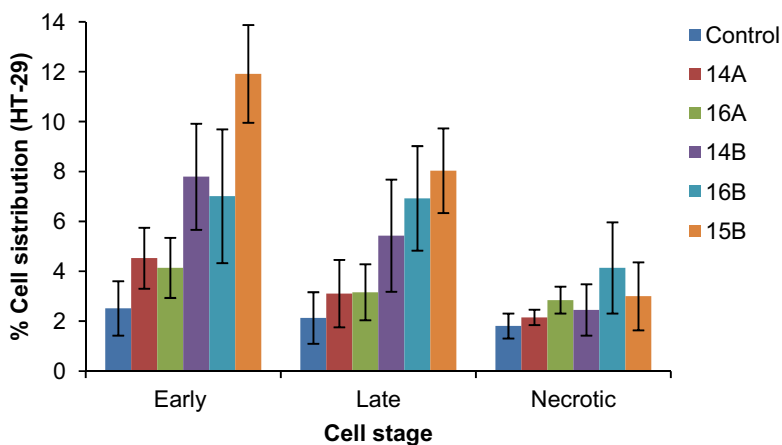
Figure 92. Induction of apoptosis in HT-29 cancer cells after treatment with different thio-flavanols at their respective IC$_{50}$ values. Percentages of cells in different cell stages are shown (cell stages are shown on the x-axis). (% cells ± SD (Standard Deviation). Number of assays performed by (poly)phenol, n= 3).

4.5.2. Biological effect of natural (poly)phenols in colon adenocarcinoma HT-29 cell line culture

4.5.2.1. Antiproliferation produced by (poly)phenols

The influence of (poly)phenols **11-21** on the viability of HT-29 colon cells was determined with the MTT assay (See Materials and Methods, Section 3.2.2.4) with and without catalase(*157*) to account for artifactual results by the formation of hydrogen peroxide (H_2O_2) from the superoxide radical generated in the medium by electron-transfer of (poly)phenols to oxygen(*35*). The results are presented in **Table 23** and the graphics of the % of viability are included as Annex 14, B without catalase and C with catalase.

Table 23. Viability of HT-29 cells in the presence of (poly)phenols.

Families of (poly)phenols	IC$_{50}$[a]	IC$_{50}$[b]
Simple phenols		
11	5.61 ± 0.50	71.4 ± 7.49
12	24.6 ± 8.29	31.6 ± 1.82
Flavanols		
13	≤ 120 ± 18.9	≤ 120 ± 51.2
14	24.1± 2.75	≤ 120 ± 5.28
15	53.7± 11.94	58.9 ± 7.98
16	17.5 ± 3.21	47.9 ± 7.97
Hydrolizable tannins		
Gallotannins		
17[c]	9.69 ± 4.50	6.30 ± 2.22
18[c]	26.3 ± 8.75	31.9 ± 1.13
Ellagitannins		
19	21.5 ± 3.53	14.4 ± 0.38
20	32.5 ± 3.88	34.1 ± 0.48
21	≤ 120 ± 27.5	≤ 120 ± 6.32

[a,b] IC$_{50}$ ± SD (SD= standard deviation) in µg per mL; values are means of two or three (n=2-3) experimental measurements; HT-29 cells were treated with the compounds for 72 h, in [a]DMEM and [b]DMEM with catalase. [c] Data from Sánchez-Tena *et al.*(*158*)

The most antiproliferative (poly)phenols assayed with HT-29 cells without catalase were pyrogallol (**11**) as simple phenol, EGC (**14**) and EGCG (**16**) from flavanols, HT (**17**) from gallotannins, and punicalagin (**19**) and DHHDP (**20**) from ellagitannins (**Table 23**). IC$_{50}$ values obtained for (poly)phenols treated with catalase differ from those obtained for simple phenols and flavanols without catalase showing that the antiproliferative effect produced by the phenol **11** and the flavanols **14** and **16** was, at least in part, artifactual since catalase diminished or eliminated their activity. This effect does not mean that those (poly)phenols were less efficient per se; the oxygen in the medium may have reacted with them before they could reach the cell. The results with catalase demonstrate only that the experimental set-up does not adequately mimic the situation *in vivo* where the extracellular oxygen concentration is much lower. Catalase did not influence the activity of the rest of (poly)phenols tested (**12**, **13**, **15**, **17-21**), which suggests that this activity was not due to extracellular hydrogen peroxide.

4.6. Comparison of the electron-transfer capacity of (poly)phenols with their biological effect on a cancer cell line.

(Poly)phenols **10**-**21** were assayed with different chemical methods to study their chemical properties and finally tested in HT-29 cells to evaluate their biological effect *in vitro*. The Radical Scavenging Capacity (RSC) of (poly)phenols was determined with HNTTM (**4**), TNPTM (**8**) and DPPH (**9**), and the Reducing Capacity (RC) with FRAP methods. The effect of (poly)phenols **11**-**21** on cell viability was determined in HT-29 cell line. All the (poly)phenols tested except the flavanol EC (**13**) and the ellagitannin EA (**21**), both bearing only two geminal hydroxyls as catechol, affected the proliferation of HT-29 cells. It is very interesting to point out that the active (poly)phenols detected with the radical **8** (pyrogallol (**11**), EGC (**14**), EGCG (**16**), HT (**17**), punicalagin (**19**) and DHHDP (**20**)), are also those that trigger the highest antiproliferative effect. As the radical **8** detects the most reactive (poly)phenols as electron donor reagents (e.g. pyrogallol moiety from tea catechins and substructures of punicalagin that contain gallate moieties linked either to each other, hexahydroxydiphenyl moiety, or to the ellagic acid moiety by C-C bonds), our results suggest that electron transfer processes should play an important role in the antiproliferative effect in colon adenocarcinoma HT-29 cell line culture. Pyrogallol and gallocatechins such as EGC (**14**) and EGCG (**16**) which contain this substructure, are among the most biologically active (poly)phenols and can be detected by TNPTM (**8**). The results with the ellagitannin punicalagin (**19**) were less expected because its substructure ellagic acid was inactive against the radical **8**. TNPTM (**8**) though revealed the punicalagin's C-C linked substructures that included hydroxyls were more active than catechols and gallates. These substructures may play a role in the biological effect of ellagitannins.

The outcome of the cell viability assay cannot be related to the redox behaviour of the (poly)phenolic structures in a straightforward way because (poly)phenols may influence cell functions by more than one mechanism and because they may not only be scavengers but actually trigger the formation of radicals. Whatever the case, the results of this thesis corroborate that pyrogallols and gallates are active against colon adenocarcinoma cells and suggest that the hydroxydiphenyl substructure of punicalagin may play a role involving a particularly reactive redox position. As some of the effects ascribed to pyrogallols *in vitro* may be due to the artifactual generation of H_2O_2 in the culture medium (*35, 159*), we ran the *in vitro* experiments in the presence of catalase.

This resulted in a significant decrease in the activity of the (poly)phenols that contained pyrogallols in their structure. This does not alter the fact that pyrogallols are the most reactive species, because they must be able to generate the superoxide radical as the first step in the formation of H_2O_2; it just shows that the experimental set-up does not adequately mimic the situation *in vivo* where the extracellular oxygen concentration is much lower.(*35*) Punicalagin (**19**) affected cell viability as effectively as gallocatechins. In this case, the effect was not artifactual since it was not affected by the addition of catalase to the medium, which suggests that punicalagin did not generate the superoxide radical extracellularly, at least not to a sufficient extent to affect cell viability.

At the level of the whole organism, the activity of (poly)phenols may come again from their scavenging activity or from their capacity to generate free radicals. This so-called pro-oxidant activity may be behind the moderate toxicity of green tea extracts at very high concentrations (*160*) and the reason why polyphenols are rapidly metabolised and excreted after ingestion. Interestingly, at concentrations that are not so high, this mild pro-oxidant activity may result in an overall antioxidant effect via a mechanism known as hormesis, which can be defined as a low-dose stimulation of defence systems with a subsequent beneficial effect.(*33*) Whatever the case, if (poly)phenols exert an influence over the redox status of any system whether it is antioxidant, toxic pro-oxidant or hormetic pro-oxidant, it is somehow related to the reactivity of the constitutive hydroxyl groups.

Independently of whether reactive (poly)phenols actually scavenge radicals or trigger hormetic responses, the use of the radical **8** as chemosensor may be a useful tool to facilitate the detection of potentially beneficial (poly)phenols in extracts and foods. Therefore, combining the outcome of HNTTM and TNPTM methods, we may generate a picture of both the RSC of (poly)phenols with a readily reactive radical and the presence of (poly)phenols with highly reactive moieties with potentially higher biological impact.

4.7. Chemo-enzymatic synthesis of (–)epigallocatechin-3-*O*-gallate glucuronides (EGCG-glucuronides)

In human biological samples, EGCG glucuronides were detected by HPLC-CEAS (coulometric array detection) albeit not isolated nor characterized.(*96*) Using an enzymatic glucuronidation with human liver microsomes, Lu and co-workers obtained the glucuronidation products of (–)-epigallocatechin-3-*O*-gallate (EGCG, **16**) at the 4" and 3' positions, the first as the major product (green arrows) (**Figure 93**).(*98*) Interestingly, Nakagawa and co-workers suggested that the hydroxyl at position 4" of EGCG (**16**) was the most reactive (violet arrow) by calculating the deprotonation energy of hydroxyl groups.(*161*) Hong and co-workers found that EGCG-4"-*O*-glucuronide was formed in HT-29 cell cultures.(*162*) In this context, we envisaged a chemo-enzymatic synthesis of EGCG-*O*-glucuronides using a chemical glycosidation. In principle, the most reactive positions of EGCG (**16**) towards its chemical glycosidation may be those that are derivatized by enzymatic glucuronidation.
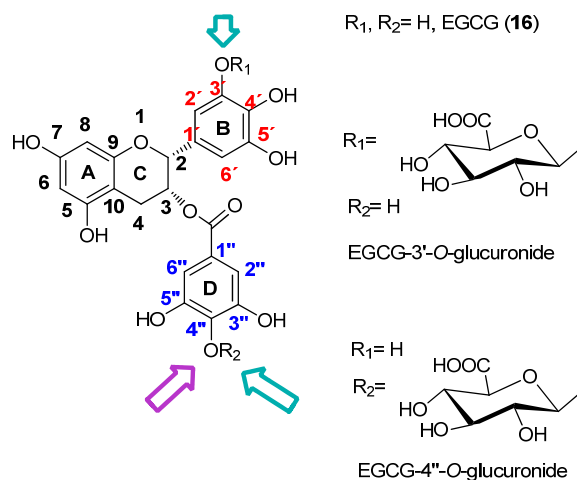
Figure 93. Main enzymatic glucuronidation positions of EGCG (**16**) (green arrows). Chemically more reactive position of EGCG (**16**) (violet arrow).

4.7.1. Chemical glucuronidation of EGCG

4.7.1.1. Optimization of the Koenigs-Knorr reaction conditions for glucuronidation of EGCG with bromo-2,3,4-tri-*O*-acetyl-α-D-glucopyranuronic acid methyl ester

The broadly used Koenigs–Knorr reaction (See Introduction, Section 1.4.4.3.1.2) was used to obtain the EGCG-*O*-acetylglucuronides methyl ester. The reaction catalyzes the formation of *O*-glycosides from an acetylated glycosyl halide and a hyroxylated compound in the presence of a promoter (e.g. silver or mercury salt (original Koenigs-Knorr reaction) and K_2CO_3). The solvents and temperature used in the reaction are chosen according to the solubility and stability of substrates and products.

In the reaction of our interest, bromo-2,3,4-tri-*O*-acetyl-α-D-glucopyranuronic acid methyl ester (**22**) and EGCG (**16**) were used as acetylated glycosyl halide (as electrophyl) and as hydroxylated compound (as nucleophile), respectively (**Figure 94**).
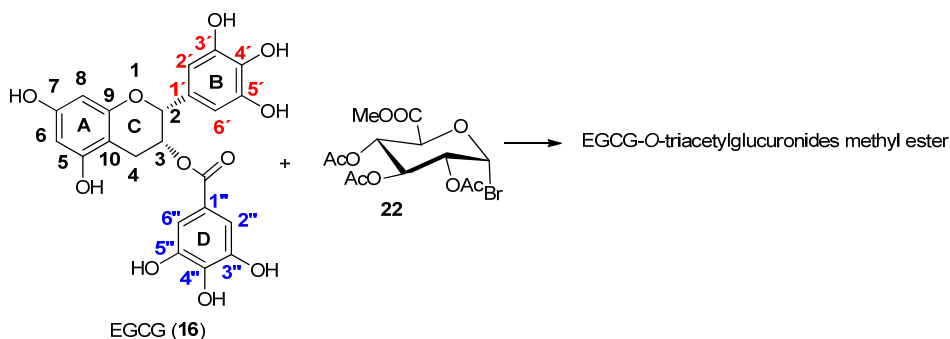
Figure 94. Koenigs-Knorr reaction of **16** with **22**.

The glucuronidation of **16** with **22** by Koenigs-Knorr reaction was assayed in different solvents, temperatures and promoters (**Table 24**) (See Materials and Methods, Section 3.2.3.1).

4. Results and discussion

Table 24. Assayed conditions for the Koenigs-Knorr reaction.

Reaction	16 (mg)	22 (mg)	Promoter (mg)[a]	Solvent (ml)	T (°C)	Peak intensity of detected products[b]
1	5.1	25.2	K_2CO_3 (5.21)	acetone (0.25)	rt	16 >> A16
2	5.2	25.2	K_2CO_3 (4.98)	CH_2Cl_2 (0.25)	rt	16
3	5.1	24.8	K_2CO_3 (4.91)	CH_2Cl_2 (0.25)	40	16
4	5.0	24.2	K_2CO_3 (5.23)	DMF (0.25)	rt	A16 = 16 > A16'
5	5.0	24.3	K_2CO_3 (5.28)	DMSO (0.25)	rt	16 > A16 > A16'
6	9.8	18.5	KOH (24 µl, 1.77 M)	DMF (0.36)	rt	polymerization
7	10.4	26.6	Cs_2CO_3 (7.11)	ACN (1)	rt	polymerization

[a]K_2CO_3(*102*), KOH(*138*), Cs_2CO_3(*139*). [b]The mass of products was identified by HPLC-HR-DAD-ESI-TOF-MS analysis. **A16** (EGCG-*O*-triacetylglucuronide methyl ester), **A16'** (EGCG-*O*-diacetylglcururonide methyl ester). Reaction time: 6 h.

Reactions were followed by HPLC-DAD according to the method described on the Materials and Methods, Section 3.2.3.3.1.1 obtaining different spectrum profiles. Those reactions with well defined new peaks, and a significant reduction of the peak corresponding to **16** were chosen to be analyzed by HPLC-HR-DAD-ESI-TOF-MS (See Materials and Methods, Section 3.2.3.3.2.1). The most efficient reaction conditions to obtain the glucuronidation of **16** was the use of DMF as solvent with K_2CO_3 as promoter at rt with gentle stirring during 6 h (reaction **4** of **Table 24**). With these conditions, different compounds were observed from the HPLC-HR-DAD-ESI-TOF-MS analysis (**Figure 95**). A peak was observed with a retention time of 21 min at *m/z* 773.1657 corresponding to one or more isomers of the desired product, EGCG-*O*-triacetylglucuronide methyl ester (**A16**) (**Figures 95** and **96**). In addition, peaks assigned to compounds derived from **A16** were observed: *m/z* value corresponding to the loss of an acetyl group, EGCG-*O*-diacetylglucuronide methyl ester (**A16'**), two *m/z* values corresponding to the addition of one and two acetyl groups, **A16(Ac)** and **A16(2Ac)**, respectively, and two *m/z* values corresponding to the oxidized and oxidized and demethoxycarbonylated compounds, **A16(O)** and **A16(-MeO,O)**, respectively (**Figures 95** and **96**).
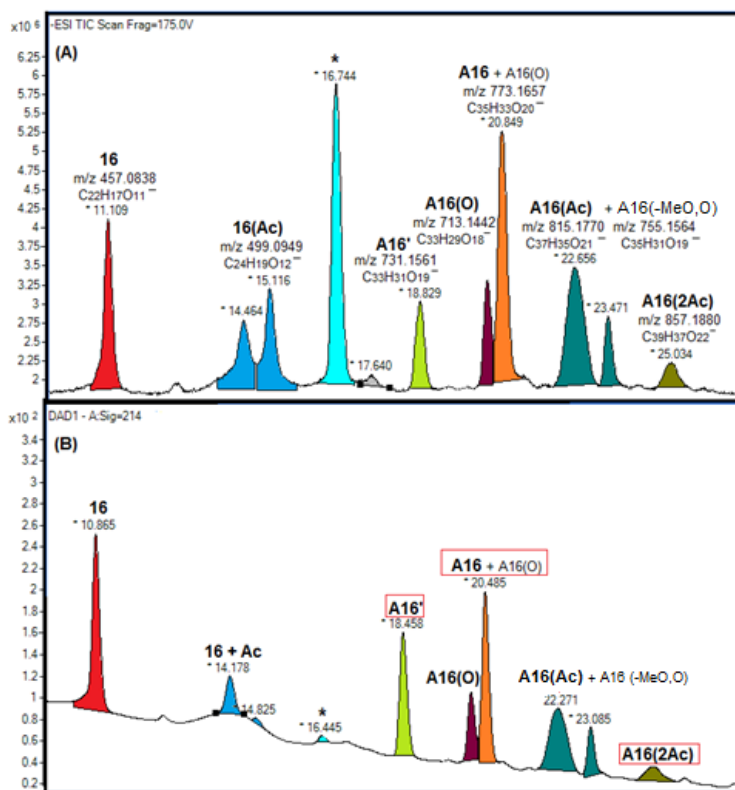
* dimer- trimer- tetramer of acetylglucuronide methyl ester.

Figure 95. Chromatograms obtained by HPLC-HR-DAD-ESI-TOF-MS analysis of the glucuronidation of EGCG (**16**) with DMF and K₂CO₃ (reaction **4** of **Table 25**). **(A)** ESI-TOF-MS chromatogram (TIC, Total Ion Count) **(B)** UV-Vis chromatogram (λ= 214 nm). Retention time of **A16**, 21 min.

4. Results and discussion
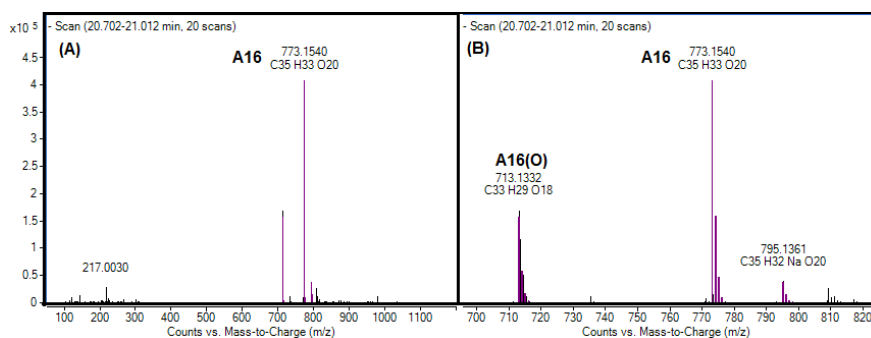
Figure 96. (A) ESI-TOF-MS chromatogram of the peak **A16 (B)** enlargement of chromatogram **(A)**.

4.7.1.2. Preparative glucuronidation of EGCG with bromo-2,3,4-tri-*O*-acetyl-α-D-glucopyranuronic acid methyl ester

The preparative glucuronidation of EGCG (**16**) was carried out in the conditions of the reaction **4** of **Table 24**, following the reaction by HPLC-HR-DAD-ESI-TOF-MS (See Materials and Methods, Section 3.2.3.1.4 and Section 3.2.3.3.2.1). The residue obtained was dissolved in MeOH and purified by semipreparative-HPLC following the method described on the Materials and Methods, Section 3.2.3.3.3.1. Three fractions were obtained:

1. fraction with three peaks with *m/z* of 731.15, 773.16 and 713.13 corresponding to the compounds **A16'**, **A16** and **A16(O)**, 20.75 mg.
2. fraction with *m/z* of 773.16 (**A16**), 18.71 mg.
3. fraction with *m/z* of 773. 16 (**A16**) and 815.17 (**A16(Ac)**), 5.17 mg.

The product EGCG-*O*-triacetylglucuronide methyl ester (**A16**) and its precursor EGCG (**16**) were characterized by NMR (CD₃OD) (¹H-NMR, ¹³C-NMR, HSQC and HMBC).

First, ¹H and ¹³C signals corresponding to the B-ring and D-ring of **16** and **A16** were assigned using ¹H-NMR, ¹³C-NMR, HSQC, and HMBC analysis (NMR spectra are included as Annex 15). The chemical shifts found for the carbon atoms of the B-ring (pyrogallol) of **A16** were very similar to those of **16**. On the other hand, the comparison of the D-ring (gallate) carbon atoms of **A16** and **16** gave different chemical shifts for the C1", C3", C4" and C5" positions (**Table 25**). The equal chemical shifts of C3" and C5"

indicate that C4" is the derivatized position of **A16**. Interestingly, the EGCG-4"-*O*-triacetylglucuronide methyl ester (**A16**) (**Figure 97**) obtained by chemical synthesis is the acetylated precursor of the major glucuronide isomer obtained enzymatically with human liver microsomes, the EGCG-4"-*O*-glucuronide.(*98*)

Table 25. Chemical shifts of atoms corresponding to the B- and D-rings of **16** and **A16**.

	Compound	
B-ring	**16**	**A16**
$H_{2'}$, $H_{6'}$ (ppm)	6.50	6.49
C_2 (ppm)	78.51	78.55
$C_{6'}$, $C_{2'}$	107.05	106.76
$C_{1'}$	130.96	130.73
$C_{4'}$	133.64	133.71
$C_{3'}$	146.66	146.72
$C_{5'}$	146.25	–
D-ring	**16**	**A16**
$H_{2''}$, $H_{6''}$ (ppm)	6.95	6.91
$C_{6''}$, $C_{2''}$	110.43	110.22
$C_{1''}$	121.61	128.29
$C_{4''}$	139.68	137.26
$C_{3''}$	146.28	151.57
C=O	167.6	166.88
$C_{5''}$	146.68	151.83
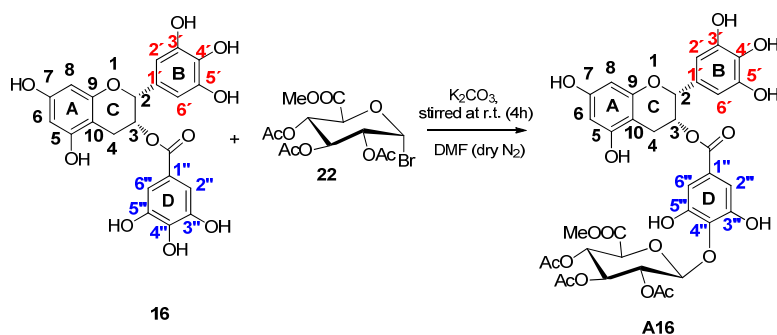
Figure 97. Koenigs-Knorr reaction. Glucuronidation reaction of **16** with **22** and the major reaction product, the **A16**.

4.7.2. Synthesis of EGCG-4''-O-glucronide methyl ester and EGCG-4''-O-glucuronide from EGCG-4''-O-triacetylglucuronide methyl ester
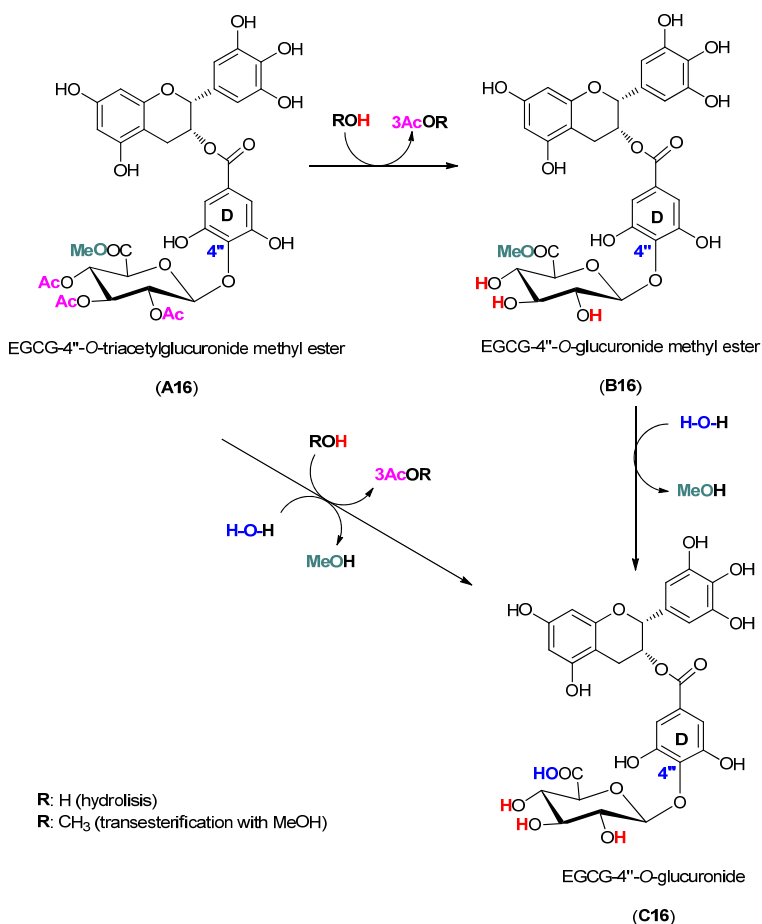
Figure 98. Schematic transformation of **A16** into **B16** or **C16**.

4.7.2.1. Chemical synthesis of EGCG-4''-O-glucuronide methyl ester or EGCG-4''-O-glucuronide from EGCG-4''-O-triacetylglucuronide methyl ester

4.7.2.1.1. Alkaline catalysis

Alkaline conditions were assayed to remove the protective acetyl groups and the methyl ester group of EGCG-4''-O-triacetylglucuronide methyl ester (**A16**), to obtain EGCG-O-glucuronide methyl ester (**B16**) and EGCG-4''-O-glucuronide (**C16**) (**Figure 98**

and **Table 26**). The utilization of NaMeO with MeOH for acetyl transesterification is broadly used in carbohydrate chemistry(*102*) albeit it may hydrolyze other chemically sensitive moieties. On the other hand, Zn(Ac)$_2$ is a milder alkaline agent that may selectively eliminate the acetyl groups of the glucuronide moiety.(*104*)

Table 26. Alkaline conditions assayed to obtain **B16** or **C16** from **A16**.

A16 (mg)	Solvent (ml)	Conditions	T (°C)	t (h)	Desired product	Peak intensity of detected products
9.10	MeOH (3)	Zn(AcO)$_2$ (11.1mg)	35	1.5	**B16**	polymerization
2.03	MeOH (5)	NaMeO/MeOH (72 µl)	4	0.5	**C16**	–

Two alkaline conditions were tested and neither of them gave the desired product (See Materials and Methods, Section 3.2.3.2.1 and Section 3.2.3.2.2). Upon these alkaline treatments, the flavanol **16** was polymerized or hydrolyzed as observed by HPLC-DAD detection, following the method described on the Materials and Methods, Section 3.2.3.3.1.2. As predicted, alkaline deprotection conditions were not compatible with **16** because a number of side reactions may occur, namely the hydrolysis of the labile ester of the C-3 position, the C-ring opening, and polymerization (**Figure 99**).(*104*)

A16
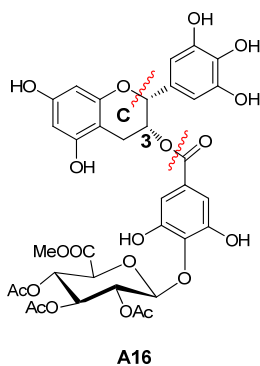
Figure 99. Sensitive chemical bonds of **A16** towards alkaline conditions.

4. Results and discussion

4.7.2.1.2. Acid catalysis

The acid conditions used by González and co-workers(*163*) to selectively deacetylate different carbohydrates containing benzyl esters, were assayed to remove the protective acetyl groups of EGCG-4''-*O*-triacetylglucuronide methyl ester (**A16**), to obtain EGCG-4''-*O*-glucuronide methyl ester (**B16**). Three different reaction conditions were assayed and followed by HPLC-HR-DAD-ESI-TOF-MS (**Table 27**) (See Materials and Methods, Section 3.2.3.2.3 and Section 3.2.3.3.2.2).

Table 27. Deacetylation conditions assayed to obtain **B16** from **A16**.

Reaction	A16 (mg)	*p*-TsOH* (mg)	Solvent (2 ml)	T (°C)	t (h)	Peak intensity of detected products[a]
1	3.96	5.20	CH₂Cl₂/MeOH (9:1)	30	48	**A16** > **A16'** > **A16''** > **B16**
2	4.00	6.93	CH₂Cl₂/MeOH (9:1)	r.t	48	**A16** > **A16'** > **A16''** > **B16**
3	3.92	6.62	MeOH/CH₂Cl₂ (4.5:1)	r.t	48	**A16** > **A16'** > **A16''** > **B16**

*p-TsOH (*para*-Toluenesulfonic acid) [a]the products were identified according to the *m/z* values obtained by HPLC-HR-DAD-ESI-TOF-MS analysis. **A16'** (EGCG-4''-*O*-diacetylglucuronide methyl ester), **A16''** (EGCG-4''-*O*-monoacetylglucuronide methyl ester) (deacetylated positions not determined).

The peak with a *m/z* 647.13 corresponding to the compound **B16** was observed by HPLC-HR-DAD-ESI-TOF-MS in the three reaction conditions, albeit the deacetylation efficiency was insufficient to obtain **B16** in a sufficient amount to be purified.

4.7.2.2. Enzymatic synthesis of EGCG-4''-*O*-glucuronide from EGCG-4''-*O*-triacetylglucuronide methyl ester

The chemical conditions assayed for the deacetylation and the hydrolysis of the methyl ester of EGCG-4''-*O*-triacetylglucuronide methyl ester (**A16**) were not compatible with the sensitive moieties found in this compound. For this reason, the use of esterases was assayed for these transformations.(*107, 164, 165*) The esterases are enzymes which hydrolyze regio- and stereoselectively the deacylation of a wide range of substances.(*105*) In organic solvent conditions, esterases are used to acylate or deacylate hydroxyl functions, showing different selectivity depending on the esterase and the precise reaction conditions. This ability is widely used to selectively protect or deprotect a certain hydroxyl position of a molecule, and for the differentiation of stereoisomers, which can be discerned and transformed by esterases.(*165*) In the present case, a number

of esterases, concretely lipases, were assayed for the non-specific transesterification or hydrolysis of the acetyl functions of EGCG-4''-*O*-triacetylglucuronide methyl ester (**A16**) in different organic solvents and in mild aqueous conditions.

Two different routes were assayed for the synthesis of EGCG-4''-*O*-glucuronide (**C16**) from **A16** (**Figure 100**). These approaches are based on those used by Baba and co-workers to obtain 1-β-*O*-acyl glucuronides of three non-steroidal anti-inflammatory drugs.(*105*)
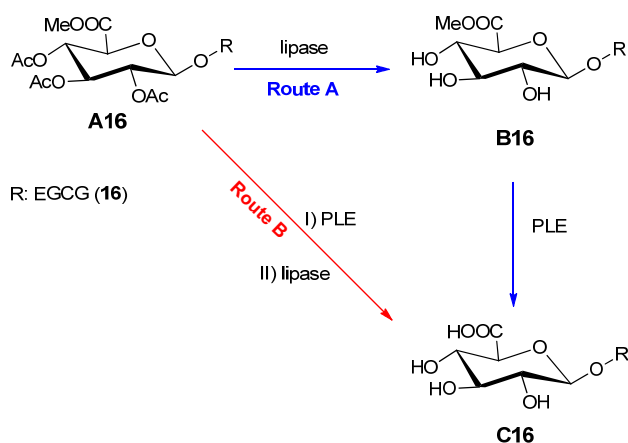
Figure 100. Proposed routes for the synthesis of **C16** from **A16**.

The effectiveness of the enzymes used in both routes strongly depends on the structure and polarity of their substrates. Hence, the order of utilization of the esterases for deacetylation and methyl ester hydrolysis of **A16** can be essential for their efficacy.

4.7.2.2.1. **Route A.** Deacetylation of the EGCG-4''-*O*-triacetylglucuronide methyl ester to obtain the EGCG-4''-*O*-glucuronide methyl ester

Five lipases at different reaction conditions were tested for the deacetylation of EGCG-4''-*O*-triacetylglucuronide methyl ester (**A16**) to obtain the EGCG-4''-*O*-glucuronide methyl ester (**B16**) following the procedure described on the Materials and Methods, Section 3.2.3.2.4: Novozyme-435 (N-345), Lipase A (LA), Lipozyme IM (LIM), Porcine pancreatic lipase (PPL), and Lipase AS (LAS). Reactions were followed by HPLC-HR-DAD-ESI-TOF-MS (See Materials and Methods, Section 3.2.3.3.2.2).

4. Results and discussion

N-345 and LIM were tested in different solvents detecting the same major product by HPLC-HR-DAD-ESI-TOF-MS with a *m/z* 713.15, corresponding to EGCG-4''-*O*-diacetylglucuronide methyl ester (**A16'**). In most reactions with LA and LAS, a peak was detected with a *m/z* 647.13 corresponding to the mass of the product **B16**. The best reaction conditions to deacetylate **A16** were the use of LAS in a proportion **A16**:LAS of 1:30 (w/w) with sodium phosphate buffer (Na_2HPO_4 buffer) (25 mM) at pH between 6-7 as solvent, DMSO as co-solvent (20 %) at 40 °C, and stirring during 4.5 h (reactions **16** and **17** of **Table 28**).

Table 28. Reaction conditions assayed with different lipases to deacetylate **A16**.

Reaction	Enzyme[a]	Solvent	A16 (mg)	Lypase (mg)	Conditions[b]	t (h)	T (°C)	Peak instesity of detected products[c]
1	N-435	THF (1ml)	3.65	50.2	IRA (50.2 mg)	24	30	**A16'**
2	N-435	diisopropyl eter (1 ml)	3.10	82.1	IRA (50.0 mg)	24	30	**A16'**
3	N-435	water (0.9 ml), MeOH (0.1 ml)	2.2	58.9	P.P.B (30 mM, pH 8.0)	44	30	**A16'**
4	LA	THF (1 ml)	3.3	50.6	IRA (50.0 mg)	24	30	Several products that disappear during reaction
5	LA	diisopropyl eter (1 ml)	2.1	28.5	IRA (70.6 mg)	24	30	Mixture of peaks and **B16** in a very low yields
6	LA	water (0.9 ml), MeOH (0.1 ml)	1.9	26.6	P.P.B (30 mM, pH 8.0)	24	30	Mixture of peaks and disappearance during reaction time
7	LA + N-435	water (0.9 ml), MeOH (0.1 ml)	2.7	10.1 (LA) + 15.7 (N-435)	P.P.B (30 mM, pH 8.0)	24	30	**A16'** and mixture of Peaks with a very low yields
8	LA	water (0.4 ml), DMSO (0.1 ml)	0.57	8.61	S.P.B (25 mM, pH 6.1)	4.5	40	**B16-H₂O** > **A16'** = **B16**
9	LA	water (0.4 ml), DMSO (0.1 ml)	0.57	15.4	S.P.B (25 mM, pH 6.1)	4.5	40	**B16-H₂O** > **B16** > **A16'**
10	LA	water (0.4 ml), DMSO (0.1 ml)	0.54	15.50	S.C.B (25 mM, pH 5.0)	4.5	40	**B16-H₂O** > **B16** = **A16'**
11	LIM[b]	THF (1 ml)	3.2	50.2	IRA (56.1 mg)	24	30	**A16'**
12	PPL	THF (1 ml)	3.4	50.1	IRA (51.4 mg)	24	30	n.r

4. Results and discussion

Reaction	Enzyme[a]	Solvent	A16 (mg)	Lypase (mg)	Conditions[b]	t (h)	T (°C)	Peak instesity of detected products[a]
13	LAS	water (0.8 ml), THF (0.2 ml)	1.07	15.3	S.P.B (25 mM, pH 6.1)	5	30	Mixture of peaks and polymerization
14	LAS	water (0.8 ml), DMSO (0.2 ml)	1.08	15.7	S.P.B (25 mM, pH 6.1)	5	30	**A16" > B16-H₂O > A16' > B16**
15	LAS	water (0.4 ml), DMSO (0.1 ml)	0.58	7.36	S.P.B (25 mM, pH 6.1)	4.5	40	**B16-H₂O > A16' > B16**
16	LAS	water (0.4 ml), DMSO (0.1 ml)	0.59	15.4	S.P.B (25 mM, pH 6.1)	4.5	40	**B16-H₂O > B16**
17	LAS	water (0.4 ml), DMSO (0.1 ml)	0.50	15.1	S.P.B (25 mM, pH 6.7)	4.5	40	**B16-H₂O > B16**
18	LAS	water (0.4 ml), DMSO (0.1 ml)	0.58	15.3	S.C.B (25 mM, pH 5.0)	4.5	40	**B16-H₂O > A16' = B16**

[a]LIM Lypase immobilized on EP-100 (polypropylene powder 200-400 microns). [b]P.P.B (Potassium Phosphate Buffer), S.P.B (Sodium Phosphate Buffer), S.C.B (Sodium Citrate Buffer). [c]The products were identified according to the m/z values obtained by HPLC-HR-DAD-ESI-TOF-MS analysis IRA (ion exchange resin). **B16-H₂O** (dehydrated **B16**). n.r : no reaction.

174

The analysis of the reaction with LAS at pH 6.1 followed by HPLC-HR-DAD-ESI-TOF-MS (See Materials and Methods, Section 3.2.3.3.2.2) gave both the *m/z* 647.13 corresponding to the mass of the desired product **B16** (**Figure 101** and **102**) and the *m/z* 629.11 corresponding to the mass of **B16-H₂O** (structure not shown).
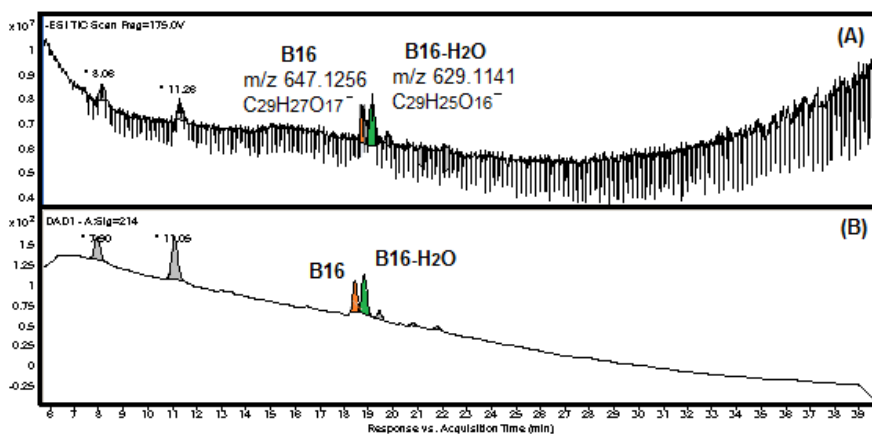
Figure 101. Chromatogram of **(A)** ESI-TOF-MS (TIC) and **(B)** UV-Vis at λ=214 nm, obtained by HPLC-HR-DAD-ESI-TOF-MS of the reaction of **A16** with LAS with a proportion of **A16**:LAS of 1:30 (w/w), with Na_2HPO_4 buffer (25 mM, pH 6.1) as solvent, and DMSO as co-solvent (20 %) (40 °C, 4.5 h). The peaks of **B16** (orange) and **B16-H₂O** (green) appear at 18 and 19 min, respectively. Peaks at 8 and 11 min are detected in LAS solution.
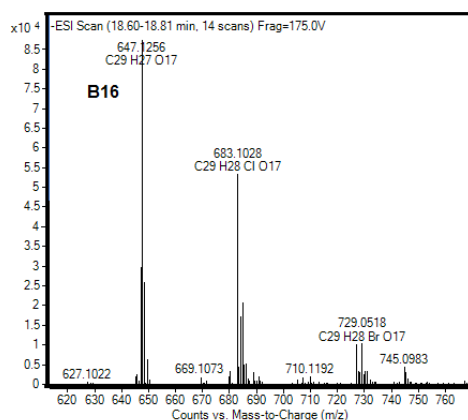
Figure 102. ESI-TOF-MS chromatogram of the peak of **B16**.

4. Results and discussion

4.7.2.2.1.1. Preparative deacetylation of the EGCG-4"-O-triacetylglucuronide methyl ester to obtain the EGCG-4"-O-glucuronide methyl ester

A preparative synthesis to obtain EGCG-4"-*O*-glucuronide methyl ester (**B16**) from EGCG-4"-O-triacetylglucuronide methyl ester (**A16**) was attempted using the conditions of the reaction **16** of **Table 28**, albeit the concentration of the enzyme LAS and the product **A16** were duplicated (See Materials and Methods, Section 3.2.3.2.4.2). The reaction was followed by HPLC-HR-DAD-ESI-TOF-MS (See Materials and Methods, Section 3.2.3.3.2.2) and the *m/z* corresponding to the desired product **B16** was detected together with that of **B16-H₂O**, in a similar concentration as in the reaction **16** of **Table 28**. The isolation of **B16** was unsuccessful due to the high amount of lipase used, which could not be efficiently separated.

4.7.2.2.2. **Route B.** Methyl ester hydrolysis and deacetylation of the EGCG-4"-*O*-triacetylglucuronide methyl ester with PLE and LAS or LA, respectivley (one-pot reaction)

This route consists in the hydrolysis of the methyl ester of the glucuronide moiety of EGCG-4"-*O*-triacetylglucuronide methyl ester (**A16**) to obtain EGCG-4"-*O*-triacetylglucuronide (**A16-Me**) with PLE (Porcine Liver Esterase) (**Figure 103**), followed by the deacetylation of **A16-Me** to obtain the final product EGCG-4"-*O*-glucuronide (**C16**) with lipases LAS or LA (**Table 29**) (See Materials and Methods, Section 3.2.3.2.4.3).

Table 29. Reaction conditions assayed to hydrolyze the methyl ester of **A16** to obtain **A16-Me** and deacetylate **A16-Me** to obtain **C16**.

Reaction	Enzyme	Solvent	A16 (mg)	Lipase (mg)	Conditions[a]	t	Detected products[b]
1	PLE/LAS	water (1.8 ml), DMSO (0.4 ml)	4.13	8.34/121.42	S.C.B (25 mM) pH 5.0	30' (PLE), 1h (LAS)	polymerization
2	PLE/LAS	water (1.8 ml), DMSO (0.4 ml)	4.08	8.35/49.9	S.C.B (25 mM) pH 5.0	30' (PLE), 4h (LAS)	**D16'** > **D16"** = **C16-H₂O** > **C16**
3	PLE/LAS	water (1.8 ml), DMSO (0.4 ml)	3.98	8.28/24.75	S.C.B (25 mM) pH 5.0	30' (PLE), 4h (LAS)	**D16'** > **D16"** > **C16-H₂O** > **C16**
4	PLE/LAS	water (1.8 ml), DMSO (0.4 ml)	4.10	8.25/25.45	S.P.B (25 mM) pH 6.2	30' (PLE), 4h (LAS)	**D16'** > **D16"** > **C16-H₂O** > **C16**
5	PLE/LA	water (1.8 ml), DMSO (0.4 ml)	3.98	8.21/24.98	S.P.B (25 mM) pH 6.2	30' (PLE), 4h (LA)	**D16'** > **D16"** = **C16-H₂O** > **C16**
6	LA/PLE	water (1.8 ml), DMSO (0.4 ml)	4.24	24.96/8.31	S.P.B (25 mM) pH 6.2	4h (LA), 30' (PLE)	**B16-H₂O** > **D16"** > **D16'** > **A16'**

4. Results and discussion

Reaction	Enzyme	Solvent	A16 (mg)	Lipase (mg)	Conditions[a]	t	Detected products[b]
7	PLE/LA	water (1.8 ml), DMSO (0.4 ml)	4.09	8.16/26.35	S.P.B (50 mM) pH 7.3	30' (PLE), 4h (LA)	**D16" > C16-H₂O>C16 > 16**
8	PLE/LA	water (1.8 ml), DMSO (0.4 ml)	4.22	8.27/25.77	S.P.B (50 mM) pH 7.3	30' (PLE), 22h (LA)	**C16-H₂O > 16 > C16 > D16"**

[a]S.C.B (Sodium Citrate Buffer), S.P.B (Sodium Phosphate Buffer). [b]Products were assigned according to the m/z values obtained by HPLC-HR-DAD-ESI-TOF-MS analysis. **D16'** (EGCG-4"-*O*-diacetylglucuronide, **D16"** (EGCG-4"-*O*-monoacetyl glucuronide) (deacetylated positions not determined), **C16-H₂O** (dehydrated EGCG-4"-*O*-glucuronide). Temperature 40 °C.
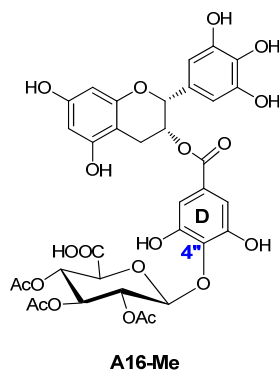
Figure 103. Structure of **A16-Me**.

178

The PLE in water at different pH values (5.0, 6.2 and 7.3) was tested to hydrolyze the methyl ester of **A16**. Reactions were followed by HPLC-HR-DAD-ESI-TOF-MS using the method described on the Materials and Methods, Section 3.2.3.3.2.2. PLE was efficient at all assayed pH values at 30 min of reaction, respectively. The two major peaks were obtained with a *m/z* of 717.13 and 759.14 at 28-30 and 31 min, corresponding to **A16-Me**, and EGCG-4''-*O*-diacetylglucuronide (**D16'**), respectively. After 30 min of reaction with PLE, LAS or LA were added to the reaction mixtures to obtain **C16** from **A16-Me** (See below).

4.7.2.2.2.1. Methyl ester hydrolysis of EGCG-4''-O-triacetylglucuronide methyl ester to obtain EGCG-4''-O-triacetylglucuronide with PLE and its further deacetylation to obtain EGCG-4''-O-glucuronide with LAS

The reaction conditions were defined attaining to the assays performed on route A, and the assays with PLE described above. Therefore, we first tested the methyl ester hydrolysis with PLE and further the deacetylation with LAS at pH 5.0 and 6.2 following changes by HPLC-HR-DAD-ESI-TOF-MS (Section 3.2.3.3.2.2). For the reaction conditions tested (reactions from **1** to **4** of **Table 29**), the amount of EGCG-4''-*O*-glucuronide (**C16**) obtained was too low (See Materials and Methods, Section 3.2.3.2.4.3).

4.7.2.2.2.2. Methyl ester hydrolysis of EGCG-4''-O-triacetylglucuronide methyl ester to obtain EGCG-4''-O-triacetylglucuronide with PLE and its further deacetylation to obtain EGCG-4''-O-glucuronide with LA

The best deacetylation conditions using the lipase LA on the route A were at pH 6.1 and DMSO as co-solvent. The methyl ester hydrolysis with PLE and the deacetylation with LA were tested at different pH values (6.2 and 7.3) and followed by HPLC-HR-DAD-ESI-TOF-MS (See Materials and Methods, Section 3.2.3.2.4.3 and Section 3.2.3.3.2.2). The methyl ester hydrolysis at both pH values gave a high peak with *m/z* 759.14 corresponding to the compound EGCG-4''-*O*-triacetylglucuronide (**A16-Me**) (**Figure 104** and **Figure 105**).
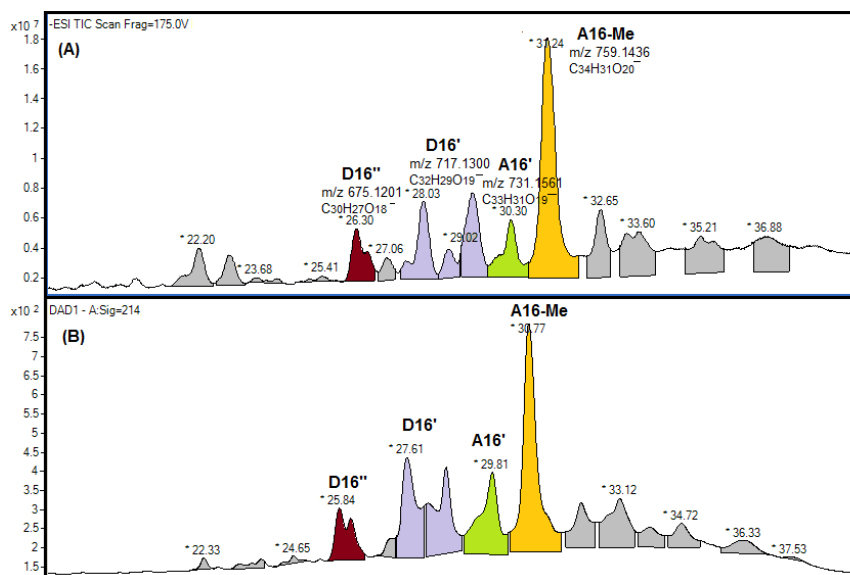
Figure 104. (A) ESI-TOF-MS chromatogram (TIC) and **(B)** UV-Vis (λ =214 nm) chromatogram of the methyl ester hydrolysis of **A16** with PLE at pH 7.3 after 30 min of reaction. (reaction **7** of **Table 29**). Retention time of **A16-Me** at 31 min.
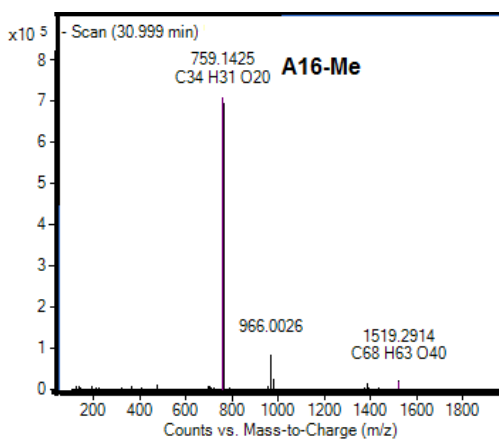
Figure 105. ESI-TOF-MS chromatogram of the **A16-Me** peak.

Further addition of LA gave the final product **C16** in low yield at pH 6.2 and higher at pH 7.3 (**Figure 106** and **107**). At pH 7.3, the precursor EGCG (**16**) was also observed owing to the hydrolysis of the glycosidic moiety.
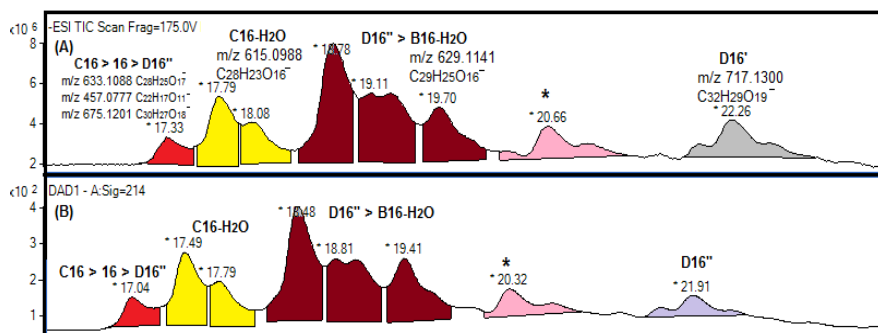
Figure 106. ESI-TOF-MS (TIC) and UV-Vis (λ =214 nm) chromatograms of deacetylation reaction of **A16** with PLE/LAS at pH 7.3 after 4 h of reaction (reaction **7** of **Table 29**). Retention time of **C16** at 17 min.
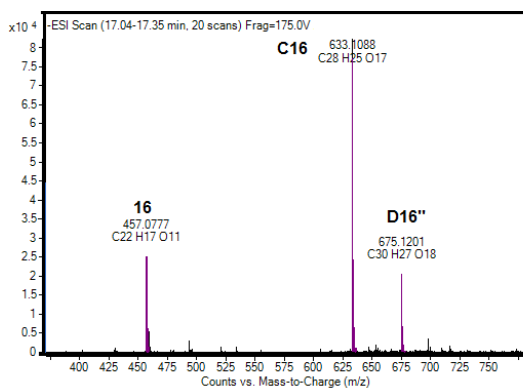
Figure 107. ESI-TOF-MS chromatogram of the **C16** peak.

The methyl ester hydrolysis and deacetylation were followed qualitatively by HPLC-DAD and by HPLC-HR-DAD-ESI-TOF-MS to detect the products of interest (See Materials and Methods, Section 3.2.3.3.1.2 and Section 3.2.3.3.2.2). Products obtained in both steps, hydrolysis and deacetylation, could not be quantified because of the lack of standards. The high absorbance of acetylated products compared to that of those deacetylated ones has to be considered.

4. Results and discussion

4.7.2.2.2.3. Preparative methyl ester hydrolysis of EGCG-4"-O-triacetylglucuronide methyl ester to obtain EGCG-4"-O-triacetylglucuronide with PLE and its further deacetylation to obtain EGCG-4"-O-glucuronide with LA

The preparative synthesis of EGCG-4"-*O*-glucuronide (**C16**) was carried out maintaining the conditions of the reaction **7** of **Table 29**, and following the reaction by HPLC-DAD (See Materials and Methods, Section 3.2.3.2.4.4 and 3.2.3.3.1.2). At the end reaction time, the obtained HPLC-DAD signal of **C16** was very low. The reaction crude was lyophilized, further dissolved in MeOH, and purified by semipreparative-HPLC following the method described on the Materials and Methods, Section 3.2.3.3.3.2. The compound with a peak at 17 min and a *m/z* 633.11 (3.7 mg) was characterized by NMR (D$_2$O). ^{1}H-NMR spectrum of **C16** was obtained with low resolution and with wide signals corresponding to impurities (e.g. the esterases).

To sum up, the hydrolysis of EGCG-4"-*O*-triacetylglucuronide methyl ester (**A16**) to obtain EGCG-4"-*O*-triacetylglucuronide (**A16-Me**) was very efficient with PLE at all tested pH values (pH 5.0, 6.2 and 7.3). The deacetylation of **A16-Me** using the best conditions with LAS (the reaction **16** of **Table 28**) was unsuccessful due to the polymerization of **A16-Me** or the low effectiveness of LAS. Deacetylation of **A16-Me** to obtain **C16** with LA was more efficient than with LAS at the same enzyme concentration. On the other hand, LA reactions provided side products of the hydrolysis of the glycosidic bond.

Preparative synthesis of **C16** was carried out with the most efficient conditions tested (LA, pH 7.3). The peak corresponding to the product **C16** was purified by semipreparative-HPLC, and we could not characterize the product by NMR owing to the low quantity of **C16** and the residual LA/PLE contained in the sample.

To solve these problems explained above, i.e. the hydrolysis of the glycosidic bond of glucuronide compounds and the separation of the final product **C16** from enzymes, we decided to assay the route A using immobilized LAS.

4.7.2.2.3. Deacetylation of EGCG-4"-*O*-triacetylglucuronide methyl ester to obtain EGCG-4"-*O*-glucuronide methyl ester with immobilized LAS

LAS was immobilized in a macroporous acrylic resin following the procedure described on the Materials and Methods, Section 3.2.3.2.4.5, to facilitate the purification

of the EGCG-4"-*O*-glucuronide methyl ester (**B16**) on the deacetylation reaction, and to increase the enzymatic activity. The results are shown in **Table 30**.

Three different LAS:resin ratios were used: A (100 mg:1 g), B (300 mg:1 g) and C (600 mg:1 g). Reaction conditions used with the immobilized LAS were those optimized for the route A at pH 6.1 (reaction **16** of **Table 28**). The first assay with immobilized LAS (the reaction **1** of **Table 30**) was followed by HPLC-HR-DAD-ESI-TOF-MS (See Materials and Methods, Section 3.2.3.3.2.3) obtaining the *m/z* corresponding to the mass of products EGCG-4"-*O*-diacetylglucuronide methyl ester (**A16'**) and EGCG-4"-*O*-monoacetylglucuronide methyl ester (**A16"**), dehydrated **A16"** (**A16"-H₂O**), and EGCG-4"-*O*- glucuronide methyl ester (**B16**), as major peaks at 22.5 h of reaction time (**Figures 108** and **109**). All other assays performed with immobilized LAS were followed by HPLC-DAD (See Materials and Methods, Section 3.2.3.3.1.3), and spectrum peaks obtained were compared with those peaks from the spectrum acquired by HPLC-HR-DAD-ESI-TOF-MS.
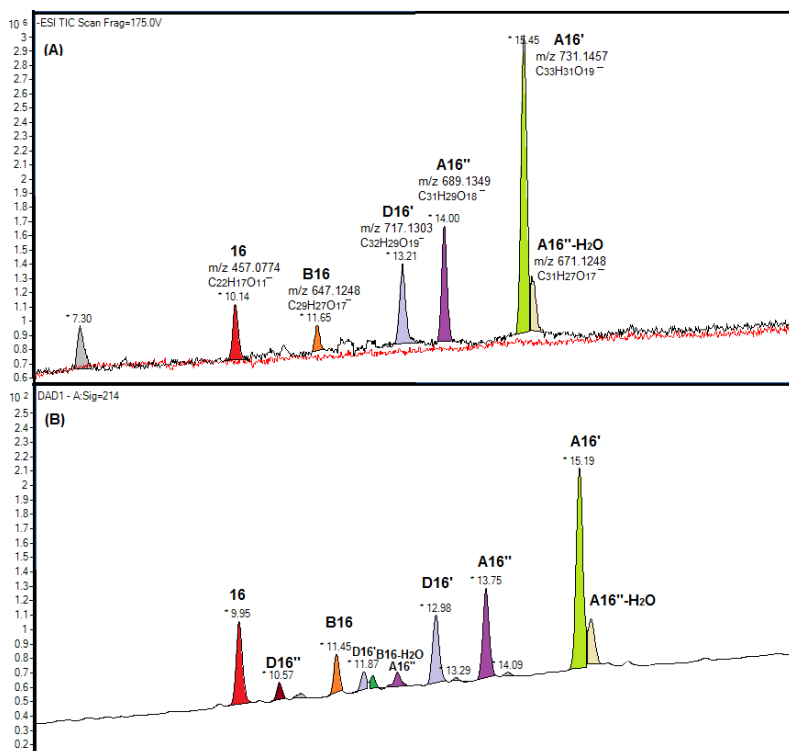
Figure 108. (A) ESI-TOF-MS chromatogram (TIC) and **(B)** UV-Vis (λ =214 nm) chromatogram of the deacetylation of **A16** to obtain **B16** with immobilized LAS at pH 6.02 after 22.5 h of reaction (reaction conditions **1** of **Table 29**).
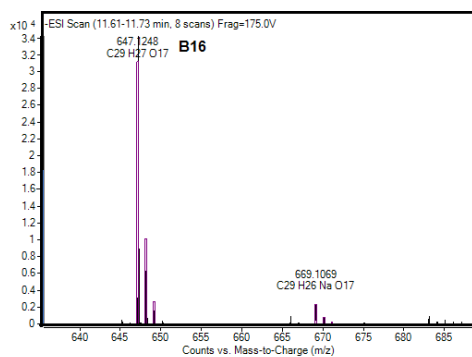
Figure 109. ESI-TOF-MS-chromatogram of **B16** peak.

Table 30. Reaction conditions to deacetylate **A16** to obtain **B16** with immobilized LAS.

Reaction	Enzyme	Solvent	A16 (mg)	LAS (mg)	Conditions[a]	t (h)	Peak intensity of detected products[b]
1	LAS	water (0.8 ml), DMSO (0.2 ml)	2.13	20.1(A)	S.P.B (25 mM) pH 6.02	22.5	**A16'** > **A16"** > **A16"-H$_2$O** > **B16**
2	LAS	water (0.8 ml), DMSO (0.2 ml)	1.90	60.0(A)	S.P.B (25 mM) pH 6.02	22.5	**A16'** > **A16"** > **B16** > **A16"-H$_2$O**
3	LAS	water (0.8 ml), DMSO (0.2 ml)	2.10	60.4(B)	S.P.B (25 mM) pH 6.02	6	**A16'** > **A16"** = **B16**
4	LAS	water (0.8 ml), DMSO (0.2 ml)	2.16	60.3(C)	S.P.B (25 mM) pH 6.02	6	**B16** > **A16'** > **A16"**

[a] S.P.B (Sodium Phosphate Buffer); [b] Products were identified according to the *m/z* values obtained by HPLC-HR-DAD-ESI-TOF-MS analysis. Temperature 40 °C.

The immobilized LAS-C, which contains the highest protein load, was the most efficient to deacetylate **A16.** The UV-Vis chromatogram obtained by HPLC-DAD was compared with that obtained by HPLC-HR-DAD-ESI-TOF-MS of the assay with immobilized LAS-A. The major peaks obtained by UV-Vis with immobilized LAS-C were **B16** > **A16'** > **A16"**. The peak of **B16-H$_2$O** was obtained with a very low intensity compared with the **B16/B16-H$_2$O** ratio obtained at the same conditions with LAS (reaction **16** of **Table 28**) (**Figure 110**).

4. Results and discussion
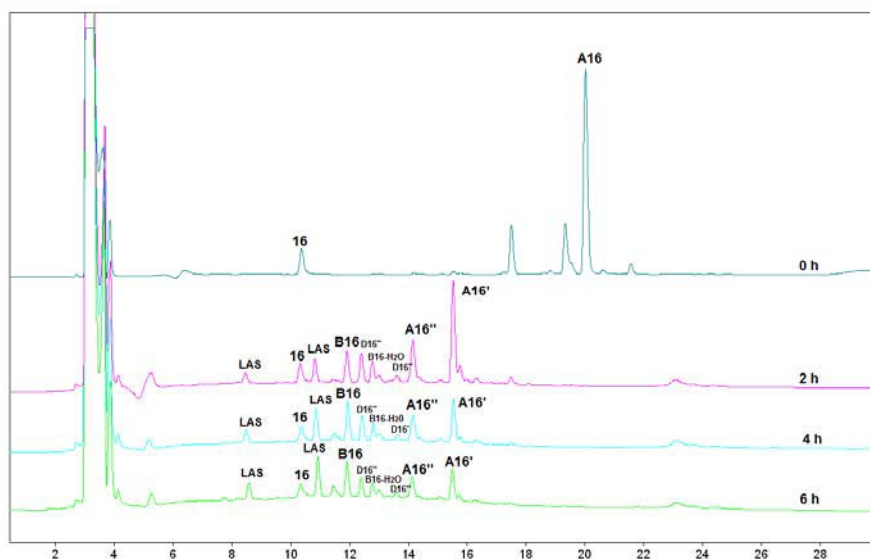
LAS (peaks detected in lipase AS solutions).

Figure 110. HPLC-DAD chromatogram of the deacetylation of **A16** with immobilized LAS-C in Na$_2$HPO$_4$ buffer (25 mM, pH 6.02) with DMSO as co-solvent (20 %) at 40 °C from 0-6 h of reaction time.

4.7.2.2.4. Methyl ester hydrolysis of EGCG-4''-*O*-glucuronide methyl ester to obtain EGCG-4''-*O*-glucuronide with PLE

After the use of the deacetylation conditions of the reaction 4 of **Table 30**, immobilized LAS-C was separated by filtration from the solution containing EGCG-4''-*O*-glucuronide methyl ester (**B16**) as the major component. PLE was added to the solution with a proportion of EGCG-4''-*O*-triacetylglucuronide methyl ester (**A16**)/PLE of 1:2 (w:w) at 40 °C and gentle stirring. The reaction was followed by HPLC-DAD (See Materials and Methods, Section 3.2.3.2.4.6 and Section 3.2.3.3.1.3) during 3 h and methyl ester hydrolysis took place with very low yield.

To conclude, the elimination of the enzyme was solved by filtration of the acrylic resin containing the enzyme. The immobilized LAS-C was more efficient than the non-immobilized LAS. The **A16**/LAS ratio used on route A was 1:26 in front of the 1:17 used with the immobilized LAS. From this, intermediates of deacetylation i.e. EGCG-4''-*O*-

diacetylglucuronide methyl ester (**A16'**) and EGCG-4''-*O*-monoacetylglucuronide methyl ester (**A16''**), and the desired product, **B16** as the major product were obtained with immobilized LAS, and **B16** and the dehydrated product of **B16**, the **B16-H2O**, as the major products were obtained with non-immobilized LAS.

The methyl ester hydrolysis of EGCG-4''-*O*-triacetylglucuronide methyl ester (**A16**) using the PLE is very efficient at all conditions tested albeit PLE does not work to hydrolyze the methyl ester of **B16**. On **Figure 111**, the scheme of the best reaction conditions assayed in this thesis to attempt the synthesis of EGCG-4''-*O*-glucuronide (**C16**) are shown.

4. Results and discussion
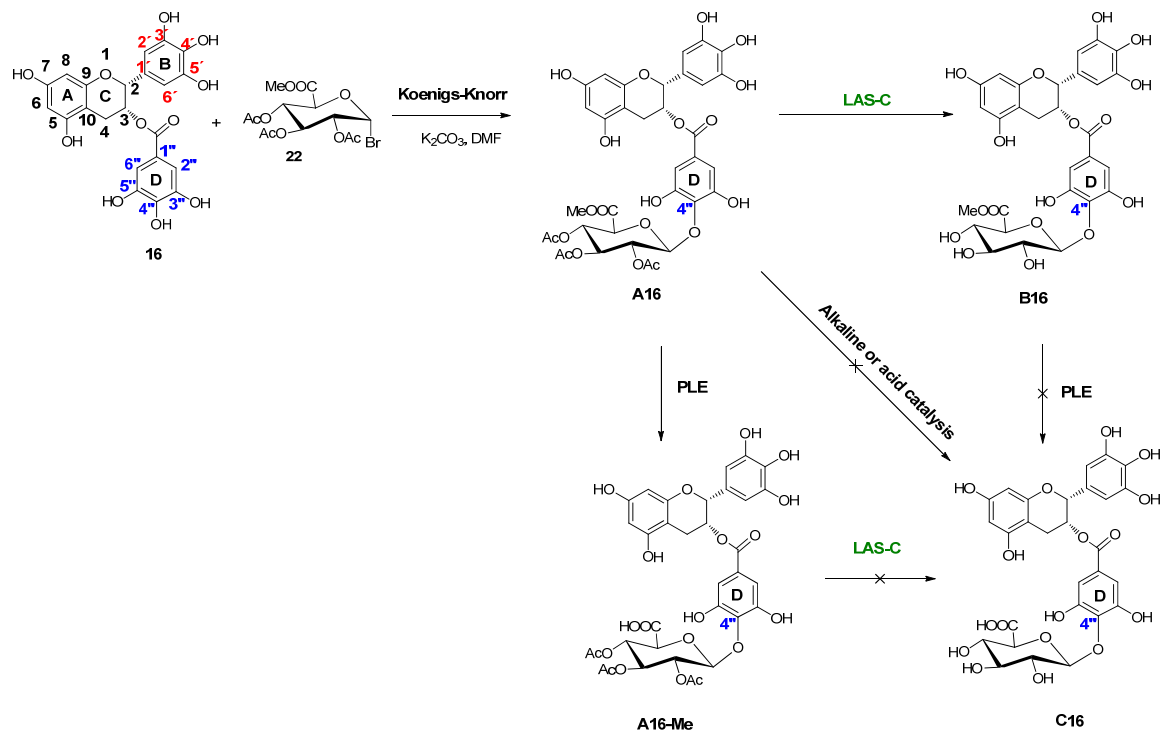
Figure 111. Scheme of the chemical and enzymatic reactions assayed to attempt the synthesis of **C16**. DMF (dimethylformamide), LAS-C (lipase AS immobilized), PLE, (Porcine Liver Esterase).

5. Conclusions

1. The tris(2,3,5,6-tetrachloro-4-nitrophenyl)methyl radical (TNPTM) was synthesized and characterized, displaying a redox potential value ($E°$) of 0.20 V in CHCl₃/MeOH (2:1).

2. TNPTM exclusively reacts with certain (poly)phenolic compounds through Electron-Transfer (ET) processes, as supported by its lack of reaction with toluene, its steric hindrance (X-ray structure), and the spectrophotometric detection of the anion of TNPTM during the reactions with (poly)phenols in CHCl₃/MeOH (2:1).

3. TNPTM and the previously described HNTTM were used to evaluate the radical scavenging activity (Kinetics and Radical Scavenging Capacity (RSC)) of a collection of (poly)phenols that comprised simple phenolics, flavanols and hydrolysable tannins. The compounds assayed were the simple phenols catechol (**10**), pyrogallol (**11**) and methylgallate (**12**), the flavanols (–)-epicatechin (EC, **13**), (–)-epigallocatechin (EGC, **14**), (–)-epicatechin-3-*O*-gallate (ECG, **15**) and (–)-epigallocatechin-3-*O*-gallate (EGCG, **16**), the gallotannins hamamelitannin (HT, **17**) and pentagalloylglucose (PGG, **18**), the ellagitannin punicalagin and its substructures dimethyl-hexahydroxydiphenyl-dicarboxylate (DHHDP, **20**), and ellagic acid (EA, **21**).

4. Only highly reactive moieties within (poly)phenols react with TNPTM. TNPTM reacted exclusively with pyrogallol (11), EGC (**14**), EGCG (**16**), HT (**17**), punicalagin (**19**), and DHHDP (**20**) in CHCl₃/MeOH (2:1). TNPTM reveals that the HHDP substructure of punicalagin (**19**) is a particularly reactive moiety. The C-C bond between gallate moieties and ellagic acid, and between two gallate moieties (HHDP group) in punicalagin (**19**) activates one of the hydroxyls of each gallate group, which are detected by TNPTM.

5. The RSC values of the (poly)phenols **10**-**21** with HNTTM were compared with the values obtained with DPPH and the FRAP method. The results were similar for the three methods, showing comparable relative results despite of their different reducing mechanisms and the different solvents used (organic solvent or water). The three methods indicate that the (poly)phenols pyrogallol (**11**), ECG (**15**), PGG (**18**), and punicalagin (**19**) are the most scavenging and reducing compounds from each group. The RSC values of (poly)phenols **10**-**21** with the radical HNTTM are roughly coincident with the number of (poly)phenolic hydroxyls, whereas with DPPH the RSC values are generally higher than those obtained with HNTTM.

5. Conclusions

6. The introduction of a cysteine group on the position 4 of EGC (**14**) and EGCG (**16**) does no modify the number of electrons transferred (n_e) per molecule of (poly)phenol to HNTTM as compared to their precursors. On the other hand, the introduction of a cysteamine group at the same position of EGC (**14**), ECG (**15**), and EGCG (**16**) increases the n_e by one.

7. The mechanism for the reactions of catechol (**10**) and pyrogallol (**11**) with HNTTM in the ionizable CHCl$_3$/MeOH (2:1) mixture is the Sequential Proton Loss Electron Transfer (SPLET) process. This is supported by electrochemical analysis (exergonic reaction only for anionic forms of the phenols) and by UV-Vis spectroscopy (HNTTM anion as the stable and characteristic intermediate). On the other hand, the mechanism in non-ionizable solvents such as CHCl$_3$ and benzene is the Proton-Coupled Electron Transfer (PCET) as suggested by the absence of detectable HNTTM anion by UV-Vis spectroscopy. Particularly, the reaction of pyrogallol (**11**) with HNTTM in benzene may take place through the formation of a complex between **11** and HNTTM and later electron-transfer into the complex to obtain the HNTTM anion which is detected by UV-Vis spectroscopy. HNTTM has a high enough oxidation potential ($E°$ (CHCl$_3$/MeOH (2:1))=0.55 V) to oxidize (poly)phenols in their neutral and anionic forms by ET.

8. The SPLET mechanism is proposed for the reaction of pyrogallol (**11**) and DHHDP (**20**) with TNTPM in CHCl$_3$/MeOH (2:1). TNPTM oxidizes those (poly)phenols with a very low anionic peak potential (E_p^a) or low anodic onset potential E_o^a (≤ 0.50 V).

9. The cyclic voltamperometries of TNTPM and DPPH show very similar redox potentials ($E°$= 0.20 V and $E°$= 0.21 V, respectively) in CHCl$_3$/MeOH (2:1). These values are not in agreement with the different reactivity of TNPTM and DPPH with (poly)phenols **10-21**. From these results is suggested that TNPTM and DPPH react with (poly)phenols in CHCl$_3$/MeOH (2:1) through different mechanisms, Electron-Transfer (ET) and Hydrogen Atom Transfer (HAT) respectively. HNTTM reacts with (poly)phenols with the same mechanism as TNPTM.

10. The kinetic studies with TNPTM show that EGCG (**16**) is the fastest agent among those tested.

11. All the (poly)phenols tested with the exception of EC (**13**) and EA (**21**), triggered antiproliferation on HT-29 cells. The most effective antiproliferative (poly)phenols on HT-29 cells when assayed without catalase (i.e. pyrogallol (**11**), EGC (**14**) and EGCG (**16**), HT (**17**), punicalagin (**19**), and DHHDP (**20**)) are those with significant radical scavenging activity with TNPTM. This suggests a possible role of a prooxidant effect.

12. EGCG-4''-*O*-glucuronide (**C16**), the most abundant EGCG metabolite in humans, was chemically synthesized and characterized in its acetylated form, EGCG-4''-*O*-triacetylglucuronide methyl ester (**A16**). The transformation of **A16** into **C16** using a set of lipases was investigated, obtaining very low yields because of the poor hydrolytic activity of the enzyme LAS towards one of the acetylated positions of EGCG-4''-*O*-triacetylglucuronide (**A16-Me**) and the poor hydrolytic activity of PLE towards the methyl ester of the EGCG-4''-*O*-glucuronide methyl ester (**B16**).

6. Bibliography

1.   Nediani, C.; Raimondi, L.; Borchi, E.; Cerbai, E. Nitric Oxide/Reactive Oxygen Species Generation and Nitroso/Redox Imbalance in Heart Failure: From Molecular Mechanisms to Therapeutic Implications. *Antiox. Redox Sig.* **2011**, *14*, 289-331.

2.   Al-Gubory, K. H.; Fowler, P. A.; Garrel, C. The roles of cellular reactive oxygen species, oxidative stress and antioxidants in pregnancy outcomes. *Int. J. Biochem. Cell B.* **2010**, *42*, 1634-1650.

3.   Koppenol, W. H. The Haber-Weiss cycle - 70 years later. *Redox Rep.* **2001**, *6*, 229-234.

4.   Goetz, M. E.; Luch, A. Reactive species: A cell damaging rout assisting to chemical carcinogens. *Cancer Lett.* **2008**, *266*, 73-83.

5.   Packer, L.; Witt, E. H.; Tritschler, H. J. Alpha-lipoic acid as a biological antioxidant. *Free Radical Biol. Med.* **1995**, *19*, 227-250.

6.   Río, L. A.; Sandalio, L. M.; Corpas, F. J.; Romero-Puertas, M. C.; Palma, J. M.; Rio, L. A.; Puppo, A., Peroxisomes as a Cellular Source of ROS Signal Molecules. Reactive Oxygen Species in Plant Signaling. *Signal. Commun. Plants* **2009**, 95-111.

7.   Watkins, P. A.; Blake, D. C.; Pedersen, J. I. Peroxisomal and mitochondrial fatty-acid oxidation in human hepatoma-cells (HEP-G2). *Federation P.* **1987**, *46*, 2008-2008.

8.   Valko, M.; Leibfritz, D.; Moncol, J.; Cronin, M. T. D.; Mazur, M.; Telser, J. Free radicals and antioxidants in normal physiological functions and human disease. *Int. J. Biochem. Cell B.* **2007**, *39*, 44-84.

9.   Boots, A. W.; Haenen, G. R. M. M.; Bast, A. Health effects of quercetin: From antioxidant to nutraceutical. *Eur. J. Pharmacol.* **2008**, *585*, 325-337.

10. Halliwell, B.; Gutteridge, J. M. C. The antioxidants of human extracellular fluids. *Arch. Biochem. Biophys.* **1990**, *280*, 1-8.

11. Podda, M.; Grundmann-Kollmann, M. Low molecular weight antioxidants and their role in skin ageing. *Clin. Exp. Dermatol.* **2001**, *26*, 578-582.

12. Moskovitz, J.; Bar-Noy, S.; Williams, W. M.; Requena, J.; Berlett, B. S.; Stadtman, E. R. Methionine sulfoxide reductase (MsrA) is a regulator of antioxidant defense and lifespan in mammals. *Proc. Natl. Acad. Sci. USA* **2001**, *98*, 12920-12925.

13. Kim, H. Y.; Gladyshev, V. N. Methionine Sulfoxide Reduction in Mammals: Characterization of Methionine-R-Sulfoxide Reductases. *Mol. Biol. Cell* **2004**, *15*, 1055-1064.

6. Bibliography

14. Ames, B. N.; Cathcart, R.; Schwiers, E.; Hochstein, P. Uric acid provides an antioxidant defense in humans against oxidant- and radical-caused aging and cancer: a hypothesis. *Proc. Natl. Acad. Sci.* **1981**, *78*, 6858-6862.

15. Roland, S.; Glazer, A. N.; Ames, B. N. Antioxidant Activity of Albumin-Bound Bilirubin. *Proc. Natl. Acad. Sci.* **1987**, *84*, 5918-5922.

16. Frei, B.; Kim, M. C.; Ames, B. N. Ubiquinol-10 is an effective lipid-soluble antioxidant at physiological concentrations. *Proc. Natl. Acad. Sci.* **1990**, *87*, 4879-4883.

17. Chauhan, A.; Chauhan, V.; Brown, W. T.; Cohen, I. Oxidative stress in autism: Increased lipid peroxidation and reduced serum levels of ceruloplasmin and transferrin - the antioxidant proteins. *Life Sci.* **2004**, *75*, 2539-2549.

18. Halliwell, B.; Cross, C. E. Oxgen-derived species-their relation to human-disease and environmental-stress. *Environ. Health Perspect.* **1994**, *102*, 5-12.

19. Cederbaum, A. Nrf2 and antioxidant defense against CYP2E1 toxicity. *Expert Opin. Drug Met.* **2009**, *5*, 1223-1244.

20. Howard, D. J.; Ota, R. B.; Briggs, L. A.; Hampton, M.; Pritsos, C. A. Environmental tobacco smoke in the workplace induces oxidative stress in employees, including increased production of 8-hydroxy-2'-deoxyguanosine. *Cancer Epidemiol. Biomarkers Prev.* **1998**, *7*, 141-146.

21. Heck, D. E.; Vetrano, A. M.; Mariano, T. M.; Laskin, J. D. UVB Light Stimulates Production of Reactive Oxygen Species. *J. Biol. Chem.* **2003**, *278*, 22432-22436.

22. King, P. D.; Perry, M. C. Hepatotoxicity of Chemotherapy. *Oncologist* **2001**, *6*, 162-176.

23. Ryrfeldt, A.; Bannenberg, G.; Moldéus, P. Free radicals and lung disease. *Br. Med. Bull.* **1993**, *49*, 588-603.

24. Hapuarachchi, J. R.; Chalmers, A. H.; Winefield, A. H.; Blake-Mortimer, J. S. Changes in clinically relevant metabolites with psychological stress parameters. *Behavior. Med.* **2003**, *29*, 52-59.

25. Ji, L. L. Antioxidants and Oxidative Stress in Exercise. *Proc. Soc. Exp. Biol. Med.* **1999**, *222*, 283-292.

26. Powers, S. K.; DeRuisseau, K. C.; Quindry, J.; Hamilton, K. L. Dietary antioxidants and exercice. *J. Sports Sci.* **2003**, *22*, 81-94

27.   Furukawa, S.; Fujita, T.; Shimabukuro, M.; Iwaki, M.; Yamada, Y.; Nakajima, Y.; Nakayama, O.; Makishima, M.; Matsuda, M.; Shimomura, I. Increased oxidative stress in obesity and its impact on metabolic syndrome. *J. Clinic. Invest.* **2004**, *114*, 1752-1761.

28.   Neri, S.; Signorelli, S. S.; Torrisi, B.; Pulvirenti, D.; Mauceri, B.; Abate, G.; Ignaccolo, L.; Bordonaro, F.; Cilio, D.; Calvagno, S.; Leotta, C. Effects of antioxidant supplementation on postprandial oxidative stress and endothelial dysfunction: A single-blind, 15-day clinical trial in patients with untreated type 2 diabetes, subjects with impaired glucose tolerance, and healthy controls. *Clinic. Therapeu.* **2005**, *27*, 1764-1773.

29.   Ames, B. N.; Shigenaga, M. K.; Hagen, T. M. Oxidants, antioxidants, and the degenerative diseases of aging. *Proc. Natl. Acad. Sci.* **1993**, *90*, 7915-7922.

30.   Halliwell, B. Oxidative stress and cancer: have we moved forward? *Biochem. J.* **2007**, *401*, 1-11.

31.   Meyer, J. W.; Schmitt, M. E. A central role for the endothelial NADPH oxidase in atherosclerosis. *FEBS Lett.* **2000**, *472*, 1-4.

32.   Jaeschke, H. Xanthine oxidase–induced oxidant stress during hepatic ischemia-reperfusion: Are we coming full circle after 20 years? *Hepatology* **2002**, *36*, 761-763.

33.   Mattson, M. P. Dietary factors, hormesis and health. *Ageing Res. Rev.* **2008**, *7*, 43-48.

34.   Bukowski, J. A.; Lewis, J. R. Hormesis and Health: A Little of What You Fancy May Be Good for You. *South. Med. J.* **2000**, *93*, 371&hyhen;374.

35.   Halliwell, B. Are polyphenols antioxidants or pro-oxidants? What do we learn from cell culture and in vivo studies? *Arch. Biochem. Biophys.* **2008**, *476*, 107-112.

36.   Surh, Y.-J. Cancer chemoprevention with dietary phytochemicals. *Nat Rev Cancer* **2003**, *3*, 768-780.

37.   Thomasset, S. C.; Berry, D. P.; Garcea, G.; Marczylo, T.; Steward, W. P.; Gescher, A. J. Dietary polyphenolic phytochemicals—promising cancer chemopreventive agents in humans? A review of their clinical properties. *Int. J. Cancer* **2007**, *120*, 451-458.

38.   D'Archivio, M.; Filesi, C. V., R.; ; Scazzocchio, B.; Masella, R. Bioavailability of the Polyphenols: Status and Controversies. *Int. J. Mol. Sci.* **2010**, *11*, 1321-1342.

39.   Manach, C.; Scalbert, A.; Morand, C.; Rémésy, C.; Jiménez, L. Polyphenols: food sources and bioavailability. *Am. J. Clinic.Nutr.* **2004**, *79*, 727-747.

40.   Larrosa, M.; García-Conesa, M. T.; Espín, J. C.; Tomás-Barberán, F. A. Ellagitannins, ellagic acid and vascular health. *Mol. Aspects Med.* **2010**, *31*, 513-539.

41.   Cassidy, A.; Hanley, B.; Lamuela-Raventós, R. M. Isoflavones, lignans and stilbenes – origins, metabolism and potential importance to human health. *J. Sci. Food Agric.* **2000**, *80*, 1044-1062.

42.   Heim, K. E.; Tagliaferro, A. R.; Bobilya, D. J. Flavonoid antioxidants: chemistry, metabolism and structure-activity relationships. *J. Nutr. Biochem.* **2002**, *13*, 572-584.

43.   Dai, J.; Mumper, R. J. Plant Phenolics: Extraction, Analysis and Their Antioxidant and Anticancer Properties. *Molecules 15*, 7313-7352.

44.   Cai, Y. Z.; Mei, S.; Jie, X.; Luo, Q.; Corke, H. Structure-radical scavenging activity relationships of phenolic compounds from traditional Chinese medicinal plants. *Life Sci.* **2006**, *78*, 2872-2888.

45.   Andrews, N. C. Probing the iron pool. Focus on "Detection of intracellular iron by its regulatory effect". *Am. J. Phys. Cell Phys.* **2004**, *287*, C1537-C1538.

46.   Perron, N. R.; Brumaghim, J. L. A Review of the Antioxidant Mechanisms of Polyphenol Compounds Related to Iron Binding. *Cell Biochem. Biophys.* **2009**, *53*, 75-100.

47.   Frei, B.; Higdon, J. V. Antioxidant Activity of Tea Polyphenols In Vivo: Evidence from Animal Studies. *J. Nutr.* **2003**, *133*, 3275S-3284S.

48.   Lin, J.-K.; Chen, P.-C.; Ho, C.-T.; Lin-Shiau, S.-Y. Inhibition of Xanthine Oxidase and Suppression of Intracellular Reactive Oxygen Species in HL-60 Cells by Theaflavin-3,3'-digallate, (-)-Epigallocatechin-3-gallate, and Propyl Gallate. *J. Agric. Food Chem.* **2000**, *48*, 2736-2743.

49.   Duthie, S. J.; Johnson, W.; Dobson, V. L. The effect of dietary flavonoids on DNA damage (strand breaks and oxidised pyrimdines) and growth in human cells. *Mutat. Res/Genet. Toxicol. Environ. Mutag.* **1997**, *390*, 141-151.

50.   Fan, P.; Lou, H. Effects of polyphenols from grape seeds on oxidative damage to cellular DNA. *Mol. Cell. Biochem.* **2004**, *267*, 67-74.

51.   Li, G. X.; Chen, Y. K.; Hou, Z.; Xiao, H.; Jin, H.; Lu, G.; Lee, M. J.; Liu, B.; Guan, F.; Yang, Z.; Yu, A.; Yang, C. S. Pro-oxidative activities and dose-response relationship of (-)-epigallocatechin-3-gallate in the inhibition of lung cancer cell growth: a comparative study in vivo and in vitro. *Carcinogenesis* **2010**, *31*, 902-910.

52.   Nakagawa, H.; Hasumi, K.; Woo, J. T.; Nagai, K.; Wachi, M. Generation of hydrogen peroxide primarily contributes to the induction of Fe(II)-dependent apoptosis in Jurkat cells by (-)-epigallocatechin gallate. *Carcinogenesis* **2004**, *25*, 1567-1574.

53.   Fassina, G.; Vené, R.; Morini, M.; Minghelli, S.; Benelli, R.; Noonan, D. M.; Albini, A. Mechanisms of Inhibition of Tumor Angiogenesis and Vascular Tumor Growth by Epigallocatechin-3-Gallate. *Clin. Cancer. Res.* **2004**, *10*, 4865-4873.

54. Long, L. H.; Kirkland, D.; Whitwell, J.; Halliwell, B. Different cytotoxic and clastogenic effects of epigallocatechin gallate in various cell-culture media due to variable rates of its oxidation in the culture medium. *Mutat. Res/Genet. Toxicol. Environ. Mutag.* **2007**, *634*, 177-183.

55.   Joubert, E.; Winterton, P.; Britz, T. J.; Gelderblom, W. C. A. Antioxidant and Pro-oxidant Activities of Aqueous Extracts and Crude Polyphenolic Fractions of Rooibos (Aspalathus linearis). *J. Agric. Food Chem.* **2005**, *53*, 10260-10267.

56.   Perron, N. R.; García, C. R.; Pinzón, J. R.; Chaur, M. N.; Brumaghim, J. L. Antioxidant and prooxidant effects of polyphenol compounds on copper-mediated DNA damage. *J. Inorg. Biochem.* **2011**, *105*, 745-753.

57.   Seeram, N. P.; Adams, L. S.; Hardy, M. L.; Heber, D. Total Cranberry Extract versus Its Phytochemical Constituents: Antiproliferative and Synergistic Effects against Human Tumor Cell Lines. *J. Agric. Food Chem.* **2004**, *52*, 2512-2517.

58.   Zhang, Y.; Seeram, N. P.; Lee, R.; Feng, L.; Heber, D. Isolation and Identification of Strawberry Phenolics with Antioxidant and Human Cancer Cell Antiproliferative Properties. *J. Agric. Food Chem.* **2008**, *56*, 670-675.

59.   Katsube, N.; Iwashita, K.; Tsushida, T.; Yamaki, K.; Kobori, M. Induction of Apoptosis in Cancer Cells by Bilberry (Vaccinium myrtillus) and the Anthocyanins. *J. Agric. Food Chem.* **2002**, *51*, 68-75.

60.   Ross, H. A.; McDougall, G. J.; Stewart, D. Antiproliferative activity is predominantly associated with ellagitannins in raspberry extracts. *Phytochemistry* **2007**, *68*, 218-228.

61.   Damianaki, A.; Bakogeorgou, E.; Kampa, M.; Notas, G.; Hatzoglou, A.; Panagiotou, S.; Gemetzi, C.; Kouroumalis, E.; Martin, P.-M.; Castanas, E. Potent inhibitory action of red wine polyphenols on human breast cancer cells. *J. Cell. Biochem.* **2000**, *78*, 429-441.

62.   Kampa, M.; Hatzoglou, A.; Notas, G.; Damianaki, A.; Bakogeorgou, E.; Gemetzi, C.; Kouroumalis, E.; Martin, P.-M.; Castanas, E. Wine Antioxidant Polyphenols Inhibit the Proliferation of Human Prostate Cancer Cell Lines. *Nutr. Cancer* **2000**, *37*, 223-233.

63.   Zhang, G.; Miura, Y.; Yagasaki, K. Induction of Apoptosis and Cell Cycle Arrest inCancer Cells by In Vivo Metabolites of Teas. *Nutr. Cancer* **2000**, *38*, 265-273.

64.   Weisburg, J. H.; Weissman, D. B.; Sedaghat, T.; Babich, H. In vitro Cytotoxicity of Epigallocatechin Gallate and Tea Extracts to Cancerous and Normal Cells from the Human Oral Cavity. *Basic Clin. Pharmacol. Toxicol.* **2004**, *95*, 191-200.

65.   McCann, M. J.; Gill, C. I. R.; O' Brien, G.; Rao, J. R.; McRoberts, W. C.; Hughes, P.; McEntee, R.; Rowland, I. R. Anti-cancer properties of phenolics from apple waste on colon carcinogenesis in vitro. *Food Chem. Toxicol.* **2007**, *45*, 1224-1230.

66.   Medina, I.; Lois, S.; Lizárraga, D.; Pazos, M.; Touriño, S.; Cascante, M.; Torres, J. L. Functional fatty fish supplemented with grape procyanidins. Antioxidant and proapoptotic properties on colon cell lines. *J. Agric. Food Chem.* **2006**, *54*, 3598-3603.

67.   Lizárraga, D.; Touriño, S.; Reyes-Zurita, F. J.; de Kok, T. M.; van Delft, J. H.; Maas, L. M.; Briede, J. J.; Centelles, J. J.; Torres, J. L.; Cascante, M. Witch Hazel (Hamamelis virginiana) Fractions and the Importance of Gallate Moieties-Electron Transfer Capacities in Their Antitumoral Properties. *J. Agric. Food Chem.* **2008**, *56*, 11675-11682.

68.   Crespy, V.; Williamson, G. A review of the health effects of green tea catechins in in vivo animal models. *J. Nutr.* **2004**, *134*, 3431S-3440S.

69.   Huang, M. T.; Lou, Y. R.; Ma, W.; Newmark, H. L.; Reuhl, K. R.; Conney, A. H. Inhibitory Effects of Dietary Curcumin on Forestomach, Duodenal, and Colon Carcinogenesis in Mice. *Cancer Res.* **1994**, *54*, 5841-5847.

70.   Mentor-Marcel, R.; Lamartiniere, C. A.; Eltoum, I. E.; Greenberg, N. M.; Elgavish, A. Genistein in the Diet Reduces the Incidence of Poorly Differentiated Prostatic Adenocarcinoma in Transgenic Mice (TRAMP). *Cancer Res.* **2001**, *61*, 6777-6782.

71.   Wang, J.; Eltoum, I. E.; Lamartiniere, C. A. Dietary genistein suppresses chemically induced prostate cancer in Lobund-Wistar rats. *Cancer Lett.* **2002**, *186*, 11-18.

72.   Sung, H.; Nah, J.; Chun, S.; Park, H.; Yang, S. E.; Min, W. K. In vivo antioxidant effect of green tea. *Eur. J. Clin. Nutr.* **2000**, *54*, 527-529.

73.   Langley-Evans, S. C. Consumption of black tea elicits an increase in plasma antioxidant potential in humans. *Int. J. Food Sci. Nutr.* **2000**, *51*, 309-315.

74.   Schwartz, J. L.; Baker, V.; Larios, E.; Chung, F. L. Molecular and cellular effects of green tea on oral cells of smokers: A pilot study. *Mol. Nutr. Food Res.* **2005**, *49*, 43-51.

75.   Hakim, I. A.; Harris, R. B.; Brown, S.; Chow, H. H. S.; Wiseman, S.; Agarwal, S.; Talbot, W. Effect of Increased Tea Consumption on Oxidative DNA Damage among Smokers: A Randomized Controlled Study. *J. Nutr.* **2003**, *133*, 3303S-3309S.

76.   Bettuzzi, S.; Brausi, M.; Rizzi, F.; Castagnetti, G.; Peracchia, G.; Corti, A. Chemoprevention of Human Prostate Cancer by Oral Administration of Green Tea Catechins in Volunteers with High-Grade Prostate Intraepithelial Neoplasia: A Preliminary Report from a One-Year Proof-of-Principle Study. *Cancer Res.* **2006**, *66*, 1234-1240.

77.   Li, N.; Sun, Z.; Han, C.; Chen, J. The Chemopreventive Effects of Tea on Human Oral Precancerous Mucosa Lesions. *Proc. Soc. Exp. Biol. Med.* **1999**, *220*, 218-224.

78.   Laurie, S. A.; Miller, V. A.; Grant, S. C.; Kris, M. G.; Ng, K. K. Phase I study of green tea extract in patients with advanced lung cancer. *Cancer Chemo. Pharma.* **2005**, *55*, 33-38.

79.   Sharma, R. A.; Euden, S. A.; Platton, S. L.; Cooke, D. N.; Shafayat, A.; Hewitt, H. R.; Marczylo, T. H.; Morgan, B.; Hemingway, D.; Plummer, S. M.; Pirmohamed, M.; Gescher, A. J.; Steward, W. P. Phase I Clinical Trial of Oral Curcumin. *Clin. Cancer. Res.* **2004**, *10*, 6847-6854.

80.   Lu, X.-Y.; Sun, D.-L.; Chen, Z.-J.; Chen, T.; Li, L.-P.; Xu, Z.-H.; Jiang, H.-D.; Zeng, S. Relative Contribution of Small and Large Intestine to Deglycosylation and Absorption of Flavonoids from Chrysanthemun morifolium Extract. *J. Agric. Food Chem.* **2010**, *58*, 10661-10667.

81.   Tsang, C.; Auger, C.; Mullen, W.; Bornet, A.; Rouanet, J. M.; Crozier, A.; Teissedre, P. L. The absorption, metabolism and excretion of flavan-3-ols and procyanidins following the ingestion of a grape seed extract by rats. *Brit. J. Nutr.* **2005**, *94*, 170-181.

82.   Urpí-Sardà, M.; Monagas, M.; Khan, N.; Lamuela-Raventós, R.; Santos-Buelga, C.; Sacanella, E.; Castell, M.; Permanyer, J.; Andrés-Lacueva, C. Epicatechin, procyanidins, and phenolic microbial metabolites after cocoa intake in humans and rats. *Anal. Bioanal. Chem.* **2009**, *394*, 1545-1556.

83.   Wu, X.; Cao, G.; Prior, R. L. Absorption and Metabolism of Anthocyanins in Elderly Women after Consumption of Elderberry or Blueberry. *J. Nutr.* **2002**, *132*, 1865-1871.

84.   Donovan, J. L.; Crespy, V.; Manach, C.; Morand, C.; Besson, C.; Scalbert, A.; Rémésy, C. Catechin Is Metabolized by Both the Small Intestine and Liver of Rats. *J. Nutr.* **2001**, *131*, 1753-1757.

85. Cheng, Z.; Radominska-Pandya, A.; Tephly, T. R. Studies on the Substrate Specificity of Human Intestinal UDP-Glucuronosyltransferases 1A8 and 1A10. *Drug Metab. Disposition* **1999**, *27*, 1165-1170.

86. Spencer, J. P. E. Metabolism of Tea Flavonoids in the Gastrointestinal Tract. *J. Nutr.* **2003**, *133*, 3255S-3261S.

87. Spencer, J. P. E.; Schroeter, H.; Rechner, A. R.; Rice-Evans, C. Bioavailability of Flavan-3-ols and Procyanidins: Gastrointestinal Tract Influences and Their Relevance to Bioactive Forms In Vivo. *Antiox. Redox Sig.* **2001**, *3*, 1023-1039.

88. Monagas, M.; Urpí-Sardà, M.; Sánchez-Patan, F.; Llorach, R. G., I.; ; Gómez-Cordovés, C.; Andrés-Lacueva, C.; Bartolome, B. Insights into the metabolism and microbial biotransformation of dietary flavan-3-ols and the bioactivity of their metabolites. *Food Funct.* **2010**, *1*, 233-253.

89. Touriño, S.; Fuguet, E.; Vinardell, M. a. P.; Cascante, M.; Torres, J. L. s. Phenolic Metabolites of Grape Antioxidant Dietary Fiber in Rat Urine. *J. Agric. Food Chem.* **2009**, *57*, 11418-11426.

90. Touriño, S.; Pérez-Jiménez, J.; Mateos-Martín, M. L.; Fuguet, E.; Vinardell, M. P.; Cascante, M.; Torres, J. L. Metabolites in Contact with the Rat Digestive Tract after Ingestion of a Phenolic-Rich Dietary Fiber Matrix. *J. Agric. Food Chem.* **2011**, *59*, 5955-5963.

91. Graham, H. N. Green tea composition, consumption, and polyphenol chemistry. *Prev. Med.* **1992**, *21*, 334-350.

92. Lambert, J. D.; Lee, M.-J.; Lu, H.; Meng, X.; Hong, J. J. J.; Seril, D. N.; Sturgill, M. G.; Yang, C. S. Epigallocatechin-3-Gallate Is Absorbed but Extensively Glucuronidated Following Oral Administration to Mice. *J. Nutr.* **2003**, *133*, 4172-4177.

93. Lee, M.-J.; Maliakal, P.; Chen, L.; Meng, X.; Bondoc, F. Y.; Prabhu, S.; Lambert, G.; Mohr, S.; Yang, C. S. Pharmacokinetics of Tea Catechins after Ingestion of Green Tea and (-)-Epigallocatechin-3-gallate by Humans. *Cancer Epidemiol. Biomarkers Prev.* **2002**, *11*, 1025-1032.

94. Chow, H. H. S.; Cai, Y. Z.; Alberts, D. S.; Hakim, I.; Dorr, R.; Shahi, F.; Crowell, J. A.; Yang, C. S.; Hara, Y. Phase I Pharmacokinetic Study of Tea Polyphenols following Single-dose Administration of Epigallocatechin Gallate and Polyphenon E. *Cancer Epidemiol. Biomarkers Prev.* **2001**, *10*, 53-58.

95. Meng, X. F.; Sang, S.; Zhu, N.; Lu, H.; Sheng, S.; Lee, M. J.; Ho, C. T.; Yang, C. S. Identification and Characterization of Methylated and Ring-Fission Metabolites of Tea Catechins Formed in Humans, Mice, and Rats. *Chem. Res. Toxicol.* **2002**, *15*, 1042-1050.

96. Lee, M. J.; Wang, Z. Y.; Li, H.; Chen, L.; Sun, Y.; Gobbo, S.; Balentine, D. A.; Yang, C. S. Analysis of plasma and urinary tea polyphenols in human subjects. *Cancer Epidemiol. Biomarkers Prev.* **1995**, *4*, 393-399.

97. Chen, L.; Lee, M. J.; Li, H.; Yang, C. S. Absorption, Distribution, and Elimination of Tea Polyphenols in Rats. *Drug Metab. Disposition* **1997**, *25*, 1045-1050.

98. Lu, H.; Meng, X. F.; Li, C.; Sang, S.; Patten, C.; Sheng, S.; Hong, J.; Bai, N.; Winnik, B.; Ho, C. T.; Yang, C. S. Glucuronides of Tea Catechins: Enzymology of Biosynthesis and Biological Activities. *Drug Metab. Disposition* **2003**, *31*, 452-461.

99. Brown, R. T.; Scheinmann, F.; Stachulski, A. V. Intermediates for glucuronide synthesis: 7-hydroxycoumarin glucuronide. *J. Chem. Res.* **1997**, 370-371.

100. Wadouachi, A.; Kovensky, J. Synthesis of Glycosides of Glucuronic, Galacturonic and Mannuronic Acids: An Overview. *Molecules* **2011**, *16*, 3933-3968.

101. Wang, P.; Zhang, Z.; Yu, B. Total Synthesis of CRM646-A and -B, Two Fungal Glucuronides with Potent Heparinase Inhibition Activities. *J. Org. Chem.* **2005**, *70*, 8884-8889.

102. González-Manzano, S.; González-Paramás, A.; Santos-Buelga, C.; Dueñas, M. Preparation and Characterization of Catechin Sulfates, Glucuronides, and Methylethers with Metabolic Interest. *J. Agric. Food Chem.* **2009**, *57*, 1231-1238.

103. Needs, P. W.; Kroon, P. A. Convenient syntheses of metabolically important quercetin glucuronides and sulfates. *Tetrahedron* **2006**, *62*, 6862-6868.

104. Boumendjel, A.; Blanc, M.; Williamson, G.; Barron, D. Efficient Synthesis of Flavanone Glucuronides. *J. Agric. Food Chem.* **2009**, *57*, 7264-7267.

105. Baba, A.; Yoshioka, T. Synthesis of 1-[β]-O-acyl glucuronides of diclofenac, mefenamic acid and (S)-naproxen by the chemo-selective enzymatic removal of protecting groups from the corresponding methyl acetyl derivatives. *Org. Biomol. Chem.* **2006**, *4*, 3303-3310.

106. Baba, A.; Yoshioka, T. An Improved Chemo-Enzymatic Synthesis of 1-β-O-Acyl Glucuronides: Highly Chemoselective Enzymatic Removal of Protecting Groups from Corresponding Methyl Acetyl Derivatives. *J. Org. Chem.* **2007**, *72*, 9541-9549.

107. Baba, A.; Yoshioka, T. Characterization of chemo- and regioselectivity in enzyme-catalyzed consecutive hydrolytic deprotection of methyl acetyl derivatives of 1-β-O-acyl glucuronides. *J. Mol. Catal. B: Enzym.* **2011**, *69*, 74-82.

108. Leopoldini, M.; Russo, N.; Toscano, M. The molecular basis of working mechanism of natural polyphenolic antioxidants. *Food Chem.* **2011**, *125*, 288-306.

109. Foti, M. C.; Daquino, C.; Mackie, I. D.; DiLabio, G. A.; Ingold, K. U. Reaction of Phenols with the 2,2-Diphenyl-1-picrylhydrazyl Radical. Kinetics and DFT Calculations Applied To Determine ArO-H Bond Dissociation Enthalpies and Reaction Mechanism. *J. Org. Chem.* **2008**, *73*, 9270-9282.

110. Galian, R. E.; Litwinienko, G.; Pérez-Prieto, J.; Ingold, K. U. Kinetic solvent effects on the reaction of an aromatic ketone л, л* triplet with phenol. Rate-retarding and rate-accelerating effects of hydrogen-bond acceptor solvents. *J. Am. Chem. Soc.* **2007**, *129*, 9280-9281.

111. Litwinienko, G.; Ingold, K. U. Abnormal Solvent Effects on Hydrogen Atom Abstraction. 3. Novel Kinetics in Sequential Proton Loss Electron Transfer Chemistry. *J. Org. Chem.* **2005**, *70*, 8982-8990.

112. Sjödin, M.; Irebo, T.; Utas, J. E.; Lind, J.; Merényi, G.; Äkermark, B.; Hammarström, L. Kinetic Effects of Hydrogen Bonds on Proton-Coupled Electron Transfer from Phenols. *J. Am. Chem. Soc.* **2006**, *128*, 13076-13083.

113. Litwinienko, G.; Ingold, K. U. Solvent Effects on the Rates and Mechanisms of Reaction of Phenols with Free Radicals. *Acc. Chem. Res.* **2007**, *40*, 222-230.

114. Hatcher, H.; Planalp, R.; Cho, J.; Torti, F.; Torti, S. Curcumin: From ancient medicine to current clinical trials. *Cell. Mol. Life Sci.* **2008**, *65*, 1631-1652.

115. Sánchez-Moreno, C. Review: Methods Used to Evaluate the Free Radical Scavenging Activity in Foods and Biological Systems. *Food Sci. Technol. Int.* **2002**, *8*, 121-137.

116. Goupy, P.; Dufour, C.; Loonis, M.; Dangles, O. Quantitative Kinetic Analysis of Hydrogen Transfer Reactions from Dietary Polyphenols to the DPPH Radical. *J. Agric. Food Chem.* **2002**, *51*, 615-622.

117. Torres, J. L.; Lozano, C.; Juliá , L.; Sánchez-Baeza, F. J.; Anglada, J. M.; Centelles, J. J.; Cascante, M. Cysteinyl-flavan-3-ol Conjugates from Grape Procyanidins. Antioxidant and Antiproliferative Properties. *Bioorgan. Med. Chem.* **2002**, *10*, 2497-2509.

118. Litwinienko, G.; Ingold, K. U. Abnormal solvent effects on hydrogen atom abstractions. 1. The reactions of phenols with 2,2-diphenyl-1-picrylhydrazyl (dpph**.**) in alcohols. *J. Org. Chem.* **2003**, *68*, 3433-3438.

119. Zulueta, A.; Esteve, M. J.; Frasquet, I.; Frígola, A. Vitamin C, vitamin A, phenolic compounds and total antioxidant capacity of new fruit juice and skim milk mixture beverages marketed in Spain. *Food Chem.* **2007**, *103*, 1365-1374.

120. Ballester, M.; Riera, J.; Castañer, J.; Badía, C.; Monsó, J. M. Inert carbon free radicals.1. Perchlorotriphenylmethyl and perchlorotriphenylmethyl radical series. *J. Am. Chem. Soc.* **1971**, *93*, 2215-2225.

121. Armet, O.; Veciana, J.; Rovira, C.; Riera, J.; Castaner, J.; Molins, E.; Rius, J.; Miravitlles, C.; Olivella, S.; Brichfeus, J. Inert carbon free-radicals .8. Polychlorotriphenylmethyl radicals - synthesis, structure, and spin-density distribution. *J. Phys. Chem.* **1987**, *91*, 5608-5616.

122. Torres, J. L.; Varela, B.; Brillas, E.; Juliá, L. Tris(2,4,6-trichloro-3,5-dinitrophenyl)methyl radical: a new stable coloured magnetic species as a chemosensor for natural polyphenols. *Chem. Commun.* **2003**, 74-75.

123. Jiménez, A.; Juliá, L.; Selga, A.; Torres, J. L. Reducing activity of polyphenols with stable radicals of the TTM series. Electron transfer versus H-abstraction reactions in flavan-3-ols. *Org. Lett.* **2004**, *6*, 4583-4586.

124. Lozano, C.; Juliá, L.; Jiménez, A.; Touriño, S.; Centelles, J. J.; Cascante, M.; Torres, J. L. Electron-transfer capacity of catechin derivatives and influence on the cell cycle and apoptosis in HT29 cells. *Febs J.* **2006**, *273*, 2475-2486.

125. Touriño, S.; Selga, A.; Jiménez, A.; Juliá, L.; Lozano, C.; Lizárraga, D. L.; Cascante, M.; Torres, J. L. Procyanidin fractions from pine (Pinus pinaster) bark: Radical scavenging power in solution, antioxidant activity in emulsion, and antiproliferative effect in melanoma cells. *J. Agric. Food Chem.* **2005**, *53*, 4728-4735.

126. Touriño, S.; Lizárraga, D.; Carreras, A.; Lorenzo, S.; Ugartondo, V.; Mitjans, M.; Vinardell, M. P.; Juliá, L.; Cascante, M.; Torres, J. L. Highly galloylated tannin fractions from witch hazel (*Hamamelis virginiana*) bark: Electron transfer capacity, in vitro antioxidant activity, and effects on skin-related cells. *Chem. Res. Toxicol.* **2008**, *21*, 696-704.

127. Benzie, I. F. F.; Strain, J. J. The ferric reducing ability of plasma (FRAP) as a measure of "antioxidant power": The FRAP assay. *Anal. Biochem.* **1996**, *239*, 70-76.

6. Bibliography

128. Berker, K. I.; Guclu, K.; Tor, I.; Apak, R. Comparative evaluation of Fe(III) reducing power-based antioxidant capacity assays in the presence of phenanthroline, batho-phenanthroline, tripyridyltriazine (FRAP), and ferricyanide reagents. *Talanta* **2007**, *72*, 1157-1165.

129. Karadag, A.; Ozcelik, B.; Saner, S. Review of Methods to Determine Antioxidant Capacities. *Food Anal. Method.* **2009**, *2*, 41-60.

130. Seeram, N. P.; Adams, L. S.; Henning, S. M.; Niu, Y. T.; Zhang, Y. J.; Nair, M. G.; Heber, D. In vitro antiproliferative, apoptotic and antioxidant activities of punicalagin, ellagic acid and a total pomegranate tannin extract are enhanced in combination with other polyphenols as found in pomegranate juice. *J. Nutr. Biochem.* **2005**, *16*, 360-367.

131. Jung, Y. D.; Ellis, L. M. Inhibition of tumour invasion and angiogenesis by epigallocatechin gallate (EGCG), a major component of green tea. *Int. J. Exp. Pathol.* **2001**, *82*, 309-316.

132. Nakagawa, H.; Hasumi, K.; Woo, J.-T.; Nagai, K.; Wachi, M. Generation of hydrogen peroxide primarily contributes to the induction of Fe(II)-dependent apoptosis in Jurkat cells by (-)-epigallocatechin gallate. *Carcinogenesis* **2004**, *25*, 1567-1574.

133. Nakagawa, H.; Wachi, M.; Woo, J.-T.; Kato, M.; Kasai, S.; Takahashi, F.; Lee, I.-S.; Nagai, K. Fenton Reaction Is Primarily Involved in a Mechanism of (-)-Epigallocatechin-3-gallate to Induce Osteoclastic Cell Death. *Biochem. Biophys. Res. Commun.* **2002**, *292*, 94-101.

134. Aziz, M. H.; R.;, K.; M., A. Cancer chemoprevention by resveratrol: In vitro and in vivo studies and the underlying mechanisms (Review). *Int. J. Oncol.* **2003**, *23*, 17-28.

135. Gibellini, L.; Pinti, M.; Nasi, M.; Montagna, J. P.; De Biasi, S.; Roat, E.; Bertoncelli, L.; Cooper, E. L.; Cossarizza, A. Quercetin and Cancer Chemoprevention. *Evid-Based Compl. Alt.* **2011**, *2011*.

136. Tognon, R.; Gasparotto, E. P. L.; Leroy, J. M. G.; Oliveira, G. L.; Peres Neves, R.; Viu Carrara, R. C.; Kashima, S.; Tadeu Covas, D.; Santana, M.; Xisto Souto, E.; Zanichelli, M. A.; Engel Velano, C. E.; Pinto Simoes, B.; Lopes Alberto, F.; Miyashiro, K.; de Souza, A. M.; Amarante-Mendes, G. P.; Attié de Castro, F. Differential expression of apoptosis-related genes from death receptor pathway in chronic myeloproliferative diseases. *J. Clin. Pathol.* **2011**, *64*, 75-82.

137. Quideau, S.; Feldman, K. S. Ellagitannin chemistry. The first synthesis of dehydrohexahydroxydiphenoate esters from oxidative coupling of unetherified methyl gallate. *J. Org. Chem.* **1997**, *62*, 8809-8813.

138. Regev-Shoshani, G.; Shoseyov, O.; Bilkis, I.; Kerem, Z. Glycosylation of resveratrol protects it from enzymic oxidation. *Biochem. J.* **2003**, *374*, 157-163.

139. Yamazoe, A.; Hayashi, K.-I.; Kuboki, A.; Ohira, S.; Nozaki, H. The isolation, structural determination, and total synthesis of terfestatin A, a novel auxin signaling inhibitor from Streptomyces sp. *Tetrahedron Lett.* **2004**, *45*, 8359-8362.

140. Touriño, S.; Fuguet, E.; Jáuregui, O.; Saura-Calixto, F.; Cascante, M.; Torres, J. L. High-resolution liquid chromatography/electrospray ionization time-of-flight mass spectrometry combined with liquid chromatography/electrospray ionization tandem mass spectrometry to identify polyphenols from grape antioxidant dietary fiber. *Rapid Commun. Mass Spectrom.* **2008**, *22*, 3489-3500.

141. Yang, J.; Liu, G.-Y.; Lu, D.-L.; Dai, F.; Qian, Y.-P.; Jin, X.-L.; Zhou, B. Hybrid-Increased Radical-Scavenging Activity of Resveratrol Derivatives by Incorporating a Chroman Moiety of Vitamin E. *Chem. Eur. J.* **2010**, *16*, 12808-12813.

142. Lorimer, J. P.; Kershaw, D.; Mason, T. J. Investigation of the consumption of diphenylpicrylhydrazyl in solution in the absence and presence of ultrasound. *J. Chem. Soc., Faraday Trans.* **1995**, *91*, 1067-1074.

143. Poirier, R. H.; Kahler, E. J.; Benington, F. The Chemistry of Hydrazyl free Radicals. I. Spectrophotometric Evidence on the Structure of α-α-Diphenyl-β-Picrylhydrazyl and α-α-Diphenyl-β-Picryl-betta-Oxyhydrazyl. *J. Org. Chem.* **1952**, *17*, 1437-1445.

144. Carreras, A.; Esparbé, I.; Brillas, E.; Rius, J.; Torres, J. L.; Juliá, L. Oxidant Activity of Tris(2,4,6-trichloro-3,5-dinitrophenyl)methyl Radical with Catechol and Pyrogallol. Mechanistic Considerations. *J. Org. Chem.* **2009**, *74*, 2368-2373.

145. Ballester, M.; Riera, J.; Castañer, J.; Rodríguez, A.; Rovira, C.; Veciana, J. Inert carbon free-radicals.3. Monofunctionalized radicals from perchlorotriphenylcarbenium hexachloroantimonate. *J. Org. Chem.* **1982**, *47*, 4498-4505.

146. Roberts, J. L.; Sugimoto, H.; Barrette, W. C.; Sawyer, D. T. One-electron reduction of anthraquinone by hydroxyde ion in aprotic media. *J. Am. Chem. Soc.* **1985**, *107*, 4556-4557.

147. Foti, M. C.; Daquino, C.; Geraci, C. Electron-Transfer Reaction of Cinnamic Acids and Their Methyl Esters with the DPPH Radical in Alcoholic Solutions. *J. Org. Chem.* **2004**, *69*, 2309-2314.

148. Nematollahi, D.; Goodarzi, H.; Tammari, E. Mechanism of electrochemical oxidation of catechol and 3-substituted catechols in the presence of barbituric acid derivatives. Synthesis of new dispiropyrimidine derivatives. *J. Chem. Soc.* **2002**, 829-834.

149. Zhu, N.; Wang, M.; Wei, G. J.; Lin, J. K.; Yang, C. S.; Ho, C. T. Identification of reaction products of (-)-epigallocatechin, (-)-epigallocatechin gallate and pyrogallol with 2,2-diphenyl-1-picrylhydrazyl radical. *Food Chem.* **2001**, *73*, 345-349.

150. Mayer, J. M.; Rhile, I. J. Thermodynamics and kinetics of proton-coupled electron transfer: stepwise vs. concerted pathways. *BBA-Bioenergetics* **2004**, *1655*, 51-58.

151. Torres, J. L.; Varela, B.; García, M. T.; Carilla, J.; Matito, C.; Centelles, J. J.; Cascante, M.; Sort, X.; Bobet, R. Valorization of grape (*Vitis vinifera*) byproducts. Antioxidant and biological properties of polyphenolic fractions differing in procyanidin composition and flavonol content. *J. Agric. Food Chem.* **2002**, *50*, 7548-7555.

152. Qian, Y.-P.; Shang, Y.-J.; Teng, Q.-F.; Chang, J.; Fan, G.-J.; Wei, X.; Li, R.-R.; Li, H.-P.; Yao, X.-J.; Dai, F.; Zhou, B. Hydroxychalcones as potent antioxidants: Structure-activity relationship analysis and mechanism considerations. *Food Chem.* **2011**, *126*, 241-248.

153. Sato, M.; Toyazaki, H.; Yoshioka, Y.; Yokoi, N.; Yamasaki, T. Structural Characteristics for Superoxide Anion Radical Scavenging and Productive Activities of Green Tea Polyphenols Including Proanthocyanidin Dimers. *Chem. Pharm. Bull.* **2010**, *58*, 98-102.

154. Nakanishi, I.; Kawashima, T.; Ohkubo, K.; Kanazawa, H.; Inami, K.; Mochizuki, M.; Fukuhara, K.; Okuda, H.; Ozawa, T.; Itoh, S.; Fukuzumi, S.; Ikota, N. Electron-transfer mechanism in radical-scavenging reactions by a vitamin E model in a protic medium. *Org. Biomol. Chem.* **2005**, *3*, 626-629.

155. Saito, S.; Gao, H.; Kawabata, J. DPPH (= 2,2-Diphenyl-1-picrylhydrazyl = 2,2-Diphenyl-1-(2,4,6-trinitrophenyl)hydrazyl) Radical-Scavenging Reaction of Protocatechuic Acid Esters (= 3,4-Dihydroxybenzoates) in Alcohols: Formation of Bis-alcohol Adduct. *Helv. Chim. Acta* **2006**, *89*, 821-831.

156. Saito, S.; Kawabata, J. DPPH (= 2,2-Diphenyl-1-picrylhydrazyl) Radical-Scavenging Reaction of Protocatechuic Acid (= 3,4-Dihydroxybenzoic Acid): Difference in Reactivity between Acids and Their Esters. *Helv. Chim. Acta* **2006**, *89*, 1395-1407.

157. Bellion, P.; Hofmann, T.; Pool-Zobel, B. L.; Will, F.; Dietrich, H.; Knaup, B.; Richling, E.; Baum, M.; Eisenbrand, G.; Janzowski, C. Antioxidant effectiveness of phenolic apple juice extracts and their gut fermentation products in the human colon carcinoma cell line caco-2. *J. Agric. Food Chem.* **2008**, *56*, 6310-6317.

158. Sánchez-Tena, S.; Fernández-Cachón, M. L.; Carreras, A.; Mateos-Martín, M. L.; Costoya, N.; Moyer, M. P.; Núñez, M. J.; Torres, J. L.; Cascante, M. Hamamelitannin from

Witch Hazel (*Hamamelis virginiana*) Displays Specific Cytotoxic Activity against Colon Cancer Cells. *J. Nat. Prod.* **2012**, *75*, 26-33.

159. Long, L. H.; Clement, M. V.; Halliwell, B. Artifacts in Cell Culture: Rapid Generation of Hydrogen Peroxide on Addition of (-)-Epigallocatechin, (-)-Epigallocatechin Gallate, (+)-Catechin, and Quercetin to Commonly Used Cell Culture Media. *Biochem. Biophys. Res. Commun.* **2000**, *273*, 50-53.

160. Lambert, J. D.; Kwon, S.-J.; Hong, J.; Yang, C. S. Salivary hydrogen peroxide produced by holding or chewing green tea in the oral cavity. *Free Radical Res.* **2007**, *41*, 850-853.

161. Nakagawa, H.; Hasumi, K.; Takami, M.; Aida-Hyugaji, S.; Woo, J.-T.; Nagai, K.; Ishikawa, T.; Wachi, M. Identification of two biologically crucial hydroxyl groups of (-)-epigallocatechin gallate in osteoclast culture. *Biochem. Pharmacol.* **2007**, *73*, 34-43.

162. Hong, J.; Lu, H.; Meng, X. F.; Ryu, J. H.; Hara, Y.; Yang, C. S. Stability, cellular uptake, biotransformation, and efflux of tea polyphenol (-)-epigallocatechin-3-gallate in HT-29 human colon adenocarcinoma cells. *Cancer Res.* **2002**, *62*, 7241-7246.

163. González, A. G.; Brouard, I.; León, F.; Padrón, J. I.; Bermejo, J. A facile chemoselective deacetylation in the presence of benzoyl and p-bromobenzoyl groups using p-toluenesulfonic acid. *Tetrahedron Lett.* **2001**, *42*, 3187-3188.

164. Hsiao, K.-F.; Wu, S.-H.; Wang, K.-T. Regioselective deacetylation of secondary acetyl esters in peracetylated methyl glycopyranosides by aspergillus niger lipase. *Bioorg. Med. Chem. Lett.* **1993**, *3*, 2125-2128.

165. La Ferla, B. Lipases as Useful Tools for the Stereo- and Regioselective Protection and Deprotection of Carbohydrates. *Monatsh. Chem.* **2002**, *133*, 351-368.